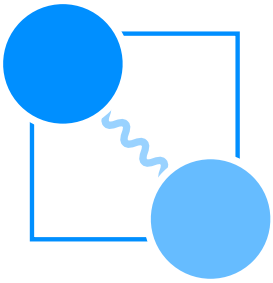

T30f
Theoretische Teilchen- und Kernphysik
Prof. Dr. Nora Brambilla

Renormalization of the Cyclic Wilson Loop

Diplomarbeit
von

Matthias Wilhelm Georg Berwein

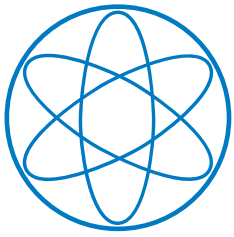

Technische Universität München Physik Department

Contents

Introduction

Ever since the discovery of the J/ψ in 1974, and of the Υ only a few years later, heavy quarkonia have been the subject of extensive study, both experimentally and theoretically. As bound states of a heavy quark and a heavy antiquark, they provide ideal opportunities to investigate various features of QCD, due to the presence of largely different scales. Having masses much larger than the typical hadronic scale Λ_{QCD} at least part of their description can be done in perturbation theory due to asymptotic freedom, while the other scales like the inverse quarkonium radius, relative momentum or the kinetic energy may or may not lie in the non-perturbative regime.

Among the first approaches to describe quarkonia were potential models in a non-relativistic Schrödinger formulation, where the basic ingredients, the potentials, were at first introduced phenomenologically and fit to experiments, but can also be obtained in various other ways. One of those is the Wilson loop approach, which will be presented in the first part of this thesis.

A more systematic treatment was found in the description of the lower energy scale dynamics through effective field theories. Two years after the formulation of a non-relativistic effective theory for QED (NRQED in [1]) the QCD analogue NRQCD was developed (see [2]), in which the mass scale m is integrated out and quarks and antiquarks are described separately through Pauli spinors. Since in this theory the energy and momentum scales are still not well separated, one can go on and integrate out all scales except for the kinetic energy. The relevant degrees of freedom are now the quark-antiquark pair in a colour singlet or a colour octet configuration plus low energy gluons and light quarks, or in the non-perturbative case only the singlet field and other light colour neutral objects like pions. The potentials enter as Wilson coefficients in the matching to NRQCD, which is why this theory has been called potential non-relativistic QCD (pNRQCD in [3], [4]).

With the original paper [5] by Matsui and Satz another application for heavy quarkonia has opened up. It has long been hypothesized that quarks and gluons at sufficiently high temperatures may undergo a phase transition into a deconfined state, the quark-gluon plasma, which is supported by recent lattice simulations as well as experimental data from heavy ion collisions. In their article they argue that heavy quarkonia pose an excellent probe for the properties of this plasma, since once the colour screening radius r_D gets smaller than the quarkonium binding radius, their formation should no longer be possible, thus providing a relation between the suppression rate of certain quarkonium states and the plasma temperature. The real situation has turned out to be more complicated, with quarkonium suppression also arising from cold-nuclear-matter effects and the possibility of secondary quarkonium production through recombination effects in heavy ion collisions, while the the results obtained from effective theories show, that the suppression is not purely related to screening effects. This necessitates a very careful treatment.

A very nice overview over all these topics with further literature, from which also this short summary was derived, can be found in references [6] and [7], shedding light on the historic development as well as the present status and future prospects of heavy quarkonia.

While perturbative approaches are usually limited to the weak coupling regime, lattice QCD computations have no such restrictions. Therefore several operators involving heavy or static quarks in a hot medium have been proposed and investigated both on the lattice and analytically, among them the Polyakov loop correlator, the singlet free energy in Coulomb gauge and the cyclic Wilson loop (compare references [8], [9], [10]). The latter is closely related to the Wilson loop in the vacuum, which we have already referred to as a quantity from which the static quark-antiquark potential can be derived. However, both suffer from divergences when calculated perturbatively even after charge renormalization, and while these have been well understood as cusp divergences in the vacuum case, there exists no such treatment for the cyclic Wilson loop yet. This will be the aim of this thesis.

The thesis is organized as follows. In the first part we will consider the Wilson loop in the vacuum. After a section introducing the Wilson loop and investigating some of its properties, a full calculation will be given at tree level and the renormalization of the cusp divergences will be discussed. This is followed by a calculation of the static quark-antiquark potential at $\mathcal{O}(\alpha_s^2)$. In the second part we turn to the cyclic Wilson loop in thermal QCD. We calculate it at $\mathcal{O}(\alpha_s^2)$ and consequently deal with its renormalization. The last section contains a summary and our conclusions. The appendices then present a lot of the details of our calculations, which were mostly omitted from the main text, and some in-depth discussions.

Part I

The Wilson Loop in the Vacuum

1 The Static Quark Potential

1.1 Colour Singlet States and Wilson Lines

Building on the original paper [11] by K. G. Wilson the connection between the static quark-antiquark potential and the Wilson loop has been shown in reference [12] and can also be found for example in references [13] and [14], which we will follow here. Let us start by defining colour neutral quark-antiquark states, because for a state to be observable it needs to be a colour singlet. Simply combining two quark field operators ψ is not enough, because quark and antiquark are in general not positioned at the same point in space. Thus under a local gauge transformation $\mathcal{V} \in SU(N_c)$ in the fundamental representation (on details of the gauge group see appendix A): $\overline{\psi}(x)\psi(y) \xrightarrow{\mathcal{V}} \overline{\psi}(x)\mathcal{V}^\dagger(x)\mathcal{V}(y)\psi(y)$, which is generally not the same. But if we introduce an operator $U(x,y)$ which compensates this transformation behaviour, we can get an invariant state:

$$|\phi_{\alpha\beta}\rangle = \hat{\phi}_{\alpha\beta}(x,y)|0\rangle = \frac{1}{\sqrt{N_c}}\overline{\psi}^{\,i}_{\alpha}(x)U^{ij}(x,y)\psi^{\,j}_{\beta}(y)\,|0\rangle\,, \tag{1.1}$$

where α and β are spinor indices, i and j colour indices, and $x_0 = y_0 = t$. The operator U is given by

$$U(x,y) = \mathcal{P}\exp\left[ig\int_{C(x,y)} \mathrm{d}z^\mu A_\mu(z)\right], \tag{1.2}$$

and we will show its behaviour under a transformation in colour space shortly. $\mathcal{P}$ denotes path ordering along the path C from y to x. This operator U is called a Wilson line. For the states $|\phi_{\alpha\beta}\rangle$ we will always take C to be a straight line, but the following properties of Wilson lines are true for a general path C.

Path ordering means that we have to expand the exponential and order the (generally not commuting) operators along the path C. So let $x^\mu(s)$, $s \in [0,1]$ be a parametrization of C, then for instance $\mathcal{P}\{O(s_3)O(s_1)O(s_4)O(s_2)\} = O(s_1)O(s_2)O(s_3)O(s_4)$ if $s_1 > s_2 > s_3 > s_4$. Let us demonstrate how this works for the Wilson line by examining the second order term in the expansion of the exponential.

$$\begin{aligned}
\frac{1}{2}\mathcal{P}\left(ig\int_C \mathrm{d}x^\mu A_\mu(x)\right)^2 &= -\frac{g^2}{2}\int_C \mathrm{d}x_1^\mu \int_C \mathrm{d}x_2^\nu \mathcal{P}A_\mu(x_1)A_\nu(x_2) \\
&= -\frac{g^2}{2}\int_0^1 \mathrm{d}s_1 \frac{\mathrm{d}x^\mu(s_1)}{\mathrm{d}s_1}\int_0^1 \mathrm{d}s_2 \frac{\mathrm{d}x^\nu(s_2)}{\mathrm{d}s_2}\mathcal{P}A_\mu(x(s_1))A_\nu(x(s_2)) \\
&= -\frac{g^2}{2}\int_0^1 \mathrm{d}s_1 \frac{\mathrm{d}x^\mu(s_1)}{\mathrm{d}s_1}\int_0^{s_1} \mathrm{d}s_2 \frac{\mathrm{d}x^\nu(s_2)}{\mathrm{d}s_2}A_\mu(x(s_1))A_\nu(x(s_2)) \\
&\quad -\frac{g^2}{2}\int_0^1 \mathrm{d}s_1 \frac{\mathrm{d}x^\mu(s_1)}{\mathrm{d}s_1}\int_{s_1}^1 \mathrm{d}s_2 \frac{\mathrm{d}x^\nu(s_2)}{\mathrm{d}s_2}A_\nu(x(s_2))A_\mu(x(s_1)) \\
&= -\frac{g^2}{2}\int_0^1 \mathrm{d}s_1 \frac{\mathrm{d}x^\mu(s_1)}{\mathrm{d}s_1}\int_0^{s_1} \mathrm{d}s_2 \frac{\mathrm{d}x^\nu(s_2)}{\mathrm{d}s_2}A_\mu(x(s_1))A_\nu(x(s_2)) \\
&\quad -\frac{g^2}{2}\int_0^1 \mathrm{d}s_2 \frac{\mathrm{d}x^\nu(s_2)}{\mathrm{d}s_2}\int_0^{s_2} \mathrm{d}s_1 \frac{\mathrm{d}x^\mu(s_1)}{\mathrm{d}s_1}A_\nu(x(s_2))A_\mu(x(s_1)) \\
&= -g^2\int_0^1 \mathrm{d}s_1 \frac{\mathrm{d}x^\mu(s_1)}{\mathrm{d}s_1}\int_0^{s_1} \mathrm{d}s_2 \frac{\mathrm{d}x^\nu(s_2)}{\mathrm{d}s_2}A_\mu(x(s_1))A_\nu(x(s_2))\,.
\end{aligned} \tag{1.3}$$

This procedure can be easily generalized to all orders, each of the $n!$ orderings of the operators $A_\mu(x_i)$ gives the same contribution after a redefinition of the integration variables, thus cancelling the factor $\frac{1}{n!}$

from the expansion of the exponential. So the Wilson line can be expressed as

$$U(C) = \sum_{n=0}^{\infty} (ig)^n \int_0^1 \mathrm{d}s_1 \frac{\mathrm{d}x^\mu(s_1)}{\mathrm{d}s_1} \int_0^{s_1} \mathrm{d}s_2 \frac{\mathrm{d}x^\nu(s_2)}{\mathrm{d}s_2} \dots \int_0^{s_{n-1}} \mathrm{d}s_n \frac{\mathrm{d}x^\rho(s_n)}{\mathrm{d}s_n} A_\mu(x(s_1)) A_\nu(x(s_2)) \dots A_\rho(x(s_n)) \,. \tag{1.4}$$

This expression of the Wilson line is the most convenient one for perturbative calculations, since it is an expansion in powers of g and path ordering has been taken care of. First, however, we want to study the behaviour of a Wilson line under a gauge transformation. For this let us have a look at a different method to achieve path ordering by discretizing the integration along C. We can split up the path C into n infinitesimal pieces ε_i with $n+1$ endpoints x_i, $\varepsilon_i = x_i - x_{i-1}$. With this we can write

$$\begin{aligned} U(C) =& \mathcal{P} \exp\left[ig \int_C \mathrm{d}x^\mu A_\mu(x)\right] = \lim_{n\to\infty} \mathcal{P} \exp\left[ig \sum_{i=1}^{n} A_\mu(x_i)\varepsilon_i^\mu\right] \\ &= \lim_{n\to\infty} \exp\left[igA_\mu(x_n)\varepsilon_n^\mu\right] \exp\left[igA_\nu(x_{n-1})\varepsilon_{n-1}^\nu\right] \cdots \exp\left[igA_\rho(x_1)\varepsilon_1^\rho\right] \\ &= \lim_{n\to\infty} \left(1 + igA_\mu(x_n)\varepsilon_n^\mu\right)\left(1 + igA_\nu(x_{n-1})\varepsilon_{n-1}^\nu\right) \cdots \left(1 + igA_\rho(x_1)\varepsilon_1^\rho\right) + \mathcal{O}(\varepsilon_i^2) \,. \end{aligned} \tag{1.5}$$

Let us note that the effect of the path ordering operator is seen in the second line. This is an exact equality, all the commutators that would usually turn up when writing $\exp[A+B] = \exp[A]\exp[B] + \dots$ vanish because of path ordering. The $\mathcal{O}(\varepsilon_i^2)$ terms in the last line vanish in the limit. Both expressions for $U(C)$ are equivalent. This can be seen by expanding the product in (1.5):

$$\begin{aligned} U(C) &= \lim_{n\to\infty} \left(1 + igA_\mu(x_n)\varepsilon_n^\mu\right)\left(1 + igA_\nu(x_{n-1})\varepsilon_{n-1}^\nu\right) \cdots \left(1 + igA_\rho(x_1)\varepsilon_1^\rho\right) \\ &= \lim_{n\to\infty} \left\{ 1 + ig \sum_{i=1}^{n} A_\mu(x_i)\varepsilon_i^\mu + (ig)^2 \sum_{i=1}^{n} \sum_{j=1}^{i} A_\mu(x_i)\varepsilon_i^\mu A_\nu(x_j)\varepsilon_j^\nu + \dots \right\} . \end{aligned} \tag{1.6}$$

In the limit we can replace the sums by integrals and get back the expression (1.4).

Now, using the transformation properties of the gauge field (for $D_\mu = \partial_\mu - igA_\mu$)

$$A_\mu(x) \xrightarrow{\mathcal{V}\in \mathrm{SU(N)}} \mathcal{V}(x) A_\mu(x) \mathcal{V}^\dagger(x) + \frac{i}{g} \mathcal{V}(x) \partial_\mu \mathcal{V}^\dagger(x) \,, \tag{1.7}$$

let us first look at the behaviour of a single factor in (1.5).

$$\begin{aligned} 1 + igA_\mu(x_i)\varepsilon_i^\mu \xrightarrow{\mathcal{V}\in \mathrm{SU(N)}} & 1 + ig\mathcal{V}(x_i)A_\mu(x_i)\mathcal{V}^\dagger(x_i)\varepsilon_i^\mu - \mathcal{V}(x_i)\partial_\mu \mathcal{V}^\dagger(x_i)\varepsilon_i^\mu \\ =& 1 + ig\mathcal{V}(x_i)A_\mu(x_i)\mathcal{V}^\dagger(x_i - \varepsilon_i)\varepsilon_i^\mu - \mathcal{V}(x_i)\left(\mathcal{V}^\dagger(x_i) - \mathcal{V}^\dagger(x_i - \varepsilon_i)\right) + \mathcal{O}(\varepsilon_i^2) \\ =& \mathcal{V}(x_i)\left(1 + igA_\mu(x_i)\varepsilon_i^\mu\right)\mathcal{V}^\dagger(x_{i-1}) + \mathcal{O}(\varepsilon_i^2) \,. \end{aligned} \tag{1.8}$$

With this we can show the transformation properties of the Wilson line.

$$\begin{aligned} U(C) =& \lim_{n\to\infty} \left(1 + igA_\mu(x_n)\varepsilon_n^\mu\right)\left(1 + igA_\nu(x_{n-1})\varepsilon_{n-1}^\nu\right) \cdots \left(1 + igA_\rho(x_1)\varepsilon_1^\rho\right) \\ \xrightarrow{\mathcal{V}\in \mathrm{SU(N)}} & \lim_{n\to\infty} \mathcal{V}(x_n)\left(1 + igA_\mu(x_n)\varepsilon_n^\mu\right)\mathcal{V}^\dagger(x_{n-1})\mathcal{V}(x_{n-1})\left(1 + igA_\nu(x_{n-1})\varepsilon_{n-1}^\nu\right)\mathcal{V}^\dagger(x_{n-2})\mathcal{V}(x_{n-2}) \cdots \\ & \cdots \mathcal{V}^\dagger(x_1)\mathcal{V}(x_1)\left(1 + igA_\rho(x_1)\varepsilon_1^\rho\right)\mathcal{V}^\dagger(x_0) \\ =& \lim_{n\to\infty} \mathcal{V}(x_n)\left(1 + igA_\mu(x_n)\varepsilon_n^\mu\right)\left(1 + igA_\nu(x_{n-1})\varepsilon_{n-1}^\nu\right) \cdots \left(1 + igA_\rho(x_1)\varepsilon_1^\rho\right)\mathcal{V}^\dagger(x_0) \\ & \Rightarrow U(x,y,C) = \mathcal{P} \exp\left[ig \int_y^x \mathrm{d}z^\mu A_\mu(z)\right] \xrightarrow{\mathcal{V}\in \mathrm{SU(N)}} \mathcal{V}(x) U(x,y,C) \mathcal{V}^\dagger(y) \,. \end{aligned} \tag{1.9}$$

Thus the states $|\phi\rangle$ indeed transform as singlets, because

$$\overline{\psi}(x) U(x,y) \psi(y) \xrightarrow{\mathcal{V}\in \mathrm{SU(N)}} \overline{\psi}(x)\mathcal{V}^\dagger(x)\mathcal{V}(x)U(x,y)\mathcal{V}^\dagger(y)\mathcal{V}(y)\psi(y) = \overline{\psi}(x)U(x,y)\psi(y) \,. \tag{1.10}$$

The transition amplitude of these states after time t is given by

$$\begin{aligned} G_{\alpha_1\alpha_2\beta_1\beta_2}(t,\mathbf{x}_1,\mathbf{x}_2,\mathbf{y}_1,\mathbf{y}_2) &= \langle \phi_{\alpha_1\alpha_2}(t,\mathbf{x}_1,\mathbf{x}_2)|\phi_{\beta_1\beta_2}(0,\mathbf{y}_1,\mathbf{y}_2)\rangle \\ &= \frac{1}{N_c}\langle 0|\,\overline{\psi}^i_{\alpha_2}(x_2)U^{ij}(x_2,x_1)\psi^j_{\alpha_1}(x_1)\overline{\psi}^k_{\beta_1}(y_1)U^{kl}(y_1,y_2)\psi^l_{\beta_2}(y_2)\,|0\rangle\ . \end{aligned} \tag{1.11}$$

This can be further transformed as follows. We will take the static limit, which means that we let the heavy quarks propagate only in time by dropping the spatial parts of the covariant derivative in the Lagrangian, and integrate out the heavy quark degrees of freedom. Doing this we can replace the heavy quark fields by static propagators in the presence of an external gluon field and the path integration is now taken only over gauge fields and light quarks. The remnants of the heavy quark field integrations is a functional determinant, which in a diagrammatic expansion consists of closed heavy fermion loops with any number of gluon fields attached. In the infinite mass limit this determinant approaches a constant, which can be taken up in the normalization of the path integral. This is called the quenched approximation. The details of this derivation can be found in appendix B, here we will just give the result.

$$\begin{aligned} G_{\alpha_1\alpha_2\beta_1\beta_2}(t,\mathbf{r}) = &-\delta^3(\mathbf{x}_1-\mathbf{y}_1)\delta^3(\mathbf{x}_2-\mathbf{y}_2)(P_+)_{\alpha_1\beta_1}(P_-)_{\beta_2\alpha_2}e^{-i(m_1+m_2)t} \\ &\frac{1}{N_c}\mathrm{Tr}\left\langle \mathcal{P}\exp\left[ig\oint_\Gamma dx^\mu A_\mu(x)\right]\right\rangle, \end{aligned} \tag{1.12}$$

where Γ represents a rectangular path running in the clockwise direction with sides of the respective time-like and space-like distances t and $\mathbf{r}=\mathbf{x}_1-\mathbf{x}_2=\mathbf{y}_1-\mathbf{y}_2$, the trace acts on the colour space, and the average is taken over the gauge fields A and the light quark degrees of freedom.

In the following we will for convenience define

$$\frac{1}{N_c}\mathrm{Tr}[\mathcal{M}] = \widetilde{\mathrm{Tr}}[\mathcal{M}]\,. \tag{1.13}$$

From this the static quark potential can be obtained via

$$\begin{aligned} G = \langle\phi(t)|\phi(0)\rangle &= \left\langle\phi(0)|e^{-i\mathcal{H}t}|\phi(0)\right\rangle \\ &= \sum_n \langle\phi(0)|\psi_n\rangle\,\langle\psi_n|\phi(0)\rangle\,e^{-iE_nt}, \end{aligned} \tag{1.14}$$

where we have introduced a complete set of energy eigenstates of the static Hamiltonian. This Hamiltonian can be obtained through quantization of the corresponding Lagrangian

$$\mathcal{L}^{(0)} = \psi^\dagger iD_0\psi + \chi^\dagger iD_0\chi - \frac{1}{4}F^{\mu\nu}_aF^a_{\mu\nu} + \mathcal{L}_q\,, \tag{1.15}$$

where $\mathcal{L}_q$ stands for the light quark degrees of freedom. This is the Lagrangian of NRQCD, which was introduced in reference [15] after the development of NRQED in reference [1], with only the terms of $\mathcal{O}(m^0)$ included, corresponding to the infinite mass limit, which is in agreement with the approximations made in the above derivation of the Wilson loop. ψ and χ are Pauli spinor fields, where ψ annihilates a heavy quark and χ creates a heavy antiquark. The next order correction would be $\mathcal{L}^{(1)} = \psi^\dagger\frac{1}{2m}\mathbf{D}^2\psi - \chi^\dagger\frac{1}{2m}\mathbf{D}^2\chi$ (see for example reference [6]).

Since the lowest energy eigenvalue gives the quark-antiquark static energy,

$$\Rightarrow\ V(\mathbf{r}) = E_0 = \lim_{t\to(1-i\epsilon)\infty}\frac{\ln G}{-it}, \tag{1.16}$$

under the assumption of a non-vanishing overlap with the ground state $\langle\phi(0)|\psi_0\rangle\,\langle\psi_0|\phi(0)\rangle$.

So for our purposes the relevant part of G is $\frac{1}{N_c}\mathrm{Tr}\left\langle\mathcal{P}\exp\left[ig\int_\Gamma dx^\mu A_\mu(x)\right]\right\rangle$, since the other terms drop out in the limit, or give the rest mass term (m_1+m_2). This quantity is what we will call the Wilson loop for short, or more exactly the vacuum expectation value or vacuum average of the Wilson loop.

To avoid confusion, let us note that we are working in the Heisenberg picture. However, the states $|\phi\rangle$ do have a time dependence due to the fact that they are defined via time dependent operators. As a consequence they transform with the opposite sign in the exponential compared to the Schrödinger picture:

$$|\phi(t)\rangle = \hat{\phi}(t)|0\rangle = e^{i\mathcal{H}t}\hat{\phi}(0)e^{-i\mathcal{H}t}|0\rangle = e^{i\mathcal{H}t}|\phi(0)\rangle\,. \tag{1.17}$$

We can also represent the Wilson loop as the product of four Wilson lines:

$$\langle W\rangle = \widetilde{\mathrm{Tr}}\left\langle U_0\left(\frac{\mathbf{r}}{2},-\frac{\mathbf{r}}{2}\right)U_{-\frac{\mathbf{r}}{2}}(0,t)\,U_t\left(-\frac{\mathbf{r}}{2},\frac{\mathbf{r}}{2}\right)U_{\frac{\mathbf{r}}{2}}(t,0)\right\rangle\,. \tag{1.18}$$

The superscripts of those straight Wilson lines denote the time or space components which are kept constant, so that we only have to show the relevant components for the start and endpoint in the argument of the Wilson line operators. We will call the contours of U_0 and U_t the strings, and the contours of $U_{\pm\frac{\mathbf{r}}{2}}$ the quark lines or, if we want to distinguish them, quark and antiquark line for the upper and lower line, respectively. An illustration of the Wilson loop can be found in the following section, where the tree level expansion diagrams are shown in figure 2.1.

1.2 The Perturbative Series for the Wilson Loop

Now, in perturbation theory the Wilson loop average can be represented as a series of diagrams γ_n multiplied by a factor $(ig)^n$. These γ_n consist of all diagrams contributing to the n-point functions $\langle A_\mu(x_1)\cdots A_\rho(x_n)\rangle$ with the n endpoints x_i ordered along the path Γ. Note that n is not an index labelling the different diagrams, but just denotes the number of endpoints a diagram has on the contour.

After calculating these contributions to the n-point functions we have to take the trace over the colour matrices and integrate over the endpoints x_i along the contour Γ as specified in equation (1.4). We can take this into account by introducing a line vertex at every point x_i on the contour. The corresponding Feynman rule for this line vertex is

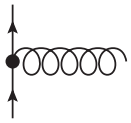

$$= ig\int \mathrm{d}x_i^\mu\,, \tag{1.19}$$

where the limits of the contour integration are given by path ordering. The colour factors will be considered separately.

According to references [16], [17], [18], the expectation value of the path ordered exponential can be re-expressed as an exponential of the sum over two-particle-irreducible (2PI) diagrams with their colour factors replaced by certain coefficients, which are called the "maximally non-Abelian" ([17]) or "colour-connected" ([18]) part of the corresponding colour factor.

$$\begin{aligned}\widetilde{\mathrm{Tr}}\left\langle \mathcal{P}\exp\left[ig\oint_\Gamma dx^\mu A_\mu(x)\right]\right\rangle &= \sum_{n=0}^{\infty}(ig)^n\sum_{\gamma_n}C(\gamma_n)W(\gamma_n)\\ &= \exp\left[\sum_{n=2}^{\infty}(ig)^n\sum_{\gamma_n\in\{\mathrm{2PI}\}}\tilde{C}(\gamma_n)W(\gamma_n)\right]\,.\end{aligned} \tag{1.20}$$

Here $W(\gamma_n)$ denotes the value of a diagram γ_n without its colour factor, $C(\gamma_n)$ the colour factor and $\tilde{C}(\gamma_n)$ the colour-connected coefficient of that diagram.

So for the static quark potential this means that we just have to sum over all 2PI diagrams, provided we know their colour connected coefficients, which greatly reduces the number of diagrams to be considered.

$$V(\mathbf{r}) = \lim_{t\to(1-i\epsilon)\infty}\frac{1}{-it}\sum_{n=2}^{\infty}(ig)^n\sum_{\gamma\in\{\mathrm{2PI}\}}\tilde{C}(\gamma_n)W(\gamma_n)\,. \tag{1.21}$$

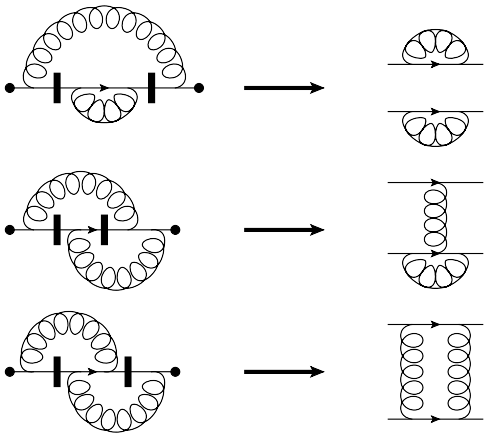

Figure 1.1: An example of a two-particle reducible and an irreducible diagram.

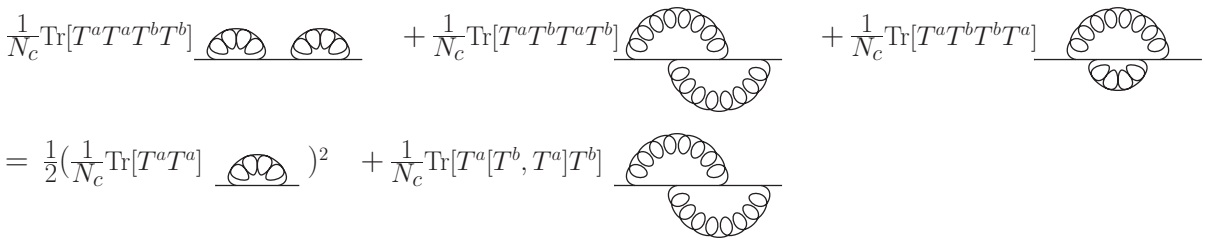

Figure 1.2: Diagrams contributing to $\mathcal{O}(g^4)$ without internal vertices.

Two-particle irreducible in this context means that the contour Γ of a diagram cannot be divided into two separate parts, which are not connected by any gluon line (or other internal lines like ghost and light fermion propagators), by cutting it in two places. In figure 1.1 two examples are given, where for simplicity the path Γ is represented as a straight line whose endpoints are to be identified (the details of the contour are not important here). If we cut the first diagram as shown, the two pieces are disconnected. The second diagram however can not be separated no matter which way we cut it (all possible ways of cutting Γ are equivalent to one of the two ways shown). So this second diagram is two-particle irreducible, while the first is reducible.

To illustrate how the coefficients $\tilde{C}(\gamma_n)$ arise, let us have a look at figure 1.2. It shows the three unconnected tree level diagrams of $\mathcal{O}(g^4)$. By unconnected we mean diagrams whose endpoints x_i are not all connected to each other via gluons or other lines. It is not to be confused with two-particle reducible, although connected diagrams are of course always irreducible. The diagram in the middle is two-particle irreducible, while the other two are reducible (compare figure 1.1).

If we neglect the colour factors for a moment it can be easily shown by a rearrangement of the integration variables that the sum over the three γ_4 diagrams in the first line factors into the square of the γ_2 diagram of $\mathcal{O}(g^0)$ and we have to include a combinatoric factor $\frac{1}{2}$. But since we have a non-Abelian theory, the 2PI diagram in the middle has a different colour factor compared to that of the other two diagrams. But still we can split that colour factor into its "Abelian" part and a rest: $T^aT^bT^aT^b = T^aT^aT^bT^b + T^a[T^b,T^a]T^b$. Then we can sum up the three terms with the coefficient $T^aT^aT^bT^b$, using the fact that T^aT^a is proportional to the unit matrix, and keep the middle diagram with the coefficient $T^a[T^b,T^a]T^b$. This leads to the second line in figure 1.2. The first term contributes to the second order of the series expansion of the exponential (1.20), while the second term belongs to the first order of that expansion. It is the only 2PI γ_4-diagram of $\mathcal{O}(g^0)$ and its colour factor $\widetilde{\mathrm{Tr}}[T^aT^bT^aT^b]$ has been replaced by its colour connected part $\widetilde{\mathrm{Tr}}[T^a[T^b,T^a]T^b]$.

The general case is explained in detail in appendix C.

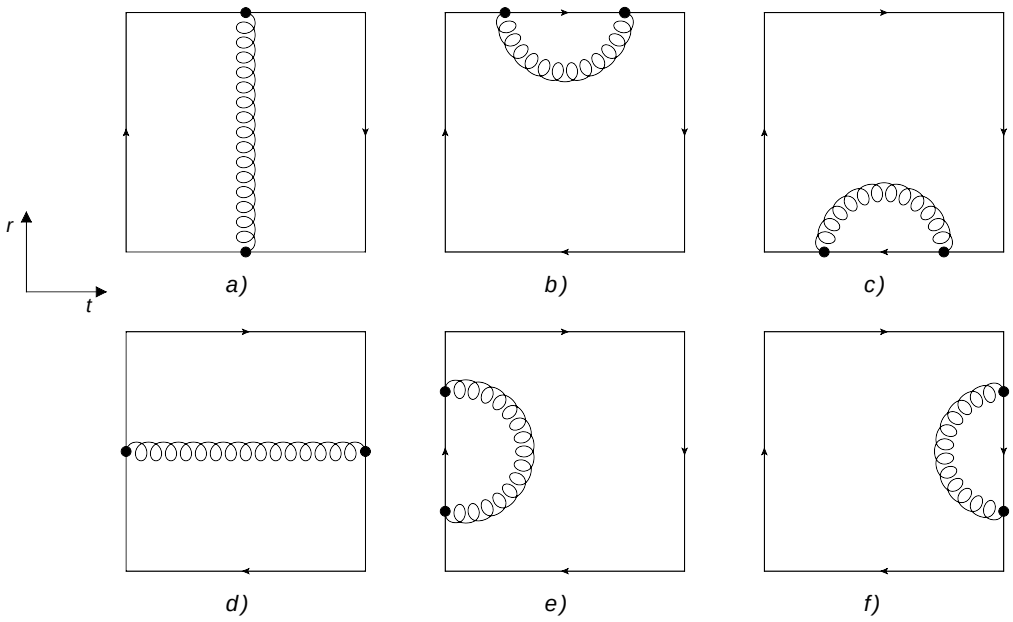

Figure 2.1: Tree level one-gluon diagrams.

2 Calculation of the Static Quark Potential

2.1 Tree Level Calculations

To lowest order in perturbation theory we have to compute the following contour integral (compare equation 1.4):

$$-\frac{g^2}{2}\oint_\Gamma dx_1^\mu \oint_\Gamma dx_2^\nu \,\widetilde{\mathrm{Tr}}\,\langle \mathcal{P} A_\mu(x_1) A_\nu(x_2)\rangle = -g^2 C_F \int_0^1 \mathrm{d}s_1 \int_0^{s_1} \mathrm{d}s_2 \frac{\mathrm{d}x^\mu}{\mathrm{d}s_1}\frac{\mathrm{d}x^\nu}{\mathrm{d}s_2} D_{\mu\nu}(x(s_1)-x(s_2))\,. \quad (2.1)$$

The six diagrams contributing to this are shown in figure 2.1 (for gauges in which the propagator is diagonal in time and space components, $D_{0i}=0$).

In the gauges we will consider, which are Feynman and Coulomb gauge, only diagrams a) and d) are not divergent and only a) will give a contribution to the potential. The reason for choosing these particular gauges is, that Feynman gauge is quite commonly used, which is helpful for comparisons to literature, while Coulomb gauge is especially apt for the Wilson loop, because it separates time- and spacelike components in a way that makes it easy to determine whether a diagram contributes to the potential or not, a feature we will make use of when calculating one-loop contributions. The divergences are treated using dimensional regularization in $D = 4-2\varepsilon$ dimensions. The explicit calculations can be found in appendix D. In the course of the calculations we have to slightly rotate t in the complex plane, so that in the following result t is assumed to have a small negative imaginary part. We get

$$\begin{aligned} &-g^2\mu^{-2\varepsilon}C_F\left\{-\frac{1}{2\pi^2\varepsilon}-\frac{1}{2\pi^2}\Big[2+\gamma_E+\ln\pi+\ln itr\mu^2\Big]-\right.\\ &\left.-\frac{1}{2\pi^2}\left[\frac{it}{r}\arctan\frac{it}{r}+\frac{r}{it}\arctan\frac{r}{it}\right]+\frac{1}{4\pi^2}\left[\ln\left(1+\frac{(it)^2}{r^2}\right)+\ln\left(1+\frac{r^2}{(it)^2}\right)\right]\right\}. \end{aligned} \quad (2.2)$$

In this expression it is easy to go to Euclidean space by substituting $it=\tau$, so that we can compare it to the QED calculation of the Wilson loop found in reference [19]. We see that the second line in equation (2.2) is identical to their result apart from the colour factor C_F. This second line gives the contributions from diagrams a) and d) in Feynman gauge for both calculations. However, they used a different regularization for the divergent integrals b), c), e), f), so we cannot make a meaningful comparison for the terms in the first line.

If we want to get the result for real time, we have to substitute $t \to t - i\varepsilon$ and take the limit $\varepsilon \to 0$, which gives

$$-g^2\mu^{-2\varepsilon}C_F\left\{-\frac{1}{2\pi^2\varepsilon}-\frac{1}{2\pi^2}\left[2+\gamma_E+\ln\pi\right]-\frac{i}{4\pi}\left(2-\frac{r}{t}\right)\Theta(r-t)-\right.$$
$$\left.-\frac{it}{4\pi r}\Theta(t-r)+\frac{1}{4\pi^2}\left(\frac{t}{r}+\frac{r}{t}\right)\ln\frac{t+r}{|t-r|}+\frac{1}{2\pi^2}\ln\frac{|t^2-r^2|}{t^2r^2\mu^2}\right\}. \tag{2.3}$$

If we neglect the divergence for a moment and take the limit $t \to \infty$, we get

$$V_{\text{tree}}(\mathbf{r}) = -C_F\frac{\alpha_s}{r}. \tag{2.4}$$

This is the classical Coulomb potential, modified by a gauge group dependent factor C_F.

Turning now to the divergence, it has been shown in reference [16] that all the divergences turning up for a loop with a smooth contour can be dealt with through a renormalization of the coupling constant and in some renormalization schemes also a "loop mass" renormalization. The divergences related to the latter case can be factored out and exponentiated, and the exponent is linearly divergent and proportional to the length $L(\Gamma)$ of the contour. If we multiply the Wilson loop by a factor $\exp[-mL(\Gamma)]$, these divergences can be taken up into the renormalization of the parameter m. In dimensional regularization these divergences are automatically put to zero, so we do not have to worry about this.

There may however be additional cusp divergences for loops with angles or intersections. These can be cancelled by multiplicative renormalization constants $Z(\gamma_i)$ to the Wilson loop, which only depend on the cusp angles γ_i ([20], [21]). Since these renormalization constants only depend on the cusp angles, they may be calculated using any convenient loop.

Following the calculation in reference [21] the tree level contribution to the simple case of a loop consisting of two straight lines, which have an angle γ and are connected at infinity, is given by

$$g^2\mu^{-2\varepsilon}C_F\left(\gamma\coth\gamma-1\right)\left[-\frac{1}{8\pi^2\varepsilon}-\frac{1}{8\pi^2}\left(\gamma_E+\ln\frac{\mu^2}{\Lambda^2}+\ln\pi\right)\right]. \tag{2.5}$$

In Minkowski space the angle γ between two vectors p^μ and q^μ, which are here used to give the directions of the two lines the loop consists of, is defined by $\cosh\gamma = \frac{p\cdot q}{\sqrt{p^2q^2}}$, while Λ is a cutoff parameter used to regulate the infrared divergence in the considered loop due to its infinite length.

Taking $\gamma = i\frac{\pi}{2}$, the corresponding renormalization constant at $\mathcal{O}(\alpha_s^1)$ in the $\overline{\text{MS}}$-scheme is

$$Z\left(i\frac{\pi}{2}\right) = \exp\left[-\frac{\alpha_s C_F}{2\pi\bar{\varepsilon}}\right]. \tag{2.6}$$

Not only the Wilson loop, but all closed loops can be expressed as an exponential of the sum over 2PI diagrams. Therefore also the $\mathcal{O}(\alpha_s)$ cusp divergence exponentiates and is removed by a renormalization constant in the form of an exponential. Since the Wilson loop has four angles, it has to be renormalized by

$$\left[Z\left(i\frac{\pi}{2}\right)\right]^4 = \exp\left[-\frac{2\alpha_s C_F}{\pi\bar{\varepsilon}}\right]. \tag{2.7}$$

If we look at equation (2.2) (which only shows the logarithm of the Wilson loop), this is indeed the case. In addition, the cusp anomalous dimension, defined as the derivative of the Wilson loop with respect to $-\ln\mu$, also depends only on the cusp angle for any loop and again both results agree by a factor 4.

2.2 One-Loop Contribution

Some of the diagrams contributing to the next order in the perturbation series are shown in figure 2.2. Basically, we have self energy corrections to the tree level one-gluon diagrams (a), connected diagrams of order $\mathcal{O}(\alpha_s^2)$, involving one three-gluon vertex (d) and the unconnected 2PI diagrams of $\mathcal{O}(\alpha_s^2)$, involving

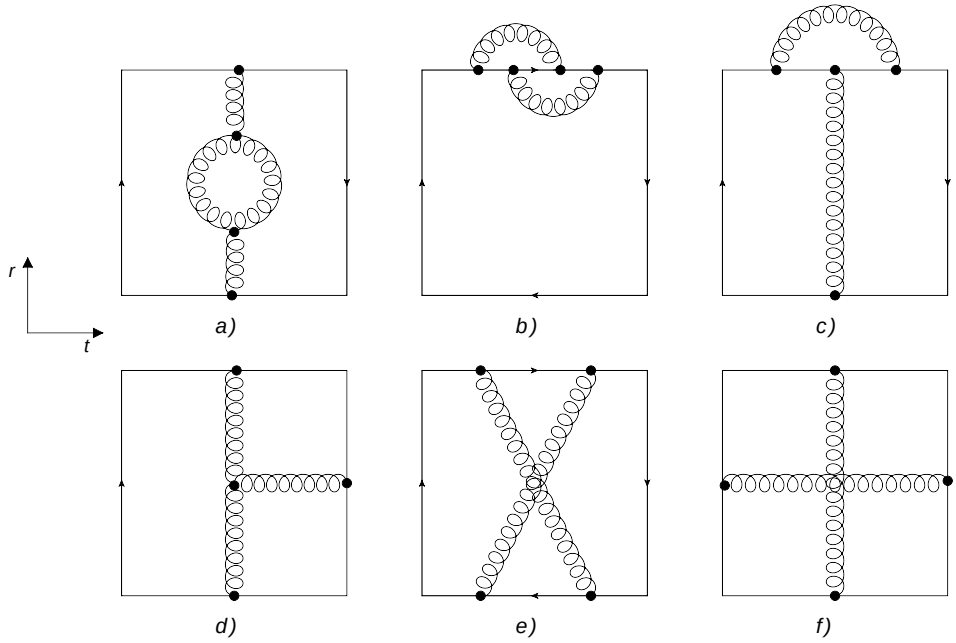

Figure 2.2: Typical diagrams contributing to $\mathcal{O}(g^4)$.

two gluons at tree level (b, c, e, f). Actually, b), c), e) and f) are of the same configuration, if we only consider constituents and path ordering, but it is useful for our calculations and further discussion to count them as separate diagrams. We already did so with the tree level diagrams, which also basically consist of just one free gluon propagator. The colour structures are the same, so b), c), e) and f) all have the same colour connected coefficient $\widetilde{\mathrm{Tr}}\{T^a[T^b,T^a]T^b\} = -\frac{1}{2}C_F C_A$, whose derivation has been shown in figure 1.2.

In Coulomb Gauge b) and c) include scaleless integrals, which vanish in dimensional regularization. Figure e) gives zero and d) and f) vanish when taking the limit $t \to \infty$. The same is true for all diagrams connecting to the vertical sides of the Wilson loop. So the only relevant diagrams left are a) and a similar one with the gluon loop replaced by a light fermion loop. The details of the calculations can be found in appendix D.3.

It simplifies the calculations a lot to take the limit $t \to \infty$ before performing the loop momentum integrations, because this basically turns $\int \mathrm{d}t \exp[-itk_0]$ into $\delta(k_0)$, so the quantity we really have to compute in a) is the vacuum polarization $\Pi_{00}(0,\mathbf{k})$. Therefore no expression for the Wilson loop expectation value will be given, but just its contribution to the static potential. The result is in agreement with references [22], [23] and reads:

$$V_{1\mathrm{loop}}^{\overline{\mathrm{MS}}}(r) = -\frac{\alpha_s^2}{4\pi r} C_F \left[\left(\frac{31}{9} C_A - \frac{20}{9} T_F n_f \right) + \left(\frac{11}{3} C_A - \frac{4}{3} T_F n_f \right) \left(\ln \mu^2 r^2 + 2\gamma_E \right) \right] \tag{2.8}$$

Since the ghost fields do not couple to the 00-component of the gluon propagator in Coulomb gauge, they need not be considered here. However, there are some ambiguities concerning ghosts in Coulomb gauge. For example one ghost loop coupling to the spatial parts of the gluon propagator leads to integrals of the type

$$\int \frac{\mathrm{d}k_0}{2\pi} \int \frac{\mathrm{d}^3 k}{(2\pi)^3} \frac{k^i (q^j - k^j)}{\mathbf{k}^2 (\mathbf{q}-\mathbf{k})^2}, \tag{2.9}$$

which is not regulated by dimensional regularization due to the divergent k_0 integration. These issues are treated for example in references [24], [25]. We will not delve further into this matter, since at no point will we have to explicitly calculate the self energy of spatial gluons in Coulomb gauge.

Part II

The Cyclic Wilson Loop

3 Wilson loops in thermal QCD

Having completed our discussion of the Wilson loop operator in the vacuum, we can turn to the in-medium case. In the imaginary time formalism, which is well suited for equilibrium systems, the biggest changes come through the introduction of periodic boundary conditions for bosons on the imaginary time axis, so $\phi(\beta + \tau, \mathbf{x}) = \phi(\tau, \mathbf{x})$, with $\beta = T^{-1}$. For fermions we get antiperiodic boundary conditions, $\psi(\beta + \tau, \mathbf{x}) = -\psi(\tau, \mathbf{x})$.

In momentum space this means that fields are no longer represented by a Fourier transform in the time variable, but by a Fourier series with discrete frequencies, called the Matsubara series and frequencies, respectively. When performing these sums, one always gets a vacuum part, which is equal to the corresponding expression in vacuum calculations after performing the k_0 integration, and a thermal part, which involves the Bose-Einstein distribution function $n_B(k)$ for bosons and the Fermi-Dirac distribution function $n_F(k)$ for fermions.

The difference, then, between a regular Wilson loop at an arbitrary imaginary time $\tau < \beta$ in the thermal medium and in the vacuum, apart from the transition to Euclidean spacetime, lies solely in the thermal parts. These do not introduce additional ultraviolet divergences, because they are exponentially suppressed at high momenta. But there may be additional infrared divergences, because the bosonic distribution functions introduce another pole at small momenta. These can be removed through a partial resummation of the perturbative series, which is best performed systematically through an effective field theory approach. However, our aim is to treat the ultraviolet divergences, and for those there is no difference to the vacuum case. Therefore, we will not discuss this scenario further.

In the previous section we took the limit $t \to \infty$ in order to obtain the static quark-antiquark potential from the Wilson loop. The corresponding procedure to get the proper thermal potential would be to rotate τ back to real time and then let it go to infinity, in other words $\tau \to i\infty$. But we could also pursue a different line of investigation and take the limit $\tau \to \beta$. In this case the Wilson loop spans the whole of the imaginary instead of the real time dimension. This quantity will be called the cyclic Wilson loop, because we go full circle on the imaginary time axis, and doing this has a lot of interesting consequences, as we will see. There are a lot of cancellations and some diagrams of $\mathcal{O}(\alpha_s^2)$ we could not calculate in the non-cyclic case turn out to be quite simple or at least manageable. Integrating all the way from 0 to β also mixes thermal and vacuum parts, and we will find that the ultraviolet divergences turn out to be very different from the non-cyclic case and cannot be removed in the same fashion.

The aforementioned infrared problems of thermal field theory make it necessary to assume a hierarchy of scales, because otherwise it is unclear which theory should be used for the contributions from different energy scales. The one which is most useful for our discussion is $\frac{1}{r} \gg T \gg m_D$. The last relation follows immediately from the weak coupling regime, since the thermal mass $m_D \sim gT$. With $\frac{1}{r}$ being the biggest scale in our system, the ultraviolet divergences must come from the contributions of this scale and we can use the unresummed thermal QCD Feynman rules to calculate them. Infrared divergences from higher scales must cancel against ultraviolet divergences from lower scales, calculated in the resummed theory. However, at $\mathcal{O}(\alpha_s^2)$ all infrared divergences in contributions from the scale $\frac{1}{r}$ cancel against each other, as it will turn out. This suggests that the contributions from the lower scales will enter at higher orders in the coupling constant, and in any case makes it unnecessary for the treatment of the ultraviolet divergences to consider the lower scales at all, so we will only concern ourselves with the contributions from the scale $\frac{1}{r}$.

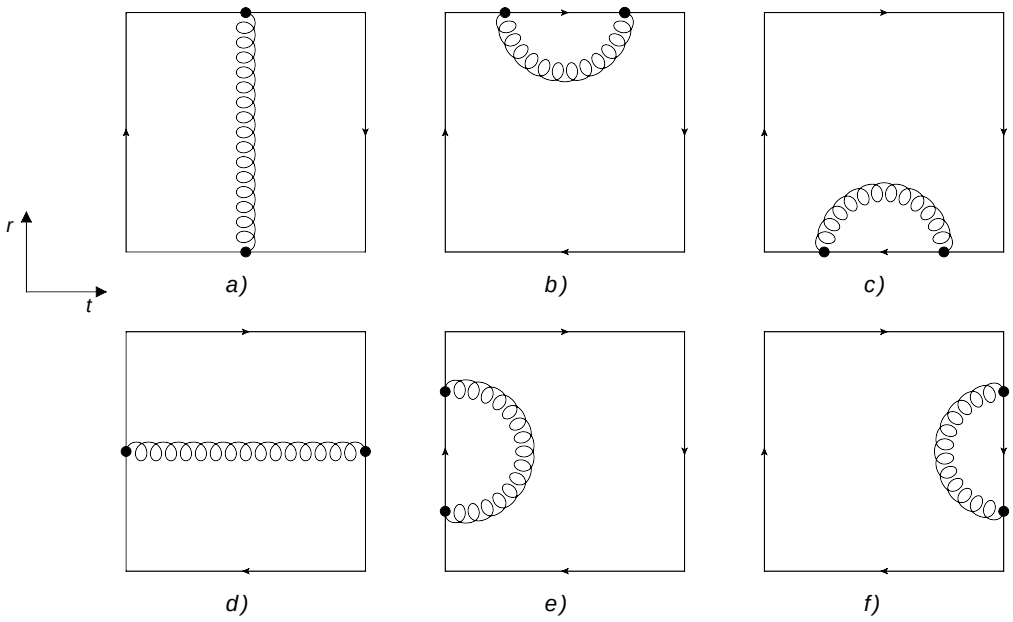

Figure 4.1: Tree level one-gluon diagrams.

4 Calculation of the Cyclic Wilson Loop to $\mathcal{O}(\alpha_s^2)$

4.1 Tree Level One-Gluon Diagrams

In figure 4.1 above, all the tree level diagrams contributing to the cyclic Wilson loop are shown, which are obviously the same as in the vacuum case. Using our previous calculations, they can be easily computed. We will be using Coulomb gauge throughout all of the cyclic Wilson loop calculations, because it quite simplifies things.

Diagram a)

$$\begin{aligned}-(ig)^2 C_F \int_0^\beta \mathrm{d}\tau_1 \int_0^\beta \mathrm{d}\tau_2 \sum\!\!\!\!\!\!\int_k \frac{e^{ik_0(\beta-\tau_1-\tau_2)-i\mathbf{r}\cdot\mathbf{k}}}{\mathbf{k}^2} &= g^2 C_F \sum\!\!\!\!\!\!\int_k \frac{\beta^2 \delta_{n_k,0}\, e^{-i\mathbf{r}\cdot\mathbf{k}}}{\mathbf{k}^2} \\ &= g^2 C_F \beta \int_k \frac{e^{-i\mathbf{r}\cdot\mathbf{k}}}{\mathbf{k}^2} \\ &= \frac{\alpha_s C_F}{rT} \end{aligned} \tag{4.1}$$

Diagrams b)+c)

$$\begin{aligned}(ig)^2 C_F \int_0^\beta \mathrm{d}\tau_1 \int_0^{\tau_1} \mathrm{d}\tau_2 \sum\!\!\!\!\!\!\int_k \frac{e^{ik_0(\tau_1-\tau_2)} + e^{-ik_0(\tau_1-\tau_2)}}{\mathbf{k}^2} &= -\, g^2 C_F \sum\!\!\!\!\!\!\int_k \frac{\beta^2 \delta_{n_k,0}}{\mathbf{k}^2} \\ &= -\, g^2 C_F \beta \int_k \frac{1}{\mathbf{k}^2} \\ &= 0 \end{aligned} \tag{4.2}$$

Diagram d)

$$\begin{aligned}&-(ig)^2 C_F \int_0^1 \mathrm{d}s_1 \int_0^1 \mathrm{d}s_2 \sum\!\!\!\!\!\!\int_k \frac{e^{-ik_0\beta + i\mathbf{r}\cdot\mathbf{k}(s_1+s_2-1)}}{k^2} \left(\mathbf{r}^2 - \frac{(\mathbf{r}\cdot\mathbf{k})^2}{\mathbf{k}^2}\right) \\ &= 2g^2 C_F \sum\!\!\!\!\!\!\int_k \frac{1-\cos(\mathbf{r}\cdot\mathbf{k})}{(\mathbf{r}\cdot\mathbf{k})^2 k^2} \left(\mathbf{r}^2 - \frac{(\mathbf{r}\cdot\mathbf{k})^2}{\mathbf{k}^2}\right) \end{aligned} \tag{4.3}$$

Diagrams e)+f)

$$
\begin{aligned}
&(ig)^2 C_F \int_0^1 \mathrm{d}s_1 \int_0^{s_1} \mathrm{d}s_2 \sum\!\!\!\!\!\!\int_k \frac{e^{i\mathbf{r}\cdot\mathbf{k}(s_1-s_2)} + e^{-i\mathbf{r}\cdot\mathbf{k}(s_1-s_2)}}{k^2} \left(\mathbf{r}^2 - \frac{(\mathbf{r}\cdot\mathbf{k})^2}{\mathbf{k}^2}\right) \\
&= -2g^2 C_F \sum\!\!\!\!\!\!\int_k \frac{1-\cos(\mathbf{r}\cdot\mathbf{k})}{(\mathbf{r}\cdot\mathbf{k})^2 k^2} \left(\mathbf{r}^2 - \frac{(\mathbf{r}\cdot\mathbf{k})^2}{\mathbf{k}^2}\right)
\end{aligned} \tag{4.4}
$$

So we see that diagrams b) and c) vanish because they contain scaleless integrals, while diagram d) has exactly the negative value of diagrams e) and f). This means that diagram a) is the only one which gives a contribution. This makes the $\mathcal{O}(\alpha_s)$ result fairly simple:

$$
\ln \langle W_c \rangle = \frac{\alpha_s C_F}{rT} + \mathcal{O}(\alpha_s^2)\,. \tag{4.5}
$$

We already see here that the ultraviolet divergences for the cyclic Wilson loop are very different from the non-cyclic case, because there are none at $\mathcal{O}(\alpha_s)$.

4.2 Systematic Cancellations

Before we go on with our calculations, it should be pointed out that for the cyclic Wilson loop a lot of diagrams cancel systematically, which greatly reduces the number of diagrams we have to consider. Of this we just saw the simplest example in the three tree level diagrams d), e) and f).

Another example would be encountered in the next section about diagrams involving the gluon self energy. Apart from the diagrams similar to the tree level ones, there could in principle appear additional contributions from another set of diagrams. Since the off-diagonal self energy components $\Pi_{0i}(k)$ are not necessarily zero, even in gauges where this is the case for the free propagator, self energy diagrams with one gluon leg attached to a quark line and the other attached to a string are not trivially vanishing. However, the four possible diagrams of this sort cancel in pairs:

- left string + quark line:

$$
\begin{aligned}
&(ig)^2 \int_0^\beta \mathrm{d}\tau \int_0^1 \mathrm{d}s \sum\!\!\!\!\!\!\int_k e^{-ik_0\tau - \frac{i}{2}\mathbf{r}\cdot\mathbf{k}} D_{00}(k)\Pi_{0i}(k) D_{ij}(k) r_j e^{i\mathbf{r}\cdot\mathbf{k}(s-\frac{1}{2})} \\
&= g^2 \int_k D_{00}(0,\mathbf{k})\Pi_{0i}(0,\mathbf{k}) D_{ij}(0,\mathbf{k}) r_j \frac{e^{-i\mathbf{r}\cdot\mathbf{k}} - 1}{i\mathbf{r}\cdot\mathbf{k}}
\end{aligned}
$$

- right string + quark line:

$$
\begin{aligned}
&(ig)^2 \int_0^\beta \mathrm{d}\tau \int_0^1 \mathrm{d}s \sum\!\!\!\!\!\!\int_k e^{-ik_0\tau - \frac{i}{2}\mathbf{r}\cdot\mathbf{k}} D_{00}(k)\Pi_{0i}(k) D_{ij}(k)(-r_j) e^{i\mathbf{r}\cdot\mathbf{k}(\frac{1}{2}-s)} \\
&= -g^2 \int_k D_{00}(0,\mathbf{k})\Pi_{0i}(0,\mathbf{k}) D_{ij}(0,\mathbf{k}) r_j \frac{e^{-i\mathbf{r}\cdot\mathbf{k}} - 1}{i\mathbf{r}\cdot\mathbf{k}}
\end{aligned}
$$

- left string + antiquark line:

$$
\begin{aligned}
&-(ig)^2 \int_0^\beta \mathrm{d}\tau \int_0^1 \mathrm{d}s \sum\!\!\!\!\!\!\int_k e^{-ik_0(\beta-\tau) + \frac{i}{2}\mathbf{r}\cdot\mathbf{k}} D_{00}(k)\Pi_{0i}(k) D_{ij}(k) r_j e^{i\mathbf{r}\cdot\mathbf{k}(s-\frac{1}{2})} \\
&= g^2 \int_k D_{00}(0,\mathbf{k})\Pi_{0i}(0,\mathbf{k}) D_{ij}(0,\mathbf{k}) r_j \frac{e^{i\mathbf{r}\cdot\mathbf{k}} - 1}{i\mathbf{r}\cdot\mathbf{k}}
\end{aligned}
$$

- right string + antiquark line:

$$
\begin{aligned}
&-(ig)^2 \int_0^\beta \mathrm{d}\tau \int_0^1 \mathrm{d}s \sum\!\!\!\!\!\!\int_k e^{-ik_0(\beta-\tau) + \frac{i}{2}\mathbf{r}\cdot\mathbf{k}} D_{00}(k)\Pi_{0i}(k) D_{ij}(k)(-r_j) e^{i\mathbf{r}\cdot\mathbf{k}(\frac{1}{2}-s)} \\
&= -g^2 \int_k D_{00}(0,\mathbf{k})\Pi_{0i}(0,\mathbf{k}) D_{ij}(0,\mathbf{k}) r_j \frac{e^{i\mathbf{r}\cdot\mathbf{k}} - 1}{i\mathbf{r}\cdot\mathbf{k}}
\end{aligned}
$$

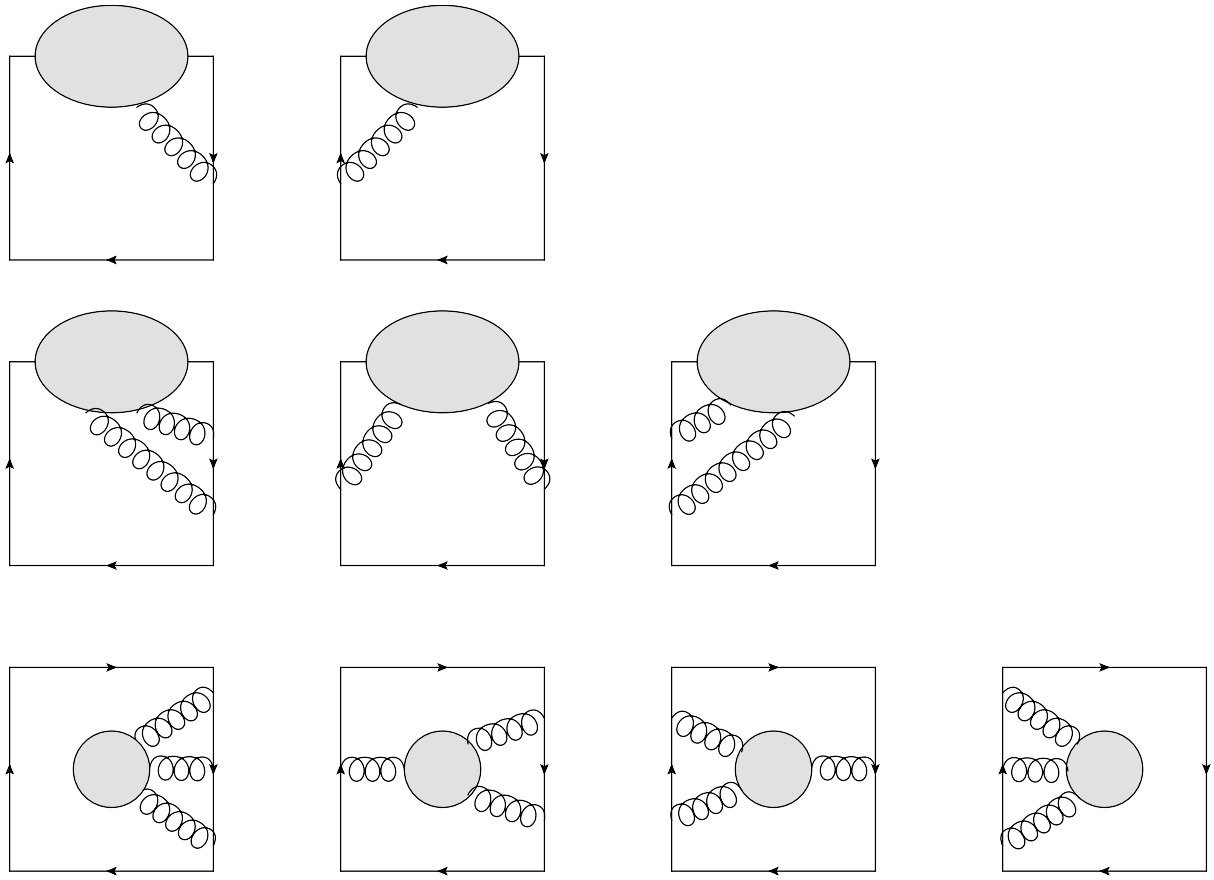

Figure 4.2: Some examples of diagrams that vanish because of cyclicity cancellation.

This result is a direct consequence of the fact that the loop is cyclic. In order to arrive at a more general statement, let us look at the Wilson loop as the expectation value of four Wilson lines:

$$\langle W_c \rangle = \widetilde{\mathrm{Tr}} \left\langle U_0 \left(\frac{\mathbf{r}}{2}, -\frac{\mathbf{r}}{2} \right) U^\dagger_{-\frac{\mathbf{r}}{2}} (\beta, 0)\, U^\dagger_\beta \left(\frac{\mathbf{r}}{2}, -\frac{\mathbf{r}}{2} \right) U_{\frac{\mathbf{r}}{2}} (\beta, 0) \right\rangle . \tag{4.6}$$

In perturbation theory we may expand each Wilson line individually. All diagrams where the quark or the antiquark line has no gluons attached to it correspond to the zeroth order expansion of the corresponding Wilson line, which is unity. But if we insert the unit matrix for one of the quark lines, we get

$$\widetilde{\mathrm{Tr}} \left\langle U_0 \left(\frac{\mathbf{r}}{2}, -\frac{\mathbf{r}}{2} \right) U^\dagger_\beta \left(\frac{\mathbf{r}}{2}, -\frac{\mathbf{r}}{2} \right) U_{\frac{\mathbf{r}}{2}} (\beta, 0) \right\rangle = \widetilde{\mathrm{Tr}} \left\langle U_{\frac{\mathbf{r}}{2}} (\beta, 0) \right\rangle = \langle W_P \rangle , \tag{4.7}$$

which is the Polyakov loop. The strings vanish because in the imaginary time formalism $\tau = 0$ and $\tau = \beta$ are identified, so the two Wilson line operators representing the strings are inverse to each other.

However, if we also expand the strings in equation (4.7), a comparison between left hand and right hand side shows, that all the non-zero order terms must cancel. These cancellations happen order by order in g, and also individually for sets of diagrams that have the same constituents and differ only in that some line vertices are switched from one string to the other.

An illustration of this statement is given in figure 4.2, where the sum over each row gives zero. The bubble may represent any diagram, as long as it stays the same in each row, and may or may not connect to one of the quark lines, but never to both. This picture shows only some of the simplest cases, but the statement is true for any number n of gluons attached to the bubble and the strings. The $n+1$ diagrams that differ only in which string these gluons are attached to, while not changing their ordering along the path, cancel when summed.

This statement is true in any gauge and we can rephrase it a bit. Whenever a diagram has at least one gluon attached to a string and at least one quark line is not connected to the other quark line or

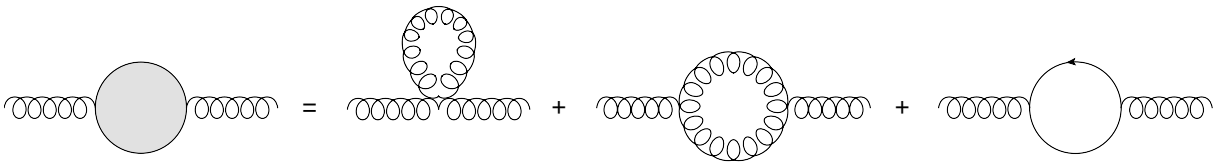

Figure 4.3: Diagrams contributing to the gluon self energy.

the strings, there will always be other similar diagrams to cancel it. We will refer to this result quite frequently in the following sections, so let us dub it "cyclicity cancellation", since it only works for the cyclic Wilson loop. Together with the restriction to 2PI diagrams this reduces the number of diagrams to be considered even more.

4.3 Gluon Self Energy Contribution

Now we can turn to the next order calculations. Let us first consider the diagrams involving the gluon self energy. Because of the cyclicity cancellation explained in the previous section, we only have to consider the tree level diagrams a), b) and c) with the free gluon propagator replaced by the 1-bubble propagator shown in figure 4.3. We can write their contribution as:

$$g^2 C_F \beta \int_k \frac{e^{-i\mathbf{r}\cdot\mathbf{k}} - 1}{\mathbf{k}^2} \left(-\Pi_{00}(0,\mathbf{k})\right) \frac{1}{\mathbf{k}^2} \,. \tag{4.8}$$

The minus sign in front of the self energy $\Pi_{00}(k)$ comes from expanding

$$\left\langle A_0^a(x_1) A_0^b(x_2) \right\rangle = \sum\!\!\!\!\!\!\int_k \frac{\delta^{ab} e^{ik(x_1-x_2)}}{\mathbf{k}^2 + \Pi_{00}(k)} = \sum\!\!\!\!\!\!\int_k \delta^{ab} e^{ik(x_1-x_2)} \left(\frac{1}{\mathbf{k}^2} - \frac{\Pi_{00}(k)}{(\mathbf{k}^2)^2} + \dots \right) , \tag{4.9}$$

and the Kronecker delta from the contour integrations $\int_0^\beta \mathrm{d}\tau \, e^{ik_0\tau} = \beta \delta_{n_k,0}$ requires $k_0 = 0$.

In order to calculate the self energy $\Pi_{00}(0,\mathbf{k})$, we have to consider the diagrams shown in figure 4.3. There is no ghost loop, because the 0-component of the gluon does not couple to ghost fields in Coulomb gauge. We can always split the calculation into a vacuum and a thermal part, because performing the thermal sums leads to a factor of $\frac{1}{2q}\left(1 \pm 2n_{B/F}(q)\right)$ for all contributions, as we will see shortly. We can then take over the result for the vacuum part from previous calculations, suitably adapted for Euclidean space (at 1-loop order and in the $\overline{\text{MS}}$-scheme):

$$-\Pi_{00}^{(0)}(0,\mathbf{k}) = \frac{\alpha_s \mathbf{k}^2}{4\pi} \left[\left(\frac{31}{9} C_A - \frac{20}{9} T_F n_f \right) + \left(\frac{11}{3} C_A - \frac{4}{3} T_F n_f \right) \ln \frac{\mu^2}{\mathbf{k}^2} \right] . \tag{4.10}$$

The details of the thermal part calculations can be found in appendix E.1. Since I know of no way to solve the last integration analytically, except for the case of the tadpole diagram, the result will be given up to that point.

$$\begin{aligned} \Pi_{00}^{(T)}(0,\mathbf{k}) =& \frac{4\alpha_s C_A}{\pi} \int_0^\infty \mathrm{d}q \, \frac{q}{e^{q\beta} - 1} \left\{ 1 - \frac{k^2}{2q^2} + \left(\frac{q}{k} - \frac{k}{2q} + \frac{k^3}{8q^3} \right) \ln \left| \frac{2q+k}{2q-k} \right| \right\} \\ &+ \frac{8\alpha_s T_F n_f}{\pi} \int_0^\infty \mathrm{d}q \, \frac{q}{e^{q\beta} + 1} \left\{ 1 + \left(\frac{q}{k} - \frac{k}{4q} \right) \ln \left| \frac{2q+k}{2q-k} \right| \right\} . \end{aligned} \tag{4.11}$$

This expression is finite for $q \to 0$, which can be seen by expanding the logarithm. It is also finite for $k \to 0$, however if we expand the logarithm as a Taylor series at $k = 0$, we get a series of divergent integrals. This means that our result cannot be represented as a power series in k.

However, we can still derive an approximation for the limit $k \ll T$ through a different approach. As explained in references [26] or [10], if we return to the start of the self energy calculation, but this time

perform the $\mathbf{q}$ integration first, then expand in $\frac{\mathbf{k}^2}{q_0^2}$ and perform the Matsubara sum last, we arrive at a series in $\frac{\mathbf{k}^2}{(\pi T)^2}$ and some non-analytic terms. Since the details of this calculation can be found in appendix E.2, we will just give the result here:

$$\begin{aligned}\Pi_{00}^{(T)}(0,\mathbf{k}) =& \frac{\alpha_s C_A (2\pi T)^2}{3\pi}\left\{1 - \frac{3\pi}{2}\frac{k}{2\pi T} - \frac{11}{2}\left[\gamma_E + \frac{1}{33} + \ln\frac{k}{4\pi T}\right]\left(\frac{k}{2\pi T}\right)^2 + \frac{\pi^3}{8}\left(\frac{k}{2\pi T}\right)^3\right\} + \\ &+ \frac{2\alpha_s T_F n_f (\pi T)^2}{3\pi}\left\{2 + \left[\gamma_E - \frac{4}{3} + \ln\frac{k}{\pi T}\right]\left(\frac{k}{\pi T}\right)^2\right\} + \mathcal{O}\left[\left(\frac{k}{\pi T}\right)^4\right]. \end{aligned} \tag{4.12}$$

The non-analyticity of the gluon self energy is contained in the logarithms and the linear and cubic terms. The calculation shows that those come from $\sqrt{k^2}$ terms, which is in accordance with equation (4.11) being even in k, so to be totally accurate we should write $|k|$ instead of just k. There are no more non-analytic contributions from higher order terms, starting from the quartic terms we only have even powers of $\frac{k}{\pi T}$. This result is in agreement with the one found in reference [27], which however does not give all of the terms above:

$$\Pi_{00}^{(T)}(0,\mathbf{k}) = 4\pi\alpha_s C_A\left(\frac{T^2}{3} - \frac{kT}{4} - \frac{11}{48\pi^2}k^2\ln\frac{k^2}{T^2}\right) + \mathcal{O}(k^2)\,. \tag{4.13}$$

Unlike the case of the small k expansion, for large k we can expand the logarithm in negative powers of k without getting divergent integrals in q and thus derive the following expression (details in appendix E.2).

$$\Pi_{00}^{(T)}(0,\mathbf{k}) = -\frac{1}{18\pi}\alpha_s C_A (2\pi T)^2 + \frac{1}{15\pi}\alpha_s (2\pi T)^2\left\{\frac{11}{15}C_A + \frac{7}{6}T_F n_f\right\}\left(\frac{2\pi T}{k}\right)^2 + \mathcal{O}\left[\left(\frac{2\pi T}{k}\right)^4\right]. \tag{4.14}$$

These expansions show that equation (4.8) is infrared (and ultraviolet) finite, because the thermal part of the gluon self energy approaches a constant for both limits $k \to 0$ and $k \to \infty$ and has no singular points in between, while the other part of the integrand is integrable in three dimensions. However, when we turn to the renormalization of the Wilson loop, we will consider the parts proportional to $\frac{\exp(i\mathbf{r}\cdot\mathbf{k})}{k^4}$ and to $\frac{1}{k^4}$ separately, which both are infrared divergent on their own. So we will just assume that these divergences have been cancelled through the inclusions of contributions from the scales T and m_D, without giving explicit values for them. The renormalization properties are unaffected by that.

4.4 3-Gluon Diagrams

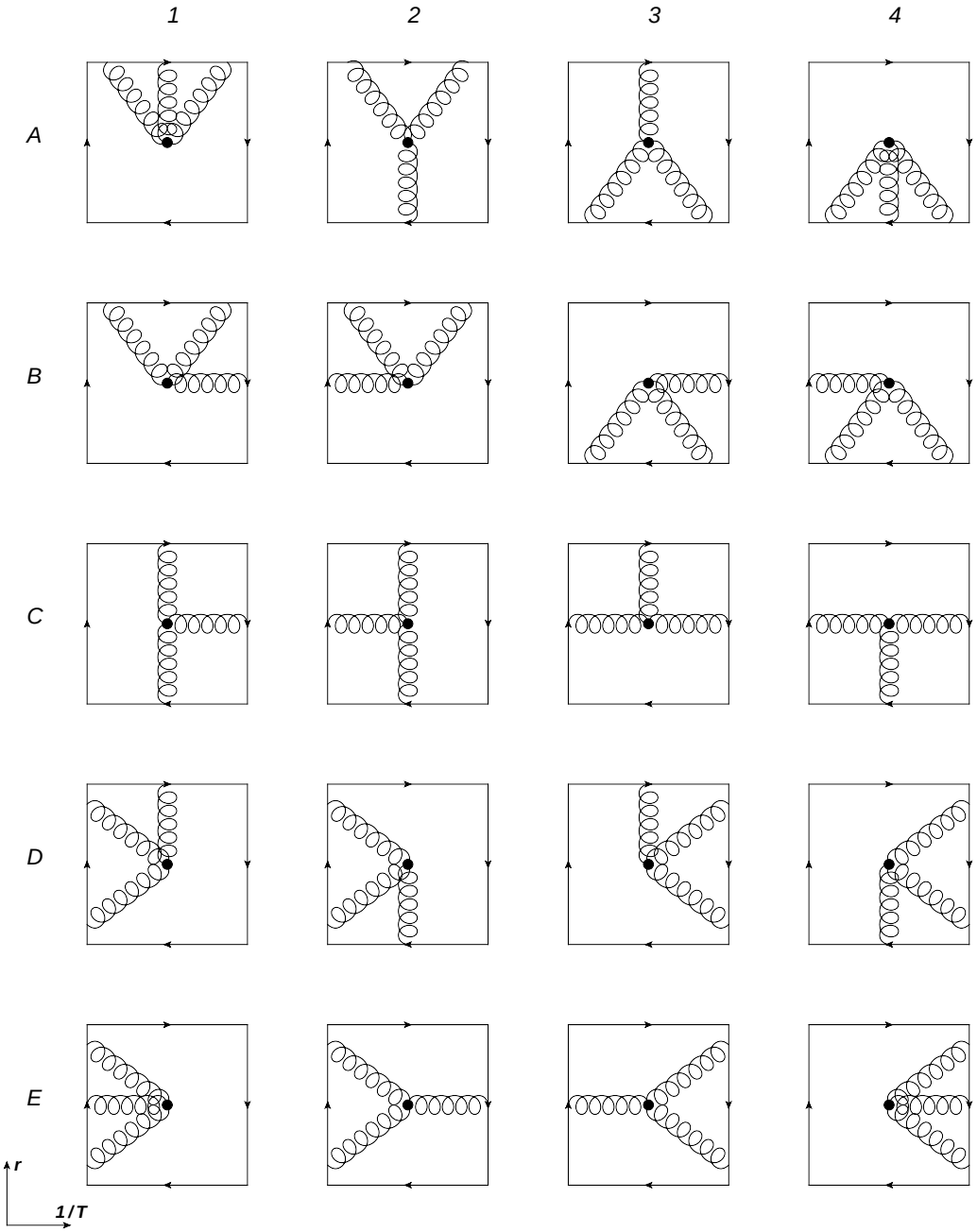

Figure 4.4: All diagrams of $\mathcal{O}\left(g^4\right)$ with a 3-gluon vertex.

Figure 4.4 above shows all the diagrams of $\mathcal{O}\left(g^4\right)$ with a 3-gluon vertex, arranged in rows of similar structures. Most of them give zero contribution to the cyclic Wilson loop, as we will show now. In the following calculations the momenta of the propagators are denoted k, p, q in counterclockwise order starting from the upper left corner. The arrows indicate the direction of the contour integration, and as always the quark lines run horizontally, the strings vertically.

Row A

All of these diagrams are zero. Since the Coulomb gauge gluon propagator is diagonal in time and space indices the vertex factor has to be taken with all Lorentz indices equal zero and thus vanishes:

$$(-ig)f^{abc}\left[(k_0-q_0)\delta_{00}+(p_0-k_0)\delta_{00}+(q_0-p_0)\delta_{00}\right]=0\,. \tag{4.15}$$

Row B

Here all diagrams cancel because of cyclicity. This example is rather similar to the previous one involving the gluon self energy. The two pairs of diagrams have the same value but different sign because of the different integration direction.

Diagrams C1, C2

These two diagrams are the only ones that give a contribution. Here we cannot invoke cyclicity cancellation. When one switches the horizontal gluon line from one side to the other, one also changes the order of the gluon legs. This gives a relative minus sign, which together with the minus from the reversed integration direction has the effect, that the diagrams C1 and C2 are actually equal, each having a value of $\frac{1}{2}C_F C_A \alpha_s^2$. The calculation itself is quite lengthy and will be given in appendix E.3.

Diagrams C3, C4 and Row D

All of these six diagrams vanish because of cyclicity, cancelling as triplets (C3, D1, D3) and (C4, D2, D4). But even if this were not the case, they would still give zero individually, because they all involve a Matsubara sum over an expression that is odd in the frequency. This will be shown for diagram C4, the expressions for the other diagrams are similar and differ only in the terms in front of the Matsubara sum:

$$\begin{aligned}
&(ig)^3(-ig)f^{abc}\widetilde{\mathrm{Tr}}\left[T^aT^bT^c\right]\int_0^1 \mathrm{d}s_1\, r_i \int_0^\beta \mathrm{d}\tau \int_0^1 \mathrm{d}s_2\, r_j \sum\!\!\!\!\!\!\int_k \sum\!\!\!\!\!\!\int_p \sum\!\!\!\!\!\!\int_q \frac{\delta_{ii'} - \frac{k_i k_{i'}}{\mathbf{k}^2}}{k^2} e^{-i\mathbf{r}\cdot\mathbf{k}\left(s_1-\frac{1}{2}\right)} \times \\
&\quad \times \frac{e^{-ip_0(\beta-\tau)+\frac{i}{2}\mathbf{r}\cdot\mathbf{p}}}{\mathbf{p}^2} \frac{\delta_{jj'} - \frac{q_j q_{j'}}{\mathbf{q}^2}}{q^2} e^{-iq_0\beta - i\mathbf{r}\cdot\mathbf{q}\left(\frac{1}{2}-s_2\right)} \delta_{i'j'}\,(k_0-q_0)\,\frac{(2\pi)^3}{T}\delta^{(3)}\left(\mathbf{k}+\mathbf{p}+\mathbf{q}\right)\delta_{-n_p,n_k+n_q} \\
&= -\frac{i}{2}g^4 C_F C_A \int_0^1 \mathrm{d}s_1 \int_0^1 \mathrm{d}s_2 \sum\!\!\!\!\!\!\int_k \sum\!\!\!\!\!\!\int_q \frac{\mathbf{r}^2 - \frac{(\mathbf{r}\cdot\mathbf{k})^2}{\mathbf{k}^2} - \frac{(\mathbf{r}\cdot\mathbf{q})^2}{\mathbf{q}^2} + \frac{(\mathbf{r}\cdot\mathbf{k})(\mathbf{r}\cdot\mathbf{q})(\mathbf{k}\cdot\mathbf{q})}{\mathbf{k}^2\mathbf{q}^2}}{(\mathbf{k}+\mathbf{q})^2 k^2 q^2} \times \\
&\quad \times e^{-i\mathbf{r}\cdot\mathbf{k}s_1 + i\mathbf{r}\cdot\mathbf{q}(s_2-1)}\beta\delta_{n_k+n_q,0}\,(k_0-q_0) \\
&= -\frac{i}{2}g^4 C_F C_A \int_k \int_q \frac{\mathbf{r}^2 - \frac{(\mathbf{r}\cdot\mathbf{k})^2}{\mathbf{k}^2} - \frac{(\mathbf{r}\cdot\mathbf{q})^2}{\mathbf{q}^2} + \frac{(\mathbf{r}\cdot\mathbf{k})(\mathbf{r}\cdot\mathbf{q})(\mathbf{k}\cdot\mathbf{q})}{\mathbf{k}^2\mathbf{q}^2}}{(\mathbf{k}+\mathbf{q})^2} \frac{\left(e^{-i\mathbf{r}\cdot\mathbf{k}}-1\right)\left(1-e^{-i\mathbf{r}\cdot\mathbf{q}}\right)}{(\mathbf{r}\cdot\mathbf{k})(\mathbf{r}\cdot\mathbf{q})} \times \\
&\quad \times \sum_{k_0} \underbrace{\frac{2k_0}{\left(k_0^2+\mathbf{k}^2\right)\left(k_0^2+\mathbf{q}^2\right)}}_{\text{odd in } k_0} = 0\,.
\end{aligned} \tag{4.16}$$

Row E

The diagrams of row E vanish again because of cyclicity. But furthermore, E1 cancels against E2 and E3 against E4. There is a nice graphic explanation for that. If we consider only the contour integration of the last gluon (the one with momentum q) in diagrams E1 and E2 and think of the other two gluons as fixed for the moment, there are three regions this integration can cover: below the other two gluons, between them or above them. In the end every region will give the same value, which can be shown by parameter substitutions like those in appendix C. Now, in diagram E2 this integration covers all three regions of the string, but runs in the opposite direction than that of diagram E1, which covers only the lower region. So in the sum of E1 and E2 the contributions from the lower region obviously cancel, leaving the contributions from the middle and upper region. But since the ordering of the gluons for the middle region differs from that of the upper region by an odd permutation, the 3-gluon vertex gives rise to a relative minus sign, which is not compensated by a different ordering of the colour matrices, so those two contributions also cancel. An exact calculation of this can be found in appendix E.4.

Result

Seeing as how many diagrams cancel or give zero contribution, the sum over all 3-gluon diagrams becomes fairly simple:

$$\ln W_c\Big|_{3g} = C_F C_A \alpha_s^2\,. \tag{4.17}$$

4.5 Unconnected Diagrams

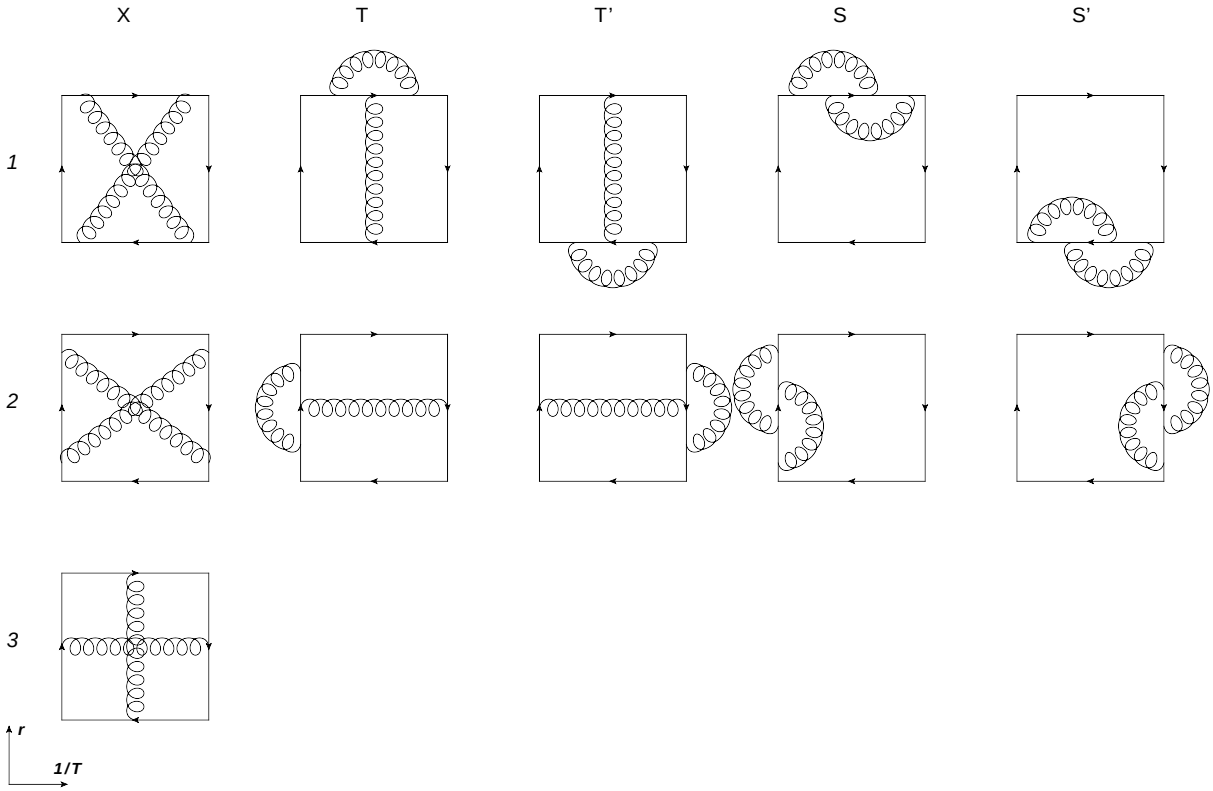

Figure 4.5: The unconnected 2PI diagrams of $\mathcal{O}(g^4)$.

In figure 4.5 there are shown all the unconnected 2PI diagrams of $\mathcal{O}(g^4)$. (For the use of the term "unconnected" see appendix C.) The columns are labelled with letters that more or less resemble the diagrams they are supposed to represent. Rows 1 and 2 vanish, but diagram 3X gives a divergent contribution, as we are about to show.

Row 1

All of these diagrams vanish individually. In Coulomb gauge the 00-component of the propagator, which is the only one relevant for these diagrams, does not contain Matsubara frequencies in the denominator. This leads to scaleless integrals, which can be neglected in dimensional regularization, in the cases 1T, 1T', 1S, 1S', since a gluon with both ends attached to the same quark line does not have any dependence on $\mathbf{r}$. But even if this were not the case, they would still vanish because of the contour integrations and Matsubara sums. We will perform this calculation explicitly for the 1X diagram, the other cases are similar.

The value of 1X is given by

$$
\begin{aligned}
&-\frac{g^4}{2}C_F C_A \int_0^\beta \mathrm{d}\tau_1 \int_0^{\tau_1} \mathrm{d}\tau_2 \int_0^\beta \mathrm{d}\tau_3 \int_0^{\tau_3} \mathrm{d}\tau_4 \sum\!\!\!\!\!\!\int_k \sum\!\!\!\!\!\!\int_q \frac{e^{ik_0(\beta-\tau_1-\tau_3)-i\mathbf{r}\cdot\mathbf{k}}}{\mathbf{k}^2}\,\frac{e^{iq_0(\beta-\tau_2-\tau_4)-i\mathbf{r}\cdot\mathbf{q}}}{\mathbf{q}^2} \\
&= -\frac{g^4}{2}C_F C_A \int_k \frac{e^{-i\mathbf{r}\cdot\mathbf{k}}}{\mathbf{k}^2} \int_q \frac{e^{-i\mathbf{r}\cdot\mathbf{q}}}{\mathbf{q}^2} \int_0^\beta \mathrm{d}\tau_1 \int_0^{\tau_1} \mathrm{d}\tau_2 \int_0^\beta \mathrm{d}\tau_3 \int_0^{\tau_3} \mathrm{d}\tau_4\, \delta(\beta-\tau_1-\tau_3)\delta(\beta-\tau_2-\tau_4) \\
&= -\frac{g^4}{2}C_F C_A \left(\frac{1}{4\pi r}\right)^2 \int_0^\beta \mathrm{d}\tau_1 \int_0^{\tau_1} \mathrm{d}\tau_2 \int_0^\beta \mathrm{d}\tau_3\, \delta(\beta-\tau_1-\tau_3)\Theta(\tau_2+\tau_3-\beta)\Theta(\beta-\tau_2) \\
&= -\frac{g^4}{2}C_F C_A \left(\frac{1}{4\pi r}\right)^2 \int_0^\beta \mathrm{d}\tau_1 \int_0^{\tau_1} \mathrm{d}\tau_2\, \Theta(\tau_1)\Theta(\beta-\tau_1)\Theta(\tau_2-\tau_1)\Theta(\beta-\tau_2) \\
&= -\frac{g^4}{2}C_F C_A \left(\frac{1}{4\pi r}\right)^2 \int_0^\beta \mathrm{d}\tau_1 \int_0^{\beta} \mathrm{d}\tau_2\, \Theta(\tau_1-\tau_2)\Theta(\tau_2-\tau_1) = 0\,.
\end{aligned}
\tag{4.18}
$$

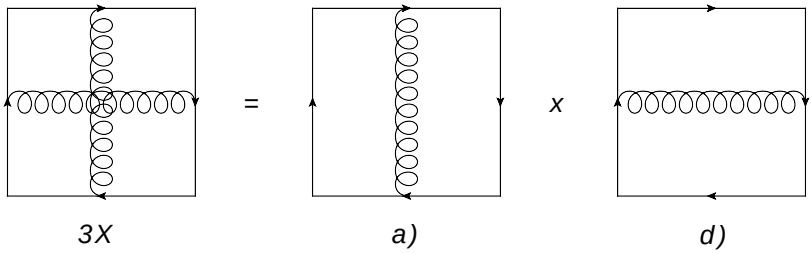

Figure 4.6: Factorization of diagram 3X (disregarding colour coefficients).

Although the Matsubara sums actually lead to an infinite sum of delta functions:

$$\sum_{k_0} e^{ik_0\tau} = \sum_n \delta(\tau - n\beta)\,, \tag{4.19}$$

their arguments lie inside the integration region only for $n = 0$.

Row 2

Again, these diagrams cancel because of cyclicity. Since this is a more complex example, the interested reader is referred to appendix E.5 for a detailed demonstration of how this cancellation works.

Diagram 3X

In this diagram the integration regions of the gluon propagator endpoints do not overlap, which means that its contribution factors into the product of two tree level diagrams with their colour factors replaced by the colour connected coefficient of the 3X diagram. As we saw in the tree level calculations, the contribution of the gluon connecting the two strings is divergent. However, unlike in the tree level case, here we have no other diagram left which could cancel this divergence. The diagrams where one gluon starts and ends at the same string are two-particle reducible and thus do not contribute here. Or to put it another way, the three tree level diagrams related to the strings, which individually are divergent but cancel each other, no longer have the same colour coefficient once we add a gluon connecting the quark lines. This leaves us with a net divergence. While we did not need to calculate diagram d) for the tree level calculations, we now have to. In addition we also have to calculate the contribution of diagram a) in d dimensions to get the correct finite parts for diagram 3X.

Let us begin with the calculation of a). Without the colour factor this is given by:

$$\begin{aligned}
W\left(\gamma_a\right) =& -(ig)^2 \int_0^\beta \mathrm{d}\tau_1 \int_0^\beta \mathrm{d}\tau_2 \sum\!\!\!\!\!\!\int_k \frac{e^{ik_0(\beta-\tau_1-\tau_2)-i\mathbf{r}\cdot\mathbf{k}}}{\mathbf{k}^2} = g^2\beta \int \frac{\mathrm{d}^d k}{(2\pi)^d} \frac{e^{-i\mathbf{r}\cdot\mathbf{k}}}{\mathbf{k}^2} \\
=& g^2\beta \frac{2\pi^{\frac{d-1}{2}}}{(2\pi)^d \Gamma\left(\frac{d-1}{2}\right)} \int_0^\infty \mathrm{d}k \int_{-1}^1 \mathrm{d}x\, k^{d-3} \left(1-x^2\right)^{\frac{d-3}{2}} e^{-ikrx} \\
=& g^2\beta \frac{2\pi^{\frac{d-1}{2}}}{(2\pi)^d \Gamma\left(\frac{d-1}{2}\right)} \int_0^\infty \mathrm{d}k \int_0^1 \mathrm{d}x\, k^{d-3} \left(1-x^2\right)^{\frac{d-3}{2}} \left(e^{ikrx} + e^{-ikrx}\right) \\
=& g^2\beta \frac{2\pi^{\frac{d-1}{2}}}{(2\pi)^d \Gamma\left(\frac{d-1}{2}\right)} 2\mathrm{Re}\left[\int_0^\infty \mathrm{d}k \int_0^1 \mathrm{d}x\, k^{d-3} \left(1-x^2\right)^{\frac{d-3}{2}} e^{ikrx}\right] \\
=& g^2\beta \frac{2\pi^{\frac{d-1}{2}}}{(2\pi)^d \Gamma\left(\frac{d-1}{2}\right)} 2\mathrm{Re}\left[\int_0^1 \mathrm{d}x \left(1-x^2\right)^{\frac{d-3}{2}} (-irx)^{2-d} \int_0^\infty \mathrm{d}k\, k^{d-3} e^{-k}\right] \\
=& g^2\beta \frac{2\pi^{\frac{d-1}{2}}}{(2\pi)^d \Gamma\left(\frac{d-1}{2}\right)} \mathrm{Re}\left[e^{-i\frac{\pi}{2}(2-d)}\right] \int_0^1 \mathrm{d}x (1-x)^{\frac{d-3}{2}} x^{\frac{1-d}{2}}\, r^{2-d}\Gamma(d-2) \\
=& g^2\beta \frac{2\pi^{\frac{d-1}{2}}\, r^{2-d}\Gamma(d-2)}{(2\pi)^d \Gamma\left(\frac{d-1}{2}\right)} \cos\left(\frac{(2-d)\pi}{2}\right) \frac{\Gamma\left(\frac{d-1}{2}\right)\Gamma\left(\frac{3-d}{2}\right)}{\Gamma(1)}
\end{aligned}$$

$$
\begin{aligned}
=&g^2\beta\frac{2\pi^{\frac{d-1}{2}}\,r^{2-d}\Gamma(d-2)}{(2\pi)^d\Gamma\left(\frac{d-1}{2}\right)}\frac{\pi}{\Gamma\left(\frac{d-1}{2}\right)\Gamma\left(\frac{3-d}{2}\right)}\frac{\Gamma\left(\frac{d-1}{2}\right)\Gamma\left(\frac{3-d}{2}\right)}{\Gamma(1)}\\
=&g^2\beta\frac{r^{2-d}\Gamma(d-2)}{(4\pi)^{\frac{d-1}{2}}\Gamma\left(\frac{d-1}{2}\right)}=\frac{\alpha_s\beta}{r}\frac{(\mu r)^{2\varepsilon}(4\pi)^{\varepsilon}\Gamma(1-2\varepsilon)}{\Gamma(1-\varepsilon)}\\
=&\frac{\alpha_s\beta}{r}\left[1+\left(\gamma_E+\ln 4\pi+\ln\mu^2r^2\right)\varepsilon+\mathcal{O}\left(\varepsilon^2\right)\right]\,.
\end{aligned}
\tag{4.20}
$$

To be honest, once we renormalize the cyclic Wilson loop in the next section, these finite terms from the $\mathcal{O}(\varepsilon^1)$ expansion of diagram $\gamma_{a)}$ will really be of no importance, since the counterterm will generate the same constant terms and they will be cancelled together with the divergence. At this stage however, we should include them.

We can split up the calculation of d) into a into a divergent "vacuum" part and a finite "thermal" part. The reason for putting in those quotation marks is that, while this nomenclature comes from the two terms in the result of the Matsubara sum $\frac{1}{2k}(1+2n_B(k))$, if we take the results of the vacuum Wilson loop calculation from the previous part and substitute $it=\beta$, we get a different split up into a vacuum and a thermal part. So, if we calculated this diagram for a generic τ and then let $\tau\to\beta$, the divergence would actually come from the thermal contribution. However, the distinction between vacuum and thermal part is of no real importance here. One could also argue, that the cyclic Wilson loop should not be viewed as the limit $\tau\to\beta$ of an ordinary Wilson loop in imaginary time, but as a different object altogether. We will return to this in the next section about the renormalization of the cyclic Wilson loop. For now, let us proceed with the calculations:

$$
\begin{aligned}
W\left(\gamma_{d)}\right)=&-(ig)^2\int_0^1\mathrm{d}s_1\int_0^1\mathrm{d}s_2\sum\!\!\!\!\!\!\int_k\frac{\mathbf{r}^2-\frac{(\mathbf{r}\cdot\mathbf{k})^2}{\mathbf{k}^2}}{k_0^2+\mathbf{k}^2}e^{-ik_0\beta+i\mathbf{r}\cdot\mathbf{k}(s_1+s_2-1)}\\
=&g^2\sum\!\!\!\!\!\!\int_k\frac{\mathbf{r}^2-\frac{(\mathbf{r}\cdot\mathbf{k})^2}{\mathbf{k}^2}}{k_0^2+\mathbf{k}^2}\frac{2-2\cos(\mathbf{r}\cdot\mathbf{k})}{(\mathbf{r}\cdot\mathbf{k})^2}\\
=&g^2\int_k\left(1+\frac{2}{e^{k\beta}-1}\right)\frac{\mathbf{r}^2-\frac{(\mathbf{r}\cdot\mathbf{k})^2}{\mathbf{k}^2}}{2k}\frac{2-2\cos(\mathbf{r}\cdot\mathbf{k})}{(\mathbf{r}\cdot\mathbf{k})^2}\,.
\end{aligned}
\tag{4.21}
$$

Now the vacuum part can be taken over from the tree level vacuum Wilson loop calculations, diagrams e) and f):

$$
\begin{aligned}
W^{(0)}\left(\gamma_{d)}\right)=&g^2\int\frac{\mathrm{d}^dk}{(2\pi)^d}\,\frac{\mathbf{r}^2-\frac{(\mathbf{r}\cdot\mathbf{k})^2}{\mathbf{k}^2}}{2k}\frac{2-2\cos(\mathbf{r}\cdot\mathbf{k})}{(\mathbf{r}\cdot\mathbf{k})^2}\\
=&-\frac{2\alpha_s}{\pi}\left(\frac{1}{\varepsilon}+1+\gamma_E+\ln\pi+\ln\mu^2r^2\right)+\mathcal{O}\left(\varepsilon\right)\,.
\end{aligned}
\tag{4.22}
$$

The calculation of the thermal part turns out to be more problematic and the result will only be given as an integral representation, or as a series expansion for $rT\ll 1$. This series expression will be used more often in subsequent results, since it is more concise and in accordance with our assumed hierarchy, but it should be understood that only the integral representation is valid for all values of rT and should be substituted whenever expanding is not allowed. (The details can be found in appendix E.6.)

$$
\begin{aligned}
W^{(T)}\left(\gamma_{d)}\right)=&\frac{4\alpha_s}{\pi}\left\{\frac{rT}{2i}\int_0^1\frac{\mathrm{d}z}{z}\left[\psi(0,1+irTz)-\psi(0,1-irTz)\right]+\frac{1}{2}\left[\ln\Gamma(1+irT)+\ln\Gamma(1-irT)\right]+\right.\\
&\left.+\frac{1}{2}\int_0^1\mathrm{d}z\,\left[\ln\Gamma(1+irTz)+\ln\Gamma(1-irTz)\right]\right\}\\
=&\frac{4\alpha_s}{\pi}\sum_{n=1}^{\infty}\frac{(-1)^{n-1}}{n(4n^2-1)}\zeta(2n)(rT)^{2n}\,.
\end{aligned}
\tag{4.23}
$$

The series expansion is obviously divergent for $rT > 1$, since the zeta function approaches 1 for large arguments and an exponential of positive n diverges more rapidly than a power of n. For $rT = 1$ it converges, because for large n it behaves as $\frac{1}{n^3}$, and a numerical calculation gives an approximate value of 0.519237 (for the sum only). So we see that the series converges for $rT \leq 1$.

The complete contribution of diagram 3X is then given by:

$$\widetilde{C}\left(\gamma_{3X}\right) W\left(\gamma_{3X}\right) = \frac{C_F C_A \alpha_s^2}{rT\pi}\left[\frac{1}{\varepsilon} + 1 + 2\gamma_E + \ln 4\pi^2 + 2\ln \mu^2 r^2 + \sum_{n=1}^{\infty} \frac{2(-1)^n \zeta(2n)}{n(4n^2-1)}(rT)^{2n} + \mathcal{O}(\varepsilon)\right]. \tag{4.24}$$

In order to compare this to the result of the calculation in [8]:

$$C_F C_A \frac{4\alpha_s^2}{T}\int_k \frac{e^{i\mathbf{r}\cdot\mathbf{k}}}{\mathbf{k}^2}\left[\frac{1}{\varepsilon} + 1 - \gamma_E + \ln\pi + \ln\frac{\mu^2}{\mathbf{k}^2}\right], \tag{4.25}$$

which only gives the leading term for small rT, we need to do one more calculation:

$$\begin{aligned}
\int_k \frac{e^{i\mathbf{r}\cdot\mathbf{k}}}{\mathbf{k}^2}\ln\frac{\mu^2}{\mathbf{k}^2} =& \frac{1}{4\pi^2}\int_0^\infty \mathrm{d}k\, \frac{e^{irk} - e^{-irk}}{irk}\ln\frac{\mu^2}{k^2} \\
=& \frac{1}{2\pi^2 r}\left\{\partial_\varepsilon \,\mathrm{Im}\left[\int_0^\infty \mathrm{d}k\, \frac{\mu^{2\varepsilon} e^{irk}}{k^{1+2\varepsilon}}\right]\right\}\Bigg|_{\varepsilon=0} \\
=& \frac{1}{2\pi^2 r}\left\{\partial_\varepsilon \,\mathrm{Im}\left[(-i\mu r)^{2\varepsilon}\int_0^\infty \mathrm{d}k\, \frac{e^{-k}}{k^{1+2\varepsilon}}\right]\right\}\Bigg|_{\varepsilon=0} \\
=& \frac{1}{2\pi^2 r}\left\{\partial_\varepsilon\left[-\sin(\pi\varepsilon)(\mu r)^{2\varepsilon}\Gamma(-2\varepsilon)\right]\right\}\Bigg|_{\varepsilon=0} \\
=& \frac{1}{2\pi^2 r}\left\{\partial_\varepsilon\left[\frac{\pi}{2} + \frac{\pi}{2}\left(2\gamma_E + \ln\mu^2 r^2\right)\varepsilon + \mathcal{O}(\varepsilon^2)\right]\right\}\Bigg|_{\varepsilon=0} \\
=& \frac{1}{4\pi r}\left(2\gamma_E + \ln\mu^2 r^2\right) \\
=& \left(2\gamma_E + \ln\mu^2 r^2\right)\int_k \frac{e^{i\mathbf{r}\cdot\mathbf{k}}}{\mathbf{k}^2}.
\end{aligned} \tag{4.26}$$

Since the logarithm is not multiplied by the singularity, we could do this calculation in three dimensions. So we can rewrite equation (4.25) to give:

$$C_F C_A \frac{4\alpha_s^2}{T}\int_k \frac{e^{i\mathbf{r}\cdot\mathbf{k}}}{\mathbf{k}^2}\left[\frac{1}{\varepsilon} + 1 + \gamma_E + \ln\pi + \ln\mu^2 r^2\right]. \tag{4.27}$$

The square brackets now correspond to what was called $W^{(0)}\left(\gamma_b\right)$ in our calculations, and it is easy to see that the coefficients are the same, apart from a factor $\frac{1}{4\pi r}$ that is still hidden in the k integration, while the rest of the constant terms comes from expanding that integral to $\mathcal{O}(\varepsilon)$. So our result agrees with that of [8].

4.6 Result

We can now put everything together to get an expression for the cyclic Wilson loop at order α_s^2, which is in agreement with reference [8]:

$$\begin{aligned}
\ln\langle W_c\rangle =& \frac{C_F\alpha_s}{rT}\left\{1 + \frac{\alpha_s}{4\pi}\left[\left(\frac{31}{9}C_A - \frac{20}{9}T_F n_f\right) + \left(\frac{11}{3}C_A - \frac{4}{3}T_F n_f\right)\left(\ln\mu^2 r^2 + 2\gamma_E\right)\right] + \right. \\
&\left. + \frac{\alpha_s C_A}{\pi}\left[\frac{1}{\varepsilon} + 1 + 2\gamma_E + \ln 4\pi^2 + 2\ln\mu^2 r^2 + \sum_{n=1}^{\infty}\frac{2(-1)^n\zeta(2n)}{n(4n^2-1)}(rT)^{2n}\right]\right\} + \\
&+ \frac{4\pi\alpha_s C_F}{T}\int_k \frac{e^{i\mathbf{r}\cdot\mathbf{k}} - 1}{(\mathbf{k}^2)^2}\left(-\Pi_{00}^{(T)}(0,\mathbf{k})\right) + C_F C_A \alpha_s^2 \quad + \mathcal{O}\left(\alpha_s^3\right).
\end{aligned} \tag{4.28}$$

5 Renormalization of the Cyclic Wilson Loop

In this section we will assume, unless otherwise specified, that a renormalization of the charge and fields has already been carried out, so that we only have to concern ourselves with the divergences due to singular points on the contour. By that we mean points where C is not differentiable (compare [16]).

As we saw in the previous section, a peculiar thing happens for the cyclic Wilson loop: The cusp divergences of $\mathcal{O}(\alpha_s)$, which we found for the vacuum case, have disappeared. But the divergence resurfaces at $\mathcal{O}(\alpha_s^2)$, this time multiplied not by a constant, but by a term depending on r and T. In order to explain this, it may be useful to look at the Wilson loop from a different angle.

Due to the periodic boundary conditions in the imaginary time formalism of finite temperature field theory, we work in a cylindric space with d infinite space dimensions and one circular time dimension. The cyclic Wilson loop wraps once around the whole of this time dimension, so that the two strings run along the same line. This means that the cyclic Wilson loop no longer has cusps, but intersections. (compare figure 5.1)

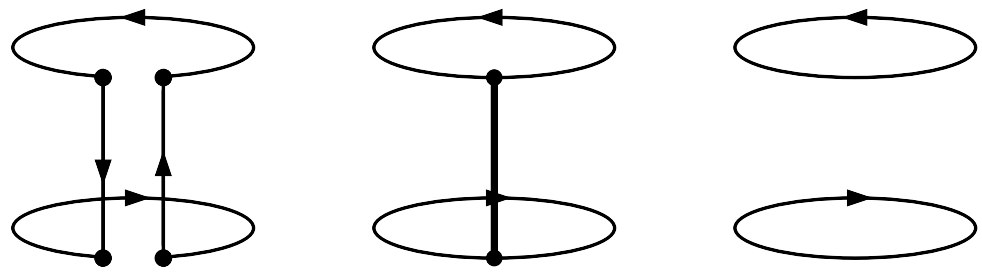

Figure 5.1: The contours for the non-cyclic (left) and the cyclic Wilson loop (middle) are shown, together with the Polyakov loop correlator (right). One can see that the cusp points turn into intersection points.

It has been shown in reference [20] that the expectation values of loops with intersections cannot be renormalized by a single multiplicative constant. One rather has to consider sets of loops and loop correlators that mix under renormalization. These sets consist of all possible path ordering prescriptions for contours that occupy the same points in space-time and retain the same direction everywhere except at the intersection points. Taking different path ordering prescriptions at the intersections will inevitably lead to contours with several disconnected loops. In this case each loop is traced separately, so as to preserve gauge invariance, and each trace is divided by the number of colours. An illustration of this is given in figure 5.2 for the simplest case of a smooth curve that intersects with itself once at a single point.

Figure 5.2: The two possible path orderings for a loop with one intersection.

Following this contour and arriving at the intersection point, there are two possible ways how to go on: one can either go straight ahead, thus following the rest of the contour, or make a turn onto the way one has come, splitting the contour into two separate loops. To highlight this last feature the two loops on the right of figure 5.2 are drawn apart, while it should be understood that they still connect at the intersection point.

Each of those two loops on the right, taken on its own, would have a normal cusp and be renormalizable through a multiplicative constant. However, when taking the average over the product of both loops there is a new source of divergences from gluon exchanges between the two loops. In order to get rid of those one has to add a multiple of the expectation value of the smooth loop on the left, for which similar divergences arise at the intersection. By choosing appropriate coefficients, combinations of both loops can be made finite.

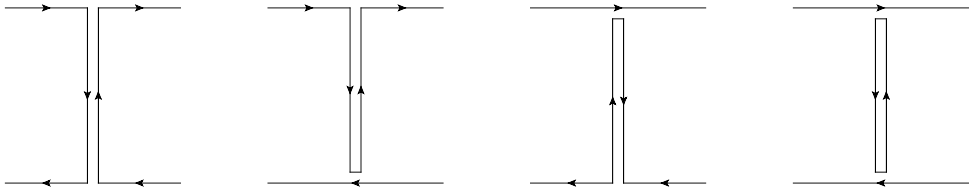

Figure 5.3: The four different path orderings of the contour of the Wilson loop. The string is represented in the middle and the endpoints at the right and left should be identified.

In general a loop may cross an intersection point more than twice and the angles at which the different lines enter that point may all be different. In that case the set of all associated loops is renormalized by a matrix of renormalization constants, which depend only on the angles at the intersection point. When a loop has more than one intersection point, then the set of associated loops takes on a tensor like structure with a renormalization matrix for each intersection point. If there are additional cusp divergences present, then those can be taken care of by multiplicative constants. So the general formula looks like this:

$$W^{(R)}_{i_1 i_2 \dots i_r} = Z_{i_1 j_1}(\beta_1) Z_{i_2 j_2}(\beta_2) \cdots Z_{i_r j_r}(\beta_r) Z(\gamma_1) Z(\gamma_2) \cdots Z(\gamma_s) W_{j_1 j_2 \dots j_r} \,. \tag{5.1}$$

Here the indices i_k label the different possible path ordering prescriptions at the r intersection points, β_k denote the angles at those intersection points and γ_l stand for the cusp angles at the s additional points of non-differentiability. As mentioned above, the loop functions W are defined such that there is a trace over each closed Wilson line, and each trace is divided by the number of colours.

Now we want to apply these results of reference [20] to the cyclic Wilson loop. Strictly speaking, we have a continuously infinite number of intersection points, namely the whole of the string. However, only the string endpoints are of real importance, as we will see shortly.

Let us first understand, which loop functions can appear, when we consider different path ordering prescriptions only at the string endpoints. We will label the loop functions L_{ij}, where $i, j = 0$ stands for taking the same path as the Wilson loop contour at the upper (i) or lower (j) intersection point and $i, j = 1$ taking the other possible path. This means that the cyclic Wilson loop is represented by L_{00}.

$$\begin{aligned}
L_{00} &= \left\langle \widetilde{\mathrm{Tr}} \left[U_0 \left(\frac{\mathbf{r}}{2}, -\frac{\mathbf{r}}{2} \right) U^\dagger_{-\frac{\mathbf{r}}{2}}(\beta, 0) U_0^\dagger \left(\frac{\mathbf{r}}{2}, -\frac{\mathbf{r}}{2} \right) U_{\frac{\mathbf{r}}{2}}(\beta, 0) \right] \right\rangle = \langle W_c \rangle \,, \\
L_{01} &= \left\langle \widetilde{\mathrm{Tr}} \left[U_0 \left(\frac{\mathbf{r}}{2}, -\frac{\mathbf{r}}{2} \right) U_0^\dagger \left(\frac{\mathbf{r}}{2}, -\frac{\mathbf{r}}{2} \right) U_{\frac{\mathbf{r}}{2}}(\beta, 0) \right] \widetilde{\mathrm{Tr}} \left[U^\dagger_{-\frac{\mathbf{r}}{2}}(\beta, 0) \right] \right\rangle \\
&= \left\langle \widetilde{\mathrm{Tr}} \left[U_{\frac{\mathbf{r}}{2}}(\beta, 0) \right] \widetilde{\mathrm{Tr}} \left[U^\dagger_{-\frac{\mathbf{r}}{2}}(\beta, 0) \right] \right\rangle = \langle P_c \rangle \,, \\
L_{10} &= \left\langle \widetilde{\mathrm{Tr}} \left[U_0 \left(\frac{\mathbf{r}}{2}, -\frac{\mathbf{r}}{2} \right) U^\dagger_{-\frac{\mathbf{r}}{2}}(\beta, 0) U_0^\dagger \left(\frac{\mathbf{r}}{2}, -\frac{\mathbf{r}}{2} \right) \right] \widetilde{\mathrm{Tr}} \left[U_{\frac{\mathbf{r}}{2}}(\beta, 0) \right] \right\rangle = \langle P_c \rangle \,, \\
L_{11} &= \left\langle \widetilde{\mathrm{Tr}} \left[U^\dagger_{-\frac{\mathbf{r}}{2}}(\beta, 0) \right] \widetilde{\mathrm{Tr}} \left[U_0 \left(\frac{\mathbf{r}}{2}, -\frac{\mathbf{r}}{2} \right) U_0^\dagger \left(\frac{\mathbf{r}}{2}, -\frac{\mathbf{r}}{2} \right) \right] \widetilde{\mathrm{Tr}} \left[U_{\frac{\mathbf{r}}{2}}(\beta, 0) \right] \right\rangle = \langle P_c \rangle \,.
\end{aligned}$$

An illustration of this is given in figure 5.3. We can see that all other options of path ordering lead to the same loop function: the expectation value of two traced Polyakov loops, or as we will call it, the Polyakov loop correlator P_c (also shown in figure 5.1 on the right). Now, if we would take into account additional intersection points along the string, this would essentially give nothing new, because any choice of path ordering different from the cyclic Wilson loop contour will lead to the Polyakov loop correlator. Furthermore, it is reasonable to take the renormalization matrix of intersection angles $(0, \pi)$ to be unity, since both possible path orderings of an otherwise smooth loop with this intersection are finite. This is, because the contour can either be smooth at this point, which does not give rise to divergences, or have two cusps of angle 0, which are also finite (compare equation (2.5)). This means that we can disregard any intersection point of angles $(0, \pi)$, because the tensor components this would create transform trivially under renormalization. So the case of considering $N \to \infty$ intersection points along the string is completely analogous to having just two at either string endpoint.

Instead of working with the tensor L_{ij} we can also represent it by a four component vector $L = (L_{00}, L_{01}, L_{10}, L_{11})$, which gets renormalized by the tensor product of the two renormalization matrices. Since the angles at both ends of the string are equal, also the renormalization matrices have to be equal.

$$\begin{pmatrix} W_c^{(R)} \\ P_c^{(R)} \\ P_c^{(R)} \\ P_c^{(R)} \end{pmatrix} = \left(\begin{array}{c|c} Z_{00}\begin{pmatrix} Z_{00} & Z_{01} \\ Z_{10} & Z_{11} \end{pmatrix} & Z_{01}\begin{pmatrix} Z_{00} & Z_{01} \\ Z_{10} & Z_{11} \end{pmatrix} \\ \hline Z_{10}\begin{pmatrix} Z_{00} & Z_{01} \\ Z_{10} & Z_{11} \end{pmatrix} & Z_{11}\begin{pmatrix} Z_{00} & Z_{01} \\ Z_{10} & Z_{11} \end{pmatrix} \end{array}\right) \begin{pmatrix} W_c \\ P_c \\ P_c \\ P_c \end{pmatrix} . \tag{5.2}$$

Since the Polyakov loop correlator is already finite, having neither cusps nor intersections, and we are employing minimal subtraction, its renormalized value is given by $P_c^{(R)} = P_c$. From this it immediately follows that Z_{10} has to be zero, otherwise $P_c^{(R)}$ would depend on W_c.

$$\begin{pmatrix} W_c^{(R)} \\ P_c \\ P_c \\ P_c \end{pmatrix} = \begin{pmatrix} Z_{00}^2 & Z_{00}Z_{01} & Z_{00}Z_{01} & Z_{01}^2 \\ 0 & Z_{00}Z_{11} & 0 & Z_{01}Z_{11} \\ 0 & 0 & Z_{00}Z_{11} & Z_{01}Z_{11} \\ 0 & 0 & 0 & Z_{11}^2 \end{pmatrix} \begin{pmatrix} W_c \\ P_c \\ P_c \\ P_c \end{pmatrix} . \tag{5.3}$$

The three equations involving P_c require $Z_{11} = 1$ and $Z_{01} = 1 - Z_{00}$ (or equivalently $Z_{11} = -1$ and $Z_{01} = -1 - Z_{00}$), which leaves only one independent renormalization constant $Z = Z_{00}^2$. So the renormalization condition for the cyclic Wilson loop and the Polyakov loop correlator reads (in compact form):

$$\begin{pmatrix} W_c^{(R)} \\ P_c \end{pmatrix} = \begin{pmatrix} Z & (1-Z) \\ 0 & 1 \end{pmatrix} \begin{pmatrix} W_c \\ P_c \end{pmatrix} . \tag{5.4}$$

Now, before we can start to determine Z, we first have to calculate P_c. We will do this in Coulomb gauge, so that we can take over results from our cyclic Wilson loop calculations. At $\mathcal{O}(\alpha_s^2)$ the expectation value of the Polyakov loop correlator is equal to twice the expectation value of a single Polyakov loop plus diagrams involving gluon exchange between the quark lines. The one-gluon exchange diagram vanishes, because it is proportional to $(\mathrm{Tr}[T^a])^2 = 0$.

There are two possible two-gluon exchange diagrams (compare figure 5.6 in the last part of this section, without the gluon connecting the strings), however the crossed one gives zero just like diagram 1X. We have not calculated the non-crossed diagram for the Wilson loop explicitly, because it is reducible (keep in mind that the exponentiation theorem does not apply to the correlator of two loops). But it is the only diagram which can contribute to the exponentiation of the tree level one-gluon exchange, due to 1X being zero, so its value without colour factor must be given by $\frac{\alpha_s^2}{2r^2T^2}$, which is the second order expansion of that exponential. However, the colour factors are different. For the Polyakov loop correlator we get:

$$\begin{aligned} \widetilde{\mathrm{Tr}}[T^aT^b]\widetilde{\mathrm{Tr}}[T^bT^a] =& \frac{T_F^2}{N_c^2}\delta^{ab}\delta^{ba} = \frac{T_F^2}{N_c^2}(N_c^2-1) = -\frac{T_F^2}{N_c^2}(N_c^4 - 2N_c^2 + 1) + \frac{T_F^2}{N_c^2}(N_c^4 - N_c^2) \\ =& -\left(C_F^2 - \frac{1}{2}C_FC_A\right) . \end{aligned} \tag{5.5}$$

So up to $\mathcal{O}(\alpha_s^2)$ we have:

$$P_c = 1 - \left(C_F^2 - \frac{1}{2}C_FC_A\right)\frac{\alpha_s^2}{2r^2T^2} + 2\widetilde{P}_L . \tag{5.6}$$

$\widetilde{P}_L$ stands for any terms coming from the Polyakov loop expectation value, but its exact value is not important for our analysis. It can be found for example in references [8], [9]. At order $\mathcal{O}(\alpha_s^2)$ it is given by the thermal part of one gluon self energy insertion into diagrams b) or c) of the tree level Wilson loop,

and in order to calculate it one has to take care of the infrared divergences arising in thermal field theory. We will not attempt that calculation here, but just present the result for the sake of completeness.

$$\widetilde{P}_L = \frac{C_F \alpha_s m_D}{2T} + C_F \alpha_s^2 \left[C_A \left(\frac{1}{4} + \ln \frac{m_D}{T} \right) - T_F n_f \ln 2 \right] \tag{5.7}$$

$$m_D^2 = \frac{4\pi}{3} \alpha_s T^2 (C_A + T_F n_f) \tag{5.8}$$

Let us also recall the unrenormalized result for the cyclic Wilson loop. In order to make the expression more concise, we will use the abbreviations f.t. for finite terms and th.p. for thermal part as well as represent the contribution coming from the gluon self energy by writing it simply as a general functional $F[\Pi]$. Note that since we consider the contributions that are also present in the Polyakov loop separately as $2\widetilde{P}_L$, the one-loop one-gluon exchange diagram will also have an infrared divergence which makes resummations necessary. So $F[\Pi]$ may stand for whatever we get from this calculation, while its details are unimportant for the treatment of the ultraviolet divergences.

$$W_c = 1 + \frac{C_F \alpha_s}{rT} + \frac{C_F^2 \alpha_s^2}{2 r^2 T^2} + C_F C_A \alpha_s^2 + \frac{C_F \alpha_s}{rT} \left(\frac{C_A \alpha_s}{\pi \varepsilon} + \text{f.t.} + \text{th.p.} + F[\Pi] \right) + 2\widetilde{P}_L + \mathcal{O}(\alpha_s^3) \,. \tag{5.9}$$

We can also expand the renormalization constant Z in powers of α_s:

$$Z = 1 + Z_1 \alpha_s + Z_2 \alpha_s^2 + \dots \tag{5.10}$$

Sometimes we will for simplicity also refer to these expansion terms Z_i as renormalization constants, since the presence or absence of an index should make clear whether we mean the whole expression or just a single term.

Now, at $\mathcal{O}(\alpha_s^2)$ we get for the renormalized cyclic Wilson loop:

$$\begin{aligned} W_c^{(R)} =& Z W_c + (1 - Z) P_c \\ =& 1 + \frac{C_F \alpha_s}{rT} + \frac{C_F^2 \alpha_s^2}{2 r^2 T^2} + C_F C_A \alpha_s^2 + \frac{C_F \alpha_s}{rT} \left(\frac{C_A \alpha_s}{\pi \varepsilon} + Z_1 \alpha_s + \text{f.t.} + \text{th.p.} + F[\Pi] \right) + 2\widetilde{P}_L \,. \end{aligned} \tag{5.11}$$

Since we have used the $\overline{\text{MS}}$-scheme for the vacuum polarization, we should also use that for cusp or intersection point divergences, so we have to take

$$Z_1 = -\frac{C_A}{\pi \overline{\varepsilon}} = -\frac{C_A}{\pi} \left(\frac{1}{\varepsilon} - \gamma_E + \ln 4\pi \right) \tag{5.12}$$

in order to make $W_c^{(R)}$ finite.

As we already commented when calculating diagram 3X, the finite terms coming from the $\mathcal{O}(\varepsilon^1)$ expansion of the tree level diagram a) can now be neglected, because it is no longer multiplied by a divergent quantity. So our expression for the renormalized cyclic Wilson loop reads:

$$\begin{aligned} \ln \langle W_c \rangle =& \frac{C_F \alpha_s}{rT} \Bigg\{ 1 + \frac{\alpha_s}{4\pi} \left[\left(\frac{31}{9} C_A - \frac{20}{9} T_F n_f \right) + \left(\frac{11}{3} C_A - \frac{4}{3} T_F n_f \right) \left(\ln \mu^2 r^2 + 2\gamma_E \right) \right] + \\ & + \frac{\alpha_s C_A}{\pi} \left[1 + 2\gamma_E - \ln 4 + 2 \ln \mu^2 r^2 + \sum_{n=1}^{\infty} \frac{2(-1)^n \zeta(2n)}{n(4n^2 - 1)} (rT)^{2n} \right] \Bigg\} + \\ & + \frac{4\pi \alpha_s C_F}{T} \int_k \frac{e^{i\mathbf{r}\cdot\mathbf{k}} - 1}{(\mathbf{k}^2)^2} \left(-\Pi_{00}^{(T)}(0, \mathbf{k}) \right) + C_F C_A \alpha_s^2 \quad + \mathcal{O}\left(\alpha_s^3\right) \,. \end{aligned} \tag{5.13}$$

This in itself may not yet be convincing enough that we have found the right renormalization procedure, since the only contribution from the Polyakov loop correlator was $-Z_1 \alpha_s$ to cancel the respective term

from the cyclic Wilson loop. We could have used any quantity equal to $1 + \mathcal{O}(\alpha_s^2)$ for that. So let us move on to $\mathcal{O}(\alpha_s^3)$.

We will not attempt to give a full expression for the cyclic Wilson loop at $\mathcal{O}(\alpha_s^3)$, but focus on the divergent contributions and how they are cancelled. For this a short discussion about different types of divergences and their origin is in order. We will summarize here the more detailed analysis found in references [16] and [20].

The exponentiation theorem allows us to only consider 2PI diagrams, which give the logarithm of the cyclic Wilson loop. Divergences come from integration regions, where two or more vertices are contracted together at one point on the contour. The superficial degree of divergence for such a configuration is

$$\omega = 1 - N_{ex} \tag{5.14}$$

at a smooth point and

$$\omega = -N_{ex} \tag{5.15}$$

at a singular point, where N_{ex} stands for the number of propagators, called external lines, which are connecting to a vertex with a finite distance from the contraction point.

Now there are three possible scenarios:

- all vertices are contracted at a smooth point, which leads to a linear divergence,
- all vertices but one are contracted at a smooth point, which leads to a logarithmic divergence, which we will call here first kind,
- all vertices are contracted at a singular point, which also gives a logarithmically divergent contribution, called second kind.

The terms linear and logarithmic apply once subdivergences have been removed.

The linear divergences are proportional to the length of the contour and can be removed by introducing a loop mass, as we already saw in the discussion of the cusp divergences of the vacuum Wilson loop. Multiplying the loop function by the exponential of this mass times the length of the loop, these divergences can be absorbed into the mass term. In dimensional regularization they are removed automatically, so we need not worry about those.

The second kind of logarithmic divergences are our main point of interest and their renormalization properties have been shown in reference [20]. These are the cusp or intersection divergences and we see that they only come from configurations where all of the vertices, or in the case of subdivergences all vertices of some constituents without external lines, approach the singular point.

But let us first comment on the first kind of logarithmic divergences. It has been shown by [16], that these divergences can be removed by using renormalized fields and couplings. In our previous calculation in Coulomb gauge this just amounted to renormalizing the gluon self energy. But in other gauges we need to be more careful, because also other diagrams can contribute to this kind of divergence.

Usually one can implement charge renormalization by simply replacing the coupling constant through its renormalized value via $g = Z_1 Z_3^{-\frac{3}{2}} g^{(R)}$ in the full unrenormalized expression at a given order in α_s, where (in a covariant gauge) Z_1 is the three-gluon vertex renormalization constant and $A = Z_3^{\frac{1}{2}} A^{(R)}$ defines the gluon field renormalization constant. At the level of the Feynman diagrams this means that we are inserting the renormalization constant Z_1 at every three-gluon vertex, while the constants $Z_3^{-\frac{1}{2}}$ from the vertices at both ends of a bare gluon propagator turn it into a renormalized propagator. The relations between renormalization constants following from the Slavnov-Taylor identities ensure that the same happens not only at three-gluon vertices, but also at the other vertices. This means that once we have found the relation between bare and renormalized charge, we no longer have to think about counterterms, because all their contributions are already included in the substitution of the charge. However, in the following we would like to distinguish exactly where divergences come from and how they are cancelled, so when we consider logarithmic divergences of the first kind, we will stick to the

cancellation by counterterms. Note also, that in addition to the usual ones we get a line vertex counterterm $(Z_1 Z_3^{-1} - 1)$, which comes from $gA = Z_1 Z_3^{-1} g^{(R)} A^{(R)}$.

We did not have to include this counterterm in our previous calculations, because we did not encounter any divergences at order $\mathcal{O}(\alpha_s^2)$ that needed it to be removed. In Coulomb gauge, line vertex corrections such as diagrams A2 and 1T for example are zero on their own, while E2 and 2T cancel because of cyclicity. Since in Coulomb gauge A_0 and $\mathbf{A}$ are treated differently, their field renormalization constants may also differ, and the absence of divergences at the quark line vertices implies $gA_0 = g^{(R)} A_0^{(R)}$, at least at this order in α_s. But for $\mathbf{A}$ we do get a line vertex counterterm, which is needed to make some higher order diagrams finite, as we will see in a moment. Let us also note that, while field and vertex renormalization constants may change in different gauges, the relation between the bare charge and its renormalized value is gauge independent in an appropriate renormalization scheme such as minimal subtraction.

In Feynman gauge, the fields A_0 and $\mathbf{A}$ are treated equally, so the corresponding renormalization constants are also equal. And indeed, diagram 1T is divergent in Feynman gauge and its logarithmic divergence of the first kind is removed by the line vertex counterterm.

Now we can turn to the second kind of logarithmic divergences. Since we would like our discussion not to depend on a specific choice of gauge, we will start by considering, which diagrams can in principle contribute to this divergence. We know that it only appears when all vertices of a diagram or at least of some constituents are drawn close together at an intersection point. If every vertex of a diagram is contracted at the intersection, then its contribution cancels because of cyclicity in all cases where at least one vertex is on the string. If, however, all vertices are on a quark line, then this diagram contributes equally to the Polyakov loop, and therefore must be finite after charge renormalization. This means that a connected diagram cannot contribute to the intersection divergence, because it either has all vertices close to an intersection and thus gives no divergent contribution, or it has some vertices with a finite distance from the intersection and therefore too many external lines to be divergent.

So diagrams with an intersection divergence have to be unconnected and only some of their constituents contribute to the divergence. This means that we can obtain every such diagram of a given order in α_s by taking lower order diagrams, which are finite after charge renormalization, and adding further constituents in such a way, that their line vertices can be drawn together at an intersection without crossing any line vertex of the finite diagram, since this would provide external lines and there would be no divergence.

In our usual representation of the cyclic Wilson loop as a rectangle, the vertices of the added diagrams may approach both the left and the right corners, since those points are identified. However, if all vertices approach only the left or only the right corner, then the diagram is two-particle reducible, so the added constituents should have vertices both on the left and on the right hand side. Note that the finite diagrams need not necessarily be 2PI, since adding constituents will often make them irreducible.

We can also state that diagrams which cancel because of cyclicity also do so after we add constituents around the corners. We can add the new constituents only to the corner of that quark line the original diagram already connects to, because otherwise it would be reducible. But then the conditions for cyclicity cancellation are still fulfilled, because there is still no connection to the other quark line. For diagrams which also contribute to the Polyakov loop, there is no way to add constituents around the corners and get a 2PI diagram, so we also do not have to consider those.

In order to illustrate these statements, we will compare the contributions to the intersection divergence in Coulomb and Feynman gauge at $\mathcal{O}(\alpha_s^2)$ before going on to $\mathcal{O}(\alpha_s^3)$. There is only one lower order diagram, the tree level one-gluon exchange between the quark lines. Its value is gauge independent, since all other tree level diagrams cancel because of cyclicity or do not contain the scale r and therefore cannot contribute to the gauge independent tree level result for the cyclic Wilson loop. The diagrams we obtain when we add another gluon whose vertices may freely approach the corners are 3X, 1T and 1T'.

In Coulomb gauge 1T and 1T' give zero and 3X is the only diagram having a logarithmic divergence of the second kind. In Feynman gauge we notice that the divergence of 3X amounts to only half of that value (compare the calculations of tree level diagrams e)+f) in appendix D). So the other half must come from 1T and 1T', which are equal. And indeed, after subtracting the logarithmic divergences of the first

kind, which are also present in these diagrams, by means of the line vertex counterterm, we get exactly the other half of the intersection divergence (compare appendix E.7).

Before we continue, let us also comment on the fact that the intersection divergence in diagrams 1T and 1T' is closely related to the concept of 2PI diagrams. One might wonder why there is a divergence at all, since the contour closes smoothly at the intersection point. To clarify this issue, figure 5.4 shows diagram 1T with the string drawn in the middle of the rectangle representing the cyclic Wilson loop. The contour is closed with the endpoints to the right and the left being identified.

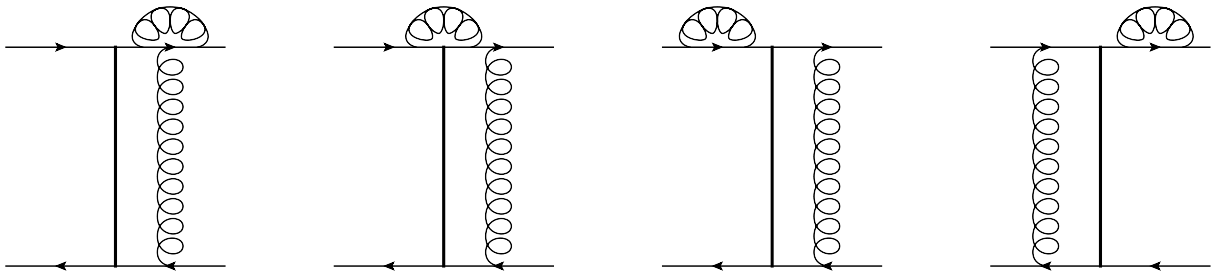

Figure 5.4: Illustration of the intersection divergence in 1T.

The figure on the left shows the basic configuration of 1T. We know that the divergence arises when the vertices of the gluon not connecting the quark lines approach the intersection from different directions, because otherwise the other gluon would be an external line. If we move the rightmost vertex all the way to the other end of the quark line, we get the configuration shown in the second diagram. Because those two vertices can only get close together at the intersection point, the divergence is logarithmic of the second kind.

If we could transport the divergent configuration across the intersection point, this would turn it into a linear divergence, vanishing in dimensional regularization (compare [16], [20]). However, the diagrams necessary for that, which are shown on the right of figure 5.4, are two-particle reducible. This means that if all three diagrams had the same colour factor, their contribution to the intersection divergence would indeed vanish, and in fact it does for the Abelian part of 1T, the part that is used in the exponentiation of its constituents. Only the 2PI rest with the colour connected coefficient remains, and its divergence contributes to the intersection divergence.

The Polyakov loop correlator does not exponentiate like the cyclic Wilson loop, so here this line of argument does not work. Diagram 1T vanishes for the Polyakov loop correlator because of the trace of a single colour matrix. But we can ignore this for now or simply replace the gluon connecting quark and antiquark line by a more complicated structure for which the trace does not vanish. The important point is that in this case the diagrams corresponding to figure 5.4 all have the same colour factor, so we can transport the divergent configuration across the (arbitrary) endpoint of the loop and the logarithmic divergence is turned into a linear one and removed accordingly. This is as expected, since the Polyakov loop correlator cannot have logarithmic divergences of the second kind.

After this short digression, let us return to the discussion of the intersection divergences of the cyclic Wilson loop at $\mathcal{O}(\alpha_s^3)$. We have seen that Coulomb gauge is advantageous for calculations, because some of the potentially divergent diagrams, and also some others like for example 1X, vanish automatically. In addition, the logarithmic divergences of the first and second kind are not entangled, like for diagram 1T in Feynman gauge for instance, at least not at this order in α_s. But we want to keep our discussion general and not depend on a specific choice of gauge, so we will consider all diagrams that can in principle contribute to the divergence.

However, in order to save space, we will not show all of those diagrams. Since we can get another diagram contributing to the intersection divergence by simply moving some of the vertices across the intersection from string to quark line or from quark line to string, it suffices to give only one of them. The colour factors remain the same, since we do not change the ordering of the colour matrices, except possibly for a cyclic permutation, which does not affect the trace. We will call these diagrams of the same type and the displayed diagrams representatives of that type.

We should also point out that, while the insertion of additional constituents around the intersections may interfere with the contour integrations of the finite diagrams, the divergence comes from integration regions, where all of the new vertices are infinitesimally close to the intersection. So if we just look at the divergent part, then this must be given by a divergent factor multiplying the value of the original diagram, and the changes in the contour integration only amount to finite corrections. The divergent factors we get, when we add all diagrams of the same type, depend only on the additional constituents and not on the finite diagram, and their contributions are gauge independent, once we sum over all constituents of a certain order in α_s.

Now, let us start with some obvious cancellations. Both W_c and P_c are equal to 1 at zeroth order in α_s, so we have $Z + (1 - Z) = 1$, which ensures that all contributions from the renormalization constant that are not multiplied by contributions from the loops cancel. The same happens for diagrams, which occur in both the cyclic Wilson loop and the Polyakov loop correlator and have the same colour factor. These are the diagrams involving only one quark line and their contribution has been included as $2\widetilde{P}_L$ in equations (5.6) and (5.9) (see for example figure 5.5, the two diagrams on the right). At higher orders one should better write $(P_L^2 - 1)$ or $(\exp[2\widetilde{P}_L] - 1)$ instead. This shows that our renormalization procedure does not introduce new divergences at higher orders. All other terms involving the renormalization constant are needed to cancel divergences from the intersections.

We can classify the diagrams contributing to the intersection divergence according to their finite lower order diagrams. At $\mathcal{O}(\alpha_s^3)$ there are only four possibilities: the tree level one-gluon exchange with added constituents of order $\mathcal{O}(\alpha_s^2)$, the one-gluon exchange with one self energy insertion and charge renormalization already performed, the two tree level two-gluon exchange diagrams, and diagrams C1 and C2, each with an added constituent of $\mathcal{O}(\alpha_s)$, which can only be a single gluon. By n-gluon exchange we always mean exchange between the quark lines. We will treat each of these cases in turn.

The cancellation of the divergences from diagrams 3X, 1T, 1T' of the cyclic Wilson loop against the tree level one-gluon exchange times $Z_1\alpha_s$ can be extended without problems to diagrams with any number of self energy terms inserted into the gluon connecting the quark lines. This is illustrated in figure 5.5, where the bubble may stand for any (possibly reducible) self energy diagram. This means that this cancellation is valid also for the full gluon propagator connecting the quark lines. Note that here we have to implement charge renormalization by considering all relevant counterterm diagrams. If we just performed the substitution of the bare charge, we could not separate this case from the next, because this substitution takes care of the logarithmic divergences of the first kind for both cases simultaneously.

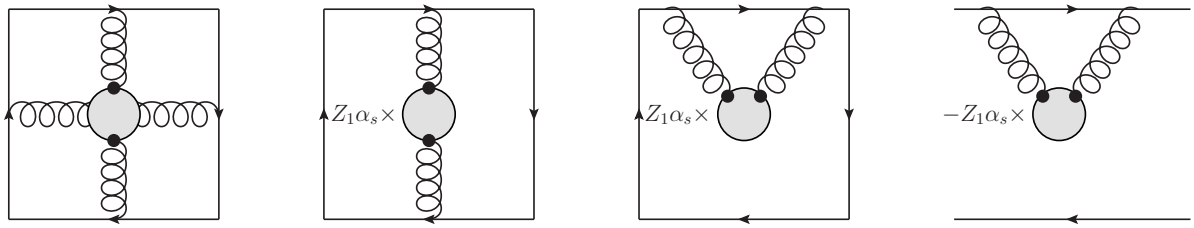

Figure 5.5: Some simple cancellations. The two diagram types on the left cancel in an analogous fashion to the tree level diagrams of W_c. The two diagrams on the right show that contributions involving only one quark line times a renormalization constant cancel between W_c and P_c.

With the two-gluon exchange diagrams, we come to the first non-trivial check of our renormalization procedure. There are two types of 2PI diagrams from the cyclic Wilson loop (see figure 5.6). We will call the type with the two exchanged gluons not crossed γ_{II} and the crossed one γ_X. The crossed one vanishes in Coulomb gauge, but not in general. Without colour factors the sum of the two finite two-gluon exchange diagrams without the added constituent gives just half of the square of the one-gluon exchange, which can be seen by combining the contour integrations. And we already know the divergent factor of a single added gluon from the $\mathcal{O}(\alpha_s^2)$ calculations. So

$$W(\gamma_{II}) + W(\gamma_X) \sim \left(\frac{\alpha_s^2}{2r^2T^2}\right)\left(-\frac{2\alpha_s}{\pi\varepsilon}\right), \tag{5.16}$$

where the $\sim$ sign is supposed to say "includes a term" rather than "is proportional to". This relation is gauge independent.

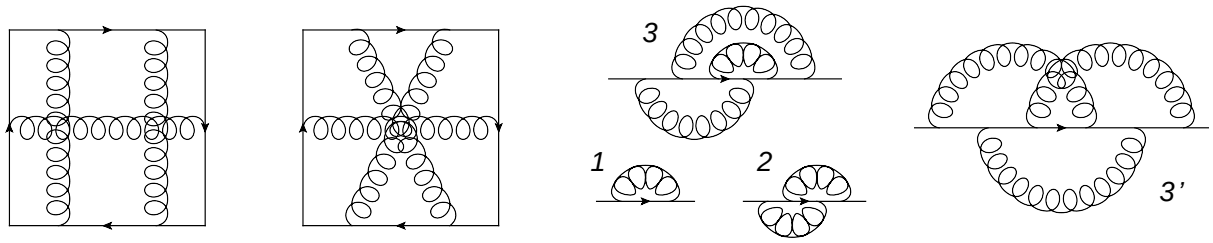

Figure 5.6: The two divergent 2PI two-gluon exchange diagram types of $\mathcal{O}(\alpha_s^3)$ are shown on the left. The diagrams on the right show the colour structure more explicitly. 3 and 3' correspond to the non-crossed and the crossed diagram on the left, respectively. 1 and 2 show the partial diagrams of 3 and 3', which are necessary for the determination of the colour connected coefficient.

But we have yet to compute the colour connected coefficients of these diagrams. Their colour structure is made clearer by representing γ_{II} and γ_X through the colour diagrams γ_3 and $\gamma_{3'}$, respectively, which are also shown in figure 5.6.

$$\begin{aligned}
C(\gamma_3) &= \widetilde{\mathrm{Tr}}[T^aT^bT^cT^aT^cT^b] \\
&= \widetilde{\mathrm{Tr}}[T^aT^bT^aT^cT^cT^b] + if^{cad}\widetilde{\mathrm{Tr}}[T^aT^bT^dT^cT^b] \\
&= C_F\widetilde{\mathrm{Tr}}[T^aT^bT^aT^b] + if^{cad}\widetilde{\mathrm{Tr}}[T^aT^bT^bT^dT^c] - f^{cad}f^{bae}\widetilde{\mathrm{Tr}}[T^eT^bT^dT^c] \\
&= C_F\left(C_F^2 - \frac{1}{2}C_FC_A\right) - \frac{1}{2}C_FC_A\widetilde{\mathrm{Tr}}[T^dT^d] + \frac{1}{4}C_A^2\widetilde{\mathrm{Tr}}[T^aT^a] \\
&= C_F^3 - C_F^2C_A + \frac{1}{4}C_FC_A^2\,, \qquad (5.17) \\
C(\gamma_{3'}) &= \widetilde{\mathrm{Tr}}[T^aT^bT^cT^aT^bT^c] \\
&= \widetilde{\mathrm{Tr}}[T^bT^cT^aT^aT^bT^c] + if^{abd}\widetilde{\mathrm{Tr}}[T^dT^cT^aT^bT^c] + if^{acd}\widetilde{\mathrm{Tr}}[T^bT^dT^aT^bT^c] \\
&= \left(C_F - \frac{1}{2}C_A - \frac{1}{2}C_A\right)\widetilde{\mathrm{Tr}}[T^bT^cT^bT^c] \\
&= (C_F - C_A)\left(C_F^2 - \frac{1}{2}C_FC_A\right) \\
&= C_F^3 - \frac{3}{2}C_F^2C_A + \frac{1}{2}C_FC_A^2\,. \qquad (5.18)
\end{aligned}$$

Now, in order to get the colour connected coefficients, we have to subtract the parts that have already been used for the exponentiation of their partial diagrams. These partial diagrams are shown as γ_1 and γ_2 in figure 5.6. The contributions we have to subtract are determined by the product of the colour connected coefficients of the partial diagrams, the number of possible distributions of these partial diagrams on γ_3 and $\gamma_{3'}$, and the coefficients we get from expanding the exponential (compare appendix C). There are 3! possible ways we can distribute three γ_1 on either γ_3 or $\gamma_{3'}$, but this factor is cancelled by $\frac{1}{3!}$, the coefficient of $(\gamma_1)^3$ in the expansion of the exponential. The coefficient in this expansion in front of $\gamma_1\gamma_2$ is 1, and there are two ways to distribute one γ_1 and one γ_2 on γ_3, and three ways to distribute them on $\gamma_{3'}$. So the colour connected coefficients are:

$$\begin{aligned}
\widetilde{C}(\gamma_3) =& C(\gamma_3) - \frac{3!}{3!}\widetilde{C}(\gamma_1)^3 - 2\widetilde{C}(\gamma_1)\widetilde{C}(\gamma_2) \\
=& C_F^3 - C_F^2C_A + \frac{1}{4}C_FC_A^2 - C_F^3 - 2C_F\left(-\frac{1}{2}C_FC_A\right) \\
=& \frac{1}{4}C_FC_A^2\,, \qquad (5.19) \\
\widetilde{C}(\gamma_{3'}) =& C(\gamma_3) - \frac{3!}{3!}\widetilde{C}(\gamma_1)^3 - 3\widetilde{C}(\gamma_1)\widetilde{C}(\gamma_2) \\
=& C_F^3 - \frac{3}{2}C_F^2C_A + \frac{1}{2}C_FC_A^2 - C_F^3 - 3C_F\left(-\frac{1}{2}C_FC_A\right) \\
=& \frac{1}{2}C_FC_A^2\,. \qquad (5.20)
\end{aligned}$$

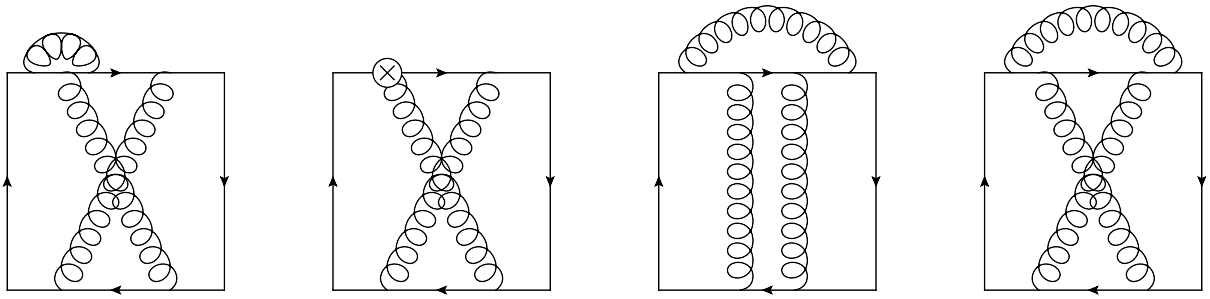

Figure 5.7: Vertex corrections to the two-gluon exchange diagrams. The two diagrams on the right belong to the same types as those shown in figure 5.6

Having determined the colour connected coefficient, we can collect all relevant contributions to the two-gluon exchange from the cyclic Wilson loop. We have:

- the renormalization constant Z_1 multiplying the second order expansion term of the tree level one-gluon exchange: $ZW_c \sim \left(-\frac{C_A\alpha_s}{\pi\varepsilon}\right)\left(\frac{C_F^2\alpha_s^2}{2r^2T^2}\right)$,
- the renormalization constant Z_1 multiplying diagram 1X:
  $ZW_c \sim \left(-\frac{C_A\alpha_s}{\pi\varepsilon}\right)\left(-\frac{1}{2}C_FC_AW(\gamma_{1X})\right) = -\frac{1}{4}C_FC_A^2W(\gamma_X)$,
- the tree level one-gluon exchange diagram times the sum of 3X, 1T, 1T' (after charge renormalization) from the expansion of the exponential: $W_c \sim \left(\frac{C_F\alpha_s}{rT}\right)^2\left(\frac{C_A\alpha_s}{\pi\varepsilon}\right)$,
- the divergent contributions from diagram types γ_{II} and γ_X:
  $W_c \sim \frac{1}{4}C_FC_A^2W(\gamma_{II}) + \frac{1}{2}C_FC_A^2W(\gamma_X)$.

Summing up all these contributions, we get

$$\begin{aligned} ZW_c \sim & \frac{1}{4}C_FC_A^2W(\gamma_{II}) + \frac{1}{2}C_FC_A^2W(\gamma_X) - \frac{1}{4}C_FC_A^2W(\gamma_X) - \frac{C_F^2\alpha_s^2}{2r^2T^2}\frac{C_A\alpha_s}{\pi\varepsilon} + \frac{C_F^2\alpha_s^2}{r^2T^2}\frac{C_A\alpha_s}{\pi\varepsilon} \\ = & \left(C_F^2 - \frac{1}{2}C_FC_A\right)\frac{\alpha_s^2}{2r^2T^2}\frac{C_A\alpha_s}{\pi\varepsilon}\,. \end{aligned} \tag{5.21}$$

This is exactly cancelled by the remaining contribution coming from the Polyakov loop correlator:

$$(1-Z)P_c \sim -\left(C_F^2 - \frac{1}{2}C_FC_A\right)\frac{\alpha_s^2}{2r^2T^2}\frac{C_A\alpha_s}{\pi\varepsilon}\,. \tag{5.22}$$

This result in particular is a strong confirmation for the renormalization procedure presented above.

Before we go on, we will give a few comments clarifying the relation between logarithmic divergences of the first and second kind in the two-gluon exchange diagrams. Diagram 5.7 gives a few examples. The diagram on the left, and also the corresponding not crossed diagram, has only a logarithmic divergence of the first kind, which is removed by the counterterm diagram next to it. We see that in this case there is no way we can contract two vertices on the intersection without external lines. Accordingly the two diagrams on the right, which are of the same type as those in figure 5.6, have no logarithmic divergence of the first kind, since here there are always two external lines when we draw vertices together on the quark line. So first and second kind of logarithmic divergences are not entangled for the two-gluon exchange diagrams at $\mathcal{O}(\alpha_s^3)$.

The next diagrams we have to consider for the intersection divergence are the ones we obtain from C1 and C2 after adding another gluon around the corners. The two types of diagram, called C11 and C12 for short, are shown on the left of figure 5.8. We could combine the integration regions of these two representatives, so that the contribution from the gluon connecting the strings factors out, and say that they belong to the same type. However, this may not be possible for higher order diagrams and considering them separately stresses the point, that the leftmost type of diagrams contributes to the divergence at the upper intersection, and the one next to it contributes to the divergence at the lower intersection.

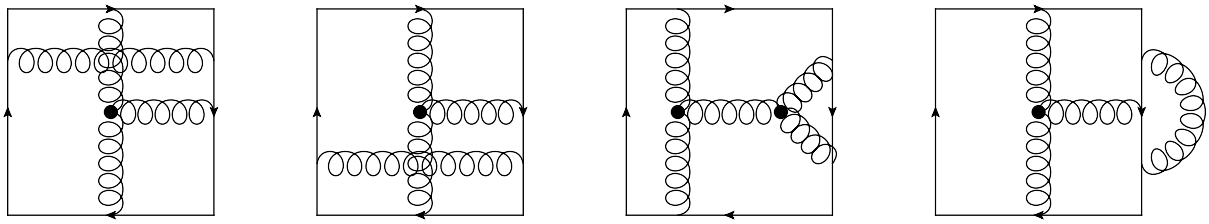

Figure 5.8: Diagram types similar to C1 with logarithmic divergences of the second kind are shown on the left. The diagrams on the right have first kind logarithmic divergences.

Both contributions are equal and summing up all diagrams of both types leads to the divergent factor of a single added gluon we obtained before.

First we have to determine the colour connected coefficients. Because of the cyclicity of the trace, both colour factors are equal.

$$\begin{aligned} C(\gamma_{C11/C12}) =& f^{bcd}\widetilde{\mathrm{Tr}}[T^aT^bT^cT^aT^d] \\ =& \frac{i}{2}C_A\widetilde{\mathrm{Tr}}[T^aT^dT^aT^d] \\ =& \frac{i}{2}C_A\left(C_F^2-\frac{1}{2}C_FC_A\right), \end{aligned} \tag{5.23}$$

$$\begin{aligned} \widetilde{C}(\gamma_{C11/C12}) =& C(\gamma_{C11/C12}) - \widetilde{C}(\gamma_1)\widetilde{C}(\gamma_{C1}) \\ =& \frac{i}{2}C_A\left(C_F^2-\frac{1}{2}C_FC_A\right) - \frac{i}{2}C_F^2C_A \\ =& -\frac{i}{4}C_FC_A^2\,. \end{aligned} \tag{5.24}$$

The case of C2 is not shown in figure 5.8, but completely analogous. Together with the term from the renormalization constant multiplying diagrams C1 and C2 we have:

$$ZW_c \sim -\frac{i}{4}C_FC_A^2\frac{C_FC_A\alpha_s^2}{\frac{i}{2}C_FC_A}\left(-\frac{2\alpha_s}{\pi\varepsilon}\right) + C_FC_A\alpha_s^2\left(-\frac{C_A\alpha_s}{\pi\varepsilon}\right) = 0\,. \tag{5.25}$$

So, again our procedure has worked fine for those diagrams.

At last, the second order expansion term Z_2 of the renormalization constant Z times the tree level diagram of the cyclic Wilson loop gives a term

$$ZW_c \sim Z_2\alpha_s^2\frac{C_F\alpha_s}{rT}\,. \tag{5.26}$$

This will be used to cancel divergent contributions from diagrams with a one-gluon exchange and constituents of $\mathcal{O}(\alpha_s^2)$ added. The different diagram types are depicted in figure 5.9. The sum of the divergent terms of all those diagrams (after charge renormalization) determines the value of Z_2.

We should comment on the left and right diagram in the first row of figure 5.9. The diagram type on the left has two different kinds of divergences related to the intersection, corresponding to different regions of the contour integration parameters: either all four vertices of the added gluons approach the intersection, or only the two vertices of one gluon do, while the vertices of the other gluon remain at a finite distance. We could call the first case an overall divergence and the second case a subdivergence, since this adequately describes the nature of the divergent terms, however, we have already used those expressions in a different context, so this would be inconsistent. The first case does not present problems and will be briefly commented on below, but the second case produces terms like $\frac{1}{\varepsilon}\ln\mu r$ or $\frac{1}{\varepsilon}$ times a thermal part, which cannot be included in the definition of Z_2. However, those are exactly cancelled by the diagram type on the right multiplied by the first order renormalization constant $Z_1\alpha_s$.

We will show this for the thermal part contributions. If we take the thermal part of the gluon propagator not connecting the quark lines in the diagrams of the type depicted on the right of figure 5.9 (diagrams

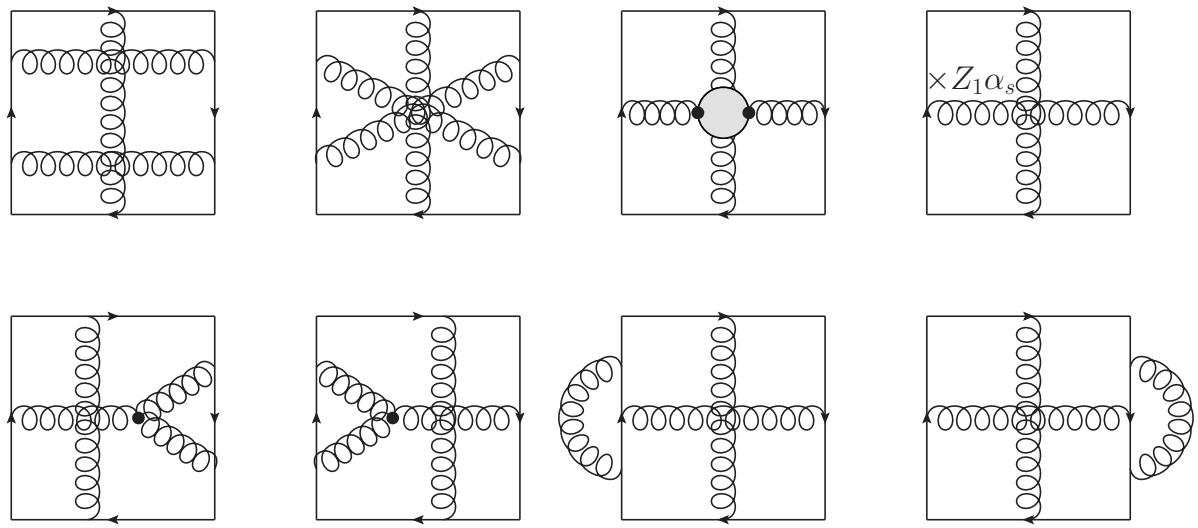

Figure 5.9: Types of diagrams that contribute to the divergence cancelled by Z_2.

3X, 1T, 1T'), then this is finite and their value will be denoted $W(\gamma_{3X})^{(T)}$ (3X stands for the type, not the specific diagram). Then, with the same line of argument as before, adding another gluon around the intersection leads to a divergence which is given by the known factor $\left(-\frac{2\alpha_s}{\pi\varepsilon}\right)$ of a single added gluon times the value of the finite diagrams. The colour connected coefficient can be taken over from the two gluon exchange calculation. Together with the first order renormalization constant, this gives:

$$ZW_c \sim \frac{1}{4}C_F C_A^2 \left(-\frac{2\alpha_s}{\pi\varepsilon}\right) W(\gamma_{3X})^{(T)} - \frac{1}{2}C_F C_A \left(-\frac{C_A\alpha_s}{\pi\varepsilon}\right) W(\gamma_{3X})^{(T)} = 0\,. \tag{5.27}$$

It has been checked that the terms involving $\ln \mu r$ cancel likewise by calculating these diagrams explicitly in Coulomb gauge, but this is quite lengthy and will not be given here. The first case of an intersection divergence, where all four vertices are contracted at the intersection points, should have no dependence on r. For the other diagram types in figure 5.9 this is the only possibility of contributing to the intersection divergence, otherwise there would be external lines, and if we take the thermal part of one of the added gluons, this reduces the superficial degree of divergence by means of one additional power of k in the denominator and thus only gives a finite contribution. So we can assume that Z_2 can indeed be defined as a constant not depending on r or T, however, we will not show this explicitly by calculating the divergent contributions of the diagrams depicted in figure 5.9, since this would go beyond the scope of this thesis.

This completes our discussion of the intersection divergences at $\mathcal{O}(\alpha_s^3)$. All other divergences are logarithmic of the first kind and therefore removed through charge renormalization, according to [16]. We will not give each and every one of them, but only a few examples.

The two diagrams on the right of figure 5.8 show the diagrams contributing to the string vertex correction to diagram C1. The divergence is removed through a line vertex counterterm on the string, which in this case is also necessary in Coulomb gauge. We also see that they cannot contribute to the intersection divergence, as expected, because there is always at least one external line. Every line vertex of the $\mathcal{O}(\alpha_s^2)$ diagrams can be modified in this way and the divergences will be removed through the corresponding counterterms. Inserted gluon self energies or vertex correction diagrams are made finite through gluon propagator or vertex counterterms, respectively.

Similarly, the lower row of diagram types in figure 5.9 has first kind logarithmic divergences, which are removed by counterterms added at the line vertices of the additional gluon in diagrams of type 3X.

Other typical diagrams are shown in figure 5.10. By switching gluons from the left to the right string or vice versa we obtain all connected diagrams with two vertices on the string and one vertex on either quark line. Most of them have at least two external lines when we draw the string vertices together, so they are finite. The only exception is the diagram on the right. The two vertices on the string can get close with only one external line, however, since they can freely move past each other this does not

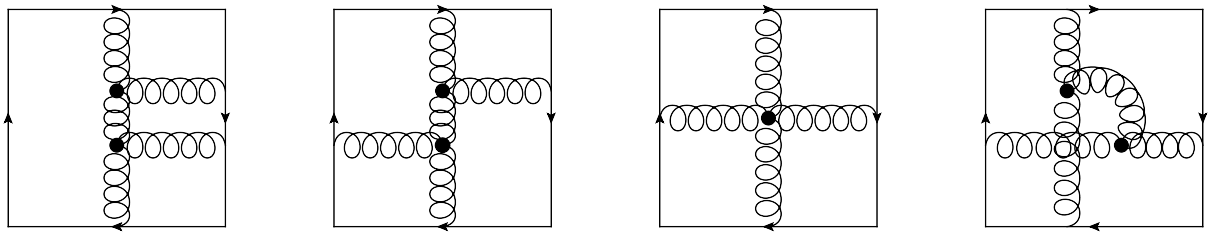

Figure 5.10: Some finite diagrams at $\mathcal{O}(\alpha_s^3)$.

lead to a divergence. To put it another way, the divergences when one vertex approaches the other from different directions have opposite sign and thus vanish. And in any case, the colour factor of this diagram is zero, which can be shown by making use of the Jacobi identity (see appendix A):

$$\begin{aligned} f^{ace}f^{bed}\widetilde{\mathrm{Tr}}[T^aT^bT^cT^d] &= \left(f^{cbe}f^{ead} + f^{bae}f^{ecd}\right)\widetilde{\mathrm{Tr}}[T^aT^bT^cT^d] \\ &= \left[\left(-\frac{i}{2}C_A\right)\left(-\frac{i}{2}C_A\right) + \left(-\frac{i}{2}C_A\right)\left(\frac{i}{2}C_A\right)\right]\widetilde{\mathrm{Tr}}[T^eT^e] \\ &= 0\,. \end{aligned} \tag{5.28}$$

So summing up our discussion, the cyclic Wilson loop is indeed finite, at least up to order $\mathcal{O}(\alpha_s^3)$, after a charge and fields renormalization and after performing the matrix renormalization together with the Polyakov loop correlator. The renormalization matrix depends on only one independent constant via equation (5.4) and this constant can be given as a power series in α_s. The first term in this expansion is given by equation (5.12) and the second has to be determined through the diagrams represented by figure 5.9, where the only thing we did not show explicitly was the independence of this second order term Z_2 on r or T.

6 Conclusions

We have calculated the Wilson loop in the vacuum analytically at $\mathcal{O}(\alpha_s)$ and found that it has cusp divergences, which can be removed through a multiplicative constant. This is in accordance with references [16], [20], and the value of the divergence agrees with [19]. At $\mathcal{O}(\alpha_s^2)$ we have calculated the relevant contributions for the static quark-antiquark potential. It is essentially a Coulomb potential with an additional colour factor C_F and higher order corrections. The result is given in equation (2.8) and agrees with references [22], [23].

In thermal QCD we have analytically calculated the cyclic Wilson loop at $\mathcal{O}(\alpha_s^2)$, except for some thermal contributions which are given as integrals or series expansions for $rT \ll 1$. The result is given in equation (4.28) and we have found that this is also divergent, however, the divergences do not have the form of usual cusp divergences. This is in agreement with the findings of reference [8]. A method for the renormalization of the cyclic Wilson loop is presented, based on the results of references [16] and [20]. It involves the mixing of the cyclic Wilson loop with the Polyakov loop correlator under renormalization, and we have shown explicitly (minus one small caveat) that this method of renormalization is valid at $\mathcal{O}(\alpha_s^3)$. The renormalized value of the cyclic Wilson loop at $\mathcal{O}(\alpha_s^2)$ is given in equation (5.13).

Acknowledgements

I would like to very warmly thank my supervisors Nora Brambilla and Antonio Vairo for their constant support and most instructive lectures, and Jacopo Ghiglieri for being a great help and always having an open ear when I got stuck somewhere.

Appendices

A Formulary and Conventions

In Minkowski space we will use the metric $\eta_{\mu\nu} = \mathrm{diag}(1,-1,-1,-1)$. The transformation to Euclidean space is performed through the substitutions

$$\begin{aligned} \tau &= it & x_i^E &= x_i^M \\ k_0^E &= -ik_0^M & k_i^E &= k_i^M \\ A_0^E &= -iA_0^M & A_i^E &= A_i^M \\ \gamma_0^E &= \gamma_0^M & \gamma_i^E &= i\gamma_i^M \,. \end{aligned} \tag{A.1}$$

The definition of the γ matrices implies $\left[\gamma_\mu^E, \gamma_\nu^E\right] = 2\delta_{\mu\nu}$. We will not display the superscripts E and M in our calculations. The Feynman rules for Euclidean space can be found in many textbooks, for example [28]. Note that there the γ matrices are defined with an additional factor i.

Our definition for the sign of the gauge coupling is given by the covariant derivative

$$D_\mu = \partial_\mu - igA_\mu \,. \tag{A.2}$$

Since we are using dimensional regularization in $d = 3-2\varepsilon$ spatial dimensions (or $D = 4-2\varepsilon$ space-time dimensions), the mass dimensions of the fields and the gauge coupling change in order to make the action a dimensionless quantity:

$$\dim[\psi] = \frac{D-1}{2} = \frac{3}{2} - \varepsilon \,, \tag{A.3}$$

$$\dim[A_\mu] = \frac{D-2}{2} = 1 - \varepsilon \,, \tag{A.4}$$

$$\dim[g] = 1 - \frac{D-2}{2} = \varepsilon \,. \tag{A.5}$$

We would like to work with a dimensionless coupling constant, so we define

$$\alpha_s = \frac{g^2 \mu^{-2\varepsilon}}{4\pi} \tag{A.6}$$

with some arbitrary mass scale μ.

In the modified minimal subtraction scheme, or $\overline{\mathrm{MS}}$-scheme, the counterterms subtract only the divergent parts proportional to

$$\frac{1}{\bar{\varepsilon}} = \frac{1}{\varepsilon} - \gamma_E + \ln 4\pi \,. \tag{A.7}$$

In thermal field theory we have the Matsubara frequencies $k_0 = 2\pi T n_k$, $n_k \in \mathbb{Z}$ for bosonic fields and $q_0 = (2n_q - 1)\pi T$, $n_q \in \mathbb{Z}$ for fermionic fields. The Matsubara sums together with the momentum integrations are abbreviated

$$\sum\!\!\!\!\!\!\int_k \qquad \text{and} \qquad \sum\!\!\!\!\!\!\int_{\{q\}}$$

for bosons and fermions respectively. If we write them separately we use the abbreviations

$$\int_k = \int \frac{\mathrm{d}^d k}{(2\pi)^d} \,, \quad \sum_{k_0} f(k_0) = T \sum_{n_k \in \mathbb{Z}} f(2\pi T n_k) \quad \text{and} \quad \sum_{\{q_0\}} f(q_0) = T \sum_{n_q \in \mathbb{Z}} f\big((2n_q - 1)\pi T\big) \,.$$

And finally, summations without the zero mode for bosons are denoted by

$$\sum\!\!\!\!\!\!\int_k{}' \,.$$

Results from group theory

We have the gauge group $SU(N_c)$ with $N_c = 3$ being the number of colours. The fundamental representation of this group consists of all $N_c \times N_c$ matrices which are unitary and have determinant one. We can represent each group element $\mathcal{V} \in SU(N_c)$ by

$$\mathcal{V} = e^{iT^a\theta^a} \tag{A.8}$$

with a suitable set of real parameters θ^a. The T^a are called the generators of this group in a specific representation.

A complex $N_c \times N_c$ matrix has $2N_c^2$ free real parameters and the requirements of unitarity and unit determinant eliminate $N_c^2 + 1$ of those. This means that we have $N_c^2 - 1$ independent parameters θ^a and therefore $N_c^2 - 1$ independent generators. In the fundamental representation the properties of unitarity and determinant equal one translate to the generators of this representation being hermitian and traceless.

We have

$$\mathrm{Tr}[T^a T^b] = \mathrm{Tr}[T^{a\dagger} T^b] = M^{ab}\,. \tag{A.9}$$

This is the Euclidean scalar product in the N_c^2 dimensional complex vector space of $N_c \times N_c$ matrices and the T^a are independent and hermitian, so M must be a positive symmetric matrix. Therefore it can be diagonalized, which means that the T^a can be chosen to be orthogonal and satisfy the normalization condition

$$\mathrm{Tr}[T^a T^b] = T_F \delta^{ab}\,, \tag{A.10}$$

where T_F is the normalization constant of the fundamental representation. Because the T^a are traceless, they are also orthogonal to the unit matrix. This means that the set $\left\{\frac{1}{\sqrt{N_c}}\mathbb{1}_{N_c}, \frac{1}{\sqrt{T_F}}T^a\right\}$ is an orthonormal base of this vector space with respect to the Euclidean scalar product. Then we can invoke the completeness relation

$$\sum_{i=1}^{N_c^2} |b_i\rangle\langle b_i| = \mathbb{1}_{N_c^2}\,. \tag{A.11}$$

Or written in components

$$\frac{1}{N_c}\delta_{ji}\delta_{kl} + \frac{1}{T_F}T^{a*}_{ji}T^a_{kl} = \delta_{jk}\delta_{il}\,, \tag{A.12}$$

$$T^a_{ij}T^a_{kl} = T_F\left(\delta_{il}\delta_{jk} - \frac{1}{N_c}\delta_{ij}\delta_{kl}\right)\,. \tag{A.13}$$

The structure constants are defined by the Lie algebra of $SU(N_c)$

$$[T^a, T^b] = i f^{abc} T^c\,. \tag{A.14}$$

Using the normalization condition we have

$$f^{abc} = \frac{1}{iT_F}\mathrm{Tr}\Big[[T^a, T^b]\,T^c\Big]\,. \tag{A.15}$$

From this it follows that f^{abc} is antisymmetric in all three components.

From

$$\Big[[T^a, T^b], T^c\Big] + \Big[[T^b, T^c], T^a\Big] + \Big[[T^c, T^a], T^b\Big] = 0 \tag{A.16}$$

follows the Jacobi identity

$$f^{abe}f^{ecd} + f^{bce}f^{ead} + f^{cae}f^{ebd} = 0\,. \tag{A.17}$$

With the Jacobi identity it is easy to show that the $(N_c^2 - 1) \times (N_c^2 - 1)$ matrices

$$(T^a_A)_{bc} = -if^{abc} \tag{A.18}$$

also fulfill the Lie algebra, since

$$\big([T^a_A, T^b_A]\big)_{cd} = -f^{ace}f^{bed} + f^{bce}f^{aed} = f^{abe}f^{ecd} = if^{abe}\,(T^e_A)_{cd}\,. \tag{A.19}$$

So the T^a_A generate another representation of $SU(N_c)$, the so called adjoint representation.

Using the Lie algebra, one can show that the quantity $T^2 = T^a T^a$ commutes with all generators in any representation:

$$\begin{aligned}[T^2, T^b] =& T^a[T^a, T^b] + [T^a, T^b]T^a \\ =& if^{abc}T^aT^c + if^{abc}T^cT^a = i(f^{abc} + f^{cba})T^aT^c = 0\,. \end{aligned} \tag{A.20}$$

Therefore, according to Schur's Lemma, it must be proportional to unity. T^2 is called the quadratic Casimir invariant, while C_F and C_A are its eigenvalues in the fundamental and the adjoint representation, respectively.

So

$$C_F = \frac{1}{N_c}\mathrm{Tr}[T^aT^a] = \frac{T_F}{N_c}\delta^{aa} = \frac{T_F}{N_c}\left(N_c^2 - 1\right)\,, \tag{A.21}$$

$$\begin{aligned} C_A =& \frac{1}{N_c^2-1}\mathrm{Tr}[T^a_A T^a_A] = -\frac{1}{N_c^2-1}f^{abc}f^{acb} \\ =& \frac{1}{N_c^2-1}f^{abc}\frac{1}{iT_F}\mathrm{Tr}\Big[[T^a,T^b]\,T^c\Big] = -\frac{1}{T_F(N_c^2-1)}\mathrm{Tr}\Big[[T^a,T^b][T^a,T^b]\Big] \\ =& -\frac{2}{T_F(N_c^2-1)}\mathrm{Tr}\Big[T^aT^bT^aT^b - T^aT^bT^bT^a\Big] \\ =& -\frac{2}{T_F(N_c^2-1)}\left[T_F\left(\delta_{il}\delta_{jk} - \frac{1}{N_c}\delta_{ij}\delta_{kl}\right)T^b_{jk}T^b_{li} - N_cC_F^2\right] \\ =& \frac{2}{T_F(N_c^2-1)}\left[\frac{T_F}{N_c}N_cC_F + N_cC_F^2\right] = 2\left[\frac{T_F}{N_c} + \frac{T_F}{N_c}\left(N_c^2-1\right)\right] \\ =& 2T_FN_c\,. \end{aligned} \tag{A.22}$$

These formulas are all we need to determine colour factors. The most common applications are

$$T^aT^a = C_F\,\mathbb{1}_{N_c}\,, \tag{A.23}$$

$$f^{acd}f^{bcd} = C_A\delta^{ab}\,, \tag{A.24}$$

$$f^{abc}T^aT^b = \frac{1}{2}f^{abc}[T^a,T^b] = \frac{i}{2}f^{abc}f^{abd}T^d = \frac{i}{2}C_AT^c\,. \tag{A.25}$$

B Detailed Derivation of the Wilson Loop

We start with the vacuum expectation value given in equation (1.11).

$$\begin{aligned} N_cG =& \frac{1}{Z}\int \mathcal{D}A\mathcal{D}\psi\mathcal{D}\bar\psi\, e^{iS}\,\bar\psi^i_{\alpha_2}(x_2)U^{ij}(x_2,x_1)\psi^j_{\alpha_1}(x_1)\bar\psi^k_{\beta_1}(y_1)U^{kl}(y_1,y_2)\psi^l_{\beta_2}(y_2) \\ =& \frac{1}{Z}\int \mathcal{D}A\, e^{iS_{YM}}U^{ij}(x_2,x_1)U^{kl}(y_1,y_2)\left(-\frac{\delta}{i\delta\eta^i_{\alpha_2}(x_2)}\right)\left(\frac{\delta}{i\delta\bar\eta^j_{\alpha_1}(x_1)}\right)\times \\ & \times\left(-\frac{\delta}{i\delta\eta^k_{\beta_1}(y_1)}\right)\left(\frac{\delta}{i\delta\bar\eta^l_{\beta_2}(y_2)}\right)\underbrace{\int \mathcal{D}\psi\mathcal{D}\bar\psi\, e^{i\int d^4x(\bar\psi(i\not{D}-m)\psi+\bar\eta\psi+\bar\psi\eta)}}_{Z_0[A,\bar\eta,\eta]}\Bigg|_{\eta=\bar\eta=0}\,. \end{aligned}$$

Integrating out the heavy quark fields we get the propagator in the presence of an external gauge field.

$$
\begin{aligned}
Z_0[A,\bar\eta,\eta] =& \int \mathcal{D}\psi\mathcal{D}\bar\psi \exp\Big\{ \int d^4x d^4y \Big[\bar\psi^a_\alpha(x) \underbrace{i(i\not{D}_x - m)^{ab}_{\alpha\beta}\delta^4(x-y)}_{iK^{ab}_{\alpha\beta}(x,y)} \psi^b_\beta(y) + \\
&+ \bar\eta^a_\alpha(x) i\delta^{ab}\delta_{\alpha\beta}\delta^4(x-y)\psi^b_\beta(y) + \bar\psi^a_\alpha(x) i\delta^{ab}\delta_{\alpha\beta}\delta^4(x-y)\eta^b_\beta(y) \Big] \Big\} \\
=& \int \mathcal{D}\psi\mathcal{D}\bar\psi \exp\Big\{ \int d^4x d^4y \Big[\Big(\bar\psi^a_\alpha(x) - i\int d^4x' \bar\eta^{a'}_{\alpha'}(x') S^{a'a}_{\alpha'\alpha}(x',x) \Big) \times \\
&\times iK^{ab}_{\alpha\beta}(x,y) \Big(\psi^b_\beta(y) - i\int d^4y' S^{bb'}_{\beta\beta'}(y,y')\eta^{b'}_{\beta'}(y') \Big) - \\
&- \bar\eta^a_\alpha(x) S^{ab}_{\alpha\beta}(x,y)\eta^b_\beta(y) \Big] \Big\} \\
=& \mathcal{N}\det[iK] \exp\Big\{ -\int d^4x d^4y\, \bar\eta^a_\alpha(x) S^{ab}_{\alpha\beta}(x,y)\eta^b_\beta(y) \Big\} ,
\end{aligned} \tag{B.1}
$$

where

$$
\int d^4y\, S^{ab}_{\alpha\beta}(x,y) K^{bc}_{\beta\gamma}(y,z) = \int d^4y\, K^{ab}_{\alpha\beta}(x,y) S^{bc}_{\beta\gamma}(y,z) = i\delta^{ab}\delta_{\alpha\beta}\delta^4(x-z) . \tag{B.2}
$$

Now we can perform the functional derivatives in equation (B.1).

$$
\begin{aligned}
&\left(\frac{\delta}{\delta\eta^i_{\alpha_2}(x_2)}\right)\left(\frac{\delta}{\delta\bar\eta^j_{\alpha_1}(x_1)}\right)\left(\frac{\delta}{\delta\eta^k_{\beta_1}(y_1)}\right)\left(\frac{\delta}{\delta\bar\eta^l_{\beta_2}(y_2)}\right) Z_0[A,\bar\eta,\eta]\Big|_{\eta=\bar\eta=0} \\
&= \left(\frac{\delta}{\delta\eta^i_{\alpha_2}(x_2)}\right)\left(\frac{\delta}{\delta\bar\eta^j_{\alpha_1}(x_1)}\right)\left(\frac{\delta}{\delta\eta^k_{\beta_1}(y_1)}\right)\left(-\int d^4y\, S^{lb}_{\beta_2\beta}(y_2,y)\eta^b_\beta(y)\right) Z_0\Big|_0 \\
&= \left(\frac{\delta}{\delta\eta^i_{\alpha_2}(x_2)}\right)\left(\frac{\delta}{\delta\bar\eta^j_{\alpha_1}(x_1)}\right)\left(-S^{lk}_{\beta_2\beta_1}(y_2,y_1) + \int d^4y\, S^{lb}_{\beta_2\beta}(y_2,y)\eta^b_\beta(y)\int d^4x\, \bar\eta^a_\alpha(x) S^{ak}_{\alpha\beta_1}(x,y_1)\right) Z_0\Big|_0 \\
&= \left(\frac{\delta}{\delta\eta^i_{\alpha_2}(x_2)}\right)\left(S^{lk}_{\beta_2\beta_1}(y_2,y_1)\int d^4y\, S^{jb}_{\alpha_1\beta}(x_1,y)\eta^b_\beta(y) - \int d^4y\, S^{lb}_{\beta_2\beta}(y_2,y)\eta^b_\beta(y) S^{jk}_{\alpha_1\beta_1}(x_1,y_1)\right) Z_0\Big|_0 \\
&= S^{lk}_{\beta_2\beta_1}(y_2,y_1) S^{ji}_{\alpha_1\alpha_2}(x_1,x_2) - S^{li}_{\beta_2\alpha_2}(y_2,x_2) S^{jk}_{\alpha_1\beta_1}(x_1,y_1) .
\end{aligned}
$$

$$
\begin{aligned}
N_c G =& \frac{1}{\mathcal{Z}}\int \mathcal{D}A\, \det[iK] e^{iS_{YM}} \{ \mathrm{Tr}[U(x_2,x_1)S_{\alpha_1\alpha_2}(x_1,x_2)]\mathrm{Tr}[U(y_1,y_2)S_{\beta_2\beta_1}(y_2,y_1)] \\
&- \mathrm{Tr}[U(x_2,x_1)S_{\alpha_1\beta_1}(x_1,y_1)U(y_1,y_2)S_{\beta_2\alpha_2}(y_2,x_2)] \} .
\end{aligned} \tag{B.3}
$$

At this point approximations are introduced: in the quenched approximation the contributions from the determinant in (B.3) are neglected (they would give corrections of order m^{-2}), and in the limit of static quarks the spatial part of the covariant derivative is set to be 0, which leaves the following condition for the propagator:

$$
(i\gamma_0 D_0 - m)S(x,y) = i\delta^4(x-y) . \tag{B.4}
$$

Now we make the following ansatz:

$$
\begin{aligned}
&S(x,y) = \delta^3(\vec x - \vec y)\mathcal{P} e^{ig\int_{y_0}^{x_0} dt\, A_0(t)} \tilde S(x_0,y_0) \\
&\quad \to (\gamma_0\partial_0 + im)\tilde S(x_0,y_0) = \delta(x_0-y_0) \\
&\tilde S(x_0,y_0) = \Theta(x_0-y_0)\frac{1+\gamma_0}{2} e^{-im(x_0-y_0)} + \Theta(y_0-x_0)\frac{1-\gamma_0}{2} e^{-im(y_0-x_0)} . \\
&S(x,y) = \delta^3(\vec x - \vec y) U(x,y) \Big[\Theta(x_0-y_0) P_+ e^{-im(x_0-y_0)} + \Theta(y_0-x_0) P_- e^{-im(y_0-x_0)} \Big]
\end{aligned} \tag{B.5}
$$

The second condition in (B.2) is easily seen to be fulfilled by noting that differentiating with respect to y yields an overall minus sign.

The term in (B.3) consisting of two traces gives 0 because of the δ-functions in S. It describes the annihilation of the quark and the antiquark, which cannot happen when both are static and at a finite distance. The other is evaluated setting $x^0_{1,2} - y^0_{1,2} = t$:

$$\begin{aligned} G_{\alpha_1\alpha_2\beta_1\beta_2}(x_1,x_2,y_1,y_2) = &-\frac{1}{\mathcal{Z}}\int \mathcal{D}A\,\widetilde{\mathrm{Tr}}\left[U(x_2,x_1)\delta^3(\vec{x_1}-\vec{y_1})U(x_1,y_1)(P_+)_{\alpha_1\beta_1}e^{-im_1t}\right. \\ &\left. U(y_1,y_2)\delta^3(\vec{x_2}-\vec{y_2})U(y_2,x_2)(P_-)_{\beta_2\alpha_2}e^{-im_2t}\right] \\ = &-\delta^3(\vec{x_1}-\vec{y_1})\delta^3(\vec{x_2}-\vec{y_2})e^{-i(m_1+m_2)t}(P_+)_{\alpha_1\beta_1}(P_-)_{\beta_2\alpha_2} \\ &\frac{1}{\mathcal{Z}}\int \mathcal{D}A\,\widetilde{\mathrm{Tr}}\left[\mathcal{P}\exp\left(ig\oint_\Gamma dx^\mu A_\mu(x)\right)\right]. \end{aligned} \tag{B.6}$$

Since the paths C connecting the endpoints x and y in $U(x,y)$ are taken to be straight lines, this gives a rectangular path Γ with endpoints y_1, x_1, x_2, y_2.

C Exponentiation Theorem

It was shown in reference [17] that the well-known exponentiation of eikonal cross sections in Abelian gauge theories can be extended to the non-Abelian case, and according to reference [18], this theorem also applies for Wilson loops. We would like, however, to give an argument for that exponentiation, which stays within the framework of Wilson lines, which we will attempt here.

We want to show through a systematic rearrangement of the perturbative series of diagrams, that they can be expressed as an exponential of the sum over a subset of these diagrams with certain coefficients. For this we will divide the set of all possible diagrams into the subsets containing all diagrams γ_n with n external points $x_1 \dots x_n$ and which are constituted of the same connected diagrams $\gamma^{(i)}_{k_i}$ ($\sum_i k_i = n$). Such a subset will be called a class $\mathcal{C}_n(\{\gamma^{(i)}_{k_i}\})$ of order n and it is uniquely defined through its constituents $\gamma^{(i)}_{k_i}$. In order to avoid cumbersome expressions, we will not distinguish between the diagram γ_n as a geometrical object and its value $W(\gamma_n)$ after integrating along the contour Γ. It should be clear from the context, which one is meant. Colour coefficients however will be treated separately and will not be considered part of a diagram.

We will show that the sum over all the diagrams γ_n belonging to the same class times their respective colour factors $C(\gamma_n)$ can be decomposed. The decomposition will only contain products of 2PI diagrams, where each diagram is multiplied by its so-called colour-connected coefficient $\tilde{C}$ and in some cases combinatoric factors. Every product of diagrams in the decomposition sum contains each constituent $\gamma^{(i)}_{k_i}$ exactly once and we sum over all possible combinations of the constituents to such products of 2PI diagrams.

Recall that irreducible means that a diagram can not be separated by cutting the path Γ in two places, whereas connected means that every endpoint x_i of γ_n is connected to every other endpoint x_j through gluon lines (or other internal lines like ghost or light fermion propagators). We will also use the term subdiagram, by which we mean the diagrams γ_m into which γ_n ($n > m$) can be reduced by cutting Γ in two places and repeating this process on the reduced diagrams until there are only irreducible diagrams left (cf. fig. C.1). It will be convenient to also refer to the intermediate reducible diagrams that occur during this process as subdiagrams. And finally those diagrams that can be obtained from γ_n by removing any number of constituents will be called, for lack of a better expression, partial diagrams of γ_n.

It is sufficient for now to consider only the case where all $\gamma^{(i)}_{k_i}$ are distinguishable, which means that we need not worry about combinatoric factors. The case where some or all of the $\gamma^{(i)}_{k_i}$ are identical can be derived from this in a quite straightforward fashion and will be treated later in this section. We will use the principle of induction in the number of constituents, so assume that for every class, whose constituents are a true subset of $\{\gamma^{(i)}_{k_i}\}$, decomposition has already been shown. This decomposition is trivially true for all classes with only one constituent, since they only contain one diagram. This is the constituent itself and it already is 2PI. So we just have to identify the colour-connected coefficients of constituents with their colour factors $C(\gamma^{(i)}_{k_i}) = \tilde{C}(\gamma^{(i)}_{k_i})$.

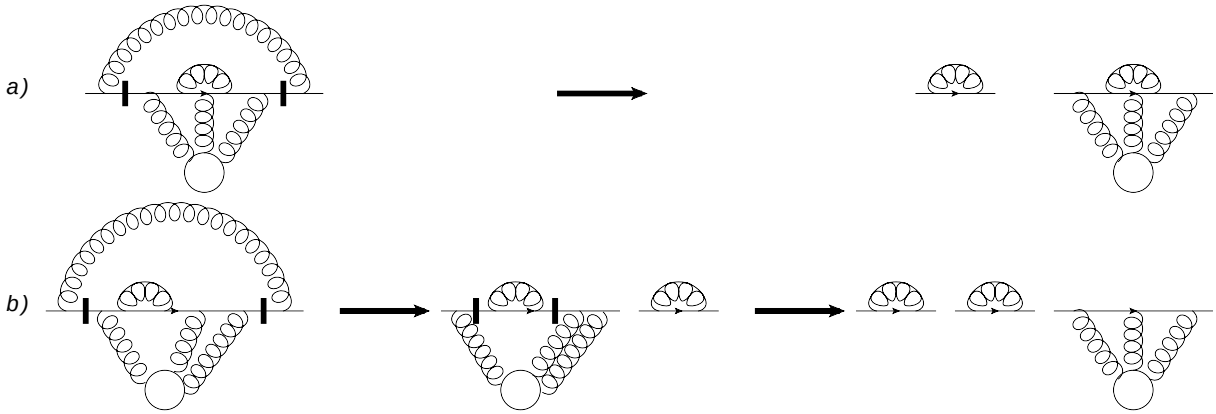

Figure C.1: Diagrams a) and b) are reduced to their subdiagrams. b) can be fully reduced to the constituents of both a) and b), whereas a) has one irreducible unconnected subdiagram.

We will start by showing that a product of colour matrices is proportional to the unit matrix, if every index is contracted with that of another colour matrix or of a structure constant. For this we will make use of the following identities (compare appendix A):

$$T^a_{ij}T^a_{kl} = T_F\left(\delta_{il}\delta_{jk} - \frac{1}{N_c}\delta_{ij}\delta_{kl}\right), \tag{C.1}$$

$$f^{abc} = \frac{1}{iT_F}\mathrm{Tr}\Big(\big[T^a, T^b\big]\,T^c\Big), \tag{C.2}$$

which follow from the T^a being independent, traceless, hermitian $N_c \times N_c$ matrices satisfying the normalization condition $\mathrm{Tr}[T^aT^b] = T_F\delta^{ab}$ and from the definition of the structure constants $[T^a, T^b] = if^{abc}T^c$.

So, in a first step we will replace all structure constants using equation (C.2). Then we can decompose every pair of colour matrices with contracted colour indices into Kronecker deltas of their matrix indices according to equation (C.1). Since all colour indices are contracted, we arrive at an expression that consists solely of Kronecker deltas. All matrix indices are also contracted, except for two (let us call them i and$j$), the initial and final indices of the original product of colour matrices. So if we perform the sums over all the matrix indices, the result can only depend on δ_{ij} times a rational function of N_c, the number of colours. This proves our statement, that a product of colour matrices and structure constants with every index contracted is proportional to the unit matrix.

Whenever a diagram has a subdiagram, the colour matrices of that subdiagram are ordered (per definition) in such a way that this theorem is applicable. Because the colour structure of this subdiagram is proportional to the unit matrix, it can be factored out of the trace. This means that the colour factor of a reducible diagram is the product of the colour factors of its subdiagrams.

One can use equations (C.1) and (C.2) to calculate all of the colour factors, however in most cases it is more convenient to use the following identities (compare appendixA):

$$T^aT^a = C_F\,\mathbb{1}_{N_c\times N_c}, \tag{C.3}$$

$$f^{abc}f^{abd} = C_A\delta^{cd}, \tag{C.4}$$

$$f^{abc}T^aT^b = \frac{i}{2}C_AT^c, \tag{C.5}$$

$$C_F = T_F\frac{\left(N_c^2-1\right)}{N_c}, \qquad C_A = 2T_FN_c. \tag{C.6}$$

Before considering the more complicated non-Abelian case, let us first show how the sum over all diagrams belonging to a class factors into the product of constituents, if we do not include colour coefficients. Since the integrand is already a product of the contributions of each constituent, we only need to concern ourselves with the integrations to show factorization.

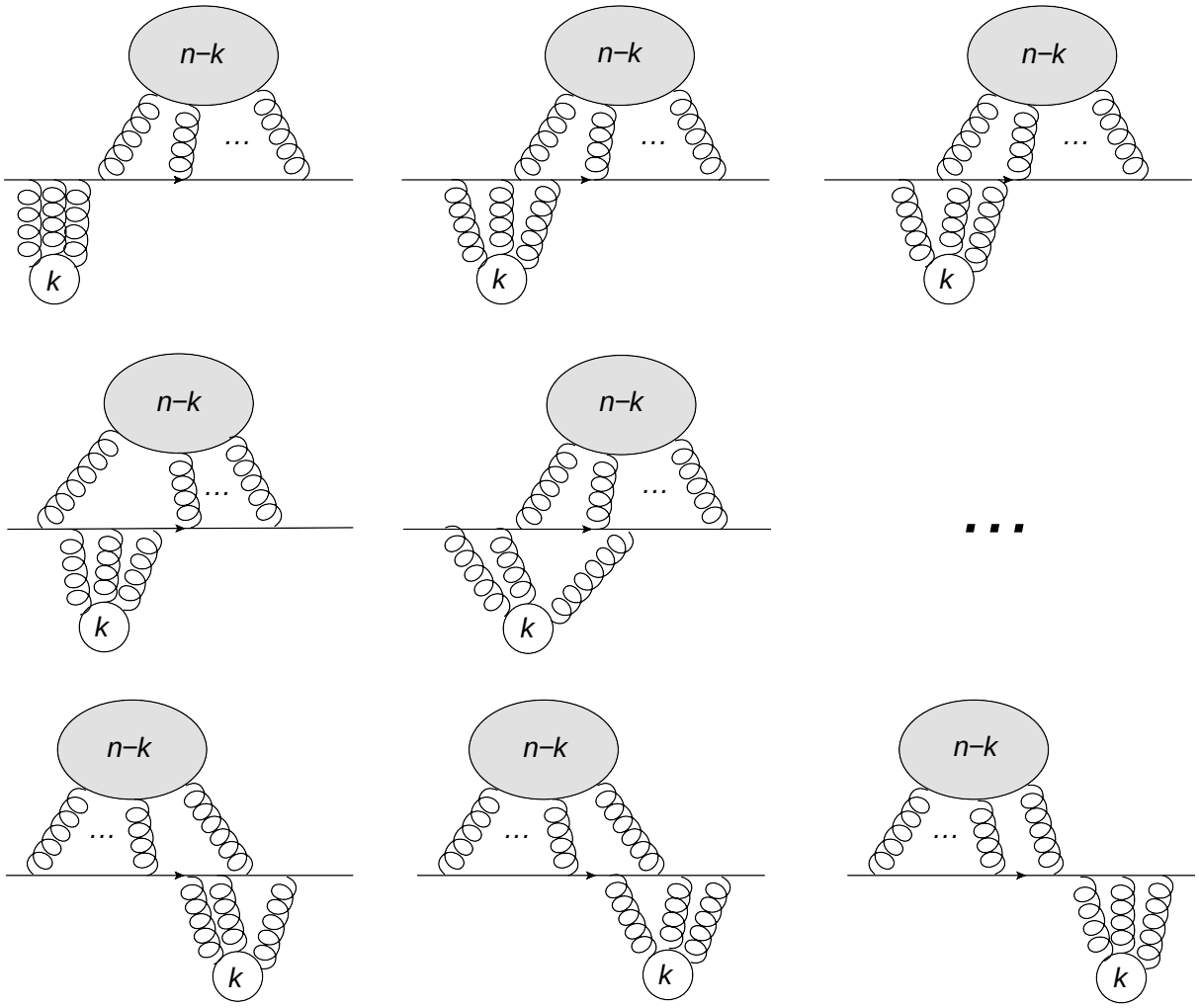

Figure C.2: A selection of diagrams contributing to the factorization of $\gamma_{k_1}^{(1)}$. The white bubble labelled k denotes $\gamma_3^{(1)}$, while the grey bubble labelled $n-k$ denotes the rest.

The crucial point here is a redefinition of the integration ranges by using the identities

$$\cdots \int_0^{s_{i+1}} \mathrm{d}s_i \int_0^{s_i} \mathrm{d}s_{i-1} \cdots = \cdots \int_0^{s_{i+1}} \mathrm{d}s_{i-1} \int_{s_{i-1}}^{s_{i+1}} \mathrm{d}s_i \cdots , \tag{C.7}$$

$$\cdots \int_0^{s_{i+1}} \mathrm{d}s_i \int_0^{s_i} \mathrm{d}s_{i-1} \int_0^{s_{i-1}} \mathrm{d}s_{i-2} \cdots = \cdots \int_0^{s_{i+1}} \mathrm{d}s_{i-2} \int_{s_{i-2}}^{s_{i+1}} \mathrm{d}s_i \int_{s_{i-2}}^{s_i} \mathrm{d}s_{i-1} \cdots , \tag{C.8}$$

and so on. This just reflects the fact, that we may chose any order in which to perform the n integrations, at each step thinking of the other integration parameters as fixed, and the integration limits change accordingly, maintaining path ordering.

Now we choose one of the constituents and call it $\gamma_{k_1}^{(1)}$. The integration parameters belonging to the endpoints of $\gamma_{k_1}^{(1)}$ will be denoted t_j, $j = 1 \ldots k_1$ and the integration parameters belonging to the rest s_i, $i = 1 \ldots n-k_1$. By repeated use of the above identities we can transform the integration ranges so that every s_i integration runs from 0 to s_{i+1}, while every t_j integration runs from $\max\{s_i | s_i \leq t_j\}$ to $\min\{t_{j+1}, s_{i+1}\}$ ($s_0 = 0$, $s_{n-k_1+1} = 1$). This means that we perform first the t_j integrations and then the s_i integrations, whatever the current path ordering may be. The s_i integrations are the same for every diagram and can be factored out, while summing over all possible diagrams means summing over all possible ranges for t_j. Now the t_j integrals can be combined so that every s_i-dependence in the integration limits drops out and the t_j integrations run from 0 to t_{j+1} ($t_{k_1+1} = 1$). This means that $\gamma_{k_1}^{(1)}$ can be factored out.

An illustration of this is given in figure C.2 for the case $k = 3$. The grey bubble denotes the rest, i.e. any possible combination of the constituents without $\gamma^{(1)}_{k_1}$, or equivalently any diagram of the class $\mathcal{C}_{n-k_1}(\{\gamma^{(j)}_{k_j}\}_{j\neq 1})$. Since the factorization procedure is the same for any rest diagram, we can also take the grey bubble to mean the sum over all rest diagrams. The integrals for the diagrams shown are given by

$$
\begin{aligned}
&\int_0^1 \mathrm{d}s_1 \cdots \int_0^{s_{n-5}} \mathrm{d}s_{n-4} \int_0^{s_{n-4}} \mathrm{d}s_{n-3} \int_0^{s_{n-3}} \mathrm{d}t_1 \int_0^{t_1} \mathrm{d}t_2 \int_0^{t_2} \mathrm{d}t_3 \\
&+ \int_0^1 \mathrm{d}s_1 \cdots \int_0^{s_{n-5}} \mathrm{d}s_{n-4} \int_0^{s_{n-4}} \mathrm{d}t_1 \int_0^{t_1} \mathrm{d}s_{n-3} \int_0^{s_{n-3}} \mathrm{d}t_2 \int_0^{t_2} \mathrm{d}t_3 \\
&+ \int_0^1 \mathrm{d}s_1 \cdots \int_0^{s_{n-5}} \mathrm{d}s_{n-4} \int_0^{s_{n-4}} \mathrm{d}t_1 \int_0^{t_1} \mathrm{d}t_2 \int_0^{t_2} \mathrm{d}s_{n-3} \int_0^{s_{n-3}} \mathrm{d}t_3 \\
&+ \int_0^1 \mathrm{d}s_1 \cdots \int_0^{s_{n-5}} \mathrm{d}s_{n-4} \int_0^{s_{n-4}} \mathrm{d}t_1 \int_0^{t_1} \mathrm{d}t_2 \int_0^{t_2} \mathrm{d}t_3 \int_0^{t_3} \mathrm{d}s_{n-3} \\
&+ \int_0^1 \mathrm{d}s_1 \cdots \int_0^{s_{n-5}} \mathrm{d}t_1 \int_0^{t_1} \mathrm{d}s_{n-4} \int_0^{s_{n-4}} \mathrm{d}s_{n-3} \int_0^{s_{n-3}} \mathrm{d}t_2 \int_0^{t_2} \mathrm{d}t_3 \\
&+ \dots \\
&+ \int_0^1 \mathrm{d}t_1 \int_0^{t_1} \mathrm{d}s_1 \int_0^{s_1} \mathrm{d}t_2 \int_0^{t_2} \mathrm{d}t_3 \int_0^{t_3} \mathrm{d}s_2 \cdots \int_0^{s_{n-4}} \mathrm{d}s_{n-3} \\
&+ \int_0^1 \mathrm{d}t_1 \int_0^{t_1} \mathrm{d}t_2 \int_0^{t_2} \mathrm{d}s_1 \int_0^{s_1} \mathrm{d}t_3 \int_0^{t_3} \mathrm{d}s_2 \cdots \int_0^{s_{n-4}} \mathrm{d}s_{n-3} \\
&+ \int_0^1 \mathrm{d}t_1 \int_0^{t_1} \mathrm{d}t_2 \int_0^{t_2} \mathrm{d}t_3 \int_0^{t_3} \mathrm{d}s_1 \int_0^{s_1} \mathrm{d}s_2 \cdots \int_0^{s_{n-4}} \mathrm{d}s_{n-3} \,.
\end{aligned}
\tag{C.9}
$$

Transforming this as specified above, we can factor out the s_i integrations and combine the t_j integrations:

$$
\begin{aligned}
&\int_0^1 \mathrm{d}s_1 \cdots \int_0^{s_{n-5}} \mathrm{d}s_{n-4} \int_0^{s_{n-4}} \mathrm{d}s_{n-3} \left\{ \int_0^{s_{n-3}} \mathrm{d}t_1 \int_0^{t_1} \mathrm{d}t_2 \int_0^{t_2} \mathrm{d}t_3 \right. \\
&+ \int_{s_{n-3}}^{s_{n-4}} \mathrm{d}t_1 \int_0^{s_{n-3}} \mathrm{d}t_2 \int_0^{t_2} \mathrm{d}t_3 + \int_{s_{n-3}}^{s_{n-4}} \mathrm{d}t_1 \int_{s_{n-3}}^{t_1} \mathrm{d}t_2 \int_0^{s_{n-3}} \mathrm{d}t_3 \\
&+ \int_{s_{n-3}}^{s_{n-4}} \mathrm{d}t_1 \int_{s_{n-3}}^{t_1} \mathrm{d}t_2 \int_{s_{n-3}}^{t_2} \mathrm{d}t_3 + \int_{s_{n-4}}^{s_{n-5}} \mathrm{d}t_1 \int_0^{s_{n-3}} \mathrm{d}t_2 \int_0^{t_2} \mathrm{d}t_3 \\
&+ \dots + \int_{s_1}^1 \mathrm{d}t_1 \int_{s_2}^{s_1} \mathrm{d}t_2 \int_{s_2}^{t_2} \mathrm{d}t_3 \\
&\left. + \int_{s_1}^1 \mathrm{d}t_1 \int_{s_1}^{t_1} \mathrm{d}t_2 \int_{s_2}^{s_1} \mathrm{d}t_3 + \int_{s_1}^1 \mathrm{d}t_1 \int_{s_1}^{t_1} \mathrm{d}t_2 \int_{s_1}^{t_2} \mathrm{d}t_3 \right\}
\end{aligned}
\tag{C.10}
$$

$$
\begin{aligned}
= &\int_0^1 \mathrm{d}s_1 \cdots \int_0^{s_{n-5}} \mathrm{d}s_{n-4} \int_0^{s_{n-4}} \mathrm{d}s_{n-3} \left\{ \int_0^{s_{n-3}} \mathrm{d}t_1 \int_0^{t_1} \mathrm{d}t_2 \int_0^{t_2} \mathrm{d}t_3 \right. \\
&+ \int_{s_{n-3}}^{s_{n-4}} \mathrm{d}t_1 \int_0^{s_{n-3}} \mathrm{d}t_2 \int_0^{t_2} \mathrm{d}t_3 + \int_{s_{n-3}}^{s_{n-4}} \mathrm{d}t_1 \int_{s_{n-3}}^{t_1} \mathrm{d}t_2 \int_0^{t_2} \mathrm{d}t_3 \\
&+ \int_{s_{n-4}}^{s_{n-5}} \mathrm{d}t_1 \int_0^{s_{n-3}} \mathrm{d}t_2 \int_0^{t_2} \mathrm{d}t_3 + \dots \\
&\left. + \int_{s_1}^1 \mathrm{d}t_1 \int_{s_2}^{s_1} \mathrm{d}t_2 \int_{s_2}^{t_2} \mathrm{d}t_3 + \int_{s_1}^1 \mathrm{d}t_1 \int_{s_1}^{t_1} \mathrm{d}t_2 \int_{s_2}^{t_2} \mathrm{d}t_3 \right\}
\end{aligned}
\tag{C.11}
$$

$$
\begin{aligned}
&= \int_0^1 \mathrm{d}s_1 \cdots \int_0^{s_{n-5}} \mathrm{d}s_{n-4} \int_0^{s_{n-4}} \mathrm{d}s_{n-3} \\
&\quad \left\{ \int_0^{s_{n-3}} \mathrm{d}t_1 \int_0^{t_1} \mathrm{d}t_2 \int_0^{t_2} \mathrm{d}t_3 + \int_{s_{n-3}}^{s_{n-4}} \mathrm{d}t_1 \int_0^{t_1} \mathrm{d}t_2 \int_0^{t_2} \mathrm{d}t_3 \right. \\
&\quad \left. + \int_{s_{n-4}}^{s_{n-5}} \mathrm{d}t_1 \int_0^{s_{n-3}} \mathrm{d}t_2 \int_0^{t_2} \mathrm{d}t_3 + \cdots + \int_{s_1}^{1} \mathrm{d}t_1 \int_{s_2}^{t_1} \mathrm{d}t_2 \int_{s_2}^{t_2} \mathrm{d}t_3 \right\} \qquad \text{(C.12)} \\
&= \int_0^1 \mathrm{d}s_1 \cdots \int_0^{s_{n-5}} \mathrm{d}s_{n-4} \int_0^{s_{n-4}} \mathrm{d}s_{n-3} \left\{ \int_0^{s_{n-4}} \mathrm{d}t_1 \int_0^{t_1} \mathrm{d}t_2 \int_0^{t_2} \mathrm{d}t_3 \right. \\
&\quad \left. + \int_{s_{n-4}}^{s_{n-5}} \mathrm{d}t_1 \int_0^{s_{n-3}} \mathrm{d}t_2 \int_0^{t_2} \mathrm{d}t_3 + \cdots + \int_{s_1}^{1} \mathrm{d}t_1 \int_{s_2}^{t_1} \mathrm{d}t_2 \int_{s_2}^{t_2} \mathrm{d}t_3 \right\} \\
&= \cdots = \int_0^1 \mathrm{d}s_1 \cdots \int_0^{s_{n-5}} \mathrm{d}s_{n-4} \int_0^{s_{n-4}} \mathrm{d}s_{n-3} \int_0^1 \mathrm{d}t_1 \int_0^{t_1} \mathrm{d}t_2 \int_0^{t_2} \mathrm{d}t_3 \,. \qquad \text{(C.13)}
\end{aligned}
$$

So now, after we have factored out $\gamma_{k_1}^{(1)}$, the rest is again the sum over all diagrams belonging to a class of smaller order: $\mathcal{C}_{n-k_1}(\{\gamma_{k_j}^{(j)}\}_{j\neq 1})$. This means that we can again apply this factorization procedure to the rest by picking a constituent $\gamma_{k_2}^{(2)}$, transforming and combining the integration ranges and factoring $\gamma_{k_2}^{(2)}$ out. In this way we can recursively show the factorization of the sum over all diagrams γ_n of the same class into the product of its constituents $\prod_i \gamma_{k_i}^{(i)}$.

In an Abelian theory we would be done here. In a non-Abelian theory, however, this method does not work because of the different colour factors. But, as already seen in the example of figure 1.2, we may split up the colour factor of every diagram $\gamma_n \in \mathcal{C}_n(\{\gamma_{k_i}^{(i)}\})$ into the colour factor of $\gamma_{k_1}^{(1)}$ times that of the partial diagram of γ_n without $\gamma_{k_1}^{(1)}$, denoted by $\gamma_n \smallsetminus \gamma_{k_1}^{(1)}$, and a rest:

$$
C(\gamma_n) = C\left(\gamma_{k_1}^{(1)}\right) C\left(\gamma_n \smallsetminus \gamma_{k_1}^{(1)}\right) + \left[C(\gamma_n) - C\left(\gamma_{k_1}^{(1)}\right) C\left(\gamma_n \smallsetminus \gamma_{k_1}^{(1)}\right) \right] \qquad \text{(C.14)}
$$

The first part is the same for every partial diagram $\gamma_n \smallsetminus \gamma_{k_1}^{(1)}$, so we can use the above method and factor out both $\gamma_{k_1}^{(1)}$ and its colour factor:

$$
\sum_{\gamma_n \in \mathcal{C}_n\left(\{\gamma_{k_i}^{(i)}\}\right)} C(\gamma_n)\,\gamma_n = C\left(\gamma_{k_1}^{(1)}\right)\gamma_{k_1}^{(1)} \cdot \left[\sum_{\gamma_{n-k_1} \in \mathcal{C}_{n-k_1}\left(\{\gamma_{k_j}^{(j)}\}_{j\neq 1}\right)} C(\gamma_{n-k_1})\,\gamma_{n-k_1} \right] + \ldots \qquad \text{(C.15)}
$$

The dots stand for the rest, to which we will turn in a moment. Here we have arrived again at the sum over all diagrams of a class, this time $\mathcal{C}_{n-k_1}\left(\{\gamma_{k_j}^{(j)}\}_{j\neq 1}\right)$ of order $n-k_1$, times their respective colour factors. So at this point we can use the induction hypothesis and replace this sum by its decomposition into products of 2PI diagrams.

The diagrams in the rest now have coefficients $\left[C(\gamma_n) - C\left(\gamma_{k_1}^{(1)}\right) C\left(\gamma_n \smallsetminus \gamma_{k_1}^{(1)}\right) \right]$. Since the colour coefficient of a diagram is the product of the coefficients of its subdiagrams, this factor vanishes whenever $\gamma_{k_1}^{(1)}$ turns up as a subdiagram. This means that the rest contains all those diagrams where $\gamma_{k_1}^{(1)}$ is combined with other $\gamma_{k_j}^{(j)}$ to 2PI (sub)diagrams.

Now, in the explanation of the factorization procedure it was never assumed that the diagram that was factored out had to be connected. So we may just as well split up the coefficients again and factor out 2PI diagrams, using the same line of argument as for factoring out constituents. Of course, only those diagrams γ_n of the rest will take part in this factorization, which contain the respective 2PI diagram as a partial diagram. We have to do these factorizations in a systematic way in order to get the right coefficients, so we will order the 2PI diagrams to be factored out according to their number of constituents.

This means that we will start with all 2PI diagrams that are a combination of $\gamma_{k_1}^{(1)}$ and $\gamma_{k_2}^{(2)}$, denoted by $\{\gamma_{k_1}^{(1)} \cup \gamma_{k_2}^{(2)}\}$, then all combinations of $\gamma_{k_1}^{(1)}$ and $\gamma_{k_3}^{(3)}$ $\{\gamma_{k_1}^{(1)} \cup \gamma_{k_3}^{(3)}\}$, etc. Since we already know the

colour-connected coefficients of the $\gamma_m \in \{\gamma_{k_1}^{(1)} \cup \gamma_{k_j}^{(j)}\}$ from the decomposition of $\mathcal{C}_m(\{\gamma_{k_1}^{(1)}, \gamma_{k_j}^{(j)}\})$ we will, like in equation (C.14), add and subtract $\tilde{C}(\gamma_m)C(\gamma_n \setminus \gamma_m)$ to the coefficients of the γ_n in the rest. So performing these factorizations we get

$$\tilde{C}\left(\gamma_m\right)\gamma_m \left\{ \sum_{\gamma_{n-m} \in \mathcal{C}\left(\left\{\gamma_{k_l}^{(l)}\right\}_{l\neq 1,j}\right)} C\left(\gamma_{n-m}\right)\gamma_{n-m} \right\} + \dots \tag{C.16}$$

Because of the induction hypothesis the sum inside curly brackets can again be replaced by the decomposition of the class $\mathcal{C}_{n-k_1-k_j}\left(\left\{\gamma_{k_l}^{(l)}\right\}_{l\neq 1,j}\right)$.

Whenever γ_m turns up as a subdiagram in γ_n, then the coefficient already has the desired form $\tilde{C}(\gamma_m)C(\gamma_n \setminus \gamma_m)$, because the coefficients of subdiagrams are independent from each other: all the adding and subtracting operations performed so far affected only the subdiagram γ_m, because $C(\gamma_n \setminus \gamma_m)$ can be factored out in all terms. This means that the coefficient of γ_m has undergone exactly the same operations as in the decomposition of the class γ_m belongs to, at the end of which it was defined to be its colour-connected coefficient $\tilde{C}(\gamma_m)$ (see below). So after factoring out all $\gamma_{k_1}^{(1)} \cup \gamma_{k_j}^{(j)}$ diagrams, the rest is reduced to all diagrams γ_n in which $\gamma_{k_1}^{(1)}$ is part of a 2PI (sub)diagram with at least three constituents.

We continue by factoring out all 2PI diagrams containing $\gamma_{k_1}^{(1)}$ that have exactly three constituents. To each coefficient of the γ_n in the rest we add and subtract, in analogy to the previous procedure, the product of the colour-connected coefficient $\tilde{C}(\gamma_m)$ of the diagram γ_m we want to factor out and the colour factor $C(\gamma_n \setminus \gamma_m)$ of the partial diagram without γ_m. After the factorization has been performed, we can use the induction hypothesis to decompose the sum over diagrams of the class of $\gamma_n \setminus \gamma_m$, like in equation (C.16). The rest now contains only diagrams in which $\gamma_{k_1}^{(1)}$ is part of a 2PI (sub)diagram with at least four constituents, because of the same line of argument as in the case of 2PI diagrams with two constituents.

This procedure can be reiterated with an increasing number of constituents of the 2PI diagrams to be factored out, each time decreasing the number of reducible diagrams in the rest, until there are only irreducible diagrams left. Now we are finished with the decomposition and define the coefficients these irreducible diagrams have acquired through this process as their colour-connected coefficients.

It remains to be shown that the result has the form we stated in the beginning: the sum over all possible combinations of the constituents $\gamma_{k_i}^{(i)}$ to products of 2PI diagrams times their respective colour-connected coefficients $\tilde{C}(\gamma_n)$. Every diagram in the above decomposition is obviously multiplied by its colour connected coefficient, so we don't have to worry about this part. The statement is true for all classes of order $< n$ because of the induction hypothesis. So we have the sum over all 2PI diagrams containing $\gamma_{k_1}^{(1)}$ times every possible combination of the remaining constituents to products of 2PI diagrams. This gives in turn the sum over all possible combinations of the constituents including $\gamma_{k_1}^{(1)}$ to products of 2PI diagrams, which is what we wanted to show. In particular this means that the decomposition does not depend on the choice of the first constituent $\gamma_{k_1}^{(1)}$ to be factored out.

Now we are only two steps away from showing exponentiation. First we have to consider the case when some of the constituents are identical. This can be done by initially treating every constituent as distinguishable, which leads to a great increase in the number of diagrams participating in the decomposition. To be specific, for every constituent $\gamma_{k_i}^{(i)}$ that turns up p_i times there are $p_i!$ as many diagrams contributing, if we distinguish among them. So we have to compensate this through a factor of $\frac{1}{\prod_i (p_i!)}$. After the decomposition has been done, we drop the distinction we have introduced. This again leads to a number of terms being identical, so the combinatoric factor is given by the number N of identical terms in the decomposition divided by $\prod_i (p_i!)$. To find N, we basically have to solve the problem, how many different ways there are to distribute the p_i constituents to the free positions inside the diagrams of the decomposition.

Let us first look at a single 2PI diagram with p identical constituents. If we treat them as distinguishable, we have to divide by $p!$. But there are also $p!$ different ways of ordering these constituents inside the

2PI diagram, since there are p distinct positions for them to occupy. If we let the constituents become identical again, those factors $p!$ exactly cancel each other. Now consider a product of two different 2PI diagrams. Again, there are p distinct places for the distinguishable constituents to occupy, so the number of possible ways to position them, i.e. the number of terms in the decomposition is $p!$, exactly cancelling the number of permutations. But in the case when the two 2PI diagrams are the same, there are only half as many possible ways of ordering the constituents, because exchanging the two diagrams gives the same contribution. So here we have to include a combinatoric factor $\frac{1}{2}$. (cf. figure C.3)

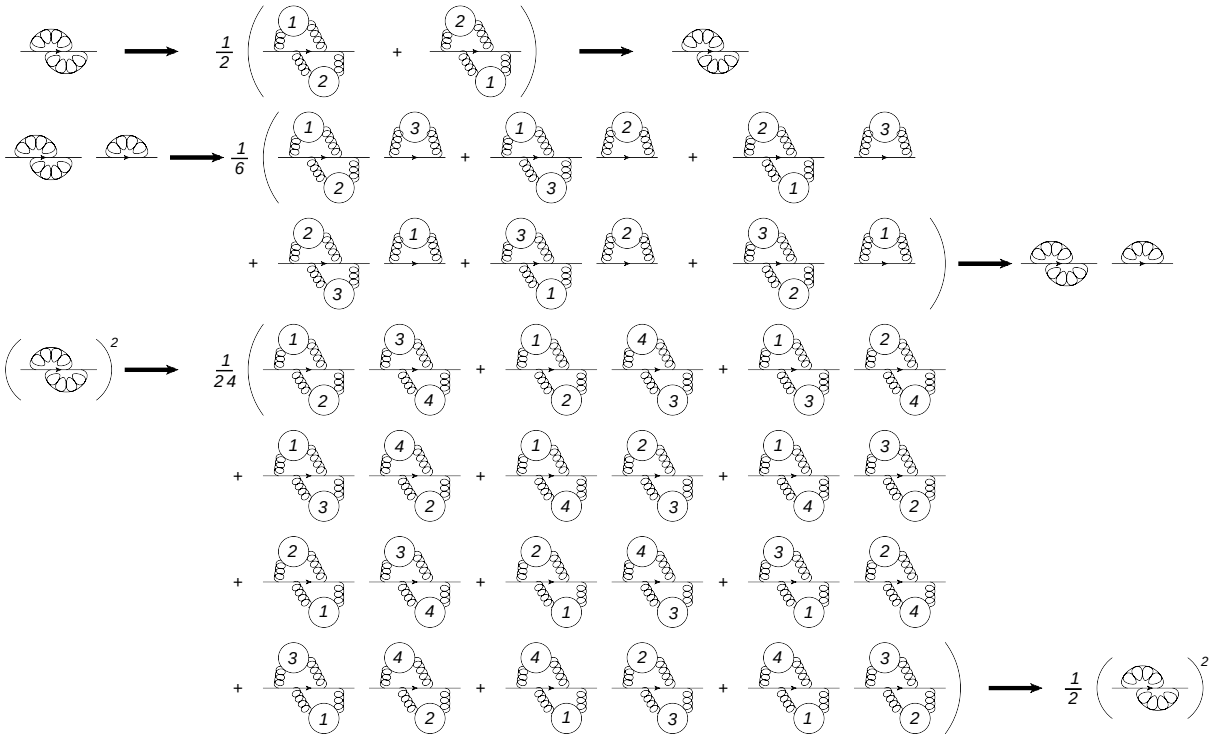

Figure C.3: Illustration for working out the combinatoric coefficients. In the first step we assign numbers $1 \dots p$ to every identical constituent (here these are simply the gluon lines), sum over all possible combinations and divide by $p!$. Then we let the constituents $1 \dots p$ become identical again, which leads to the coefficient $\frac{N}{p!}$, where N is the number of diagrams.

In general, the positions inside a diagram are distinct, but the diagrams themselves are not. So we can again treat diagrams that turn up to the power of q in the decomposition series as distinguishable and divide by the number $q!$ of permutations of those diagrams. Now all the free positions for the constituents are distinguishable by the diagram and the position inside that diagram, leading to $p_i!$ different terms for every constituent $\gamma_{k_i}^{(i)}$. So the number of permutations of the constituents always drops out and only the number of permutations of diagrams remains. This means that we have to include the combinatoric factor $\frac{1}{q!}$ for every power q of a diagram in the decomposition series.

In the last step we want to show that this decomposition series can be summed up in an exponential of the sum over all 2PI diagrams times their colour-connected coefficients. This can be easily done in the following way:

$$\begin{aligned} \exp\left[\sum_{\gamma_n \in \mathrm{2PI}} \tilde{C}(\gamma_n)\gamma_n\right] &= \prod_{\gamma_n \in \mathrm{2PI}} \exp\left[\tilde{C}(\gamma_n)\gamma_n\right] \\ &= \prod_{\gamma_n \in \mathrm{2PI}} \left[\sum_{q=0}^{\infty} \frac{\left(\tilde{C}(\gamma_n)\gamma_n\right)^q}{q!}\right] . \end{aligned} \tag{C.17}$$

If we expand the product, we see that this is exactly the decomposition series we have constructed, when summed over all classes: a sum over all possible products of powers of 2PI diagrams and their colour connected coefficients times a factor $\frac{1}{q!}$ for every power q.

On a side note, we never used the fact that Γ represented a closed path or the invariance of the trace under cyclic permutations, so this theorem also applies to the expectation values of Wilson lines in general, and not just to loops.

D Details of the Vacuum Calculations

Since it is too cumbersome to put all the integrations in the main text, they will be given here instead. Let us first define the parametrization chosen for the four sides of the Wilson loop, starting with the upper left corner:

$$\begin{array}{rlll} \text{I}: & x^\mu = \left(\tau, \frac{1}{2}\vec{r}\right) & \tau \in [0,t] & dx^\mu = (1,0)d\tau \\ \text{II}: & x^\mu = \left(t, (\frac{1}{2}-s)\vec{r}\right) & s \in [0,1] & dx^\mu = (0,-\vec{r})ds \\ \text{III}: & x^\mu = \left((t-\tau), -\frac{1}{2}\vec{r}\right) & \tau \in [0,t] & dx^\mu = (-1,0)d\tau \\ \text{IV}: & x^\mu = \left(0, (s-\frac{1}{2})\vec{r}\right) & s \in [0,1] & dx^\mu = (0,\vec{r})ds\,. \end{array} \tag{D.1}$$

This means that I and III stand for the quark and antiquark line, respectively, while II and IV represent left and right string.

The contributions from different parts of the contour integration are denoted by $I_{i,j}$ where the index i stands for the range of the x variable and j for y. Because the gluon propagator is diagonal with respect to time and space components in Feynman and Coulomb gauge, there are only six contributions to be considered, shown in figure 2.1. It can be easily checked that the gauge fixing parameter ξ dependent contributions in arbitrary covariant gauges cancel, but that calculation will not be shown here.

D.1 Tree Level Calculations (Feynman Gauge)

propagator

$$D_{\mu\nu}(k) = \frac{-i\eta_{\mu\nu}}{k^2 + i\epsilon} \tag{D.2}$$

figures b), c)

$$\begin{aligned} I_{\text{I,I}} + I_{\text{III,III}} &= \int \frac{\mathrm{d}^4k}{(2\pi)^4} \frac{-i}{k^2+i\epsilon} \int_0^t \mathrm{d}\tau \int_0^\tau \mathrm{d}\tau' \left(e^{ik_0(\tau-\tau')} + e^{-ik_0(\tau-\tau')}\right) \\ &= \int \frac{\mathrm{d}^4k}{(2\pi)^4} \frac{-i}{k^2+i\epsilon} \frac{1}{k_0^2} \left(2 - e^{ik_0t} - e^{-ik_0t}\right)\,. \end{aligned} \tag{D.3}$$

Despite the factor $\frac{1}{k_0^2}$, this expression does not have a pole at $k_0 = 0$, because it is cancelled by the zero in $(2 - e^{ik_0t} - e^{-ik_0t})$. But if we tried to split this up into three integrals and calculate them separately, each would be divergent. We may however introduce a new parameter m^2 in the denominator that shifts the pole on the imaginary axis, perform the integration and in the end take the limit $m \to 0$. Now we can manipulate each term independently from the others. In this case we will switch the sign of k_0 in the last term so that we can close the integration in the upper half of the complex plane and use the residue theorem.

$$\begin{aligned} I_{\text{I,I}} + I_{\text{III,III}} &= \lim_{m\to 0} \int \frac{\mathrm{d}^3k}{(2\pi)^3} \int \frac{\mathrm{d}k_0}{2\pi} \frac{-i}{k_0^2 - k^2 + i\epsilon} \frac{2 - e^{ik_0t} - e^{-ik_0t}}{k_0^2 + m^2} \\ &= \lim_{m\to 0} \int \frac{\mathrm{d}^3k}{(2\pi)^3} \int \frac{\mathrm{d}k_0}{2\pi} \frac{-2i}{k_0^2 - k^2 + i\epsilon} \frac{1 - e^{ik_0t}}{k_0^2 + m^2} \\ &= \lim_{m\to 0} \int \frac{\mathrm{d}^3k}{(2\pi)^3} \left(\frac{2}{-2k} \frac{1 - e^{-ikt}}{k^2+m^2} + \frac{2}{-m^2-k^2} \frac{1-e^{-mt}}{2mi}\right) \\ &= \int \frac{\mathrm{d}^3k}{(2\pi)^3} \frac{e^{-ikt} + ikt - 1}{k^3}\,. \end{aligned} \tag{D.4}$$

This procedure is a useful trick if one wants to perform integrals over a sum of functions, where each separate integral would be divergent, but the sum is not. However it is only valid, if we can exchange integrating over k_0 and taking the limit $m \to 0$. For this to be the case we must be careful not to create new divergences when introducing the parameter m, for example terms like $\frac{1}{m}$ for certain values of k_0, that diverge when taking $m \to 0$. Here this is obviously not the case, since the only possible point where $m \to 0$ might diverge is $k_0 = 0$, but there the numerator also gives 0, so we need not worry.

The integral in (D.4) is divergent, so we have to regularize it, preferably by dimensional regularization. We will use $d = 3 - 2\varepsilon$ and include the factor μ^{3-d} introduced through the usage of a dimensionless coupling constant α_s (compare appendix A).

$$\begin{aligned} I_{\mathrm{I,I}} + I_{\mathrm{III,III}} =& \frac{2\mu^{3-d}}{(4\pi)^{\frac{d}{2}}\Gamma\left(\frac{d}{2}\right)} \int_0^\infty \mathrm{d}k\, k^{d-4} \left(e^{-ikt} + ikt - 1\right) \\ =& \frac{2\mu^{3-d}}{(4\pi)^{\frac{d}{2}}\Gamma\left(\frac{d}{2}\right)} \int_0^\infty \mathrm{d}k\, \frac{k^{d-4}}{(it)^{d-3}} e^{-k} \\ =& \frac{2\mu^{3-d}}{(4\pi)^{\frac{d}{2}}\Gamma\left(\frac{d}{2}\right)} \frac{\Gamma(d-3)}{(it)^{d-3}} = \frac{2(it\mu)^{2\varepsilon}\Gamma(-2\varepsilon)}{(4\pi)^{\frac{3}{2}-\varepsilon}\Gamma\left(\frac{3}{2}-\varepsilon\right)} \\ =& -\frac{1}{4\pi^2\varepsilon} - \frac{1}{4\pi^2}\left(2 + \gamma_E + \ln\pi + 2\ln it\mu\right) + \mathcal{O}(\epsilon)\,. \end{aligned} \tag{D.5}$$

figures e), f)

$$\begin{aligned} I_{\mathrm{II,II}} + I_{\mathrm{IV,IV}} =& \int \frac{\mathrm{d}^4k}{(2\pi)^4} \frac{i\mathbf{r}^2}{k^2 + i\epsilon} \int_0^1 \mathrm{d}s \int_0^s \mathrm{d}s' \left(e^{i(s-s')\mathbf{k}\cdot\mathbf{r}} + e^{-i(s-s')\mathbf{k}\cdot\mathbf{r}}\right) \\ =& \int \frac{\mathrm{d}^4k}{(2\pi)^4} \frac{i}{k^2 + i\epsilon} \frac{\mathbf{r}^2}{(\mathbf{k}\cdot\mathbf{r})^2} \left(2 - e^{i\mathbf{k}\cdot\mathbf{r}} - e^{-i\mathbf{k}\cdot\mathbf{r}}\right) \\ =& \int \frac{\mathrm{d}^3k}{(2\pi)^3} \frac{1}{2k} \frac{\mathbf{r}^2}{(\mathbf{k}\cdot\mathbf{r})^2} \left(2 - e^{i\mathbf{k}\cdot\mathbf{r}} - e^{-i\mathbf{k}\cdot\mathbf{r}}\right)\,. \end{aligned} \tag{D.6}$$

Since this integral also diverges, we will use dimensional regularization again, but this time we still have an angular dependence resulting from the $\mathbf{k}\cdot\mathbf{r}$ terms. Switching to d-dimensional spherical coordinates we can write

$$\int \mathrm{d}\Omega_d = \int \mathrm{d}\Omega_{d-1} \int_{-1}^1 \mathrm{d}x (1-x^2)^{\frac{d-3}{2}}\,, \tag{D.7}$$

where $x = \cos\theta$ is the cosine of the angle defined by $\mathbf{r}$ and $\mathbf{k}$, so $\mathbf{k}\cdot\mathbf{r} = krx$.

$$\begin{aligned} I_{\mathrm{II,II}} + I_{\mathrm{IV,IV}} =& \mu^{3-d} \int \frac{\mathrm{d}^dk}{(2\pi)^d} \frac{\mathbf{r}^2}{2k(\mathbf{k}\cdot\mathbf{r})^2} \left(2 - e^{i\mathbf{k}\cdot\mathbf{r}} - e^{-i\mathbf{k}\cdot\mathbf{r}}\right) \\ =& -\frac{2\pi^{\frac{d-1}{2}}\mu^{3-d}}{(2\pi)^d\Gamma\left(\frac{d-1}{2}\right)} \int_0^\infty \mathrm{d}k\, k^{d-4}\, 2\int_0^1 \mathrm{d}x \frac{(1-x^2)^{\frac{d-3}{2}}}{2x^2} \left(e^{ikrx} + e^{-ikrx}\right) \\ =& -\frac{4\mu^{3-d}}{(4\pi)^{\frac{d+1}{2}}\Gamma\left(\frac{d-1}{2}\right)} 2\,\mathrm{Re}\left[\int_0^1 \mathrm{d}x\,(1-x^2)^{\frac{d-3}{2}}(-irx)^{3-d}x^{-2}\int_0^\infty \mathrm{d}k\, k^{d-4}e^{-k}\right] \\ =& -\frac{4\mu^{3-d}}{(4\pi)^{\frac{d+1}{2}}\Gamma\left(\frac{d-1}{2}\right)} \mathrm{Re}\left[(-ir)^{3-d}\right] \int_0^1 \mathrm{d}x\,(1-x)^{\frac{d-3}{2}}x^{-\frac{d}{2}}\,\Gamma(d-3) \\ =& -\frac{4(\mu r)^{3-d}}{(4\pi)^{\frac{d+1}{2}}\Gamma\left(\frac{d-1}{2}\right)} \cos\left(\frac{d-3}{2}\pi\right) \frac{\Gamma\left(\frac{d-1}{2}\right)\Gamma\left(1-\frac{d}{2}\right)}{\Gamma\left(\frac{1}{2}\right)}\Gamma(d-3) \\ =& \frac{2(\mu r)^{3-d}}{(4\pi)^{\frac{d}{2}}} \frac{\Gamma(d-3)}{\Gamma\left(\frac{d}{2}\right)} = \frac{2(\mu r)^{2\varepsilon}}{(4\pi)^{\frac{3}{2}-\varepsilon}} \frac{\Gamma(-2\varepsilon)}{\Gamma\left(\frac{3}{2}-\varepsilon\right)} \\ =& -\frac{1}{4\pi^2\varepsilon} - \frac{1}{4\pi^2}\left(2 + \gamma_E + \ln\pi + 2\ln\mu r\right) + \mathcal{O}(\varepsilon)\,. \end{aligned} \tag{D.8}$$

figure a)

$$\begin{aligned}
I_{\mathrm{III,I}} &= \int \frac{\mathrm{d}^4k}{(2\pi)^4}\frac{i}{k^2+i\epsilon}\int_0^t \mathrm{d}\tau \int_0^t \mathrm{d}\tau' e^{ik_0(t-\tau-\tau')}e^{i\mathbf{k}\cdot\mathbf{r}} \\
&= \int \frac{\mathrm{d}^4k}{(2\pi)^4}\,\frac{i\,e^{i\mathbf{k}\cdot\mathbf{r}}}{k^2+i\epsilon}\,\frac{2-e^{ik_0t}-e^{-ik_0t}}{k_0^2} \\
&= \int \frac{\mathrm{d}^3k}{(2\pi)^3}e^{i\mathbf{k}\cdot\mathbf{r}}\left(\frac{1-e^{-ikt}}{k^3}-\frac{it}{k^2}\right) \\
&= \frac{1}{4\pi^2}\int_0^\infty \mathrm{d}k \int_{-1}^1 \mathrm{d}x\, e^{ikrx}\left(\frac{1-e^{-ikt}}{k}-it\right) \\
&= \frac{1}{2\pi^2 r}\int_0^\infty \mathrm{d}k\,\sin(kr)\left(\frac{1-e^{-ikt}}{k^2}-\frac{it}{k}\right). \qquad \text{(D.9)}
\end{aligned}$$

In order to solve this integration we will integrate by parts:

$$\begin{aligned}
\int_0^\infty \mathrm{d}k\,\sin(kr)\frac{1-e^{-ikt}}{k^2} &= \left[-\sin(kr)\frac{1-e^{-ikt}}{k}\right]_0^\infty + \int_0^\infty \mathrm{d}k\left(r\cos(kr)\frac{1-e^{-ikt}}{k}+\sin(kr)\frac{it\,e^{-ikt}}{k}\right) \\
&= \int_0^\infty \mathrm{d}k\left(ir\cos(kr)\int_0^t \mathrm{d}\tau\, e^{-ik\tau} - t\sin(kr)\int_t^\infty \mathrm{d}\tau\, e^{-ik\tau}\right) \\
&= \int_0^t \mathrm{d}\tau\,\frac{ir}{2}\int_0^\infty \mathrm{d}k\left(e^{-i(\tau-r)k}+e^{-i(\tau+r)k}\right) + \int_t^\infty \mathrm{d}\tau\,\frac{it}{2}\int_0^\infty \mathrm{d}k\left(e^{-i(\tau-r)k}-e^{-i(\tau+r)k}\right) \\
&= \int_0^t \mathrm{d}\tau\,\frac{r\tau}{\tau^2-r^2}+\int_t^\infty \mathrm{d}\tau\,\frac{tr}{\tau^2-r^2} = \int_0^t \mathrm{d}\tau\,\frac{i(i\tau)r}{(i\tau)^2+r^2} - \frac{t}{r}\int_t^\infty \mathrm{d}\tau\,\frac{1}{\left(\frac{i\tau}{r}\right)^2+1} \\
&= \frac{r}{2}\ln\frac{(it)^2+r^2}{r^2} + it\left(\frac{\pi}{2}-\arctan\frac{it}{r}\right). \qquad \text{(D.10)}
\end{aligned}$$

For this we assumed t to have a small negative imaginary part, i.e. $t \to t - i\varepsilon$, in order to make some of the integrals converge. It is important to keep this in mind, since we have to be careful not to cross the branch cut on the negative real axis when adding up complex logarithms. And also the formula

$$\frac{\pi}{2} - \arctan x = \arctan\frac{1}{x}\,, \qquad \text{(D.11)}$$

which we will use several times, is only valid for $\mathrm{Re}\,x > 0$. These issues have been considered in the rest of this section, but will not be pointed out again. It is assumed throughout that $t = |t| - i\varepsilon$ and the limit $\varepsilon \to 0$ then gives the right result for real t.

So now equation (D.9) gives

$$\begin{aligned}
I_{\mathrm{III,I}} &= \frac{1}{2\pi^2 r}\left(\frac{r}{2}\ln\left(1+\frac{(it)^2}{r^2}\right)+it\left(\frac{\pi}{2}-\arctan\frac{it}{r}\right)\right) - \frac{it}{2\pi^2 r}\int_0^\infty \mathrm{d}k\,\frac{\sin(kr)}{k} \\
&= -\frac{it}{2\pi^2 r}\arctan\frac{it}{r} + \frac{1}{4\pi^2}\ln\left(1+\frac{(it)^2}{r^2}\right). \qquad \text{(D.12)}
\end{aligned}$$

figure d)

$$\begin{aligned}
I_{\mathrm{IV,II}} &= \int \frac{\mathrm{d}^4k}{(2\pi)^4}\frac{-ir^2}{k^2+i\epsilon}\int_0^1 \mathrm{d}s\int_0^1 \mathrm{d}s' e^{-i(s+s'-1)\mathbf{k}\cdot\mathbf{r}}e^{-ik_0t} \\
&= \int \frac{\mathrm{d}^4k}{(2\pi)^4}\frac{-ir^2e^{-ik_0t}}{k^2+i\epsilon}\frac{2-e^{i\mathbf{k}\cdot\mathbf{r}}-e^{-i\mathbf{k}\cdot\mathbf{r}}}{(\mathbf{k}\cdot\mathbf{r})^2} \\
&= -\int \frac{\mathrm{d}^3k}{(2\pi)^3}\frac{r^2e^{-ikt}}{2k}\frac{2-e^{i\mathbf{k}\cdot\mathbf{r}}-e^{-i\mathbf{k}\cdot\mathbf{r}}}{(\mathbf{k}\cdot\mathbf{r})^2} \\
&= -\frac{1}{4\pi^2}\int_0^\infty \mathrm{d}k\int_{-1}^1 \mathrm{d}x\,\frac{1-\cos(krx)}{kx^2}e^{-ikt}\,. \qquad \text{(D.13)}
\end{aligned}$$

Again we integrate by parts

$$\begin{aligned}\int_{-1}^{1}\mathrm{d}x\,\frac{1-\cos(krx)}{kx^2} &= \left[-\frac{1-\cos(krx)}{kx}\right]_{-1}^{1}+\int_{-1}^{1}\mathrm{d}x\,\frac{r\sin(krx)}{x}\\ &= -\,2\,\frac{1-\cos(kr)}{k}+2r\,\mathrm{Si}(kr)\,.\end{aligned}\tag{D.14}$$

Putting this in (D.13) we get

$$\begin{aligned}I_{\mathrm{IV,II}} &= \frac{1}{2\pi^2}\int_0^\infty \mathrm{d}k\left(\frac{1-\cos(kr)}{k}-r\,\mathrm{Si}(kr)\right)e^{-ikt}\\
&= \frac{1}{2\pi^2}\int_0^\infty \mathrm{d}k\left(\frac{1-\cos(kr)}{k}-\frac{r^2}{it}\frac{\sin(kr)}{kr}\right)e^{-ikt}-\frac{1}{2\pi^2}\left[\frac{r}{-it}e^{-ikt}\mathrm{Si}(kr)\right]_0^\infty\\
&= \frac{i}{4\pi^2}\int_t^\infty \mathrm{d}\tau\int_0^\infty \mathrm{d}k\left(2e^{-ik\tau}-e^{-i(\tau-r)k}-e^{-i(\tau+r)k}+\frac{r}{t}\left(e^{-i(t-r)k}-e^{-i(t+r)k}\right)\right)\\
&= \frac{1}{4\pi^2}\int_t^\infty \mathrm{d}\tau\left(\frac{2}{\tau}-\frac{1}{\tau-r}-\frac{1}{\tau+r}+\frac{r}{t}\left(\frac{1}{\tau-r}-\frac{1}{\tau+r}\right)\right)\\
&= \frac{1}{2\pi^2}\int_t^\infty \mathrm{d}\tau\left(\frac{1}{\tau}-\frac{\tau}{\tau^2-r^2}+\frac{r^2}{t(\tau^2-r^2)}\right)\\
&= \frac{1}{2\pi^2}\int_t^\infty \mathrm{d}\tau\left(\frac{i}{i\tau}-\frac{i(i\tau)}{(i\tau)^2+r^2}-\frac{1}{t}\frac{1}{\left(\frac{i\tau}{r}\right)^2+1}\right)\\
&= \frac{1}{2\pi^2}\left(-\frac{1}{2}\ln\frac{(it)^2}{(it)^2+r^2}-\frac{r}{it}\left(\frac{\pi}{2}-\arctan\frac{it}{r}\right)\right)\\
&= -\frac{r}{2\pi^2 it}\arctan\frac{r}{it}+\frac{1}{4\pi^2}\ln\left(1+\frac{r^2}{(it)^2}\right)\,.\end{aligned}\tag{D.15}$$

Finally the sum over all contributions gives

$$\begin{aligned}&-\frac{1}{2\pi^2\varepsilon}-\frac{1}{2\pi^2}\left[2+\gamma_E+\ln\pi+\ln itr\mu^2\right]-\frac{1}{2\pi^2}\left[\frac{it}{r}\arctan\frac{it}{r}+\frac{r}{it}\arctan\frac{r}{it}\right]+\\
&+\frac{1}{4\pi^2}\left[\ln\left(1+\frac{(it)^2}{r^2}\right)+\ln\left(1+\frac{r^2}{(it)^2}\right)\right]\,.\end{aligned}\tag{D.16}$$

In this expression it is still assumed that t has a small negative imaginary part. To get the expression for real t we make the substitution $t\to t-i\varepsilon$ and take the limit $\varepsilon\to 0$. Using $\arctan(ix)=\frac{i}{2}(\ln(1+x)-\ln(1-x))$ we get

$$\begin{aligned}&\frac{1}{4\pi^2}\left(\frac{t}{r}+\frac{r}{t}\right)\ln\frac{t+r}{|t-r|}-\frac{it}{4\pi r}\Theta(t-r)+\frac{ir}{4\pi t}\Theta(r-t)+\\
&+\frac{1}{2\pi^2}\ln\frac{|t^2-r^2|}{tr}+\frac{i}{4\pi}\Theta(t-r)-\frac{i}{4\pi}\Theta(r-t)-\\
&-\frac{1}{2\pi^2\varepsilon}-\frac{1}{2\pi^2}\left[2+\gamma_E+\ln\pi+\ln tr\mu^2+i\frac{\pi}{2}\right]\\
=&-\frac{it}{4\pi r}\Theta(t-r)+\frac{1}{4\pi^2}\left(\frac{t}{r}+\frac{r}{t}\right)\ln\frac{t+r}{|t-r|}+\frac{1}{2\pi^2}\ln\frac{|t^2-r^2|}{t^2r^2\mu^2}-\\
&-\frac{1}{2\pi^2\varepsilon}-\frac{1}{2\pi^2}\left[2+\gamma_E+\ln\pi\right]-\frac{i}{4\pi}\left(2-\frac{r}{t}\right)\Theta(r-t)\,.\end{aligned}\tag{D.17}$$

D.2 Tree Level Calculations (Coulomb Gauge)

propagator

$$D_{\mu\nu}(k)=\frac{i\eta_{\mu0}\eta_{\nu0}}{\mathbf{k}^2}+\frac{i\eta_{\mu i}\eta_{\nu j}}{k^2+i\epsilon}\left(\delta^{ij}-\frac{\mathbf{k}^i\mathbf{k}^j}{\mathbf{k}^2}\right)\tag{D.18}$$

figures b), c)

$$\begin{aligned} I_{\mathrm{I,I}} + I_{\mathrm{III,III}} &= \int \frac{\mathrm{d}^4k}{(2\pi)^4} \frac{i}{\mathbf{k}^2} \int_0^t \mathrm{d}\tau \int_0^\tau \mathrm{d}\tau' \left(e^{ik_0(\tau-\tau')} + e^{-ik_0(\tau-\tau')} \right) \\ &= \int \frac{\mathrm{d}^4k}{(2\pi)^4} \frac{i}{\mathbf{k}^2} \frac{1}{k_0^2} \left(2 - e^{ik_0 t} - e^{-ik_0 t} \right) \\ &= \int \frac{\mathrm{d}^3k}{(2\pi)^3} \frac{it}{\mathbf{k}^2} \,. \end{aligned} \tag{D.19}$$

This is a scaleless integral and vanishes in dimensional regularization.

figures e), f)

$$\begin{aligned} I_{\mathrm{II,II}} + I_{\mathrm{IV,IV}} &= \int \frac{\mathrm{d}^4k}{(2\pi)^4} \frac{i}{k^2 + i\epsilon} \left(r^2 - \frac{(\mathbf{k}\cdot\mathbf{r})^2}{\mathbf{k}^2} \right) \int_0^1 \mathrm{d}s \int_0^s \mathrm{d}s' \left(e^{i(s-s')\mathbf{k}\cdot\mathbf{r}} + e^{-i(s-s')\mathbf{k}\cdot\mathbf{r}} \right) \\ &= \int \frac{\mathrm{d}^4k}{(2\pi)^4} \frac{i}{k^2 + i\epsilon} \left(r^2 - \frac{(\mathbf{k}\cdot\mathbf{r})^2}{\mathbf{k}^2} \right) \frac{2 - e^{i\mathbf{k}\cdot\mathbf{r}} - e^{-i\mathbf{k}\cdot\mathbf{r}}}{(\mathbf{k}\cdot\mathbf{r})^2} \\ &= \int \frac{\mathrm{d}^3k}{(2\pi)^3} \frac{1}{2k} \left(r^2 - \frac{(\mathbf{k}\cdot\mathbf{r})^2}{\mathbf{k}^2} \right) \frac{2 - e^{i\mathbf{k}\cdot\mathbf{r}} - e^{-i\mathbf{k}\cdot\mathbf{r}}}{(\mathbf{k}\cdot\mathbf{r})^2} \,. \end{aligned} \tag{D.20}$$

Again using dimensional regularization.

$$\begin{aligned} I_{\mathrm{II,II}} + I_{\mathrm{IV,IV}} &= \mu^{3-d} \int \frac{\mathrm{d}^dk}{(2\pi)^d} \frac{1}{2k} \left(\mathbf{r}^2 - \frac{(\mathbf{k}\cdot\mathbf{r})^2}{\mathbf{k}^2} \right) \frac{2 - e^{i\mathbf{k}\cdot\mathbf{r}} - e^{-i\mathbf{k}\cdot\mathbf{r}}}{(\mathbf{k}\cdot\mathbf{r})^2} \\ &= - \frac{2\pi^{\frac{d-1}{2}} \mu^{3-d}}{(2\pi)^d \Gamma\left(\frac{d-1}{2}\right)} \int_0^\infty \mathrm{d}k\, k^{d-4}\, 2 \int_0^1 \mathrm{d}x \frac{(1-x^2)^{\frac{d-1}{2}}}{2x^2} \left(e^{ikrx} + e^{-ikrx} \right) \\ &= - \frac{4\mu^{3-d}}{(4\pi)^{\frac{d+1}{2}} \Gamma\left(\frac{d-1}{2}\right)} 2\,\mathrm{Re} \left[\int_0^1 \mathrm{d}x\, (1-x^2)^{\frac{d-1}{2}} (-irx)^{3-d} x^{-2} \int_0^\infty \mathrm{d}k\, k^{d-4} e^{-k} \right] \\ &= - \frac{4\mu^{3-d}}{(4\pi)^{\frac{d+1}{2}} \Gamma\left(\frac{d-1}{2}\right)} \mathrm{Re}\left[(-ir)^{3-d} \right] \int_0^1 \mathrm{d}x\, (1-x)^{\frac{d-1}{2}} x^{-\frac{d}{2}}\, \Gamma(d-3) \\ &= - \frac{4(\mu r)^{3-d}}{(4\pi)^{\frac{d+1}{2}} \Gamma\left(\frac{d-1}{2}\right)} \cos\left(\frac{d-3}{2}\pi \right) \frac{\Gamma\left(\frac{d+1}{2}\right) \Gamma\left(1 - \frac{d}{2}\right)}{\Gamma\left(\frac{3}{2}\right)} \Gamma(d-3) \\ &= \frac{2(\mu r)^{3-d}}{(4\pi)^{\frac{d}{2}}} (d-1) \frac{\Gamma(d-3)}{\Gamma\left(\frac{d}{2}\right)} = \frac{4(\mu r)^{2\varepsilon}}{(4\pi)^{\frac{3}{2}-\varepsilon}} (1-\varepsilon) \frac{\Gamma(-2\varepsilon)}{\Gamma\left(\frac{3}{2}-\varepsilon\right)} \\ &= - \frac{1}{2\pi^2 \varepsilon} - \frac{1}{2\pi^2} \left(1 + \gamma_E + \ln\pi + 2\ln \mu r \right) + \mathcal{O}(\varepsilon) \,. \end{aligned} \tag{D.21}$$

figure a)

$$\begin{aligned} I_{\mathrm{III,I}} &= \int \frac{\mathrm{d}^4k}{(2\pi)^4} \frac{-i}{\mathbf{k}^2} \int_0^t \mathrm{d}\tau \int_0^t \mathrm{d}\tau' e^{ik_0(t-\tau-\tau')} e^{i\mathbf{k}\cdot\mathbf{r}} \\ &= \int \frac{\mathrm{d}^4k}{(2\pi)^4} \frac{-ie^{i\mathbf{k}\cdot\mathbf{r}}}{\mathbf{k}^2} \frac{2 - e^{ik_0 t} - e^{-ik_0 t}}{k_0^2} \\ &= \int \frac{\mathrm{d}^3k}{(2\pi)^3} \frac{-it}{\mathbf{k}^2} e^{i\mathbf{k}\cdot\mathbf{r}} \\ &= - \frac{it}{4\pi^2} \int_0^\infty \mathrm{d}k \int_{-1}^1 \mathrm{d}x\, e^{ikrx} \\ &= - \frac{it}{4\pi^2 r} \int_0^\infty \mathrm{d}k\, \frac{2\sin(kr)}{k} \\ &= - \frac{it}{4\pi r} \,. \end{aligned} \tag{D.22}$$

figure d)

$$
\begin{aligned}
I_{\mathrm{IV,II}} &= \int \frac{\mathrm{d}^4k}{(2\pi)^4} \frac{-ie^{-ik_0t}}{k^2+i\epsilon} \left(r^2 - \frac{(\mathbf{k}\cdot\mathbf{r})^2}{\mathbf{k}^2} \right) \int_0^1 \mathrm{d}s \int_0^1 \mathrm{d}s' e^{-i(s+s'-1)\mathbf{k}\cdot\mathbf{r}} \\
&= \int \frac{\mathrm{d}^4k}{(2\pi)^4} \frac{-ie^{-ik_0t}}{k^2+i\epsilon} \left(r^2 - \frac{(\mathbf{k}\cdot\mathbf{r})^2}{\mathbf{k}^2} \right) \frac{2 - e^{i\mathbf{k}\cdot\mathbf{r}} - e^{-i\mathbf{k}\cdot\mathbf{r}}}{(\mathbf{k}\cdot\mathbf{r})^2} \\
&= -\int \frac{\mathrm{d}^3k}{(2\pi)^3} \frac{e^{-ikt}}{2k} \left(r^2 - \frac{(\mathbf{k}\cdot\mathbf{r})^2}{\mathbf{k}^2} \right) \frac{2 - e^{i\mathbf{k}\cdot\mathbf{r}} - e^{-i\mathbf{k}\cdot\mathbf{r}}}{(\mathbf{k}\cdot\mathbf{r})^2} \\
&= -\frac{1}{4\pi^2} \int_0^\infty \mathrm{d}k \int_{-1}^1 \mathrm{d}x \, \left(1-x^2\right) \frac{1-\cos(krx)}{kx^2} e^{-ikt} \\
&\overset{\text{(D.14)}}{=} -\frac{1}{2\pi^2} \int_0^\infty \mathrm{d}k \left(r\,\mathrm{Si}(kr) - \frac{1-\cos(kr)}{k} - \frac{kr-\sin(kr)}{k^2r} \right) e^{-ikt} \,. \qquad \text{(D.23)}
\end{aligned}
$$

For the last term in (D.23) we will again use integration by parts:

$$
\begin{aligned}
\int_0^\infty \mathrm{d}k \, \frac{kr-\sin(kr)}{k^2r} e^{-ikt} &= \left[-\frac{kr-\sin(kr)}{kr} e^{-ikt} \right]_0^\infty + \int_0^\infty \mathrm{d}k \left(\frac{1-\cos(kr)}{k} - it \frac{kr-\sin(kr)}{kr} \right) e^{-ikt} \\
&= \int_0^\infty \mathrm{d}k \left(\frac{1-\cos(kr)}{k} - it \left(1 - \frac{\sin(kr)}{kr} \right) \right) e^{-ikt} \,. \qquad \text{(D.24)}
\end{aligned}
$$

Putting this back into (D.23), all integrals are already familiar from the Feynman gauge calculations. So we get

$$
\begin{aligned}
&= -\frac{1}{2\pi^2} \int_0^\infty \mathrm{d}k \left(r\,\mathrm{Si}(kr) - 2\,\frac{1-\cos(kr)}{k} - \frac{it\sin(kr)}{kr} + it \right) e^{-ikt} \\
&= -\frac{1}{2\pi^2} \left[\frac{r}{it} \arctan\frac{r}{it} - \frac{it}{r} \arctan\frac{r}{it} - \ln\left(1 + \frac{r^2}{(it)^2} \right) + 1 \right] . \qquad \text{(D.25)}
\end{aligned}
$$

result

$$
\begin{aligned}
&-\frac{1}{2\pi^2\varepsilon} - \frac{1}{2\pi^2} \left[2 + \gamma_E + \ln\pi + \ln\mu^2r^2 \right] - \frac{it}{4\pi r} + \\
&+ \frac{1}{2\pi^2} \left[\frac{it}{r} \arctan\frac{r}{it} - \frac{r}{it} \arctan\frac{r}{it} \right] + \frac{1}{2\pi^2} \ln\left(1 + \frac{r^2}{(it)^2} \right) . \qquad \text{(D.26)}
\end{aligned}
$$

This result is equal to the one in Feynman gauge, as it should be. To see this we make the following transformations:

$$
\frac{it}{2\pi^2 r} \arctan\frac{r}{it} - \frac{it}{4\pi r} = -\frac{it}{2\pi^2 r} \arctan\frac{it}{r} \,, \qquad \text{(D.27)}
$$

$$
\frac{1}{2\pi^2} \ln\left(1 + \frac{r^2}{(it)^2} \right) = \frac{1}{4\pi^2} \left[\ln\left(1 + \frac{r^2}{(it)^2} \right) + \ln\left(1 + \frac{(it)^2}{r^2} \right) - \ln\frac{(it)^2}{r^2} \right] , \qquad \text{(D.28)}
$$

$$
\ln\mu^2r^2 + \frac{1}{2}\ln\frac{(it)^2}{r^2} = \ln itr\mu^2 \,. \qquad \text{(D.29)}
$$

D.3 Unconnected Two-Gluon Diagrams

All calculations are done in Coulomb gauge. This has the advantage that some contributions can be immediately seen to be zero, but on the other hand it rather complicates some other calculations like the vacuum polarization in the next section. We will now give the values for the diagrams shown in figure 2.2.

$$
\text{b)} \quad \int_0^t \mathrm{d}\tau_1 \int_0^{\tau_1} \mathrm{d}\tau_2 \int_0^{\tau_2} \mathrm{d}\tau_3 \int_0^{\tau_3} \mathrm{d}\tau_4 \int \frac{\mathrm{d}^4k}{(2\pi)^4} \int \frac{\mathrm{d}^4q}{(2\pi)^4} \frac{i}{\mathbf{k}^2} \frac{i}{\mathbf{q}^2} e^{ik_0(\tau_1-\tau_3)} e^{iq_0(\tau_2-\tau_4)} \qquad \text{(D.30)}
$$

$$\text{c)} - \int_0^t \mathrm{d}\tau_1 \int_0^t \mathrm{d}\tau_2 \int_0^{\tau_2} \mathrm{d}\tau_3 \int_0^{\tau_3} \mathrm{d}\tau_4 \int \frac{\mathrm{d}^4k}{(2\pi)^4} \int \frac{\mathrm{d}^4q}{(2\pi)^4} \frac{i}{\mathbf{k}^2} \frac{i}{\mathbf{q}^2} e^{ik_0(t-\tau_1-\tau_3)i\mathbf{k}\cdot\mathbf{r}} e^{iq_0(\tau_2-\tau_4)} \tag{D.31}$$

Both of these integrals vanish in dimensional regularization because of the scaleless $\mathbf{k}$ or $\mathbf{q}$ integrations. But even without regularizing they give zero because of the k_0, q_0 and τ_i integrations in a way quite analogous to the next example.

$$\begin{aligned}
\text{e)} \quad & \int_0^t \mathrm{d}\tau_1 \int_0^{\tau_1} \mathrm{d}\tau_2 \int_0^t \mathrm{d}\tau_3 \int_0^{\tau_3} \mathrm{d}\tau_4 \int \frac{\mathrm{d}^4k}{(2\pi)^4} \int \frac{\mathrm{d}^4q}{(2\pi)^4} \frac{i}{\mathbf{k}^2} \frac{i}{\mathbf{q}^2} e^{ik_0(t-\tau_1-\tau_3)+i\mathbf{k}\cdot\mathbf{r}} e^{iq_0(t-\tau_2-\tau_4)+i\mathbf{q}\cdot\mathbf{r}} \\
&= -\left(\frac{1}{4\pi r}\right)^2 \int_0^t \mathrm{d}\tau_1 \int_0^{\tau_1} \mathrm{d}\tau_2 \int_0^t \mathrm{d}\tau_3 \int_0^{\tau_3} \mathrm{d}\tau_4\, \delta(t-\tau_1-\tau_3)\delta(t-\tau_2-\tau_4) \\
&= -\left(\frac{1}{4\pi r}\right)^2 \int_0^t \mathrm{d}\tau_1 \int_0^{\tau_1} \mathrm{d}\tau_2 \int_0^t \mathrm{d}\tau_3\, \delta(t-\tau_1-\tau_3)\Theta(\tau_2+\tau_3-t) \\
&= -\left(\frac{1}{4\pi r}\right)^2 \int_0^t \mathrm{d}\tau_1 \int_0^{\tau_1} \mathrm{d}\tau_2\, \Theta(\tau_2-\tau_1) = 0\,.
\end{aligned} \tag{D.32}$$

In the next diagram f) there is no overlap between the regions of integration for the two propagators, so they factor to give the product of the corresponding tree level contributions (D.22) and (D.25), with their colour factors replaced by the colour connected coefficient.

$$\text{f)} \ -\frac{1}{2} C_F C_A\, g^4 \left(\frac{-it}{4\pi r}\right) \cdot \left(-\frac{1}{2\pi^2}\left[\frac{r}{it}\arctan\frac{r}{it} - \frac{it}{r}\arctan\frac{r}{it} - \ln\left(1-\frac{r^2}{t^2}\right)+1\right]\right), \tag{D.33}$$

$$\lim_{t\to(1-i\epsilon)\infty} \frac{W(\gamma_\mathrm{f})}{-it} = 0\,. \tag{D.34}$$

In d) the colour factor is given by

$$f^{abc}\widetilde{\mathrm{Tr}}\{T^aT^bT^c\} = \frac{i}{2} C_A \widetilde{\mathrm{Tr}}\{T^cT^c\} = \frac{i}{2} C_F C_A\,. \tag{D.35}$$

After contracting all the indices at the three gluon vertex, d) reads

$$\begin{aligned}
-\frac{1}{2} C_F C_A g^4 \int_0^t \mathrm{d}\tau_1 \int_0^1 \mathrm{d}s \int_0^t \mathrm{d}\tau_2 \int \frac{\mathrm{d}^4k}{(2\pi)^4} \int \frac{\mathrm{d}^4q}{(2\pi)^4} \frac{i}{(\mathbf{k}+\mathbf{q})^2} \frac{2i\left(\mathbf{r}\cdot\mathbf{k} - \frac{(\mathbf{r}\cdot\mathbf{q})(\mathbf{k}\cdot\mathbf{q})}{\mathbf{q}^2}\right)}{q^2+i\varepsilon} \frac{i}{\mathbf{k}^2} \times \\
\times\, e^{i(k_0+q_0)(t-\tau_1)+\frac{i}{2}(\mathbf{k}+\mathbf{q})\cdot\mathbf{r}} e^{-iq_0t+i\mathbf{q}\cdot\mathbf{r}(\frac{1}{2}-s)} e^{-ik_0\tau_2+\frac{i}{2}\mathbf{k}\cdot\mathbf{r}}\,.
\end{aligned} \tag{D.36}$$

Now let us concentrate only on the parts relevant for taking the limit to show that this diagram gives no contribution.

$$\begin{aligned}
& \lim_{t\to(1-i\epsilon)\infty} \frac{1}{-it} \int_0^t \mathrm{d}\tau_1 \int_0^t \mathrm{d}\tau_2 \int \frac{\mathrm{d}k_0}{2\pi} \int \frac{\mathrm{d}q_0}{2\pi} e^{ik_0(t-\tau_1-\tau_2)} \frac{e^{-iq_0\tau_1}}{q^2+i\varepsilon} \\
&= \lim_{t\to(1-i\epsilon)\infty} \frac{1}{-it} \int_0^t \mathrm{d}\tau_1 \int_0^t \mathrm{d}\tau_2\, \delta(t-\tau_1-\tau_2) \frac{ie^{-i|\mathbf{q}|\tau_1}}{-2|\mathbf{q}|} \\
&= \lim_{t\to(1-i\epsilon)\infty} \frac{1}{-it} \int_0^t \mathrm{d}\tau_1 \frac{ie^{-i|\mathbf{q}|\tau_1}}{-2|\mathbf{q}|} \\
&= \lim_{t\to(1-i\epsilon)\infty} \frac{1-e^{-i|\mathbf{q}|t}}{-it\,2|\mathbf{q}|^2} = 0
\end{aligned} \tag{D.37}$$

It can be shown in a similar fashion that other diagrams involving one or more of the vertical sides of the Wilson loop give no contribution. The three gluon diagrams with all endpoints on the horizontal sides of the Wilson loop are zero because of the structure of the three gluon vertex:

$$\eta^{\mu\nu}(k-q)^\rho + \eta^{\nu\rho}(q-p)^\mu + \eta^{\rho\mu}(p-k)^\nu = 0 \quad \text{for } \mu=\nu=\rho=0. \tag{D.38}$$

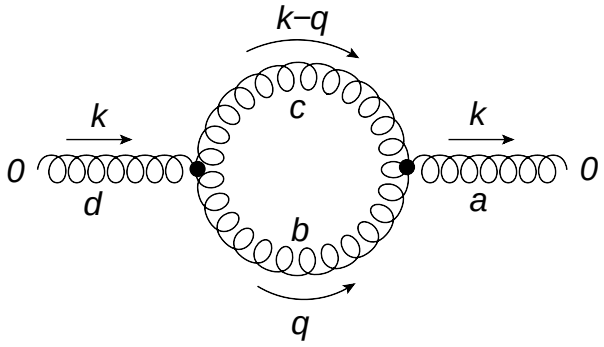

Figure D.1: Feynman diagram for the vacuum polarization (gluon loop).

D.4 Vacuum Polarization

Now the only diagram left is a), which involves the vacuum polarization. It will make things easier later on if we take the limit first and then do the momentum integrations.

$$\begin{aligned}
&\lim_{t\to\infty}\frac{1}{-it}\int_0^t \mathrm{d}\tau_1\int_0^t \mathrm{d}\tau_2\, e^{-ik_0(\tau_1-\tau_2)}\\
=&i\lim_{t\to\infty}\int_0^t \mathrm{d}\tau\,\left(e^{ik_0(t-\tau)}+e^{-ik_0(t-\tau)}\right)\\
=&i\lim_{t\to\infty}\int_{-t}^t \mathrm{d}\tau\, e^{ik_0\tau} = i\,\delta(k_0)\,.
\end{aligned} \tag{D.39}$$

This means that in the calculation of the vacuum polarization we can use $k_0 = 0$. We also only need the 00 component of the vacuum polarization, so for the gluonic part we have to integrate over the following (compare figure D.1)

$$\begin{aligned}
&\frac{1}{2}D_{00}(k)\left(-gf^{abc}\right)\left[\eta^{0\mu}(-k-q)^\nu+\eta^{\mu\nu}(q_0-(k_0-q_0))+\eta^{\nu 0}(k-q+k)^\mu\right]D_{\mu\rho}(q)\times\\
&\times D_{\nu\sigma}(k-q)\left(-gf^{bdc}\right)\left[\eta^{\rho 0}(-q-k)^\sigma+\eta^{0\sigma}(k+k-q)^\rho+\eta^{\sigma\rho}(-(k_0-q_0)+q_0)\right]D_{00}(k)\\
=&-\frac{g^2}{2}C_A\delta^{ad}\left(\frac{1}{\mathbf{k}^2}\right)^2\left\{\frac{4q_0^2}{(q^2+i\varepsilon)((k-q)^2+i\varepsilon)}\left[d-2+\frac{((\mathbf{k}-\mathbf{q})\cdot\mathbf{q})^2}{(\mathbf{k}-\mathbf{q})^2\mathbf{q}^2}\right]+\right.\\
&\left.+\frac{1}{\mathbf{q}^2((k-q)^2+i\varepsilon)}\left[(\mathbf{k}+\mathbf{q})^2-\frac{(\mathbf{k}^2-\mathbf{q}^2)^2}{(\mathbf{k}-\mathbf{q})^2}\right]+\frac{1}{(\mathbf{k}-\mathbf{q})^2(q^2+i\varepsilon)}\left[(2\mathbf{k}-\mathbf{q})^2-\frac{(2\mathbf{k}\cdot\mathbf{q}-\mathbf{q}^2)^2}{\mathbf{q}^2}\right]\right\}.
\end{aligned} \tag{D.40}$$

Note that there is a symmetry factor $\frac{1}{2}$ from the two interchangeable gluon lines. We will use the convention $d = 3-2\varepsilon$ and $D = 4-2\varepsilon$ throughout. The last two terms are actually the same under the substitution $q \leftrightarrow k-q$. This integral will be computed by combining the denominators using Feynman parameters and the following formulae:

$$\begin{aligned}
I_a =&\int\frac{\mathrm{d}^dq}{(2\pi)^d}\frac{1}{(\mathbf{q}^2+2\mathbf{b}\cdot\mathbf{q}+c)^a} = \frac{1}{\Gamma(a)}\int\frac{\mathrm{d}^dq}{(2\pi)^d}\int_0^\infty \mathrm{d}x\, x^{a-1}e^{-x(\mathbf{q}+\mathbf{b})^2-x(c-\mathbf{b}^2)}\\
=&\frac{1}{\Gamma(a)}\int_0^\infty \mathrm{d}x\, x^{a-1-\frac{d}{2}}e^{-x(c-b^2)}\int\frac{\mathrm{d}^dq}{(2\pi)^d}e^{-q^2}\\
=&\frac{\Gamma(a-\frac{d}{2})}{(4\pi)^{\frac{d}{2}}\Gamma(a)(c-b^2)^{a-\frac{d}{2}}}\,,
\end{aligned} \tag{D.41}$$

$$I_a^k = \int\frac{\mathrm{d}^dq}{(2\pi)^d}\frac{q^k}{(\mathbf{q}^2+2\mathbf{b}\cdot\mathbf{q}+c)^a} = -b^kI_a\,, \tag{D.42}$$

$$I_a^{kl} = \int \frac{\mathrm{d}^d q}{(2\pi)^d} \frac{q^k q^l}{(\mathbf{q}^2 + 2\mathbf{b}\cdot\mathbf{q} + c)^a} = b^k b^l I_a + \frac{1}{2(a-1)} \delta^{kl} I_{a-1} \,. \tag{D.43}$$

The second two equations can be obtained from the first by differentiating with respect to b^k.

Now we will integrate the different parts separately.

$$\begin{aligned}
&\int \frac{\mathrm{d}^D q}{(2\pi)^D} \frac{2}{\mathbf{q}^2((k-q)^2 + i\varepsilon)} \left[(\mathbf{k}+\mathbf{q})^2 - \frac{(\mathbf{k}^2 - \mathbf{q}^2)^2}{(\mathbf{k}-\mathbf{q})^2} \right] \\
&= -i \int \frac{\mathrm{d}^d q}{(2\pi)^d} \frac{1}{\mathbf{q}^2 |\mathbf{k}-\mathbf{q}|} \left[(\mathbf{k}+\mathbf{q})^2 - \frac{(\mathbf{k}^2 - \mathbf{q}^2)^2}{(\mathbf{k}-\mathbf{q})^2} \right] \\
&= -i \int \frac{\mathrm{d}^d q}{(2\pi)^d} \left[\frac{1}{|\mathbf{k}-\mathbf{q}|} + \frac{2\mathbf{k}\cdot\mathbf{q}}{\mathbf{q}^2|\mathbf{k}-\mathbf{q}|} + \frac{\mathbf{k}^2}{\mathbf{q}^2|\mathbf{k}-\mathbf{q}|} - \frac{(\mathbf{k}^2)^2}{\mathbf{q}^2|\mathbf{k}-\mathbf{q}|^3} + \frac{2\mathbf{k}^2}{|\mathbf{k}-\mathbf{q}|^3} - \frac{\mathbf{q}^2}{|\mathbf{k}-\mathbf{q}|^3} \right] .
\end{aligned} \tag{D.44}$$

Many of the above terms are scaleless integrals after shifting $\mathbf{q} \to \mathbf{k} - \mathbf{q}$. We are left with

$$\begin{aligned}
&= -i \int \frac{\mathrm{d}^d q}{(2\pi)^d} \left[\frac{3\mathbf{k}^2}{(\mathbf{k}-\mathbf{q})^2 q} - \frac{2\mathbf{k}\cdot\mathbf{q}}{(\mathbf{k}-\mathbf{q})^2 q} - \frac{(\mathbf{k}^2)^2}{(\mathbf{k}-\mathbf{q})^2 q^3} \right] \\
&= -i \int_0^1 \mathrm{d}x \int \frac{\mathrm{d}^d q}{(2\pi)^d} \left[\frac{\Gamma(\frac{3}{2})}{\Gamma(\frac{1}{2})\Gamma(1)} \frac{(3\mathbf{k}^2 - 2\mathbf{k}\cdot\mathbf{q})(1-x)^{-\frac{1}{2}}}{(\mathbf{q}^2 - 2x\mathbf{k}\cdot\mathbf{q} + x\mathbf{k}^2)^{\frac{3}{2}}} - \frac{\Gamma(\frac{5}{2})}{\Gamma(\frac{3}{2})\Gamma(1)} \frac{(\mathbf{k}^2)^2 (1-x)^{\frac{1}{2}}}{(\mathbf{q}^2 - 2x\mathbf{k}\cdot\mathbf{q} + x\mathbf{k}^2)^{\frac{5}{2}}} \right] \\
&= -\frac{i}{2} \int_0^1 \mathrm{d}x \left[3k^2 (1-x)^{-\frac{1}{2}} I_{\frac{3}{2}}(-x\mathbf{k}, xk^2) - 2(1-x)^{-\frac{1}{2}} k^l I^l_{\frac{3}{2}}(-x\mathbf{k}, xk^2) - 3k^4 (1-x)^{\frac{1}{2}} I_{\frac{5}{2}}(-x\mathbf{k}, xk^2) \right] \\
&= -i \frac{k^{d-1}}{2(4\pi)^{\frac{d}{2}}} \int_0^1 \mathrm{d}x \left[3\frac{\Gamma(\frac{3-d}{2})}{\Gamma(\frac{3}{2})} x^{\frac{d-3}{2}} (1-x)^{\frac{d-4}{2}} - 2\frac{\Gamma(\frac{3-d}{2})}{\Gamma(\frac{3}{2})} x^{\frac{d-1}{2}} (1-x)^{\frac{d-4}{2}} - 3\frac{\Gamma(\frac{5-d}{2})}{\Gamma(\frac{5}{2})} x^{\frac{d-5}{2}} (1-x)^{\frac{d-4}{2}} \right] \\
&= -i \frac{k^{d-1}}{2(4\pi)^{\frac{d}{2}}} \left[3\frac{\Gamma(\frac{3-d}{2})\Gamma(\frac{d-1}{2})\Gamma(\frac{d-2}{2})}{\Gamma(\frac{3}{2})\Gamma(d-\frac{3}{2})} - 2\frac{\Gamma(\frac{3-d}{2})\Gamma(\frac{d+1}{2})\Gamma(\frac{d-2}{2})}{\Gamma(\frac{3}{2})\Gamma(d-\frac{1}{2})} - 3\frac{\Gamma(\frac{5-d}{2})\Gamma(\frac{d-3}{2})\Gamma(\frac{d-2}{2})}{\Gamma(\frac{5}{2})\Gamma(d-\frac{5}{2})} \right] \\
&= i \frac{k^{d-1}}{(4\pi)^{\frac{d-1}{2}}} 2(d-1) \frac{\Gamma(\frac{d}{2}) \sec(d\frac{\pi}{2})}{\Gamma(d-\frac{1}{2})} \\
&= -i \frac{2k^2}{3\pi^2} \left(\frac{1}{\varepsilon} + \frac{7}{3} - \gamma_E - \ln k^2 + \ln \pi + \mathcal{O}(\varepsilon^1) \right) .
\end{aligned} \tag{D.45}$$

Now to the other term:

$$\begin{aligned}
&\int \frac{\mathrm{d}^D q}{(2\pi)^D} \frac{4q_0^2}{(q^2 + i\varepsilon)((k-q)^2 + i\varepsilon)} \left[d - 2 + \frac{((\mathbf{k}-\mathbf{q})\cdot\mathbf{q})^2}{(\mathbf{k}-\mathbf{q})^2 \mathbf{q}^2} \right] \\
&= \int_0^1 \mathrm{d}x \int \frac{\mathrm{d}^D q}{(2\pi)^D} \frac{4q_0^2}{(q_0^2 - \mathbf{q}^2 + 2x\mathbf{k}\cdot\mathbf{q} - x\mathbf{k}^2 + i\varepsilon)^2} \left[d - 1 + \frac{(\mathbf{k}\cdot\mathbf{q})^2}{(\mathbf{k}-\mathbf{q})^2\mathbf{q}^2} - \frac{\mathbf{k}^2}{(\mathbf{k}-\mathbf{q})^2} \right] \\
&= -i \int_0^1 \mathrm{d}x \int_0^1 \mathrm{d}y \int \frac{\mathrm{d}^d q}{(2\pi)^d} \frac{1}{(\mathbf{q}^2 - 2x\mathbf{k}\cdot\mathbf{q} + x\mathbf{k}^2)^{\frac{1}{2}}} \left[d - 1 + \frac{(\mathbf{k}\cdot\mathbf{q})^2}{(\mathbf{q}^2 - 2y\mathbf{k}\cdot\mathbf{q} + y\mathbf{k}^2)^2} - \frac{\mathbf{k}^2}{(\mathbf{k}-\mathbf{q})^2} \right] \\
&= -i \int_0^1 \mathrm{d}x \int_0^1 \mathrm{d}y \int_0^1 \mathrm{d}z \int \frac{\mathrm{d}^d q}{(2\pi)^d} \left[\frac{d-1}{(\mathbf{q}^2 - 2x\mathbf{k}\cdot\mathbf{q} + x\mathbf{k}^2)^{\frac{1}{2}}} - \right. \\
&\quad - \frac{\Gamma(\frac{3}{2})}{\Gamma(\frac{1}{2})\Gamma(1)} \frac{z^{-\frac{1}{2}} \mathbf{k}^2}{(\mathbf{q}^2 - 2(xz+1-z)\mathbf{k}\cdot\mathbf{q} + (xz+1-z)\mathbf{k}^2)^{\frac{3}{2}}} + \\
&\quad \left. + \frac{\Gamma(\frac{5}{2})}{\Gamma(\frac{1}{2})\Gamma(2)} \frac{z^{-\frac{1}{2}}(1-z)(\mathbf{k}\cdot\mathbf{q})^2}{(\mathbf{q}^2 - 2(xz + y(1-z))\mathbf{k}\cdot\mathbf{q} + (xz+y(1-z))\mathbf{k}^2)^{\frac{5}{2}}} \right] \\
&= -i \int_0^1 \mathrm{d}x \int_0^1 \mathrm{d}y \int_0^1 \mathrm{d}z \left[(d-1) I_{\frac{1}{2}} \left(-x\mathbf{k}, x\mathbf{k}^2\right) - \right. \\
&\quad - \frac{\Gamma(\frac{3}{2})}{\Gamma(\frac{1}{2})\Gamma(1)} z^{-\frac{1}{2}} \mathbf{k}^2 I_{\frac{3}{2}}(-(xz+1-z)\mathbf{k}, \left(xz+1-z\right)\mathbf{k}^2) + \\
&\quad \left. + \frac{\Gamma(\frac{5}{2})}{\Gamma(\frac{1}{2})\Gamma(2)} z^{-\frac{1}{2}}(1-z) k^i k^j I^{ij}_{\frac{5}{2}} \left(-(xz + y(1-z))\mathbf{k}, (xz+y(1-z))\mathbf{k}^2\right) \right]
\end{aligned}$$

$$
\begin{aligned}
=&-i\frac{k^{d-1}}{(4\pi)^{\frac{d}{2}}}\int_0^1\mathrm{d}x\int_0^1\mathrm{d}y\int_0^1\mathrm{d}z\left[(d-1)\frac{\Gamma(\frac{1-d}{2})}{\Gamma(\frac{1}{2})}x^{\frac{d-1}{2}}(1-x)^{\frac{d-1}{2}}-\right.\\
&-\frac{\Gamma(\frac{3-d}{2})}{\Gamma(\frac{1}{2})}z^{-\frac{1}{2}}\left[z(1-x)(1-z(1-x))\right]^{\frac{d-3}{2}}+\\
&+\frac{\Gamma(\frac{5-d}{2})}{\Gamma(\frac{1}{2})}z^{-\frac{1}{2}}(1-z)(xz+y(1-z))^{\frac{d-1}{2}}(1-xz-y(1-z))^{\frac{d-5}{2}}+\\
&\left.+\frac{\Gamma(\frac{3-d}{2})}{2\Gamma(\frac{1}{2})}z^{-\frac{1}{2}}(1-z)(xz+y(1-z))^{\frac{d-3}{2}}(1-xz-y(1-z))^{\frac{d-3}{2}}\right].
\end{aligned}
\tag{D.46}
$$

Now there are only the Feynman parameter integrals left. Those can be computed in this way:

$$
\begin{aligned}
(d-1)\frac{\Gamma(\frac{1-d}{2})}{\Gamma(\frac{1}{2})}\int_0^1\mathrm{d}x\,x^{\frac{d-1}{2}}(1-x)^{\frac{d-1}{2}}&=-2\frac{\Gamma(\frac{3-d}{2})\Gamma(\frac{d+1}{2})^2}{\Gamma(\frac{1}{2})\Gamma(d+1)},\\
i\frac{2k^{d-1}}{(4\pi)^{\frac{d}{2}}}\frac{\Gamma(\frac{3-d}{2})\Gamma(\frac{d+1}{2})^2}{\Gamma(\frac{1}{2})\Gamma(d+1)}&=i\frac{k^2}{24\pi^2}\left(\frac{1}{\varepsilon}+\frac{5}{3}-\gamma_E+\ln 4\pi-\ln k^2\right).
\end{aligned}
\tag{D.47}
$$

In the next term we will make the substitution $u=z(1-x)$:

$$
\begin{aligned}
&-\frac{\Gamma(\frac{3-d}{2})}{\Gamma(\frac{1}{2})}\int_0^1\mathrm{d}x\int_0^1\mathrm{d}z\,z^{-\frac{1}{2}}\left[z(1-x)(1-z(1-x))\right]^{\frac{d-3}{2}}\\
=&-\frac{\Gamma(\frac{3-d}{2})}{\Gamma(\frac{1}{2})}\int_0^1\mathrm{d}z\int_0^z\mathrm{d}u\,z^{-\frac{3}{2}}(u(1-u))^{\frac{d-3}{2}}\\
=&-\frac{\Gamma(\frac{3-d}{2})}{\Gamma(\frac{1}{2})}\int_0^1\mathrm{d}u\,(u(1-u))^{\frac{d-3}{2}}\int_u^1\mathrm{d}z\,z^{-\frac{3}{2}}\\
=&-2\frac{\Gamma(\frac{3-d}{2})}{\Gamma(\frac{1}{2})}\int_0^1\mathrm{d}u\,(u(1-u))^{\frac{d-3}{2}}(u^{-\frac{1}{2}}-1)\\
=&-2\frac{\Gamma(\frac{3-d}{2})\Gamma(\frac{d-2}{2})\Gamma(\frac{d-1}{2})}{\Gamma(\frac{1}{2})\Gamma(d-\frac{3}{2})}-2\frac{\Gamma(\frac{3-d}{2})\Gamma(\frac{d-1}{2})^2}{\Gamma(\frac{1}{2})\Gamma(d-1)}\\
=&\sqrt{4\pi}\sec\left(d\frac{\pi}{2}\right)\left(\frac{\Gamma(\frac{d-2}{2})}{\Gamma(d-\frac{3}{2})}-\frac{\Gamma(\frac{d-1}{2})}{\Gamma(d-1)}\right),
\end{aligned}
$$

$$
-i\frac{k^{d-1}}{(4\pi)^{\frac{d-1}{2}}}\sec\left(d\frac{\pi}{2}\right)\left(\frac{\Gamma(\frac{d-2}{2})}{\Gamma(d-\frac{3}{2})}-\frac{\Gamma(\frac{d-1}{2})}{\Gamma(d-1)}\right)=i\frac{k^2}{4\pi^2}\left(\frac{1}{\varepsilon}+6-\gamma_E-\ln 4-\ln k^2+\ln\pi\right).
\tag{D.48}
$$

And for the last two terms we use $u=xz+y(1-z)$ and $v=y(1-z)$:

$$
\begin{aligned}
&\frac{\Gamma(\frac{3-d}{2})}{2\Gamma(\frac{1}{2})}\int_0^1\mathrm{d}x\int_0^1\mathrm{d}y\int_0^1\mathrm{d}z\left[z^{-\frac{1}{2}}(1-z)(3-d)(xz+y(1-z))^{\frac{d-1}{2}}(1-xz-y(1-z))^{\frac{d-5}{2}}\right.\\
&\qquad\left.+z^{-\frac{1}{2}}(1-z)(xz+y(1-z))^{\frac{d-3}{2}}(1-xz-y(1-z))^{\frac{d-3}{2}}\right]\\
=&\frac{\Gamma(\frac{3-d}{2})}{2\Gamma(\frac{1}{2})}\int_0^1\mathrm{d}z\int_0^1\mathrm{d}y\int_{y(1-z)}^{z+y(1-z)}\mathrm{d}u\,z^{-\frac{3}{2}}(1-z)\left[(3-d)u^{\frac{d-1}{2}}(1-u)^{\frac{d-5}{2}}+(u(1-u))^{\frac{d-3}{2}}\right]\\
=&\frac{\Gamma(\frac{3-d}{2})}{2\Gamma(\frac{1}{2})}\int_0^1\mathrm{d}z\int_0^{1-z}\mathrm{d}v\int_v^{z+v}\mathrm{d}u\,z^{-\frac{3}{2}}\left[(3-d)u^{\frac{d-1}{2}}(1-u)^{\frac{d-5}{2}}+\frac{1}{2}(u(1-u))^{\frac{d-3}{2}}\right]\\
=&\frac{\Gamma(\frac{3-d}{2})}{2\Gamma(\frac{1}{2})}\int_0^1\mathrm{d}v\int_0^{1-v}\mathrm{d}z\int_v^{z+v}\mathrm{d}u\,z^{-\frac{3}{2}}\left[(3-d)u^{\frac{d-1}{2}}(1-u)^{\frac{d-5}{2}}+\frac{1}{2}(u(1-u))^{\frac{d-3}{2}}\right]\\
=&\frac{\Gamma(\frac{3-d}{2})}{2\Gamma(\frac{1}{2})}\int_0^1\mathrm{d}v\int_v^1\mathrm{d}u\int_{u-v}^{1-v}\mathrm{d}z\,z^{-\frac{3}{2}}\left[(3-d)u^{\frac{d-1}{2}}(1-u)^{\frac{d-5}{2}}+\frac{1}{2}(u(1-u))^{\frac{d-3}{2}}\right]
\end{aligned}
$$

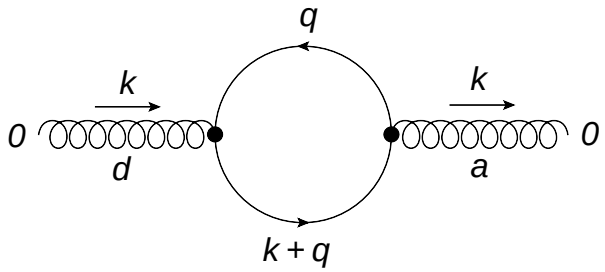

Figure D.2: Feynman diagram for the vacuum polarization (fermion loop).

$$
\begin{aligned}
=&-\frac{\Gamma(\frac{3-d}{2})}{\Gamma(\frac{1}{2})}\int_0^1 \mathrm{d}u\int_0^u \mathrm{d}v\left((1-v)^{-\frac{1}{2}}-(u-v)^{-\frac{1}{2}}\right)\left[(3-d)u^{\frac{d-1}{2}}(1-u)^{\frac{d-5}{2}}+\frac{1}{2}(u(1-u))^{\frac{d-3}{2}}\right]\\
=&2\frac{\Gamma(\frac{3-d}{2})}{\Gamma(\frac{1}{2})}\int_0^1 \mathrm{d}u\left((1-u)^{\frac{1}{2}}-1+u^{\frac{1}{2}}\right)\left[(3-d)u^{\frac{d-1}{2}}(1-u)^{\frac{d-5}{2}}+\frac{1}{2}(u(1-u))^{\frac{d-3}{2}}\right]\\
=&2\frac{\Gamma(\frac{3-d}{2})}{\Gamma(\frac{1}{2})}(3-d)\left(\frac{\Gamma(\frac{d+1}{2})\Gamma(\frac{d-2}{2})}{\Gamma(d-\frac{1}{2})}+\frac{\Gamma(\frac{d+2}{2})\Gamma(\frac{d-3}{2})}{\Gamma(d-\frac{1}{2})}-\frac{\Gamma(\frac{d+1}{2})\Gamma(\frac{d-3}{2})}{\Gamma(d-1)}\right)\\
&+2\frac{\Gamma(\frac{3-d}{2})}{\Gamma(\frac{1}{2})}\left(2\frac{\Gamma(\frac{d}{2})\Gamma(\frac{d-1}{2})}{\Gamma(d-\frac{1}{2})}-\frac{\Gamma(\frac{d-1}{2})^2}{\Gamma(d-1)}\right)\\
=&2(3-d)\frac{\Gamma(\frac{3-d}{2})\Gamma(\frac{d+1}{2})\Gamma(\frac{d-2}{2})}{\Gamma(\frac{1}{2})\Gamma(d-\frac{1}{2})}+2(2-d)\frac{\Gamma(\frac{3-d}{2})\Gamma(\frac{d}{2})\Gamma(\frac{d-1}{2})}{\Gamma(\frac{1}{2})\Gamma(d-\frac{1}{2})}+2\frac{\Gamma(\frac{3-d}{2})\Gamma(\frac{d-1}{2})^2}{\Gamma(\frac{1}{2})\Gamma(d-2)}\\
=&\sqrt{4\pi}\sec\left(d\frac{\pi}{2}\right)\left(\left(d^2-4d+\frac{7}{2}\right)\frac{\Gamma(\frac{d-2}{2})}{\Gamma(d-\frac{1}{2})}-\frac{\Gamma(\frac{d-1}{2})}{\Gamma(d-2)}\right).
\end{aligned}
$$

So finally

$$
\begin{aligned}
&-i\frac{k^{d-1}}{(4\pi)^{\frac{d-1}{2}}}\sec\left(d\frac{\pi}{2}\right)\left(\left(d^2-4d+\frac{7}{2}\right)\frac{\Gamma(\frac{d-2}{2})}{\Gamma(d-\frac{1}{2})}-\frac{\Gamma(\frac{d-1}{2})}{\Gamma(d-2)}\right)\\
=&-i\frac{k^2}{12\pi^2}\left(\frac{1}{\varepsilon}+\frac{16}{3}-\gamma_E+3\ln 4-\ln k^2+\ln\pi\right).
\end{aligned}
\tag{D.49}
$$

Putting everything together (and including the mass scale μ) we get

$$
-i\frac{g^2\mu^{-2\varepsilon}}{(4\pi)^2k^2}C_A\delta^{ab}\left(-\frac{11}{3}\left(\frac{1}{\varepsilon}-\gamma_E+\ln 4\pi\right)+\frac{11}{3}\ln\frac{k^2}{\mu^2}-\frac{31}{9}\right). \tag{D.50}
$$

This completes the gluonic part of the vacuum polarization, since the tadpole diagram vanishes in dimensional regularization. The ghost fields do not couple to the time components of the propagator, so the only contribution left is the fermion loop with light quarks. So for one flavour of light quarks we have to compute the following (compare figure D.2):

$$
\begin{aligned}
&-(-ig)^2\mathrm{Tr}[T^aT^d]\left(\frac{i}{\mathbf{k}^2}\right)^2\int\frac{\mathrm{d}^Dq}{(2\pi)^D}\mathrm{Tr}\left[\gamma^0\frac{i(\not{k}+\not{q})}{(k+q)^2+i\varepsilon}\gamma^0\frac{i\not{q}}{q^2+i\varepsilon}\right]\\
&\quad=g^2T_F\delta^{ad}\left(\frac{1}{\mathbf{k}^2}\right)^2\int\frac{\mathrm{d}^Dq}{(2\pi)^D}4\frac{2q_0^2-(k+q)\cdot q}{((k+q)^2+i\varepsilon)\,(q^2+i\varepsilon)}\\
&\quad=4g^2T_F\delta^{ad}\left(\frac{1}{\mathbf{k}^2}\right)^2\int\frac{\mathrm{d}^Dq}{(2\pi)^D}\frac{2q_0^2-(k+q)\cdot q}{((k+q)^2+i\varepsilon)(q^2+i\varepsilon)}\\
&\quad=4ig^2T_F\delta^{ad}\left(\frac{1}{\mathbf{k}^2}\right)^2\int\frac{\mathrm{d}^Dq_E}{(2\pi)^D}\frac{k\cdot q-2q_0^2}{(k+q)^2q^2}\\
&\quad=4ig^2T_F\delta^{ad}\left(\frac{1}{\mathbf{k}^2}\right)^2\int_0^1\mathrm{d}x\int\frac{\mathrm{d}^Dq_E}{(2\pi)^D}\frac{k\cdot q-2q_0^2}{(q^2+2xk\cdot q+xk^2)^2}
\end{aligned}
$$

$$
\begin{aligned}
&= 4ig^2 T_F \delta^{ad} \left(\frac{1}{\mathbf{k}^2}\right)^2 \int_0^1 \mathrm{d}x \left[k^\mu I_2^\mu(xk, xk^2) - 2I_2^{00}(xk, xk^2)\right] \\
&= 4ig^2 T_F \delta^{ad} \left(\frac{1}{\mathbf{k}^2}\right)^2 \int_0^1 \mathrm{d}x \left[-x\mathbf{k}^2 \frac{\Gamma\left(2-\frac{D}{2}\right)}{(4\pi)^{\frac{D}{2}}(x(1-x)\mathbf{k}^2)^{2-\frac{D}{2}}} - \frac{\Gamma\left(1-\frac{D}{2}\right)}{(4\pi)^{\frac{D}{2}}(x(1-x)\mathbf{k}^2)^{1-\frac{D}{2}}}\right] \\
&= -4ig^2 T_F \delta^{ad} \frac{(\mathbf{k}^2)^{\frac{D}{2}-3}}{(4\pi)^{\frac{D}{2}}} \left[\frac{\Gamma\left(2-\frac{D}{2}\right)\Gamma\left(\frac{D}{2}\right)\Gamma\left(\frac{D}{2}-1\right)}{\Gamma(D-1)} + \frac{\Gamma\left(1-\frac{D}{2}\right)\Gamma\left(\frac{D}{2}\right)^2}{\Gamma(D)}\right] \\
&= -i\frac{g^2\mu^{-2\varepsilon}T_F\delta^{ab}}{(4\pi)^2\mathbf{k}^2}\left(\frac{4}{3}\left(\frac{1}{\varepsilon} - \gamma_E + \ln 4\pi\right) + \frac{20}{9} - \frac{4}{3}\ln\frac{\mathbf{k}^2}{\mu^2}\right). \qquad \text{(D.51)}
\end{aligned}
$$

So in the $\overline{\text{MS}}$-scheme the 00-part of the vacuum polarization times the two external propagators is given by

$$
\frac{i}{\mathbf{k}^2}\left[-\Pi_{00}^{\overline{\text{MS}}}(0,\mathbf{k})\right]\frac{i}{\mathbf{k}^2} = -i\frac{\alpha_s}{4\pi\mathbf{k}^2}\delta^{ab}\left(-\left(\frac{31}{9}C_A - \frac{20}{9}T_F n_f\right) + \left(\frac{11}{3}C_A - \frac{4}{3}T_F n_f\right)\ln\frac{\mathbf{k}^2}{\mu^2}\right). \qquad \text{(D.52)}
$$

Putting this into the calculation for the Wilson loop (with the limit $t \to \infty$ already taken) we have

$$
\begin{aligned}
&ig^2\widetilde{\text{Tr}}[T^a T^d]\left(-i\frac{\alpha_s}{4\pi}\right)\delta^{ad}\int\frac{\mathrm{d}k^3}{(2\pi)^3}\frac{e^{i\mathbf{k}\cdot\mathbf{r}}}{\mathbf{k}^2}\left(-\left(\frac{31}{9}C_A - \frac{20}{9}T_F n_f\right) + \left(\frac{11}{3}C_A - \frac{4}{3}T_F n_f\right)\ln\frac{\mathbf{k}^2}{\mu^2}\right) \\
&= -\frac{\alpha_s^2 C_F}{4\pi r}\left(\frac{31}{9}C_A - \frac{20}{9}T_F n_f + \left(\frac{11}{3}C_A - \frac{4}{3}T_F n_f\right)\left(\ln\mu^2 r^2 + 2\gamma_E\right)\right). \qquad \text{(D.53)}
\end{aligned}
$$

The Integral involving the logarithm can be computed in this way:

$$
\begin{aligned}
\int\frac{\mathrm{d}^3k}{(2\pi)^3}\frac{e^{i\mathbf{k}\cdot\mathbf{r}}}{k^2}\ln k^2 &= \lim_{\epsilon\to 0}\frac{\partial}{\partial\epsilon}\int\frac{\mathrm{d}^3k}{(2\pi)^3}k^{2\epsilon-2}e^{i\mathbf{k}\cdot\mathbf{r}} \\
&= \lim_{\epsilon\to 0}\frac{\partial}{\partial\epsilon}\frac{1}{4\pi^2}\int_0^\infty \mathrm{d}k\int_{-1}^1 \mathrm{d}x\, k^{2\epsilon}e^{ikrx} \\
&= \lim_{\epsilon\to 0}\frac{\partial}{\partial\epsilon}\frac{1}{4\pi^2}\int_0^\infty \mathrm{d}k\,\frac{k^{2\epsilon-1}}{ir}\left(e^{ikr} - e^{-ikr}\right) \\
&= \lim_{\epsilon\to 0}\frac{\partial}{\partial\epsilon}\frac{1}{4\pi^2}2\text{Re}\left[\int_0^\infty \mathrm{d}k\,\frac{k^{2\epsilon-1}}{ir}e^{ikr}\right] \\
&= \lim_{\epsilon\to 0}\frac{\partial}{\partial\epsilon}\frac{1}{4\pi^2}2\text{Re}\left[-(-ir)^{-2\epsilon-1}\int_0^\infty \mathrm{d}k\,k^{2\epsilon-1}e^{-k}\right] \\
&= \lim_{\epsilon\to 0}\frac{\partial}{\partial\epsilon}\frac{2\sin(\epsilon\pi)}{4\pi^2 r^{2\epsilon+1}}\Gamma(2\epsilon) \\
&= \lim_{\epsilon\to 0}\frac{\partial}{\partial\epsilon}\frac{1}{4\pi r}\left(1 - (2\gamma_E + \ln r^2)\epsilon + \mathcal{O}(\epsilon^2)\right) \\
&= -\frac{1}{4\pi r}(2\gamma_E + \ln r^2). \qquad \text{(D.54)}
\end{aligned}
$$

E Details of the in Medium Calculations

E.1 The Gluon Self Energy (Thermal Part)

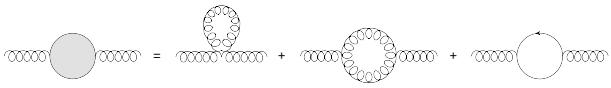

Figure E.1: Diagrams contributing to the gluon self energy.

Contribution from the tadpole diagram

$$\begin{aligned}
&-\frac{g^2}{2}\left(\frac{1}{\mathbf{k}^2}\right)^2 2\, f^{abe} f^{dbe}(\delta_{00}\delta_{\mu\nu}-\delta_{\mu 0}\delta_{\nu 0}) \sum\!\!\!\!\!\!\int_q D_{\mu\nu(q)} \\
&= -\, g^2 C_A \delta^{ad}\left(\frac{1}{\mathbf{k}^2}\right)^2 \sum\!\!\!\!\!\!\int_q D_{ii}(q) \\
&= -\, g^2 C_A \delta^{ad}\left(\frac{1}{\mathbf{k}^2}\right)^2 \sum\!\!\!\!\!\!\int_q \frac{d-1}{q_0^2+\mathbf{q}^2} \\
&= -\, g^2 C_A \delta^{ad}\left(\frac{1}{\mathbf{k}^2}\right)^2 \int_q \frac{d-1}{2q}\left(1+\frac{2}{e^{q\beta}-1}\right), \qquad \text{(E.1)}
\end{aligned}$$

$$\Pi_{00}^{(T)}(0,\mathbf{q})\Big|_{\text{tadpole}} = g^2 C_A \frac{1}{\pi^2}\int_0^\infty \mathrm{d}q\, \frac{q}{e^{q\beta}-1} = g^2 C_A \frac{T^2}{\pi^2}\zeta(2) = \frac{2\pi}{3}\alpha_s C_A T^2\,. \qquad \text{(E.2)}$$

While this part of the thermal gluon self energy can be calculated exactly, we will still give it as a part of the integral in the end result for aesthetic reasons.

Contribution from the gluon ring

Here we need not do all the index algebra of vertices and propagators again, we can just take over the corresponding expression from the vacuum calculations and replace the vacuum propagators by the thermal ones. So this diagram gives:

$$\begin{aligned}
&\frac{g^2}{2} C_A \delta^{ad}\left(\frac{1}{\mathbf{k}^2}\right)^2 \sum\!\!\!\!\!\!\int_q \left\{ \frac{4q_0^2}{(q_0^2+\mathbf{q}^2)\,(q_0^2+(\mathbf{k}-\mathbf{q})^2)}\left[d-2+\frac{\left(\mathbf{k}\cdot\mathbf{q}-\mathbf{q}^2\right)^2}{\mathbf{q}^2(\mathbf{k}-\mathbf{q})^2}\right]+\right. \\
&\left.+\frac{1}{(\mathbf{k}-\mathbf{q})^2\,(q_0^2+\mathbf{q}^2)}\left[(2\mathbf{k}-\mathbf{q})^2-\frac{\left(2\mathbf{k}\cdot\mathbf{q}-\mathbf{q}^2\right)^2}{\mathbf{q}^2}\right]+\frac{1}{\mathbf{q}^2\,(q_0^2+(\mathbf{k}-\mathbf{q})^2)}\left[(\mathbf{k}+\mathbf{q})^2-\frac{\left(\mathbf{k}^2-\mathbf{q}^2\right)^2}{(\mathbf{k}-\mathbf{q})^2}\right]\right\} \\
=&\frac{g^2}{2} C_A \delta^{ad}\left(\frac{1}{\mathbf{k}^2}\right)^2 \sum\!\!\!\!\!\!\int_q \left\{ \frac{4\mathbf{q}^2}{(q_0^2+\mathbf{q}^2)\,(\mathbf{q}^2-(\mathbf{k}-\mathbf{q})^2)}\left[d-2+\frac{\left(\mathbf{k}\cdot\mathbf{q}-\mathbf{q}^2\right)^2}{\mathbf{q}^2(\mathbf{k}-\mathbf{q})^2}\right]+\right. \\
&\left.+\frac{4}{(q_0^2+\mathbf{q}^2)}\left[1-\frac{\left(\mathbf{k}\cdot\mathbf{q}-\mathbf{q}^2\right)^2}{\mathbf{q}^2(\mathbf{k}-\mathbf{q})^2}\right]+(\mathbf{q}\leftrightarrow\mathbf{k}-\mathbf{q})\right\} \\
=&\, g^2 C_A \delta^{ad}\left(\frac{1}{\mathbf{k}^2}\right)^2 \int_q \left(1+\frac{2}{e^{q\beta}-1}\right)\left\{ \frac{q}{2\mathbf{k}\cdot\mathbf{q}-\mathbf{k}^2}\left[d-2+\frac{\left(\mathbf{k}\cdot\mathbf{q}-\mathbf{q}^2\right)^2}{\mathbf{q}^2(\mathbf{k}-\mathbf{q})^2}\right]+\right. \\
&\left.+\frac{1}{q}\left[1-\frac{\left(\mathbf{k}\cdot\mathbf{q}-\mathbf{q}^2\right)^2}{\mathbf{q}^2(\mathbf{k}-\mathbf{q})^2}\right]\right\}+(\mathbf{q}\leftrightarrow\mathbf{k}-\mathbf{q})\,. \qquad \text{(E.3)}
\end{aligned}$$

Here we used some algebraic transformations, in particular

$$\frac{q_0^2}{(q_0^2+\mathbf{q}^2)\,(q_0^2+(\mathbf{k}-\mathbf{q})^2)} = \frac{1}{\mathbf{q}^2-(\mathbf{k}-\mathbf{q})^2}\left(\frac{\mathbf{q}^2}{q_0^2+\mathbf{q}^2}-\frac{(\mathbf{k}-\mathbf{q})^2}{q_0^2+(\mathbf{k}-\mathbf{q})^2}\right) \qquad \text{(E.4)}$$

and

$$
\begin{aligned}
(2\mathbf{k}-\mathbf{q})^2-\frac{\left(2\mathbf{k}\cdot\mathbf{q}-\mathbf{q}^2\right)^2}{\mathbf{q}^2} =& \frac{(2\mathbf{k}-\mathbf{q})^2\mathbf{q}^2-\left(2\mathbf{k}\cdot\mathbf{q}-\mathbf{q}^2\right)^2}{\mathbf{q}^2}\\
=& \frac{4\mathbf{k}^2\mathbf{q}^2-4(\mathbf{k}\cdot\mathbf{q})^2}{\mathbf{q}^2}\\
=& \frac{4\mathbf{q}^2(\mathbf{k}-\mathbf{q})^2+8\mathbf{q}^2(\mathbf{k}\cdot\mathbf{q})-4(\mathbf{q}^2)^2-4(\mathbf{k}\cdot\mathbf{q})^2}{\mathbf{q}^2}\\
=& 4(\mathbf{k}-\mathbf{q})^2-4\frac{\left(\mathbf{k}\cdot\mathbf{q}-\mathbf{q}^2\right)^2}{\mathbf{q}^2}\,. \qquad \text{(E.5)}
\end{aligned}
$$

We can also exploit the symmetry of the whole expression under $\mathbf{q}\leftrightarrow\mathbf{k}-\mathbf{q}$, so that we can at least perform the angular integrations. These are only integrations of rational functions for the term with $n_B(q)$, but get more complicated for the term with $n_B(|\mathbf{k}-\mathbf{q}|)$. However, because both are symmetric under this change of variables, they should give the same contribution. There is a singularity in both terms for the value of $\mathbf{q}=\frac{1}{2}\mathbf{k}$, but each cancels the other, because for this value of $\mathbf{q}$ both terms are equal but have opposite sign. This means that we need not worry about that point and just take the principal value of the integral.

$$
\begin{aligned}
\Pi_{00}^{(T)}(0,\mathbf{k})\Big|_{\text{ring}} =& -g^2C_A\frac{1}{4\pi^2}2\,\mathrm{P}\int_0^\infty \mathrm{d}q\int_{-1}^1\mathrm{d}x\,\frac{2\,q^2}{e^{q\beta}-1}\left\{\frac{q}{2kqx-k^2}\left[1+\frac{\left(kqx-q^2\right)^2}{q^2(k^2-2kqx+q^2)}\right]+\right.\\
&\left.+\frac{1}{q}\left[1-\frac{\left(kqx-q^2\right)^2}{q^2(k^2-2kqx+q^2)}\right]\right\}\\
=& -g^2C_A\frac{1}{\pi^2}\mathrm{P}\int_0^\infty\frac{\mathrm{d}q\,q}{e^{q\beta}-1}\int_{-1}^1\mathrm{d}x\left\{\frac{q^2}{2kqx-k^2}\left[2-\frac{(1-x^2)k^2}{k^2-2kqx+q^2}\right]+\frac{(1-x^2)k^2}{k^2-2kqx+q^2}\right\}\\
=& -g^2C_A\frac{1}{\pi^2}\mathrm{P}\int_0^\infty\frac{\mathrm{d}q\,q}{e^{q\beta}-1}\int_{-1}^1\mathrm{d}x\left\{\frac{2\,q^2}{2kqx-k^2}-\frac{(1-x^2)k^2}{2kqx-k^2}\right\}\\
=& -g^2C_A\frac{1}{\pi^2}\mathrm{P}\int_0^\infty\frac{\mathrm{d}q\,q}{e^{q\beta}-1}\int_{-1}^1\mathrm{d}x\left\{\frac{q}{k}\frac{1}{x-\frac{k}{2q}}+\frac{k}{2q}\frac{x^2-1}{x-\frac{k}{2q}}\right\}\\
=& -g^2C_A\frac{1}{\pi^2}\mathrm{P}\int_0^\infty\frac{\mathrm{d}q\,q}{e^{q\beta}-1}\int_{-1}^1\mathrm{d}x\left\{\frac{q}{k}\frac{1}{x-\frac{k}{2q}}+\frac{k}{2q}\left(x+\frac{k}{2q}+\frac{\frac{k^2}{4q^2}-1}{x-\frac{k}{2q}}\right)\right\}\\
=& -g^2C_A\frac{1}{\pi^2}\int_0^\infty\frac{\mathrm{d}q\,q}{e^{q\beta}-1}\left\{\frac{k^2}{2q^2}+\left(\frac{q}{k}-\frac{k}{2q}+\frac{k^3}{8q^3}\right)\ln\left|\frac{1-\frac{k}{2q}}{-1-\frac{k}{2q}}\right|\right\}\\
=& \frac{4\alpha_sC_A}{\pi}\int_0^\infty\frac{\mathrm{d}q\,q}{e^{q\beta}-1}\left\{-\frac{k^2}{2q^2}+\left(\frac{q}{k}-\frac{k}{2q}+\frac{k^3}{8q^3}\right)\ln\left|\frac{2q+k}{2q-k}\right|\right\}.
\end{aligned}
$$

Contribution from the fermion loop

$$
\begin{aligned}
&-(ig)^2\mathrm{Tr}[T^aT^d]\left(\frac{1}{\mathbf{k}^2}\right)^2\sum\!\!\!\!\!\!\int_{\{q\}}\mathrm{Tr}\left[\gamma_0\frac{-i\left(\not{k}+\not{q}\right)}{(k+q)^2}\gamma_0\frac{-i\not{q}}{q^2}\right]\\
=& -4g^2T_f\delta^{ad}\left(\frac{1}{\mathbf{k}^2}\right)^2\sum\!\!\!\!\!\!\int_{\{q\}}\frac{q_0^2-(\mathbf{k}+\mathbf{q})\cdot\mathbf{q}}{(q_0^2+\mathbf{q}^2)(q_0^2+(\mathbf{k}+\mathbf{q})^2)}\\
=& -4g^2T_f\delta^{ad}\left(\frac{1}{\mathbf{k}^2}\right)^2\sum\!\!\!\!\!\!\int_{\{q\}}\left\{\frac{1}{\mathbf{q}^2-(\mathbf{k}+\mathbf{q})^2}\left(\frac{\mathbf{q}^2}{q_0^2+\mathbf{q}^2}-\frac{(\mathbf{k}+\mathbf{q})^2}{q_0^2+(\mathbf{k}+\mathbf{q})^2}\right)+\right.\\
&\left.+\frac{(\mathbf{k}+\mathbf{q})\cdot\mathbf{q}}{\mathbf{q}^2-(\mathbf{k}+\mathbf{q})^2}\left(\frac{1}{q_0^2+\mathbf{q}^2}-\frac{1}{q_0^2+(\mathbf{k}+\mathbf{q})^2}\right)\right\}\\
=& 4g^2T_f\delta^{ad}\left(\frac{1}{\mathbf{k}^2}\right)^2\int_q\frac{1}{2q}\left(1-\frac{2}{e^{q\beta}+1}\right)\frac{\mathbf{k}\cdot\mathbf{q}+2\mathbf{q}^2}{2\mathbf{k}\cdot\mathbf{q}+\mathbf{k}^2}+(\mathbf{q}\leftrightarrow-\mathbf{k}-\mathbf{q})\,. \qquad \text{(E.6)}
\end{aligned}
$$

$$\begin{aligned}\Pi_{00}^{(T)}(0,\mathbf{k})\Big|_{\text{fermion}} =& 4g^2T_Fn_f\frac{1}{4\pi^2}2\mathrm{P}\int_0^\infty \mathrm{d}q\int_{-1}^1 \mathrm{d}x\,\frac{q}{e^{q\beta}+1}\left(\frac{1}{2}+\frac{2q^2-\frac{k^2}{2}}{2kqx+k^2}\right)\\ =&\frac{2g^2T_Fn_f}{\pi^2}\int_0^\infty \mathrm{d}q\,\frac{q}{e^{q\beta}+1}\left\{1+\left(\frac{q}{k}-\frac{k}{4q}\right)\ln\left|\frac{1+\frac{k}{2q}}{-1+\frac{k}{2q}}\right|\right\}\\ =&\frac{8\alpha_sT_Fn_f}{\pi}\int_0^\infty \mathrm{d}q\,\frac{q}{e^{q\beta}+1}\left\{1+\left(\frac{q}{k}-\frac{k}{4q}\right)\ln\left|\frac{2q+k}{2q-k}\right|\right\}. \end{aligned}\tag{E.7}$$

Result

$$\begin{aligned}\Pi_{00}^{(T)}(0,\mathbf{k}) =&\frac{4\alpha_sC_A}{\pi}\int_0^\infty \mathrm{d}q\,\frac{q}{e^{q\beta}-1}\left\{1-\frac{k^2}{2q^2}+\left(\frac{q}{k}-\frac{k}{2q}+\frac{k^3}{8q^3}\right)\ln\left|\frac{2q+k}{2q-k}\right|\right\}\\ &+\frac{8\alpha_sT_Fn_f}{\pi}\int_0^\infty \mathrm{d}q\,\frac{q}{e^{q\beta}+1}\left\{1+\left(\frac{q}{k}-\frac{k}{4q}\right)\ln\left|\frac{2q+k}{2q-k}\right|\right\}. \end{aligned}\tag{E.8}$$

E.2 Expansions of the Gluon Self Energy

$k \ll T$ Expansion

The procedure we will follow here (as described in [26] and [10]) is to start from the initial expression, perform the $\mathbf{q}$ integration, expand in $\frac{\mathbf{k}^2}{q_0^2}$, and then perform the Matsubara sum last. Since we do not split off the vacuum part, we have to do this in d space dimensions. The vacuum part has already been calculated separately, so after we subtract it from the expression obtained by this procedure, we get the desired approximation for the thermal part.

For these calculations it will be convenient to give some standard formulae and calculations beforehand. The most general formula for the standard Feynman parameter method is given by:

$$\begin{aligned}\frac{1}{A_1^{n_1}A_2^{n_2}\cdots A_k^{n_k}} =&\frac{\Gamma(n_1+n_2+\cdots+n_k)}{\Gamma(n_1)\Gamma(n_2)\cdots\Gamma(n_k)}\int_0^1\mathrm{d}x_1\int_0^1\mathrm{d}x_2\cdots\int_0^1\mathrm{d}x_k\times\\ &\times\frac{x_1^{n_1-1}x_2^{n_2-1}\cdots x_k^{n_k-1}}{\left(x_1A_1+x_2A_2+\cdots+x_kA_k\right)^{n_1+n_2+\cdots+n_k}}\delta\left(1-x_1-x_2-\cdots-x_k\right)\\ =&\frac{\Gamma(n_1+n_2+\cdots+n_k)}{\Gamma(n_1)\Gamma(n_2)\cdots\Gamma(n_k)}\int_0^1\mathrm{d}x_1\int_0^{1-x_1}\mathrm{d}x_2\cdots\int_0^{1-x_1-x_2-\cdots-x_{k-2}}\mathrm{d}x_{k-1}\times\\ &\times\frac{x_1^{n_1-1}x_2^{n_2-1}\cdots x_{k-1}^{n_{k-1}-1}\left(1-x_1-x_2-\cdots-x_{k-1}\right)^{n_k-1}}{\left(x_1\left(A_1-A_k\right)+x_2\left(A_2-A_k\right)+\cdots+x_{k-1}\left(A_{k-1}-A_k\right)+A_k\right)^{n_1+n_2+\cdots+n_k}}. \end{aligned}\tag{E.9}$$

The expansion we are going to use is described by:

$$(1+x)^\alpha=\sum_{l=0}^\infty\frac{\Gamma(\alpha+1)}{\Gamma(l+1)\Gamma(\alpha+1-l)}\,x^l\,.\tag{E.10}$$

After making use of the Feynman parameters, the standard integral we have to solve is:

$$\begin{aligned}\int_q\frac{\left(\mathbf{q}^2\right)^k}{\left(\mathbf{q}^2+m^2\right)^n} =&\frac{1}{\Gamma(n)}\int_0^\infty\mathrm{d}z\int_q z^{n-1}\left(\mathbf{q}^2\right)^k e^{-z\left(\mathbf{q}^2+m^2\right)}\\ =&\frac{1}{\Gamma(n)}\int_0^\infty\mathrm{d}z\,z^{n-1}e^{-zm^2}\left(-\partial_z\right)^k\int_q e^{-z\mathbf{q}^2}\end{aligned}$$

$$
\begin{aligned}
&= \frac{1}{\Gamma(n)} \int_0^\infty \mathrm{d}z\, z^{n-1} e^{-zm^2} \left(-\partial_z\right)^k \frac{1}{(4\pi z)^{\frac{d}{2}}} \\
&= \frac{1}{(4\pi)^{\frac{d}{2}}\Gamma(n)} \int_0^\infty \mathrm{d}z\, z^{n-1} e^{-zm^2} \frac{\Gamma\left(\frac{d}{2}+k\right)}{\Gamma\left(\frac{d}{2}\right)} z^{-\left(\frac{d}{2}+k\right)} \\
&= \frac{\left(m^2\right)^{\frac{d}{2}+k-n}}{(4\pi)^{\frac{d}{2}}} \frac{\Gamma\left(n-k-\frac{d}{2}\right)}{\Gamma(n)} \frac{\Gamma\left(\frac{d}{2}+k\right)}{\Gamma\left(\frac{d}{2}\right)} .
\end{aligned} \tag{E.11}
$$

Now we can turn to the calculation of the three relevant diagrams. The tadpole contribution is independent of k and can be calculated exactly (see E.1). It is given by:

$$
-\left.\Pi_{00}(0,\mathbf{k})\right|_{\text{tadpole}} = -\frac{2\pi}{3}\alpha_s C_A T^2 . \tag{E.12}
$$

The gluon ring contribution has the most complicated expression and its calculation will be split into five parts, after some transformations have been performed.

$$
\begin{aligned}
-\left.\Pi_{00}(0,\mathbf{k})\right|_{\text{ring}} &= \frac{g^2}{2} C_A \sum\!\!\!\!\!\!\int_q \left\{ \frac{2q_0^2}{\left(q_0^2+\mathbf{q}^2\right)\left(q_0^2+(\mathbf{k}-\mathbf{q})^2\right)} \left[d-2+\frac{\left(\mathbf{k}\cdot\mathbf{q}-\mathbf{q}^2\right)^2}{\mathbf{q}^2(\mathbf{k}-\mathbf{q})^2} \right] + \right. \\
&\quad \left. + \frac{1}{(\mathbf{k}-\mathbf{q})^2\left(q_0^2+\mathbf{q}^2\right)} \left[(2\mathbf{k}-\mathbf{q})^2 - \frac{\left(2\mathbf{k}\cdot\mathbf{q}-\mathbf{q}^2\right)^2}{\mathbf{q}^2} \right] + (\mathbf{q}\leftrightarrow\mathbf{k}-\mathbf{q}) \right\} \\
&= 2\pi\alpha_s\mu^{2\varepsilon} C_A \sum\!\!\!\!\!\!\int_q \left\{ \frac{4q_0^2}{\left(q_0^2+\mathbf{q}^2\right)\left(q_0^2+(\mathbf{k}-\mathbf{q})^2\right)} \left[\underbrace{d-1}_{[1]} + \underbrace{\frac{(\mathbf{k}\cdot\mathbf{q})^2}{\mathbf{q}^2(\mathbf{k}-\mathbf{q})^2}}_{[2]} - \underbrace{\frac{\mathbf{k}^2}{(\mathbf{k}-\mathbf{q})^2}}_{[3]} \right] + \right. \\
&\quad \left. + \frac{8}{\left(q_0^2+\mathbf{q}^2\right)} \left[-\underbrace{\frac{(\mathbf{k}\cdot\mathbf{q})^2}{\mathbf{q}^2(\mathbf{k}-\mathbf{q})^2}}_{[4]} + \underbrace{\frac{\mathbf{k}^2}{(\mathbf{k}-\mathbf{q})^2}}_{[5]} \right] \right\} \\
&= 2\pi\alpha_s C_A \left(I_1+I_2+I_3+I_4+I_5\right) .
\end{aligned} \tag{E.13}
$$

Since the calculation of the zero mode is usually different from the rest, we will denote the Matsubara sum without the zero mode with a prime. It is, however, not necessary to calculate everything separately for the zero modes, so we will make the distinction only where we have to. For each of the five contributions we will first give a general expression and then the terms up to cubic order. We will see that the divergence lies only in the quadratic terms. The factors $\mu^{2\varepsilon}$ will not be displayed explicitly.

$$
\begin{aligned}
I_1 &= \sum\!\!\!\!\!\!\int_q \frac{4(d-1)q_0^2}{\left(q_0^2+\mathbf{q}^2\right)\left(q_0^2+(\mathbf{k}-\mathbf{q})^2\right)} \\
&= \int_0^1 \mathrm{d}x \sum\!\!\!\!\!\!\int_q \frac{4(d-1)q_0^2}{\left(\mathbf{q}^2-2x\mathbf{k}\cdot\mathbf{q}+x\mathbf{k}^2+q_0^2\right)^2} \\
&= \int_0^1 \mathrm{d}x \sum\!\!\!\!\!\!\int_q \frac{4(d-1)q_0^2}{\left(\mathbf{q}^2+x(1-x)k^2+q_0^2\right)^2} \\
&= \int_0^1 \mathrm{d}x \sum_{q_0} \frac{4(d-1)q_0^2}{(4\pi)^{\frac{d}{2}}} \Gamma\left(2-\frac{d}{2}\right) \left(x(1-x)k^2+q_0^2\right)^{\frac{d}{2}-2} \\
&= \int_0^1 \mathrm{d}x \sum_{q_0}{}' \frac{4(d-1)q_0^{d-2}}{(4\pi)^{\frac{d}{2}}} \Gamma\left(2-\frac{d}{2}\right) \sum_{l=0}^\infty \frac{\Gamma\left(\frac{d}{2}-1\right)}{\Gamma(l+1)\Gamma\left(\frac{d}{2}-l-1\right)} x^l (1-x)^l \left(\frac{k^2}{q_0^2}\right)^l \\
&= \frac{4(d-1)(2\pi T)^{d-2}}{(4\pi)^{\frac{d}{2}}} \Gamma\left(2-\frac{d}{2}\right) \sum_{l=0}^\infty \frac{\Gamma\left(\frac{d}{2}-1\right)}{\Gamma(l+1)\Gamma\left(\frac{d}{2}-l-1\right)} \frac{\Gamma(l+1)^2}{\Gamma(2l+2)} \left(\frac{k}{2\pi T}\right)^{2l} 2T \sum_{n=1}^\infty \frac{1}{n^{2l+2-d}}
\end{aligned}
$$

$$
\begin{aligned}
&= \frac{16(d-1)(2\pi T)^{d-1}}{(4\pi)^{\frac{d}{2}+1}}\Gamma\left(2-\frac{d}{2}\right)\sum_{l=0}^{\infty}\left(\frac{k}{2\pi T}\right)^{2l}\frac{\Gamma(l+1)\Gamma\left(\frac{d}{2}-1\right)}{\Gamma(2l+2)\Gamma\left(\frac{d}{2}-l-1\right)}\zeta(2l+2-d)\\
&= -\frac{(2\pi T)^2}{12\pi^2}-\frac{(2\pi T)^2}{24\pi^2}\left[\frac{1}{\varepsilon}+1+\gamma_E+\ln\pi-2\ln\frac{2\pi T}{\mu}\right]\left(\frac{k}{2\pi T}\right)^2+\mathcal{O}\left[\left(\frac{k}{2\pi T}\right)^4\right]. \qquad \text{(E.14)}
\end{aligned}
$$

$$
\begin{aligned}
I_2 &= \sum\!\!\!\!\!\!\int_q \frac{4q_0^2(\mathbf{k}\cdot\mathbf{q})^2}{\left(q_0^2+\mathbf{q}^2\right)\left(q_0^2+(\mathbf{k}-\mathbf{q})^2\right)\mathbf{q}^2(\mathbf{k}-\mathbf{q})^2}\\
&= \int_0^1 \mathrm{d}x\int_0^1 \mathrm{d}y \sum\!\!\!\!\!\!\int_q \frac{4q_0^2(\mathbf{k}\cdot\mathbf{q})^2}{\left(xq_0^2+\mathbf{q}^2\right)^2\left(yq_0^2+(\mathbf{k}-\mathbf{q})^2\right)^2}\\
&= \int_0^1 \mathrm{d}x\int_0^1 \mathrm{d}y\int_0^1 \mathrm{d}z \sum\!\!\!\!\!\!\int_q \frac{4q_0^2(\mathbf{k}\cdot\mathbf{q})^2 6z(1-z)}{\left(\mathbf{q}^2-2z\mathbf{k}\cdot\mathbf{q}+z\mathbf{k}^2+(x(1-z)+yz)q_0^2\right)^4}\\
&= \int_0^1 \mathrm{d}x\int_0^1 \mathrm{d}y\int_0^1 \mathrm{d}z \sum\!\!\!\!\!\!\int_q \frac{4q_0^2(\mathbf{k}\cdot\mathbf{q}+z\mathbf{k}^2)^2 6z(1-z)}{\left(\mathbf{q}^2+z(1-z)\mathbf{k}^2+(x(1-z)+yz)q_0^2\right)^4}\\
&= \int_0^1 \mathrm{d}x\int_0^1 \mathrm{d}y\int_0^1 \mathrm{d}z \sum\!\!\!\!\!\!\int_q \frac{4q_0^2k^2\left(\frac{1}{d}\mathbf{q}^2+z^2k^2\right)6z(1-z)}{\left(\mathbf{q}^2+z(1-z)k^2+(x(1-z)+yz)q_0^2\right)^4}\\
&= \int_0^1 \mathrm{d}x\int_0^1 \mathrm{d}y\int_0^1 \mathrm{d}z \sum_{q_0} \frac{4q_0^2k^2z(1-z)}{(4\pi)^{\frac{d}{2}}}\left[\frac{1}{2}\Gamma\left(3-\frac{d}{2}\right)\left(z(1-z)k^2+(x(1-z)+yz)q_0^2\right)^{\frac{d}{2}-3}+\right.\\
&\qquad\left.+\,z^2k^2\Gamma\left(4-\frac{d}{2}\right)\left(z(1-z)k^2+(x(1-z)+yz)q_0^2\right)^{\frac{d}{2}-4}\right]\\
&= \int_0^1 \mathrm{d}z \sum_{q_0}{}' \frac{4}{(4\pi)^{\frac{d}{2}}}\frac{k^2}{q_0^2}\left\{\frac{1}{2}\Gamma\left(1-\frac{d}{2}\right)\left[\left(z(1-z)k^2+q_0^2\right)^{\frac{d}{2}-1}-\left(z(1-z)k^2+zq_0^2\right)^{\frac{d}{2}-1}-\right.\right.\\
&\qquad\left.-\left(z(1-z)k^2+(1-z)q_0^2\right)^{\frac{d}{2}-1}+\left(z(1-z)k^2\right)^{\frac{d}{2}-1}\right]+\\
&\qquad+z^2k^2\Gamma\left(2-\frac{d}{2}\right)\left[\left(z(1-z)k^2+q_0^2\right)^{\frac{d}{2}-2}-\left(z(1-z)k^2+zq_0^2\right)^{\frac{d}{2}-2}-\right.\\
&\qquad\left.\left.-\left(z(1-z)k^2+(1-z)q_0^2\right)^{\frac{d}{2}-2}+\left(z(1-z)k^2\right)^{\frac{d}{2}-2}\right]\right\}\\
&= \int_0^1 \mathrm{d}z \sum_{q_0}{}' \frac{4q_0^{d-2}}{(4\pi)^{\frac{d}{2}}}\sum_{l=0}^{\infty}\frac{\left(\frac{k^2}{q_0^2}\right)^{l+1}}{\Gamma(l+1)}\left\{\frac{\Gamma\left(1-\frac{d}{2}\right)\Gamma\left(\frac{d}{2}\right)}{2\Gamma\left(\frac{d}{2}-l\right)}\left[z^l(1-z)^l-z^{\frac{d}{2}-1}(1-z)^l-z^l(1-z)^{\frac{d}{2}-1}\right]+\right.\\
&\qquad\left.+\,\frac{k^2}{q_0^2}\frac{\Gamma\left(2-\frac{d}{2}\right)\Gamma\left(\frac{d}{2}-1\right)}{\Gamma\left(\frac{d}{2}-1-l\right)}\left[z^{l+2}(1-z)^l-z^{\frac{d}{2}}(1-z)^l-z^{l+2}(1-z)^{\frac{d}{2}-2}\right]\right\}+\\
&\quad+\sum_{q_0}{}' \frac{4}{(4\pi)^{\frac{d}{2}}}\frac{k^2}{q_0^2}\left\{\frac{1}{2}\Gamma\left(1-\frac{d}{2}\right)\frac{\Gamma\left(\frac{d}{2}\right)^2}{\Gamma(d)}+\Gamma\left(2-\frac{d}{2}\right)\frac{\Gamma\left(\frac{d}{2}+1\right)\Gamma\left(\frac{d}{2}-1\right)}{\Gamma(d)}\right\}k^{d-2}\\
&= \frac{16(2\pi T)^{d-1}}{(4\pi)^{\frac{d}{2}+1}}\sum_{l=0}^{\infty}\left(\frac{k}{2\pi T}\right)^{2(l+1)}\left\{\frac{1}{2}\zeta(2l+4-d)\frac{\Gamma\left(1-\frac{d}{2}\right)\Gamma\left(\frac{d}{2}\right)}{\Gamma\left(\frac{d}{2}-l\right)}\left[\frac{\Gamma(l+1)}{\Gamma(2l+2)}-2\frac{\Gamma\left(\frac{d}{2}\right)}{\Gamma\left(\frac{d}{2}+l+1\right)}\right]+\right.\\
&\qquad+\left(\frac{k}{2\pi T}\right)^2\zeta(2l+6-d)\frac{\Gamma\left(2-\frac{d}{2}\right)\Gamma\left(\frac{d}{2}-1\right)}{\Gamma\left(\frac{d}{2}-l-1\right)}\times\\
&\qquad\left.\times\left[\frac{\Gamma(l+3)}{\Gamma(2l+4)}-\frac{\Gamma\left(\frac{d}{2}+1\right)}{\Gamma\left(\frac{d}{2}+l+2\right)}-\frac{\Gamma(l+3)\Gamma\left(\frac{d}{2}-1\right)}{\Gamma(l+1)\Gamma\left(\frac{d}{2}+l+2\right)}\right]\right\}+\\
&\quad+\frac{16(2\pi T)^{d-1}}{(4\pi)^{\frac{d}{2}+1}}\left(\frac{k}{2\pi T}\right)^d\left\{\frac{1}{2}\Gamma\left(1-\frac{d}{2}\right)\frac{\Gamma\left(\frac{d}{2}\right)^2}{\Gamma(d)}+\Gamma\left(2-\frac{d}{2}\right)\frac{\Gamma\left(\frac{d}{2}+1\right)\Gamma\left(\frac{d}{2}-1\right)}{\Gamma(d)}\right\}\\
&= \frac{(2\pi T)^2}{12\pi^2}\left[\frac{1}{\varepsilon}+\frac{14}{3}+\gamma_E+\ln\pi-2\ln\frac{2\pi T}{\mu}\right]\left(\frac{k}{2\pi T}\right)^2+\frac{\pi(2\pi T)^2}{48}\left(\frac{k}{2\pi T}\right)^3+\mathcal{O}\left[\left(\frac{k}{2\pi T}\right)^4\right]. \qquad \text{(E.15)}
\end{aligned}
$$

$$
\begin{aligned}
I_3 &= -\sum\!\!\!\!\!\!\int_q \frac{4q_0^2\mathbf{k}^2}{(q_0^2+\mathbf{q}^2)\,(q_0^2+(\mathbf{k}-\mathbf{q})^2)\,(\mathbf{k}-\mathbf{q})^2} \\
&= -\int_0^1 \mathrm{d}x \sum\!\!\!\!\!\!\int_q \frac{4q_0^2\mathbf{k}^2}{(q_0^2+\mathbf{q}^2)\,(xq_0^2+(\mathbf{k}-\mathbf{q})^2)^2} \\
&= -\int_0^1 \mathrm{d}x \int_0^1 \mathrm{d}y \sum\!\!\!\!\!\!\int_q \frac{8q_0^2\mathbf{k}^2 y}{(\mathbf{q}^2-2y\mathbf{k}\cdot\mathbf{q}+y\mathbf{k}^2+(1-y+xy)q_0^2)^3} \\
&= -\int_0^1 \mathrm{d}x \int_0^1 \mathrm{d}y \sum\!\!\!\!\!\!\int_q \frac{8q_0^2k^2 y}{(\mathbf{q}^2+y(1-y)k^2+(1-y+xy)q_0^2)^3} \\
&= -\int_0^1 \mathrm{d}x \int_0^1 \mathrm{d}y \sum_{q_0} \frac{4q_0^2k^2 y}{(4\pi)^{\frac{d}{2}}}\Gamma\left(3-\frac{d}{2}\right)\left(y(1-y)k^2+(1-y+xy)q_0^2\right)^{\frac{d}{2}-3} \\
&= \int_0^1 \mathrm{d}y \sum_{q_0}{}' \frac{4k^2}{(4\pi)^{\frac{d}{2}}}\Gamma\left(2-\frac{d}{2}\right)\left[\left(y(1-y)k^2+q_0^2\right)^{\frac{d}{2}-2}-\left(y(1-y)k^2+(1-y)q_0^2\right)^{\frac{d}{2}-2}\right] \\
&= \int_0^1 \mathrm{d}y \sum_{q_0}{}' \frac{4q_0^{d-2}}{(4\pi)^{\frac{d}{2}}}\Gamma\left(2-\frac{d}{2}\right)\sum_{l=0}^{\infty}\frac{\Gamma\left(\frac{d}{2}-1\right)}{\Gamma(l+1)\Gamma\left(\frac{d}{2}-l-1\right)}\left(\frac{k^2}{q_0^2}\right)^{l+1}\left[y^l(1-y)^l-y^l(1-y)^{\frac{d}{2}-2}\right] \\
&= \frac{16(2\pi T)^{d-1}}{(4\pi)^{\frac{d}{2}+1}}\Gamma\left(2-\frac{d}{2}\right)\sum_{l=0}^{\infty}\left(\frac{k}{2\pi T}\right)^{2(l+1)}\frac{\Gamma\left(\frac{d}{2}-1\right)}{\Gamma\left(\frac{d}{2}-l-1\right)}\left[\frac{\Gamma(l+1)}{\Gamma(2l+2)}-\frac{\Gamma\left(\frac{d}{2}-1\right)}{\Gamma\left(\frac{d}{2}+l\right)}\right]\zeta(2l+4-d) \\
&= -\frac{(2\pi T)^2}{4\pi^2}\left[\frac{1}{\varepsilon}+4+\gamma_E+\ln\pi-2\ln\frac{2\pi T}{\mu}\right]\left(\frac{k}{2\pi T}\right)^2+\mathcal{O}\left[\left(\frac{k}{2\pi T}\right)^4\right]. \qquad \text{(E.16)}
\end{aligned}
$$

$$
\begin{aligned}
I_4 &= -\sum\!\!\!\!\!\!\int_q \frac{8(\mathbf{k}\cdot\mathbf{q})^2}{(q_0^2+\mathbf{q}^2)\,\mathbf{q}^2(\mathbf{k}-\mathbf{q})^2} \\
&= -\int_0^1 \mathrm{d}x \sum\!\!\!\!\!\!\int_q \frac{8(\mathbf{k}\cdot\mathbf{q})^2}{(xq_0^2+\mathbf{q}^2)^2\,(\mathbf{k}-\mathbf{q})^2} \\
&= -\int_0^1 \mathrm{d}x \int_0^1 \mathrm{d}y \sum\!\!\!\!\!\!\int_q \frac{16(\mathbf{k}\cdot\mathbf{q})^2(1-y)}{(\mathbf{q}^2-2y\mathbf{k}\cdot\mathbf{q}+y\mathbf{k}^2+x(1-y)q_0^2)^3} \\
&= -\int_0^1 \mathrm{d}x \int_0^1 \mathrm{d}y \sum\!\!\!\!\!\!\int_q \frac{16k^2\left(\frac{1}{d}\mathbf{q}^2+y^2k^2\right)(1-y)}{(\mathbf{q}^2+y(1-y)k^2+x(1-y)q_0^2)^3} \\
&= -\int_0^1 \mathrm{d}x \int_0^1 \mathrm{d}y \sum_{q_0} \frac{8k^2(1-y)}{(4\pi)^{\frac{d}{2}}}\left[\frac{1}{2}\Gamma\left(2-\frac{d}{2}\right)\left(y(1-y)k^2+x(1-y)q_0^2\right)^{\frac{d}{2}-2}+\right. \\
&\qquad\qquad \left.+y^2k^2\Gamma\left(3-\frac{d}{2}\right)\left(y(1-y)k^2+x(1-y)q_0^2\right)^{\frac{d}{2}-3}\right] \\
&= \int_0^1 \mathrm{d}y \sum_{q_0}{}' \frac{8}{(4\pi)^{\frac{d}{2}}}\frac{k^2}{q_0^2}\left\{\frac{1}{2}\Gamma\left(1-\frac{d}{2}\right)\left[\left(y(1-y)k^2+(1-y)q_0^2\right)^{\frac{d}{2}-1}-\left(y(1-y)k^2\right)^{\frac{d}{2}-1}\right]+\right. \\
&\qquad\qquad \left.+y^2k^2\Gamma\left(2-\frac{d}{2}\right)\left[\left(y(1-y)k^2+(1-y)q_0^2\right)^{\frac{d}{2}-2}-\left(y(1-y)k^2\right)^{\frac{d}{2}-2}\right]\right\}- \\
&\quad -\frac{8Tk^{d-2}}{(4\pi)^{\frac{d}{2}}}\left[\frac{1}{2}\Gamma\left(2-\frac{d}{2}\right)\frac{\Gamma\left(\frac{d}{2}\right)\Gamma\left(\frac{d}{2}-1\right)}{\Gamma(d-1)}+\Gamma\left(3-\frac{d}{2}\right)\frac{\Gamma\left(\frac{d}{2}\right)\Gamma\left(\frac{d}{2}-1\right)}{\Gamma(d-1)}\right]
\end{aligned}
$$

$$
\begin{aligned}
&= \int_0^1 \mathrm{d}y \sum_{q_0}{}' \frac{8}{(4\pi)^{\frac{d}{2}}} \sum_{l=0}^{\infty} \frac{q_0^{d-2}}{\Gamma(l+1)} \left(\frac{k^2}{q_0^2}\right)^{l+1} \left\{ \frac{1}{2}\Gamma\left(1-\frac{d}{2}\right) \frac{\Gamma\left(\frac{d}{2}\right)}{\Gamma\left(\frac{d}{2}-l\right)} y^l (1-y)^{\frac{d}{2}-1} + \right. \\
&\qquad \left. + \frac{k^2}{q_0^2}\Gamma\left(2-\frac{d}{2}\right) \frac{\Gamma\left(\frac{d}{2}-1\right)}{\Gamma\left(\frac{d}{2}-l-1\right)} y^{l+2} (1-y)^{\frac{d}{2}-2} \right\} - \\
&\quad - \frac{32(2\pi T)k^{d-2}}{(4\pi)^{\frac{d}{2}+1}} \left(\frac{k}{2\pi T}\right)^2 \frac{\pi^2}{6} \left\{ \frac{1}{2}\Gamma\left(1-\frac{d}{2}\right) \frac{\Gamma\left(\frac{d}{2}\right)^2}{\Gamma(d)} + \Gamma\left(2-\frac{d}{2}\right) \frac{\Gamma\left(\frac{d}{2}+1\right)\Gamma\left(\frac{d}{2}-1\right)}{\Gamma(d)} \right\} - \\
&\quad - \frac{16(2\pi T)k^{d-2}}{(4\pi)^{\frac{d}{2}+1}} \left[\frac{1}{2}\Gamma\left(2-\frac{d}{2}\right) \frac{\Gamma\left(\frac{d}{2}\right)\Gamma\left(\frac{d}{2}-1\right)}{\Gamma(d-1)} + \Gamma\left(3-\frac{d}{2}\right) \frac{\Gamma\left(\frac{d}{2}\right)\Gamma\left(\frac{d}{2}-1\right)}{\Gamma(d-1)} \right] \\
&= \frac{32(2\pi T)^{d-1}}{(4\pi)^{\frac{d}{2}+1}} \sum_{l=0}^{\infty} \left(\frac{k}{2\pi T}\right)^{2(l+1)} \left\{ \frac{1}{2}\zeta(2l+4-d)\Gamma\left(1-\frac{d}{2}\right) \frac{\Gamma\left(\frac{d}{2}\right)^2}{\Gamma\left(\frac{d}{2}-l\right)\Gamma\left(\frac{d}{2}+l+1\right)} + \right. \\
&\qquad \left. + \left(\frac{k}{2\pi T}\right)^2 \zeta(2l+6-d)\Gamma\left(2-\frac{d}{2}\right) \frac{\Gamma\left(\frac{d}{2}-1\right)}{\Gamma\left(\frac{d}{2}-l-1\right)} \frac{\Gamma(l+3)\Gamma\left(\frac{d}{2}-1\right)}{\Gamma(l+1)\Gamma\left(\frac{d}{2}+l+2\right)} \right\} - \\
&\quad - \frac{32(2\pi T)^{d-1}}{(4\pi)^{\frac{d}{2}+1}} \left(\frac{k}{2\pi T}\right)^d \frac{\pi^2}{6} \left\{ \frac{1}{2}\Gamma\left(1-\frac{d}{2}\right) \frac{\Gamma\left(\frac{d}{2}\right)^2}{\Gamma(d)} + \Gamma\left(2-\frac{d}{2}\right) \frac{\Gamma\left(\frac{d}{2}+1\right)\Gamma\left(\frac{d}{2}-1\right)}{\Gamma(d)} \right\} - \\
&\quad - \frac{16(2\pi T)^{d-1}}{(4\pi)^{\frac{d}{2}+1}} \left(\frac{k}{2\pi T}\right)^{d-2} \left[\frac{1}{2}\Gamma\left(2-\frac{d}{2}\right) \frac{\Gamma\left(\frac{d}{2}\right)\Gamma\left(\frac{d}{2}-1\right)}{\Gamma(d-1)} + \Gamma\left(3-\frac{d}{2}\right) \frac{\Gamma\left(\frac{d}{2}\right)\Gamma\left(\frac{d}{2}-1\right)}{\Gamma(d-1)} \right] \\
&= -\frac{(2\pi T)^2}{4\pi} \frac{k}{2\pi T} - \frac{(2\pi T)^2}{3\pi^2} \left[\frac{1}{\varepsilon} + \frac{8}{3} + \gamma_E + \ln\pi - 2\ln\frac{2\pi T}{\mu} \right] \left(\frac{k}{2\pi T}\right)^2 - \frac{\pi(2\pi T)^2}{24} \left(\frac{k}{2\pi T}\right)^3 + \\
&\quad + \mathcal{O}\left[\left(\frac{k}{2\pi T}\right)^4 \right] .
\end{aligned}
\tag{E.17}
$$

$$
\begin{aligned}
I_5 &= \sum\!\!\!\!\!\!\int_q \frac{8\mathbf{k}^2}{(q_0^2+\mathbf{q}^2)\,(\mathbf{k}-\mathbf{q})^2} \\
&= \int_0^1 \mathrm{d}x \sum\!\!\!\!\!\!\int_q \frac{8\mathbf{k}^2}{\left(\mathbf{q}^2 - 2x\mathbf{k}\cdot\mathbf{q} + x\mathbf{k}^2 + (1-x)q_0^2\right)^2} \\
&= \int_0^1 \mathrm{d}x \sum\!\!\!\!\!\!\int_q \frac{8k^2}{\left(\mathbf{q}^2 + x(1-x)k^2 + (1-x)q_0^2\right)^2} \\
&= \int_0^1 \mathrm{d}x \sum_{q_0} \frac{8k^2}{(4\pi)^{\frac{d}{2}}} \Gamma\left(2-\frac{d}{2}\right) \left(x(1-x)k^2 + (1-x)q_0^2\right)^{\frac{d}{2}-2} \\
&= \int_0^1 \mathrm{d}x \sum_{q_0}{}' \frac{8q_0^{d-2}}{(4\pi)^{\frac{d}{2}}} \frac{k^2}{q_0^2} \Gamma\left(2-\frac{d}{2}\right) \sum_{l=0}^{\infty} \frac{\Gamma\left(\frac{d}{2}-1\right)}{\Gamma(l+1)\Gamma\left(\frac{d}{2}-l-1\right)} \left(\frac{k^2}{q_0^2}\right)^l x^l (1-x)^{\frac{d}{2}-2} + \\
&\quad + \frac{8Tk^2}{(4\pi)^{\frac{d}{2}}} \Gamma\left(2-\frac{d}{2}\right) \frac{\Gamma\left(\frac{d}{2}-1\right)^2}{\Gamma(d-2)} k^{d-4} \\
&= \frac{32(2\pi T)^{d-1}}{(4\pi)^{\frac{d}{2}+1}} \Gamma\left(2-\frac{d}{2}\right) \sum_{l=0}^{\infty} \left(\frac{k}{2\pi T}\right)^{2(l+1)} \frac{\Gamma\left(\frac{d}{2}-1\right)^2}{\Gamma\left(\frac{d}{2}-l-1\right)\Gamma\left(\frac{d}{2}+l\right)} \zeta(2l+4-d) + \\
&\quad + \frac{16(2\pi T)^{d-1}}{(4\pi)^{\frac{d}{2}+1}} \left(\frac{k}{2\pi T}\right)^{d-2} \Gamma\left(2-\frac{d}{2}\right) \frac{\Gamma\left(\frac{d}{2}-1\right)^2}{\Gamma(d-2)} \\
&= \frac{(2\pi T)^2}{2\pi} \frac{k}{2\pi T} + \frac{(2\pi T)^2}{\pi^2} \left[\frac{1}{\varepsilon} + 2 + \gamma_E + \ln\pi - 2\ln\frac{2\pi T}{\mu} \right] \left(\frac{k}{2\pi T}\right)^2 + \mathcal{O}\left[\left(\frac{k}{2\pi T}\right)^4 \right] .
\end{aligned}
\tag{E.18}
$$

Adding everything up, we get the gluonic contribution to the gluon self energy:

$$\Pi_{00}(0,\mathbf{k})\Big|_{\text{gluon}} = \frac{\alpha_s C_A (2\pi T)^2}{4\pi}\left\{\frac{4}{3} - 2\pi\frac{k}{2\pi T} - \frac{11}{3}\left[\frac{1}{\varepsilon} + 1 + \gamma_E + \ln\pi - 2\ln\frac{2\pi T}{\mu}\right]\left(\frac{k}{2\pi T}\right)^2 + \right.$$
$$\left. + \frac{\pi^3}{6}\left(\frac{k}{2\pi T}\right)^3 + \mathcal{O}\left[\left(\frac{k}{2\pi T}\right)^4\right]\right\}. \tag{E.19}$$

The vacuum part has already been calculated in a previous section:

$$\Pi_{00}^{(0)}(0,\mathbf{k})\Big|_{\text{gluon}} = -\frac{\alpha_s C_A\, k^2}{4\pi}\frac{11}{3}\left[\frac{1}{\varepsilon} + \frac{31}{33} - \gamma_E + \ln 4\pi - 2\ln\frac{k}{\mu}\right]. \tag{E.20}$$

This gives the following gluonic contribution to thermal part:

$$\Pi_{00}^{(T)}(0,\mathbf{k})\Big|_{\text{gluon}} = \frac{\alpha_s C_A (2\pi T)^2}{3\pi}\left\{1 - \frac{3\pi}{2}\frac{k}{2\pi T} - \frac{11}{2}\left[\gamma_E + \frac{1}{33} + \ln\frac{k}{4\pi T}\right]\left(\frac{k}{2\pi T}\right)^2 + \right.$$
$$\left. + \frac{\pi^3}{8}\left(\frac{k}{2\pi T}\right)^3 + \mathcal{O}\left[\left(\frac{k}{2\pi T}\right)^4\right]\right\}. \tag{E.21}$$

Now to the fermionic part:

$$\begin{aligned}
\Pi_{00}(0,\mathbf{k})\Big|_{\text{fermion}} &= g^2 T_F n_f\, 4 \sum\!\!\!\!\!\!\int_{\{q\}} \frac{q_0^2 - (\mathbf{k}+\mathbf{q})\cdot\mathbf{q}}{(q_0^2+\mathbf{q}^2)\,(q_0^2+(\mathbf{k}+\mathbf{q})^2)} \\
&= 4g^2 T_F n_f \int_0^1 \mathrm{d}x \sum\!\!\!\!\!\!\int_{\{q\}} \frac{q_0^2 - (\mathbf{k}+\mathbf{q})\cdot\mathbf{q}}{\left(\mathbf{q}^2 + 2x\mathbf{k}\cdot\mathbf{q} + x\mathbf{k}^2 + q_0^2\right)^2} \\
&= 4g^2 T_F n_f \int_0^1 \mathrm{d}x \sum\!\!\!\!\!\!\int_{\{q\}} \frac{q_0^2 + x(1-x)k^2 - \mathbf{q}^2}{\left(\mathbf{q}^2 + x(1-x)k^2 + q_0^2\right)^2} \\
&= 4g^2 T_F n_f \int_0^1 \mathrm{d}x \sum_{\{q_0\}} \frac{1}{(4\pi)^{\frac{d}{2}}}\left[\Gamma\left(2-\frac{d}{2}\right) - \frac{d}{2}\Gamma\left(1-\frac{d}{2}\right)\right]\left(x(1-x)k^2 + q_0^2\right)^{\frac{d}{2}-1} \\
&= 4g^2 T_F n_f \int_0^1 \mathrm{d}x \sum_{\{q_0\}} \frac{q_0^{d-2}}{(4\pi)^{\frac{d}{2}}}(1-d)\Gamma\left(1-\frac{d}{2}\right)\sum_{l=0}^{\infty}\frac{\Gamma\left(\frac{d}{2}\right)}{\Gamma(l+1)\Gamma\left(\frac{d}{2}-l\right)}x^l(1-x)^l\left(\frac{k^2}{q_0^2}\right)^l \\
&= 4g^2 T_F n_f \frac{(1-d)(\pi T)^{d-2}}{(4\pi)^{\frac{d}{2}}}\Gamma\left(1-\frac{d}{2}\right)\sum_{l=0}^{\infty}\frac{\Gamma(l+1)\Gamma\left(\frac{d}{2}\right)}{\Gamma(2l+2)\Gamma\left(\frac{d}{2}-l\right)}\left(\frac{k}{\pi T}\right)^{2l}\times \\
&\qquad\qquad \times \sum_{n=1}^{\infty}\frac{2T}{(2n-1)^{2l+2-d}} \\
&= g^2 T_F n_f \frac{32(1-d)(\pi T)^{d-1}}{(4\pi)^{\frac{d}{2}+1}}\Gamma\left(1-\frac{d}{2}\right)\sum_{l=0}^{\infty}\left(\frac{k}{\pi T}\right)^{2l}\frac{\Gamma(l+1)\Gamma\left(\frac{d}{2}\right)}{\Gamma(2l+2)\Gamma\left(\frac{d}{2}-l\right)}\times \\
&\qquad\qquad \times \left(1-2^{d-2-2l}\right)\zeta(2l+2-d) \\
&= \frac{\alpha_s T_F n_f (\pi T)^2}{3\pi}\left\{4 + \left[\frac{1}{\varepsilon} - 1 + \gamma_E + \ln 4\pi - 2\ln\frac{\pi T}{\mu}\right]\left(\frac{k}{\pi T}\right)^2 + \mathcal{O}\left[\left(\frac{k}{\pi T}\right)^4\right]\right\}.
\end{aligned} \tag{E.22}$$

$$\Pi_{00}^{(0)}(0,\mathbf{k})\Big|_{\text{fermion}} = \frac{\alpha_s T_F n_f\, k^2}{3\pi}\left[\frac{1}{\varepsilon} + \frac{5}{3} - \gamma_E + \ln 4\pi - 2\ln\frac{k}{\mu}\right]. \tag{E.23}$$

$$\Pi_{00}^{(T)}(0,\mathbf{k})\Big|_{\text{fermion}} = \frac{2\alpha_s T_F n_f (\pi T)^2}{3\pi}\left\{2 + \left[\gamma_E - \frac{4}{3} + \ln\frac{k}{\pi T}\right]\left(\frac{k}{\pi T}\right)^2 + \mathcal{O}\left[\left(\frac{k}{\pi T}\right)^4\right]\right\}. \tag{E.24}$$

In all contributions, the divergences come always from the zeta function, since the negative arguments of the gamma functions are always half integers. These divergences must be, and indeed are, in the quadratic terms only, since they all must be contained in the vacuum part, which is quadratic in k. Apart from the linear and cubic terms, there are no other terms of odd power.

$k \gg T$ Expansion

We start with expanding the logarithm:

$$\begin{aligned}\ln\frac{k+2q}{k-2q} =& \ln\frac{1+\frac{2q}{k}}{1-\frac{2q}{k}} = \int_0^{\frac{2q}{k}} \mathrm{d}x \left(\frac{1}{1+x}+\frac{1}{1-x}\right)\\ =& \int_0^{\frac{2q}{k}} \mathrm{d}x\, \frac{2}{1-x^2} = \sum_{n=0}^{\infty}\int_0^{\frac{2q}{k}} \mathrm{d}x\, 2x^{2n}\\ =& \sum_{n=0}^{\infty}\frac{2}{2n+1}\left(\frac{2q}{k}\right)^{2n+1}. \end{aligned} \tag{E.25}$$

$$\begin{aligned}1-\frac{k^2}{2q^2}+\left(\frac{q}{k}-\frac{k}{2q}+\frac{k^3}{8q^3}\right)\ln\frac{k+2q}{k-2q} =& 1-\frac{k^2}{2q^2}+\sum_{n=0}^{\infty}\frac{2}{2n+1}\left[\frac{1}{2}\left(\frac{2q}{k}\right)^{2n+2}-\left(\frac{2q}{k}\right)^{2n}+\left(\frac{2q}{k}\right)^{2n-2}\right]\\ =& 1-\frac{k^2}{2q^2}-2+2\left(\frac{2q}{k}\right)^{-2}+\frac{2}{3}\\ &+\sum_{n=1}^{\infty}\left[\frac{1}{2n-1}-\frac{2}{2n+1}+\frac{2}{2n+3}\right]\left(\frac{2q}{k}\right)^{2n}\\ =& -\frac{1}{3}+\sum_{n=1}^{\infty}\frac{4n^2+7}{(2n-1)(2n+1)(2n+3)}\left(\frac{2q}{k}\right)^{2n}. \end{aligned} \tag{E.26}$$

$$\begin{aligned}1+\left(\frac{q}{k}-\frac{k}{4q}\right)\ln\frac{k+2q}{k-2q} =& 1+\sum_{n=0}^{\infty}\frac{1}{2n+1}\left[\left(\frac{2q}{k}\right)^{2n+2}-\left(\frac{2q}{k}\right)^{2n}\right]\\ =& 1-1+\sum_{n=1}^{\infty}\left[\frac{1}{2n-1}-\frac{1}{2n+1}\right]\left(\frac{2q}{k}\right)^{2n}\\ =& \sum_{n=1}^{\infty}\frac{2}{(2n-1)(2n+1)}\left(\frac{2q}{k}\right)^{2n}. \end{aligned} \tag{E.27}$$

Then the q integrations can be performed using the integral representation of the Riemann zeta function.

$$\int_0^{\infty}\mathrm{d}q\,\frac{q^{n-1}}{e^{q\beta}-1} = T^n\Gamma(n)\zeta(n)\,, \tag{E.28}$$

$$\int_0^{\infty}\mathrm{d}q\,\frac{q^{n-1}}{e^{q\beta}+1} = \int_0^{\infty}\mathrm{d}q\left(\frac{q^{n-1}}{e^{q\beta}-1}-\frac{2q^{n-1}}{e^{2q\beta}-1}\right) = \left(1-2^{1-n}\right)T^n\Gamma(n)\zeta(n)\,. \tag{E.29}$$

$$\begin{aligned}\Pi_{00}^{(T)}(0,\mathbf{k}) =& \frac{4\alpha_s C_A}{\pi}\int_0^{\infty}\mathrm{d}q\,\frac{q}{e^{q\beta}-1}\left\{1-\frac{k^2}{2q^2}+\left(\frac{q}{k}-\frac{k}{2q}+\frac{k^3}{8q^3}\right)\ln\left|\frac{2q+k}{2q-k}\right|\right\}\\ &+\frac{8\alpha_s T_F n_f}{\pi}\int_0^{\infty}\mathrm{d}q\,\frac{q}{e^{q\beta}+1}\left\{1+\left(\frac{q}{k}-\frac{k}{4q}\right)\ln\left|\frac{2q+k}{2q-k}\right|\right\}\\ =& \frac{4\alpha_s C_A}{\pi}\int_0^{\infty}\mathrm{d}q\,\frac{q}{e^{q\beta}-1}\left\{-\frac{1}{3}+\sum_{n=1}^{\infty}\frac{4n^2+7}{(2n-1)(2n+1)(2n+3)}\left(\frac{2q}{k}\right)^{2n}\right\}\\ &+\frac{8\alpha_s T_F n_f}{\pi}\int_0^{\infty}\mathrm{d}q\,\frac{q}{e^{q\beta}+1}\left\{\sum_{n=1}^{\infty}\frac{2}{(2n-1)(2n+1)}\left(\frac{2q}{k}\right)^{2n}\right\}\end{aligned}$$

$$
\begin{aligned}
&= -\frac{2}{9}\alpha_s\pi C_A T^2 + \frac{4\alpha_s T^2}{\pi}\sum_{n=1}^{\infty}\Gamma(2n+2)\zeta(2n+2)\times \\
&\quad\times\left\{\frac{(4n^2+7)C_A}{(2n-1)(2n+1)(2n+3)} + \frac{4T_F n_f(1-2^{-2n-1})}{(2n-1)(2n+1)}\right\}\left(\frac{2T}{k}\right)^{2n} \\
&= -\frac{2}{9}\alpha_s\pi C_A T^2 + \frac{4}{15}\alpha_s\pi^3 T^2\left\{\frac{11}{15}C_A + \frac{7}{6}T_F n_f\right\}\frac{4T^2}{k^2} + \dots
\end{aligned}
\tag{E.30}
$$

We have obtained an asymptotic series; it diverges when summed to infinity because of the gamma function, but gives a good approximation when truncated after a few terms. The reason for this is, that the series expansion of the logarithm is only valid for $k > 2q$, but we ignored this when performing the q integration. However, the region with $2q > k$ is exponentially suppressed through the Bose and Fermi distribution functions. So, as a justification for our procedure, we can split up the integration into a region $q < \Lambda$ with $T \ll \Lambda \ll \frac{k}{2}$, where we may expand the integrand, and a region $q > \Lambda$, that is exponentially suppressed:

$$
\begin{aligned}
\int_0^\infty \mathrm{d}q\, q\, n_{B/F}(q) f\left(\frac{2q}{k}\right) &= \int_0^\Lambda \mathrm{d}q\, q\, n_{B/F}(q)\sum_{n=0}^{\infty} f_n\left(\frac{2q}{k}\right)^n + \int_\Lambda^\infty \mathrm{d}q\, q\, n_{B/F}(q) f\left(\frac{2q}{k}\right) \\
&= \int_0^\Lambda \mathrm{d}q\, q\, n_{B/F}(q)\sum_{n=0}^{N} f_n\left(\frac{2q}{k}\right)^n + \mathcal{O}\left[\int_0^\Lambda \mathrm{d}q\, q\, n_{B/F}(q)\left(\frac{2q}{k}\right)^{N+1}\right] \\
&\quad + \int_\Lambda^\infty \mathrm{d}q\, q\, n_{B/F}(q) f\left(\frac{2q}{k}\right) \\
&= \int_0^\infty \mathrm{d}q\, q\, n_{B/F}(q)\sum_{n=0}^{N} f_n\left(\frac{2q}{k}\right)^n + \mathcal{O}\left[T^2\int_0^{\frac{\Lambda}{T}} \mathrm{d}x\, \frac{x}{e^x \pm 1}\left(\frac{2T}{k}x\right)^{N+1}\right] \\
&\quad + T^2\int_{\frac{\Lambda}{T}}^\infty \mathrm{d}x\, \frac{x}{e^x \pm 1}\left[f\left(\frac{2T}{k}x\right) - \sum_{n=0}^{N} f_n\left(\frac{2T}{k}x\right)^n\right] \\
&= \int_0^\infty \mathrm{d}q\, q\, n_{B/F}(q)\sum_{n=0}^{N} f_n\left(\frac{2q}{k}\right)^n + \mathcal{O}\left[\frac{T^2}{N+1}\left(\frac{2\Lambda}{k}\right)^{N+1}\right] \\
&\quad + \mathcal{O}\left[T^2 e^{-\frac{\Lambda}{T}}\right] + \mathcal{O}\left[T^2\Gamma(N+2)\left(\frac{2T}{k}\right)^N e^{-\frac{\Lambda}{T}}\right].
\end{aligned}
\tag{E.31}
$$

For the estimation of the correction terms we used $\frac{x^2}{e^x \pm 1} < 1$ in the first term, which is a far too conservative but simple choice. The last term was included, despite it being suppressed by additional powers of $\frac{2T}{k}$, because it shows that the corrections may get big for large N by means of the gamma function. This is the reason why the series obtained in (E.30) diverges. However, we are only interested in the first few terms anyway, so the above procedure leads to a good approximation. The equlities in (E.30) are to be understood in this context and not to be taken literally.

E.3 Diagram C1

Since this diagram is finite (as it will turn out) we may perform all the integrations in 3 dimensions.

$$
\begin{aligned}
&(ig)^3(-ig)f^{abc}\widetilde{\mathrm{Tr}}\left[T^aT^bT^c\right]\int_0^\beta(-\mathrm{d}\tau_1)\int_0^1 \mathrm{d}s\ (-r_i)\int_0^\beta \mathrm{d}\tau_2 \sum\!\!\!\!\!\!\int_k \sum\!\!\!\!\!\!\int_p \sum\!\!\!\!\!\!\int_q \frac{e^{-i(\beta-\tau_1)k_0+\frac{i}{2}\mathbf{r}\cdot\mathbf{k}}}{\mathbf{k}^2}\times \\
&\times\frac{\delta_{ij}-\frac{p_ip_j}{\mathbf{p}^2}}{p^2}e^{-i\beta p_0 - i\left(\frac{1}{2}-s\right)\mathbf{r}\cdot\mathbf{p}}\frac{e^{-i\tau_2 q_0-\frac{i}{2}\mathbf{r}\cdot\mathbf{q}}}{\mathbf{q}^2}\left(k_j-q_j\right)\frac{(2\pi)^3}{T}\delta^{(3)}\left(\mathbf{k}+\mathbf{p}+\mathbf{q}\right)\delta_{-n_k,n_p+n_q}
\end{aligned}
$$

$$
\begin{aligned}
=&-\frac{i}{2}g^4C_FC_A\sum\!\!\!\!\!\!\int_p\sum\!\!\!\!\!\!\int_q\frac{-2\left(\mathbf{r}\cdot\mathbf{q}-\frac{(\mathbf{r}\cdot\mathbf{p})(\mathbf{p}\cdot\mathbf{q})}{\mathbf{p}^2}\right)}{(\mathbf{p}+\mathbf{q})^2\,p^2\,\mathbf{q}^2}\int_0^\beta \mathrm{d}\tau_1\int_0^1\mathrm{d}s\int_0^\beta\mathrm{d}\tau_2\,e^{-i\tau_1p_0-i(1-s)\mathbf{r}\cdot\mathbf{p}}e^{-i(\tau_1+\tau_2)q_0-i\mathbf{r}\cdot\mathbf{q}}\\
=&ig^4C_FC_A\int_0^1\mathrm{d}s\sum\!\!\!\!\!\!\int_p\sum\!\!\!\!\!\!\int_q\frac{\left(\mathbf{r}\cdot\mathbf{q}-\frac{(\mathbf{r}\cdot\mathbf{p})(\mathbf{p}\cdot\mathbf{q})}{\mathbf{p}^2}\right)}{(\mathbf{p}+\mathbf{q})^2\,p^2\,\mathbf{q}^2}e^{-i\mathbf{r}\cdot\mathbf{q}}e^{-is\mathbf{r}\cdot\mathbf{p}}\beta^2\delta_{n_p+n_q,0}\delta_{n_q,0}\\
=&-g^4C_FC_A\int_0^1\mathrm{d}s\int_p\frac{r_i-\frac{\mathbf{r}\cdot\mathbf{p}}{\mathbf{p}^2}p_i}{\mathbf{p}^2}e^{-is\mathbf{r}\cdot\mathbf{p}}\,\nabla_i^{(\mathbf{r})}\int_q\frac{e^{-i\mathbf{r}\cdot\mathbf{q}}}{(\mathbf{p}+\mathbf{q})^2\,\mathbf{q}^2}\,.
\end{aligned}
\tag{E.32}
$$

$$
\begin{aligned}
\int_q\frac{e^{-i\mathbf{r}\cdot\mathbf{q}}}{(\mathbf{p}+\mathbf{q})^2\,\mathbf{q}^2}&=\int_0^1\mathrm{d}x\int_q\frac{e^{-i\mathbf{r}\cdot\mathbf{q}}}{\left(\mathbf{q}^2+2x\mathbf{p}\cdot\mathbf{q}+x\mathbf{p}^2\right)^2}\\
&=\int_0^1\mathrm{d}x\,e^{ix\mathbf{r}\cdot\mathbf{p}}\int_q\frac{e^{-i\mathbf{r}\cdot\mathbf{q}}}{\left(\mathbf{q}^2+x(1-x)\mathbf{p}^2\right)^2}\\
&=\int_0^1\mathrm{d}x\,e^{ix\mathbf{r}\cdot\mathbf{p}}\frac{1}{4\pi^2}\int_0^\infty\mathrm{d}q\,\frac{q^2}{\left(q^2+x(1-x)p^2\right)^2}\frac{e^{irq}-e^{-irq}}{irq}\\
&=\int_0^1\mathrm{d}x\,e^{ix\mathbf{r}\cdot\mathbf{p}}\frac{1}{4\pi^2ir}\int_{-\infty}^\infty\mathrm{d}q\,\frac{q\,e^{irq}}{\left(q^2+x(1-x)p^2\right)^2}\\
&=\int_0^1\mathrm{d}x\,e^{ix\mathbf{r}\cdot\mathbf{p}}\frac{1}{4\pi^2ir}\left\{\left[-\frac{1}{2}\frac{e^{irq}}{q^2+x(1-x)p^2}\right]_{-\infty}^\infty+\frac{1}{2}\int_{-\infty}^\infty\mathrm{d}q\,\frac{ir\,e^{irq}}{q^2+x(1-x)p^2}\right\}\\
&=\int_0^1\mathrm{d}x\,e^{ix\mathbf{r}\cdot\mathbf{p}}\frac{1}{8\pi^2}\left\{2\pi i\frac{e^{-\sqrt{x(1-x)}rp}}{2i\sqrt{x(1-x)}\,p}\right\}\\
&=\frac{1}{8\pi}\int_0^1\mathrm{d}x\,\frac{e^{ix\mathbf{r}\cdot\mathbf{p}}e^{-\sqrt{x(1-x)}rp}}{\sqrt{x(1-x)}\,p}\,.
\end{aligned}
\tag{E.33}
$$

$$
\begin{aligned}
&-g^4C_FC_A\int_0^1\mathrm{d}s\int_p\frac{r_i-\frac{\mathbf{r}\cdot\mathbf{p}}{\mathbf{p}^2}p_i}{\mathbf{p}^2}e^{-is\mathbf{r}\cdot\mathbf{p}}\,\nabla_i^{(\mathbf{r})}\int_q\frac{e^{-i\mathbf{r}\cdot\mathbf{q}}}{(\mathbf{p}+\mathbf{q})^2\,\mathbf{q}^2}\\
=&-g^4C_FC_A\int_0^1\mathrm{d}s\int_p\frac{r_i-\frac{\mathbf{r}\cdot\mathbf{p}}{\mathbf{p}^2}p_i}{\mathbf{p}^2}e^{-is\mathbf{r}\cdot\mathbf{p}}\,\frac{1}{8\pi}\int_0^1\mathrm{d}x\,\left[ixp^i-\sqrt{x(1-x)}\,p\frac{r^i}{r}\right]\frac{e^{ix\mathbf{r}\cdot\mathbf{p}}e^{-\sqrt{x(1-x)}rp}}{\sqrt{x(1-x)}\,p}\\
=&\frac{g^4C_FC_A}{8\pi}\int_0^1\mathrm{d}x\int_0^1\mathrm{d}s\int_p\frac{\mathbf{r}^2-\frac{(\mathbf{r}\cdot\mathbf{p})^2}{\mathbf{p}^2}}{r\,\mathbf{p}^2}e^{i(x-s)\mathbf{r}\cdot\mathbf{p}}e^{-\sqrt{x(1-x)}rp}\\
=&\frac{g^4C_FC_A}{8\pi}\int_0^1\mathrm{d}x\int_0^1\mathrm{d}s\frac{r}{4\pi^2}\int_0^\infty\mathrm{d}p\int_{-1}^1\mathrm{d}y\left(1-y^2\right)e^{i(x-s)yrp}e^{-\sqrt{x(1-x)}rp}\,.
\end{aligned}
\tag{E.34}
$$

$$
\begin{aligned}
\int_{-1}^1\mathrm{d}y\left(1-y^2\right)e^{iay}&=\left[\left(1-y^2\right)\frac{e^{iay}}{ia}\right]_{-1}^1+\frac{2}{ia}\int_0^1\mathrm{d}y\,ye^{iay}\\
&=\frac{2}{ia}\left[y\frac{e^{ia}}{ia}\right]_{-1}^1-\frac{2}{(ia)^2}\int_{-1}^1\mathrm{d}y\,e^{iay}\\
&=-\frac{4\cos a}{a^2}+\frac{4\sin a}{a^3}\,.
\end{aligned}
\tag{E.35}
$$

$$
\begin{aligned}
&\frac{g^4C_FC_A}{8\pi}\int_0^1\mathrm{d}x\int_0^1\mathrm{d}s\frac{r}{4\pi^2}\int_0^\infty\mathrm{d}p\int_{-1}^1\mathrm{d}y\left(1-y^2\right)e^{i(x-s)yrp}e^{-\sqrt{x(1-x)}rp}\\
=&\frac{g^4C_FC_A}{8\pi^3}\int_0^1\mathrm{d}x\int_0^1\mathrm{d}s\int_0^\infty\mathrm{d}p\,r\left[-\frac{\cos\left[(x-s)rp\right]}{(x-s)^2r^2p^2}+\frac{\sin\left[(x-s)rp\right]}{(x-s)^3r^3p^3}\right]e^{-\sqrt{x(1-x)}rp}\\
=&\frac{g^4C_FC_A}{8\pi^3}\int_0^1\mathrm{d}x\int_0^1\mathrm{d}s\int_0^\infty\frac{\mathrm{d}p}{|x-s|}\left[-\frac{\cos p}{p^2}+\frac{\sin p}{p^3}\right]e^{-\frac{\sqrt{x(1-x)}}{|x-s|}p}\,.
\end{aligned}
\tag{E.36}
$$

$$
\begin{aligned}
-\frac{\cos p}{p^2}+\frac{\sin p}{p^3} &= \partial_p\left[-\frac{1}{2p^2}\left(-p\cos p+\sin p\right)\right]+\frac{1}{2p^2}\left(-\cos p+p\sin p+\cos p\right)\\
&= \partial_p^2\left[\frac{1}{2p}\left(-p\cos p+\sin p\right)\right]-\partial_p\left[\frac{1}{2}\sin p\right]+\frac{1}{2}\frac{\sin p}{p}\,. \qquad \text{(E.37)}
\end{aligned}
$$

$$
\begin{aligned}
&\frac{g^4C_FC_A}{8\pi^3}\int_0^1\mathrm{d}x\int_0^1\mathrm{d}s\int_0^\infty\frac{\mathrm{d}p}{|x-s|}\left[-\frac{\cos p}{p^2}+\frac{\sin p}{p^3}\right]e^{-\frac{\sqrt{x(1-x)}}{|x-s|}p}\\
&=\frac{g^4C_FC_A}{16\pi^3}\int_0^1\mathrm{d}x\int_0^1\mathrm{d}s\int_0^\infty\frac{\mathrm{d}p\,e^{-\frac{\sqrt{x(1-x)}}{|x-s|}p}}{|x-s|}\left[\frac{x(1-x)}{|x-s|^2}\left(-\cos p+\frac{\sin p}{p}\right)-\frac{\sqrt{x(1-x)}}{|x-s|}\sin p+\frac{\sin p}{p}\right]. \qquad \text{(E.38)}
\end{aligned}
$$

$$
\begin{aligned}
\int_0^\infty\mathrm{d}p\left(b^2\cos p+b\sin p\right)\,e^{-bp} &= \int_0^\infty\mathrm{d}p\left[\left(\frac{b^2}{2}+\frac{b}{2i}\right)e^{-(b-i)p}+\left(\frac{b^2}{2}-\frac{b}{2i}\right)e^{-(b+i)p}\right]\\
&=\frac{b}{2}\left(\frac{b-i}{b-i}+\frac{b+i}{b+i}\right)=b \qquad \text{(E.39)}\\
\int_0^\infty\mathrm{d}p\,\frac{\sin p}{p}e^{-bp} &= \int_0^\infty\mathrm{d}p\sum_{n=0}^\infty\frac{(-1)^np^{2n}}{(2n+1)!}e^{-bp}=\sum_{n=0}^\infty\frac{(-1)^n}{2n+1}\frac{1}{b^{2n+1}}\\
&=\sum_{n=0}^\infty(-1)^n\int_0^{\frac{1}{b}}\mathrm{d}x\,x^{2n}=\int_0^{\frac{1}{b}}\mathrm{d}x\sum_{n=0}^\infty\left(-x^2\right)^n\\
&=\int_0^{\frac{1}{b}}\mathrm{d}x\,\frac{1}{1-(-x^2)}=\arctan\frac{1}{b}\,. \qquad \text{(E.40)}
\end{aligned}
$$

Actually, the intermediate steps in the derivation of equation (E.40), in particular exchanging summation and integration, are only valid for $b>1$, but since both the initial and the final expression are analytic functions of b, their equality holds for all $b\geq 0$.

$$
\begin{aligned}
&\frac{g^4C_FC_A}{16\pi^3}\int_0^1\mathrm{d}x\int_0^1\mathrm{d}s\int_0^\infty\frac{\mathrm{d}p\,e^{-\frac{\sqrt{x(1-x)}}{|x-s|}p}}{|x-s|}\left[\frac{x(1-x)}{|x-s|^2}\left(-\cos p+\frac{\sin p}{p}\right)-\frac{\sqrt{x(1-x)}}{|x-s|}\sin p+\frac{\sin p}{p}\right]\\
&=\frac{g^4C_FC_A}{16\pi^3}\int_0^1\mathrm{d}x\int_0^1\mathrm{d}s\left[-\frac{\sqrt{x(1-x)}}{|x-s|^2}+\left(\frac{x(1-x)}{|x-s|^3}+\frac{1}{|x-s|}\right)\arctan\frac{|x-s|}{\sqrt{x(1-x)}}\right]\\
&=\frac{g^4C_FC_A}{16\pi^3}\int_0^1\mathrm{d}x\int_0^1\mathrm{d}s\left[-\frac{\sqrt{x(1-x)}}{(s-x)^2}+\left(\frac{x(1-x)}{(s-x)^3}+\frac{1}{s-x}\right)\arctan\frac{s-x}{\sqrt{x(1-x)}}\right]. \qquad \text{(E.41)}
\end{aligned}
$$

$$
\begin{aligned}
\frac{1}{x}\arctan\frac{x}{c} &= \sum_{n=0}^\infty\frac{(-1)^n}{(2n+1)c}\left(\frac{x}{c}\right)^{2n}=\partial_x\left[\sum_{n=0}^\infty\frac{(-1)^n}{(2n+1)^2}\left(\frac{x}{c}\right)^{2n+1}\right]\\
&=\partial_x\left[\mathrm{Im}\sum_{n=0}^\infty\frac{1}{(2n+1)^2}\left(\frac{ix}{c}\right)^{2n+1}\right]=\partial_x\left[\mathrm{Im}\sum_{n=1}^\infty\frac{1}{n^2}\left(\frac{ix}{c}\right)^n\right]\\
&=\partial_x\mathrm{Im}\left[\mathrm{Li}_2\left(\frac{ix}{c}\right)\right]=\partial_x\frac{1}{2i}\left[\mathrm{Li}_2\left(\frac{ix}{c}\right)-\mathrm{Li}_2\left(\frac{-ix}{c}\right)\right]\\
&\equiv\partial_x L\left(\frac{x}{c}\right)\,. \qquad \text{(E.42)}
\end{aligned}
$$

Again, the sum representations in the intermediate steps are strictly speaking only valid for $x < c$. However, the analytic continuation in terms of the complex dilogarithm does have no such restriction. Anyway, we will never need any property of L in the following, apart from it being an integral function of $\frac{1}{x}\arctan(x)$ with $L(-x) = -L(x)$, so this is a moot point.

$$\begin{aligned}
\frac{1}{x^3}\arctan\frac{x}{c} &= \partial_x\left[-\frac{1}{2x^2}\arctan\frac{x}{c}\right] + \frac{1}{2x^2}\frac{c}{x^2+c^2} \\
&= \partial_x\left[-\frac{1}{2x^2}\arctan\frac{x}{c}\right] + \frac{1}{2c}\left(\frac{1}{x^2} - \frac{1}{x^2+c^2}\right) \\
&= \partial_x\left[-\frac{1}{2x^2}\arctan\frac{x}{c} - \frac{1}{2cx} - \frac{1}{2c^2}\arctan\frac{x}{c}\right] .
\end{aligned} \tag{E.43}$$

$$\begin{aligned}
&\frac{g^4 C_F C_A}{16\pi^3}\int_0^1 \mathrm{d}x \int_0^1 \mathrm{d}s \left[-\frac{\sqrt{x(1-x)}}{(s-x)^2} + \left(\frac{x(1-x)}{(s-x)^3} + \frac{1}{s-x}\right)\arctan\frac{s-x}{\sqrt{x(1-x)}}\right] \\
&= \frac{g^4 C_F C_A}{16\pi^3}\int_0^1 \mathrm{d}x \left[\frac{\sqrt{x(1-x)}}{(s-x)} - \frac{x(1-x)}{2(s-x)^2}\arctan\frac{s-x}{\sqrt{x(1-x)}} - \frac{\sqrt{x(1-x)}}{2(s-x)} - \right. \\
&\qquad \left. - \frac{1}{2}\arctan\frac{s-x}{\sqrt{x(1-x)}} + L\left(\frac{s-x}{\sqrt{x(1-x)}}\right)\right]_{s=0}^{s=1} \\
&= \frac{g^4 C_F C_A}{32\pi^3}\int_0^1 \mathrm{d}x \left[\sqrt{\frac{x}{1-x}} - \left(\frac{x}{1-x}+1\right)\arctan\sqrt{\frac{1-x}{x}} + 2L\left(\sqrt{\frac{1-x}{x}}\right) + \right. \\
&\qquad \left. + \sqrt{\frac{1-x}{x}} - \left(\frac{1-x}{x}+1\right)\arctan\sqrt{\frac{x}{1-x}} + 2L\left(\sqrt{\frac{x}{1-x}}\right)\right] \\
&= \frac{g^4 C_F C_A}{16\pi^3}\int_0^1 \mathrm{d}x \left[\sqrt{\frac{x}{1-x}} - \left(\frac{x}{1-x}+1\right)\arctan\sqrt{\frac{1-x}{x}} + 2L\left(\sqrt{\frac{1-x}{x}}\right)\right] .
\end{aligned} \tag{E.44}$$

In the last step we used the symmetry of this expression under $x \leftrightarrow 1-x$. Now we can simplify things by making the following substitution:

$$z = \sqrt{\frac{1-x}{x}}, \qquad x = \frac{1}{1+z^2}, \qquad \mathrm{d}x = \frac{-2z}{(1+z^2)^2}\mathrm{d}z . \tag{E.45}$$

$$\begin{aligned}
&\frac{g^4 C_F C_A}{16\pi^3}\int_0^1 \mathrm{d}x \left[\sqrt{\frac{x}{1-x}} - \left(\frac{x}{1-x}+1\right)\arctan\sqrt{\frac{1-x}{x}} + 2L\left(\sqrt{\frac{1-x}{x}}\right)\right] \\
&= \frac{g^4 C_F C_A}{16\pi^3}\int_0^\infty \mathrm{d}z \left(-\partial_z \frac{1}{1+z^2}\right)\left[\frac{1}{z} - \left(\frac{1}{z^2}+1\right)\arctan z + 2L(z)\right] \\
&= \frac{g^4 C_F C_A}{16\pi^3}\int_0^\infty \mathrm{d}z \left\{-\partial_z\left[\frac{1}{z(1+z^2)} - \frac{1}{z^2}\arctan z + \frac{2L(z)}{1+z^2}\right] + \right. \\
&\qquad \left. + \frac{1}{1+z^2}\left[-\frac{1}{z^2} + \frac{2}{z^3}\arctan z - \frac{1}{z^2} + \frac{2}{z}\arctan z\right]\right\} \\
&= \frac{g^4 C_F C_A}{16\pi^3}\int_0^\infty \mathrm{d}z \left\{-\partial_z\left[\frac{1}{z(1+z^2)} - \frac{1}{z^2}\arctan z + \frac{2L(z)}{1+z^2}\right] - \frac{2}{z^2} + \frac{2}{1+z^2} + \frac{2}{z^3}\arctan z\right\} \\
&= \frac{g^4 C_F C_A}{16\pi^3}\left[-\frac{1}{z(1+z^2)} + \frac{1}{z^2}\arctan z - \frac{2L(z)}{1+z^2} + \frac{2}{z} + 2\arctan z - \frac{1}{z^2}\arctan z - \frac{1}{z} - \arctan z\right]_0^\infty
\end{aligned}$$

$$= \frac{g^4 C_F C_A}{16\pi^3} \left[\frac{z}{1+z^2} + \arctan z - \frac{2L(z)}{1+z^2} \right]_0^\infty$$
$$= \frac{g^4 C_F C_A}{16\pi^3} \left[\frac{\pi}{2} \right] = \frac{g^4 C_F C_A}{32\pi^2} = \frac{1}{2} C_F C_A \alpha_s^2 \,. \tag{E.46}$$

Now the only thing left to show is that the integral function $L(x)$ does not diverge faster than $1+x^2$. This can be done using l'Hôpital's rule.

$$\lim_{x\to\infty} \frac{2L(x)}{1+x^2} = \lim_{x\to\infty} \frac{\frac{2}{x}\arctan x}{2x} = 0 \,. \tag{E.47}$$

$L(0) = 0$ follows from $L(-x) = -L(x)$.

E.4 Diagrams E1, E2

The colour factor, gluon propagators and vertex factor are the same for every diagram, so we will start with the terms describing the contour integrations.

$$\begin{aligned} I_{\mathrm{E1}}(\mathbf{k},\mathbf{p},\mathbf{q}) &= \int_0^1 \mathrm{d}s_1 \int_0^{s_1} \mathrm{d}s_2 \int_0^{s_2} \mathrm{d}s_3 \, e^{i\mathbf{r}\cdot\mathbf{k}\left(s_1-\frac{1}{2}\right)} e^{i\mathbf{r}\cdot\mathbf{p}\left(s_2-\frac{1}{2}\right)} e^{i\mathbf{r}\cdot\mathbf{q}\left(s_3-\frac{1}{2}\right)} \\ &= \int_0^1 \mathrm{d}s_1 \int_0^{s_1} \mathrm{d}s_2 \int_0^{s_2} \mathrm{d}s_3 \, e^{i\mathbf{r}\cdot\mathbf{k}s_1} e^{i\mathbf{r}\cdot\mathbf{p}s_2} e^{i\mathbf{r}\cdot\mathbf{q}s_3} \,, \end{aligned} \tag{E.48}$$

$$\begin{aligned} I_{\mathrm{E2}}(\mathbf{k},\mathbf{p},\mathbf{q}) &= -\int_0^1 \mathrm{d}s_1 \int_0^{s_1} \mathrm{d}s_2 \int_0^{1} \mathrm{d}s_3 \, e^{i\mathbf{r}\cdot\mathbf{k}\left(s_1-\frac{1}{2}\right)} e^{i\mathbf{r}\cdot\mathbf{p}\left(s_2-\frac{1}{2}\right)} e^{i\mathbf{r}\cdot\mathbf{q}\left(\frac{1}{2}-s_3\right)} \\ &= -\int_0^1 \mathrm{d}s_1 \int_0^{s_1} \mathrm{d}s_2 \int_0^{1} \mathrm{d}s_3 \, e^{i\mathbf{r}\cdot\mathbf{k}s_1} e^{i\mathbf{r}\cdot\mathbf{p}s_2} e^{i\mathbf{r}\cdot\mathbf{q}(1-s_3)} \\ &= -\int_0^1 \mathrm{d}s_1 \int_0^{s_1} \mathrm{d}s_2 \int_0^{1} \mathrm{d}s_3 \, e^{i\mathbf{r}\cdot\mathbf{k}s_1} e^{i\mathbf{r}\cdot\mathbf{p}s_2} e^{i\mathbf{r}\cdot\mathbf{q}s_3} \,. \end{aligned} \tag{E.49}$$

Here we have used $\mathbf{k}+\mathbf{p}+\mathbf{q}=0$ because of the δ-function in the vertex factor and in the last line made the substitution $s_3 \to 1-s_3$.

$$\begin{aligned} I_{\mathrm{E1}}(\mathbf{k},\mathbf{p},\mathbf{q}) + I_{\mathrm{E2}}(\mathbf{k},\mathbf{p},\mathbf{q}) &= -\int_0^1 \mathrm{d}s_1 \int_0^{s_1} \mathrm{d}s_2 \int_{s_2}^{1} \mathrm{d}s_3 \, e^{i\mathbf{r}\cdot\mathbf{k}s_1} e^{i\mathbf{r}\cdot\mathbf{p}s_2} e^{i\mathbf{r}\cdot\mathbf{q}s_3} \\ &= -\int_0^1 \mathrm{d}s_1 \int_0^{s_1} \mathrm{d}s_2 \left[\int_{s_2}^{s_1} \mathrm{d}s_3 + \int_{s_1}^{1} \mathrm{d}s_3 \right] e^{i\mathbf{r}\cdot\mathbf{k}s_1} e^{i\mathbf{r}\cdot\mathbf{p}s_2} e^{i\mathbf{r}\cdot\mathbf{q}s_3} \\ &= -\int_0^1 \mathrm{d}s_1 \int_0^{s_1} \mathrm{d}s_3 \int_0^{s_3} \mathrm{d}s_2 \, e^{i\mathbf{r}\cdot\mathbf{k}s_1} e^{i\mathbf{r}\cdot\mathbf{p}s_2} e^{i\mathbf{r}\cdot\mathbf{q}s_3} - \\ &\quad -\int_0^1 \mathrm{d}s_3 \int_0^{s_3} \mathrm{d}s_1 \int_0^{s_1} \mathrm{d}s_2 \, e^{i\mathbf{r}\cdot\mathbf{k}s_1} e^{i\mathbf{r}\cdot\mathbf{p}s_2} e^{i\mathbf{r}\cdot\mathbf{q}s_3} \\ &= -I_{\mathrm{E1}}(\mathbf{k},\mathbf{q},\mathbf{p}) - I_{\mathrm{E1}}(\mathbf{q},\mathbf{k},\mathbf{p}) \,. \end{aligned} \tag{E.50}$$

Now, $\mathbf{k}$, $\mathbf{p}$ and $\mathbf{q}$ are just integration variables, so we may rename them to get back $I_{\mathrm{E1}}(\mathbf{k},\mathbf{p},\mathbf{q})$. To see what happens after this change of variables, we give the rest of the integrand:

$$r_i r_j r_k \frac{\delta_{il} - \frac{k_i k_l}{\mathbf{k}^2}}{k^2} \frac{\delta_{jm} - \frac{p_j p_m}{\mathbf{p}^2}}{p^2} \frac{\delta_{kn} - \frac{q_k q_n}{\mathbf{q}^2}}{q^2} \left[\delta_{lm}(p_n - k_n) + \delta_{mn}(q_l - p_l) + \delta_{nl}(k_m - q_m) \right] \frac{(2\pi)^3}{T} \delta^{(4)}(k+p+q) \,. \tag{E.51}$$

This does not change under cyclic permutations of $(\mathbf{k},\mathbf{p},\mathbf{q})$, but gives an additional minus sign under odd permutations. So the sum of diagrams E1 and E2 is $\sim [I_{\mathrm{E1}}(\mathbf{k},\mathbf{p},\mathbf{q}) - I_{\mathrm{E1}}(\mathbf{k},\mathbf{p},\mathbf{q})] = 0$. The case of E3 and E4 is analogous.

E.5 Diagrams 2X, 2T, 2T', 2S, 2S'

Colour coefficients and propagator terms are the same for every diagram, so the important part lies in the parameter integrations of the exponentials. The value for the sum of all diagrams is given by

$$-\frac{g^4}{2}C_F C_A \sum\!\!\!\!\!\!\int_k \sum\!\!\!\!\!\!\int_q \frac{\mathbf{r}^2-\frac{(\mathbf{r}\cdot\mathbf{k})^2}{\mathbf{k}^2}}{k^2}\frac{\mathbf{r}^2-\frac{(\mathbf{r}\cdot\mathbf{q})^2}{\mathbf{q}^2}}{q^2} I(\mathbf{k},\mathbf{q})\,, \tag{E.52}$$

where $I(\mathbf{k},\mathbf{q})$ represents the terms from the parameter integrations:

$$I(\mathbf{k},\mathbf{q}) = I_{2X}(\mathbf{k},\mathbf{q}) + I_{2T}(\mathbf{k},\mathbf{q}) + I_{2T'}(\mathbf{k},\mathbf{q}) + I_{2S}(\mathbf{k},\mathbf{q}) + I_{2S'}(\mathbf{k},\mathbf{q})\,. \tag{E.53}$$

$$\begin{aligned}
I_{2X}(\mathbf{k},\mathbf{q}) &= \int_0^1 \mathrm{d}s_1 \int_0^{s_1} \mathrm{d}s_2 \int_0^1 \mathrm{d}s_3 \int_0^{s_3} \mathrm{d}s_4\, e^{i\mathbf{r}\cdot\mathbf{k}(s_1+s_3-1)} e^{i\mathbf{r}\cdot\mathbf{q}(s_2+s_4-1)} \\
&= \int_0^1 \mathrm{d}s_1 \int_0^1 \mathrm{d}s_3\, e^{i\mathbf{r}\cdot\mathbf{k}(s_1+s_3-1)} \frac{\left(e^{i\mathbf{r}\cdot\mathbf{q}s_1}-1\right)\left(e^{i\mathbf{r}\cdot\mathbf{q}s_3}-1\right)e^{-i\mathbf{r}\cdot\mathbf{q}}}{-(\mathbf{r}\cdot\mathbf{q})^2} \\
&= \frac{e^{-i\mathbf{r}\cdot\mathbf{k}}e^{-i\mathbf{r}\cdot\mathbf{q}}}{(\mathbf{r}\cdot\mathbf{q})^2}\left(\frac{e^{i\mathbf{r}\cdot\mathbf{k}+i\mathbf{r}\cdot\mathbf{q}}-1}{\mathbf{r}\cdot\mathbf{k}+\mathbf{r}\cdot\mathbf{q}} - \frac{e^{i\mathbf{r}\cdot\mathbf{k}}-1}{\mathbf{r}\cdot\mathbf{k}}\right)\left(\frac{e^{i\mathbf{r}\cdot\mathbf{k}+i\mathbf{r}\cdot\mathbf{q}}-1}{\mathbf{r}\cdot\mathbf{k}+\mathbf{r}\cdot\mathbf{q}} - \frac{e^{i\mathbf{r}\cdot\mathbf{k}}-1}{\mathbf{r}\cdot\mathbf{k}}\right) \\
&= \frac{\left(e^{i\mathbf{r}\cdot\mathbf{k}}-e^{-i\mathbf{r}\cdot\mathbf{q}}\right)\left(e^{i\mathbf{r}\cdot\mathbf{q}}-e^{-i\mathbf{r}\cdot\mathbf{k}}\right)}{(\mathbf{r}\cdot\mathbf{q})^2(\mathbf{r}\cdot\mathbf{k}+\mathbf{r}\cdot\mathbf{q})^2} - 2\frac{\left(1-e^{-i\mathbf{r}\cdot\mathbf{k}}\right)\left(e^{i\mathbf{r}\cdot\mathbf{k}}-e^{-i\mathbf{r}\cdot\mathbf{q}}\right)}{(\mathbf{r}\cdot\mathbf{k})(\mathbf{r}\cdot\mathbf{q})^2(\mathbf{r}\cdot\mathbf{k}+\mathbf{r}\cdot\mathbf{q})} + \\
&\quad + \frac{\left(1-e^{-i\mathbf{r}\cdot\mathbf{k}}\right)\left(e^{i(\mathbf{r}\cdot\mathbf{k}-\mathbf{r}\cdot\mathbf{q})}-e^{-i\mathbf{r}\cdot\mathbf{q}}\right)}{(\mathbf{r}\cdot\mathbf{k})^2(\mathbf{r}\cdot\mathbf{q})^2} \\
&= \frac{e^{i(\mathbf{r}\cdot\mathbf{k}+\mathbf{r}\cdot\mathbf{q})}}{(\mathbf{r}\cdot\mathbf{q})^2(\mathbf{r}\cdot\mathbf{k}+\mathbf{r}\cdot\mathbf{q})^2} + \frac{e^{-i(\mathbf{r}\cdot\mathbf{k}+\mathbf{r}\cdot\mathbf{q})}}{(\mathbf{r}\cdot\mathbf{k})^2(\mathbf{r}\cdot\mathbf{k}+\mathbf{r}\cdot\mathbf{q})^2} + \frac{e^{i(\mathbf{r}\cdot\mathbf{k}-\mathbf{r}\cdot\mathbf{q})}}{(\mathbf{r}\cdot\mathbf{k})^2(\mathbf{r}\cdot\mathbf{q})^2} - \\
&\quad - \frac{2\,e^{i\mathbf{r}\cdot\mathbf{k}}}{(\mathbf{r}\cdot\mathbf{k})(\mathbf{r}\cdot\mathbf{q})^2(\mathbf{r}\cdot\mathbf{k}+\mathbf{r}\cdot\mathbf{q})} - \frac{2\,e^{-i\mathbf{r}\cdot\mathbf{q}}}{(\mathbf{r}\cdot\mathbf{k})^2(\mathbf{r}\cdot\mathbf{q})(\mathbf{r}\cdot\mathbf{k}+\mathbf{r}\cdot\mathbf{q})} + \\
&\quad + \frac{2}{(\mathbf{r}\cdot\mathbf{k})(\mathbf{r}\cdot\mathbf{q})(\mathbf{r}\cdot\mathbf{k}+\mathbf{r}\cdot\mathbf{q})^2}\,.
\end{aligned} \tag{E.54}$$

$$\begin{aligned}
I_{2T}(\mathbf{k},\mathbf{q}) &= -\int_0^1 \mathrm{d}s_1 \int_0^{s_1} \mathrm{d}s_2 \int_0^{s_2} \mathrm{d}s_3 \int_0^1 \mathrm{d}s_4\, e^{i\mathbf{r}\cdot\mathbf{k}(s_1-s_3)} e^{i\mathbf{r}\cdot\mathbf{q}(s_2+s_4-1)} \\
&= -\int_0^1 \mathrm{d}s_1 \int_0^{s_1} \mathrm{d}s_2\, e^{i\mathbf{r}\cdot\mathbf{k}s_1} e^{i\mathbf{r}\cdot\mathbf{q}s_2} \frac{\left(e^{-i\mathbf{r}\cdot\mathbf{k}s_2}-1\right)}{\mathbf{r}\cdot\mathbf{k}} \frac{\left(1-e^{-i\mathbf{r}\cdot\mathbf{q}}\right)}{\mathbf{r}\cdot\mathbf{q}} \\
&= -\int_0^1 \mathrm{d}s_1\, \frac{e^{i\mathbf{r}\cdot\mathbf{k}s_1}}{\mathbf{r}\cdot\mathbf{k}}\left(\frac{e^{-i(\mathbf{r}\cdot\mathbf{k}-\mathbf{r}\cdot\mathbf{q})s_1}-1}{-i(\mathbf{r}\cdot\mathbf{k}-\mathbf{r}\cdot\mathbf{q})} - \frac{e^{i\mathbf{r}\cdot\mathbf{q}s_1}-1}{i\mathbf{r}\cdot\mathbf{q}}\right)\frac{\left(1-e^{-i\mathbf{r}\cdot\mathbf{q}}\right)}{\mathbf{r}\cdot\mathbf{q}} \\
&= \frac{\left(e^{-i\mathbf{r}\cdot\mathbf{q}}-1\right)}{(\mathbf{r}\cdot\mathbf{k})(\mathbf{r}\cdot\mathbf{q})}\left(\frac{e^{i\mathbf{r}\cdot\mathbf{q}}-1}{(\mathbf{r}\cdot\mathbf{q})(\mathbf{r}\cdot\mathbf{k}-\mathbf{r}\cdot\mathbf{q})} - \frac{e^{i\mathbf{r}\cdot\mathbf{k}}-1}{(\mathbf{r}\cdot\mathbf{k})(\mathbf{r}\cdot\mathbf{k}-\mathbf{r}\cdot\mathbf{q})} + \frac{e^{i(\mathbf{r}\cdot\mathbf{k}+\mathbf{r}\cdot\mathbf{q})}-1}{(\mathbf{r}\cdot\mathbf{q})(\mathbf{r}\cdot\mathbf{k}+\mathbf{r}\cdot\mathbf{q})} - \frac{e^{i\mathbf{r}\cdot\mathbf{k}}-1}{(\mathbf{r}\cdot\mathbf{k})(\mathbf{r}\cdot\mathbf{q})}\right) \\
&= \frac{\left(e^{-i\mathbf{r}\cdot\mathbf{q}}-1\right)\left(e^{i\mathbf{r}\cdot\mathbf{q}}-1\right)}{(\mathbf{r}\cdot\mathbf{k})(\mathbf{r}\cdot\mathbf{q})^2(\mathbf{r}\cdot\mathbf{k}-\mathbf{r}\cdot\mathbf{q})} - \frac{\left(e^{i\mathbf{r}\cdot\mathbf{k}}-1\right)\left(e^{-i\mathbf{r}\cdot\mathbf{q}}-1\right)}{(\mathbf{r}\cdot\mathbf{k})(\mathbf{r}\cdot\mathbf{q})^2(\mathbf{r}\cdot\mathbf{k}-\mathbf{r}\cdot\mathbf{q})} + \frac{\left(e^{-i\mathbf{r}\cdot\mathbf{q}}-1\right)\left(e^{i(\mathbf{r}\cdot\mathbf{k}+\mathbf{r}\cdot\mathbf{q})}-1\right)}{(\mathbf{r}\cdot\mathbf{k})(\mathbf{r}\cdot\mathbf{q})^2(\mathbf{r}\cdot\mathbf{k}+\mathbf{r}\cdot\mathbf{q})} \\
&= -\frac{e^{i(\mathbf{r}\cdot\mathbf{k}+\mathbf{r}\cdot\mathbf{q})}}{(\mathbf{r}\cdot\mathbf{k})(\mathbf{r}\cdot\mathbf{q})^2(\mathbf{r}\cdot\mathbf{k}+\mathbf{r}\cdot\mathbf{q})} - \frac{e^{i(\mathbf{r}\cdot\mathbf{k}-\mathbf{r}\cdot\mathbf{q})}}{(\mathbf{r}\cdot\mathbf{k})(\mathbf{r}\cdot\mathbf{q})^2(\mathbf{r}\cdot\mathbf{k}-\mathbf{r}\cdot\mathbf{q})} + \\
&\quad + \frac{2\,e^{i\mathbf{r}\cdot\mathbf{k}}}{(\mathbf{r}\cdot\mathbf{q})^2(\mathbf{r}\cdot\mathbf{k}+\mathbf{r}\cdot\mathbf{q})(\mathbf{r}\cdot\mathbf{k}-\mathbf{r}\cdot\mathbf{q})} - \frac{e^{i\mathbf{r}\cdot\mathbf{q}}}{(\mathbf{r}\cdot\mathbf{k})(\mathbf{r}\cdot\mathbf{q})^2(\mathbf{r}\cdot\mathbf{k}-\mathbf{r}\cdot\mathbf{q})} - \\
&\quad - \frac{e^{-i\mathbf{r}\cdot\mathbf{q}}}{(\mathbf{r}\cdot\mathbf{k})(\mathbf{r}\cdot\mathbf{q})^2(\mathbf{r}\cdot\mathbf{k}+\mathbf{r}\cdot\mathbf{q})} + \frac{2}{(\mathbf{r}\cdot\mathbf{q})^2(\mathbf{r}\cdot\mathbf{k}+\mathbf{r}\cdot\mathbf{q})(\mathbf{r}\cdot\mathbf{k}-\mathbf{r}\cdot\mathbf{q})}\,.
\end{aligned} \tag{E.55}$$

$$
\begin{aligned}
I_{2T'}(\mathbf{k},\mathbf{q}) &= -\int_0^1 \mathrm{d}s_1 \int_0^1 \mathrm{d}s_2 \int_0^{s_2} \mathrm{d}s_3 \int_0^{s_3} \mathrm{d}s_4\, e^{i\mathbf{r}\cdot\mathbf{k}(s_1+s_3-1)} e^{-i\mathbf{r}\cdot\mathbf{q}(s_2-s_4)} = I_{2T}(-\mathbf{q},\mathbf{k}) \\
&= \frac{e^{i(\mathbf{r}\cdot\mathbf{k}-\mathbf{r}\cdot\mathbf{q})}}{(\mathbf{r}\cdot\mathbf{k})^2(\mathbf{r}\cdot\mathbf{q})(\mathbf{r}\cdot\mathbf{k}-\mathbf{r}\cdot\mathbf{q})} - \frac{e^{-i(\mathbf{r}\cdot\mathbf{k}+\mathbf{r}\cdot\mathbf{q})}}{(\mathbf{r}\cdot\mathbf{k})^2(\mathbf{r}\cdot\mathbf{q})(\mathbf{r}\cdot\mathbf{k}+\mathbf{r}\cdot\mathbf{q})} - \\
&\quad - \frac{2\,e^{-i\mathbf{r}\cdot\mathbf{q}}}{(\mathbf{r}\cdot\mathbf{k})^2(\mathbf{r}\cdot\mathbf{k}+\mathbf{r}\cdot\mathbf{q})(\mathbf{r}\cdot\mathbf{k}-\mathbf{r}\cdot\mathbf{q})} - \frac{e^{i\mathbf{r}\cdot\mathbf{k}}}{(\mathbf{r}\cdot\mathbf{k})^2(\mathbf{r}\cdot\mathbf{q})(\mathbf{r}\cdot\mathbf{k}+\mathbf{r}\cdot\mathbf{q})} + \\
&\quad + \frac{e^{-i\mathbf{r}\cdot\mathbf{k}}}{(\mathbf{r}\cdot\mathbf{k})^2(\mathbf{r}\cdot\mathbf{q})(\mathbf{r}\cdot\mathbf{k}-\mathbf{r}\cdot\mathbf{q})} - \frac{2}{(\mathbf{r}\cdot\mathbf{k})^2(\mathbf{r}\cdot\mathbf{k}+\mathbf{r}\cdot\mathbf{q})(\mathbf{r}\cdot\mathbf{k}-\mathbf{r}\cdot\mathbf{q})}\,.
\end{aligned}
\tag{E.56}
$$

$$
\begin{aligned}
I_{2S}(\mathbf{k},\mathbf{q}) &= \int_0^1 \mathrm{d}s_1 \int_0^{s_1} \mathrm{d}s_2 \int_0^{s_2} \mathrm{d}s_3 \int_0^{s_3} \mathrm{d}s_4\, e^{i\mathbf{r}\cdot\mathbf{k}(s_1-s_3)} e^{i\mathbf{r}\cdot\mathbf{q}(s_2-s_4)} \\
&= -\frac{1}{i(\mathbf{r}\cdot\mathbf{q})} \int_0^1 \mathrm{d}s_1 \int_0^{s_1} \mathrm{d}s_2 \int_0^{s_2} \mathrm{d}s_3\, e^{i\mathbf{r}\cdot\mathbf{k}s_1} e^{i\mathbf{r}\cdot\mathbf{q}s_2} \left(e^{-i(\mathbf{r}\cdot\mathbf{k}+\mathbf{r}\cdot\mathbf{q})s_3} - e^{-i\mathbf{r}\cdot\mathbf{k}s_3} \right) \\
&= -\frac{1}{\mathbf{r}\cdot\mathbf{q}} \int_0^1 \mathrm{d}s_1 \int_0^{s_1} \mathrm{d}s_2\, e^{i\mathbf{r}\cdot\mathbf{k}s_1} \left(\frac{e^{-i\mathbf{r}\cdot\mathbf{k}s_2}}{\mathbf{r}\cdot\mathbf{k}+\mathbf{r}\cdot\mathbf{q}} - \frac{e^{-i(\mathbf{r}\cdot\mathbf{k}-\mathbf{r}\cdot\mathbf{q})s_2}}{\mathbf{r}\cdot\mathbf{k}} + \frac{(\mathbf{r}\cdot\mathbf{q})\, e^{i\mathbf{r}\cdot\mathbf{q}s_2}}{(\mathbf{r}\cdot\mathbf{k})(\mathbf{r}\cdot\mathbf{k}+\mathbf{r}\cdot\mathbf{q})} \right) \\
&= \frac{1}{\mathbf{r}\cdot\mathbf{q}} \int_0^1 \mathrm{d}s_1 \left(\frac{1-e^{i\mathbf{r}\cdot\mathbf{k}s_1}}{i(\mathbf{r}\cdot\mathbf{k})(\mathbf{r}\cdot\mathbf{k}+\mathbf{r}\cdot\mathbf{q})} - \frac{e^{i\mathbf{r}\cdot\mathbf{q}s_1}-e^{i\mathbf{r}\cdot\mathbf{k}s_1}}{i(\mathbf{r}\cdot\mathbf{k})(\mathbf{r}\cdot\mathbf{k}-\mathbf{r}\cdot\mathbf{q})} - \frac{e^{i(\mathbf{r}\cdot\mathbf{k}+\mathbf{r}\cdot\mathbf{q})s_1}-e^{i\mathbf{r}\cdot\mathbf{k}s_1}}{i(\mathbf{r}\cdot\mathbf{k})(\mathbf{r}\cdot\mathbf{k}+\mathbf{r}\cdot\mathbf{q})} \right) \\
&= \frac{1}{i(\mathbf{r}\cdot\mathbf{k})(\mathbf{r}\cdot\mathbf{q})} \int_0^1 \mathrm{d}s_1 \left(\frac{1-e^{i(\mathbf{r}\cdot\mathbf{k}+\mathbf{r}\cdot\mathbf{q})s_1}}{\mathbf{r}\cdot\mathbf{k}+\mathbf{r}\cdot\mathbf{q}} - \frac{e^{i\mathbf{r}\cdot\mathbf{q}s_1}-e^{i\mathbf{r}\cdot\mathbf{k}s_1}}{\mathbf{r}\cdot\mathbf{k}-\mathbf{r}\cdot\mathbf{q}} \right) \\
&= \frac{1}{i(\mathbf{r}\cdot\mathbf{k})(\mathbf{r}\cdot\mathbf{q})(\mathbf{r}\cdot\mathbf{k}+\mathbf{r}\cdot\mathbf{q})} + \frac{e^{i(\mathbf{r}\cdot\mathbf{k}+\mathbf{r}\cdot\mathbf{q})}-1}{(\mathbf{r}\cdot\mathbf{k})(\mathbf{r}\cdot\mathbf{q})(\mathbf{r}\cdot\mathbf{k}+\mathbf{r}\cdot\mathbf{q})^2} + \\
&\quad + \frac{e^{i\mathbf{r}\cdot\mathbf{q}}-1}{(\mathbf{r}\cdot\mathbf{k})(\mathbf{r}\cdot\mathbf{q})^2(\mathbf{r}\cdot\mathbf{k}-\mathbf{r}\cdot\mathbf{q})} - \frac{e^{i\mathbf{r}\cdot\mathbf{k}}-1}{(\mathbf{r}\cdot\mathbf{k})^2(\mathbf{r}\cdot\mathbf{q})(\mathbf{r}\cdot\mathbf{k}-\mathbf{r}\cdot\mathbf{q})}\,.
\end{aligned}
\tag{E.57}
$$

$$
\begin{aligned}
I_{2S'}(\mathbf{k},\mathbf{q}) &= \int_0^1 \mathrm{d}s_1 \int_0^{s_1} \mathrm{d}s_2 \int_0^{s_2} \mathrm{d}s_3 \int_0^{s_3} \mathrm{d}s_4\, e^{-i\mathbf{r}\cdot\mathbf{k}(s_1-s_3)} e^{-i\mathbf{r}\cdot\mathbf{q}(s_2-s_4)} = I_{2S}(-\mathbf{k},-\mathbf{q}) \\
&= -\frac{1}{i(\mathbf{r}\cdot\mathbf{k})(\mathbf{r}\cdot\mathbf{q})(\mathbf{r}\cdot\mathbf{k}+\mathbf{r}\cdot\mathbf{q})} + \frac{e^{-i(\mathbf{r}\cdot\mathbf{k}+\mathbf{r}\cdot\mathbf{q})}-1}{(\mathbf{r}\cdot\mathbf{k})(\mathbf{r}\cdot\mathbf{q})(\mathbf{r}\cdot\mathbf{k}+\mathbf{r}\cdot\mathbf{q})^2} + \\
&\quad + \frac{e^{-i\mathbf{r}\cdot\mathbf{q}}-1}{(\mathbf{r}\cdot\mathbf{k})(\mathbf{r}\cdot\mathbf{q})^2(\mathbf{r}\cdot\mathbf{k}-\mathbf{r}\cdot\mathbf{q})} - \frac{e^{-i\mathbf{r}\cdot\mathbf{k}}-1}{(\mathbf{r}\cdot\mathbf{k})^2(\mathbf{r}\cdot\mathbf{q})(\mathbf{r}\cdot\mathbf{k}-\mathbf{r}\cdot\mathbf{q})}\,.
\end{aligned}
\tag{E.58}
$$

$$
\begin{aligned}
I(\mathbf{k},\mathbf{q}) &= I_{2X}(\mathbf{k},\mathbf{q}) + I_{2T}(\mathbf{k},\mathbf{q}) + I_{2T'}(\mathbf{k},\mathbf{q}) + I_{2S}(\mathbf{k},\mathbf{q}) + I_{2S'}(\mathbf{k},\mathbf{q}) \\
&= e^{i(\mathbf{r}\cdot\mathbf{k}+\mathbf{r}\cdot\mathbf{q})} \left(\frac{1}{(\mathbf{r}\cdot\mathbf{q})^2(\mathbf{r}\cdot\mathbf{k}+\mathbf{r}\cdot\mathbf{q})^2} - \frac{1}{(\mathbf{r}\cdot\mathbf{k})(\mathbf{r}\cdot\mathbf{q})^2(\mathbf{r}\cdot\mathbf{k}+\mathbf{r}\cdot\mathbf{q})} + \frac{1}{(\mathbf{r}\cdot\mathbf{k})(\mathbf{r}\cdot\mathbf{q})(\mathbf{r}\cdot\mathbf{k}+\mathbf{r}\cdot\mathbf{q})^2} \right) + \\
&\quad + e^{-i(\mathbf{r}\cdot\mathbf{k}+\mathbf{r}\cdot\mathbf{q})} \left(\frac{1}{(\mathbf{r}\cdot\mathbf{k})^2(\mathbf{r}\cdot\mathbf{k}+\mathbf{r}\cdot\mathbf{q})^2} - \frac{1}{(\mathbf{r}\cdot\mathbf{k})^2(\mathbf{r}\cdot\mathbf{q})(\mathbf{r}\cdot\mathbf{k}+\mathbf{r}\cdot\mathbf{q})} + \frac{1}{(\mathbf{r}\cdot\mathbf{k})(\mathbf{r}\cdot\mathbf{q})(\mathbf{r}\cdot\mathbf{k}+\mathbf{r}\cdot\mathbf{q})^2} \right) + \\
&\quad + e^{i(\mathbf{r}\cdot\mathbf{k}-\mathbf{r}\cdot\mathbf{q})} \left(\frac{1}{(\mathbf{r}\cdot\mathbf{k})^2(\mathbf{r}\cdot\mathbf{q})^2} - \frac{1}{(\mathbf{r}\cdot\mathbf{k})(\mathbf{r}\cdot\mathbf{q})^2(\mathbf{r}\cdot\mathbf{k}-\mathbf{r}\cdot\mathbf{q})} + \frac{1}{(\mathbf{r}\cdot\mathbf{k})^2(\mathbf{r}\cdot\mathbf{q})(\mathbf{r}\cdot\mathbf{k}-\mathbf{r}\cdot\mathbf{q})} \right) + \\
&\quad + e^{i\mathbf{r}\cdot\mathbf{k}} \left(-\frac{2}{(\mathbf{r}\cdot\mathbf{k})(\mathbf{r}\cdot\mathbf{q})^2(\mathbf{r}\cdot\mathbf{k}+\mathbf{r}\cdot\mathbf{q})} + \frac{2}{(\mathbf{r}\cdot\mathbf{q})^2(\mathbf{r}\cdot\mathbf{k}+\mathbf{r}\cdot\mathbf{q})(\mathbf{r}\cdot\mathbf{k}-\mathbf{r}\cdot\mathbf{q})} - \right. \\
&\qquad \left. - \frac{1}{(\mathbf{r}\cdot\mathbf{k})^2(\mathbf{r}\cdot\mathbf{q})(\mathbf{r}\cdot\mathbf{k}+\mathbf{r}\cdot\mathbf{q})} - \frac{1}{(\mathbf{r}\cdot\mathbf{k})^2(\mathbf{r}\cdot\mathbf{q})(\mathbf{r}\cdot\mathbf{k}-\mathbf{r}\cdot\mathbf{q})} \right) + \\
&\quad + e^{-i\mathbf{r}\cdot\mathbf{k}} \left(\frac{1}{(\mathbf{r}\cdot\mathbf{k})^2(\mathbf{r}\cdot\mathbf{q})(\mathbf{r}\cdot\mathbf{k}-\mathbf{r}\cdot\mathbf{q})} - \frac{1}{(\mathbf{r}\cdot\mathbf{k})^2(\mathbf{r}\cdot\mathbf{q})(\mathbf{r}\cdot\mathbf{k}-\mathbf{r}\cdot\mathbf{q})} \right) + \\
&\quad + e^{i\mathbf{r}\cdot\mathbf{q}} \left(-\frac{1}{(\mathbf{r}\cdot\mathbf{k})(\mathbf{r}\cdot\mathbf{q})^2(\mathbf{r}\cdot\mathbf{k}-\mathbf{r}\cdot\mathbf{q})} + \frac{1}{(\mathbf{r}\cdot\mathbf{k})(\mathbf{r}\cdot\mathbf{q})^2(\mathbf{r}\cdot\mathbf{k}-\mathbf{r}\cdot\mathbf{q})} \right) +
\end{aligned}
$$

$$
\begin{aligned}
&+e^{-i\mathbf{r}\cdot\mathbf{q}}\left(-\frac{2}{(\mathbf{r}\cdot\mathbf{k})^2(\mathbf{r}\cdot\mathbf{q})(\mathbf{r}\cdot\mathbf{k}+\mathbf{r}\cdot\mathbf{q})}-\frac{1}{(\mathbf{r}\cdot\mathbf{k})(\mathbf{r}\cdot\mathbf{q})^2(\mathbf{r}\cdot\mathbf{k}+\mathbf{r}\cdot\mathbf{q})}-\right.\\
&\qquad\left.-\frac{2}{(\mathbf{r}\cdot\mathbf{k})^2(\mathbf{r}\cdot\mathbf{k}+\mathbf{r}\cdot\mathbf{q})(\mathbf{r}\cdot\mathbf{k}-\mathbf{r}\cdot\mathbf{q})}+\frac{1}{(\mathbf{r}\cdot\mathbf{k})(\mathbf{r}\cdot\mathbf{q})^2(\mathbf{r}\cdot\mathbf{k}-\mathbf{r}\cdot\mathbf{q})}\right)+\\
&+\frac{2}{(\mathbf{r}\cdot\mathbf{k})(\mathbf{r}\cdot\mathbf{q})(\mathbf{r}\cdot\mathbf{k}+\mathbf{r}\cdot\mathbf{q})^2}+\frac{2}{(\mathbf{r}\cdot\mathbf{q})^2(\mathbf{r}\cdot\mathbf{k}+\mathbf{r}\cdot\mathbf{q})(\mathbf{r}\cdot\mathbf{k}-\mathbf{r}\cdot\mathbf{q})}-\\
&-\frac{2}{(\mathbf{r}\cdot\mathbf{k})^2(\mathbf{r}\cdot\mathbf{k}+\mathbf{r}\cdot\mathbf{q})(\mathbf{r}\cdot\mathbf{k}-\mathbf{r}\cdot\mathbf{q})}-\frac{2}{(\mathbf{r}\cdot\mathbf{k})(\mathbf{r}\cdot\mathbf{q})(\mathbf{r}\cdot\mathbf{k}+\mathbf{r}\cdot\mathbf{q})^2}-\\
&-\frac{2}{(\mathbf{r}\cdot\mathbf{k})(\mathbf{r}\cdot\mathbf{q})^2(\mathbf{r}\cdot\mathbf{k}-\mathbf{r}\cdot\mathbf{q})}+\frac{2}{(\mathbf{r}\cdot\mathbf{k})^2(\mathbf{r}\cdot\mathbf{q})(\mathbf{r}\cdot\mathbf{k}-\mathbf{r}\cdot\mathbf{q})}+\\
&+\frac{1}{i(\mathbf{r}\cdot\mathbf{k})(\mathbf{r}\cdot\mathbf{q})(\mathbf{r}\cdot\mathbf{k}+\mathbf{r}\cdot\mathbf{q})}-\frac{1}{i(\mathbf{r}\cdot\mathbf{k})(\mathbf{r}\cdot\mathbf{q})(\mathbf{r}\cdot\mathbf{k}+\mathbf{r}\cdot\mathbf{q})}\\
&=0\,.
\end{aligned}
\tag{E.59}
$$

E.6 Diagram 3X (Thermal Part)

Since the thermal part is finite, we may compute it in 3 dimensions. The angular integration has already been done for diagram d) in the tree level vacuum Wilson loop calculations:

$$
\begin{aligned}
W^{(T)}\left(\gamma_{d)}\right)&=\frac{g^2}{2\pi^2}\int_0^\infty \mathrm{d}k\int_{-1}^1 \mathrm{d}x\,\frac{1}{e^{k\beta}-1}\left(1-x^2\right)\frac{1-\cos(krx)}{kx^2}\\
&=\frac{g^2}{\pi^2}\int_0^\infty \mathrm{d}k\,\frac{1}{e^{\frac{k}{rT}}-1}\left(\mathrm{Si}(k)-\frac{1-\cos k}{k}-\frac{k-\sin k}{k^2}\right)\,.
\end{aligned}
\tag{E.60}
$$

To (at least partially) solve this integral, we will look at each term individually and make the substitution $x=e^{-\frac{k}{rT}}$:

$$
\begin{aligned}
\bullet\int_0^\infty \mathrm{d}k\frac{\mathrm{Si}(k)}{e^{\frac{k}{rT}}-1}&=\int_0^1 \mathrm{d}z\int_0^\infty \mathrm{d}k\frac{1}{e^{\frac{k}{rT}}-1}\frac{\sin(kz)}{z}\\
&=rT\int_0^1\frac{\mathrm{d}z}{z}\int_0^1 \mathrm{d}x\frac{1}{1-x}\frac{1}{2i}\left(x^{-irTz}-x^{irTz}\right)\\
&=\frac{rT}{2i}\int_0^1\frac{\mathrm{d}z}{z}\lim_{\epsilon\to0}\left[\int_0^1 \mathrm{d}x(1-x)^{\epsilon-1}\left(x^{-irTz}-x^{irTz}\right)\right]\\
&=\frac{rT}{2i}\int_0^1\frac{\mathrm{d}z}{z}\lim_{\epsilon\to0}\left[\frac{\Gamma(\epsilon)\Gamma(1-irTz)}{\Gamma(\epsilon+1-irTz)}-\frac{\Gamma(\epsilon)\Gamma(1+irTz)}{\Gamma(\epsilon+1+irTz)}\right]\\
&=\frac{rT}{2i}\int_0^1\frac{\mathrm{d}z}{z}\left[\frac{\Gamma'(1+irTz)}{\Gamma(1+irTz)}-\frac{\Gamma'(1-irTz)}{\Gamma(1-irTz)}\right]\\
&=\frac{rT}{2i}\int_0^1\frac{\mathrm{d}z}{z}\left[\psi(1+irTz)-\psi(1-irTz)\right]\,.
\end{aligned}
\tag{E.61}
$$

In the last line we used the digamma function $\psi(x)=\partial_x\ln\Gamma(x)$. This expression is finite for $z\to0$, but I'm not aware of a way to calculate it analytically.

$$
\begin{aligned}
\bullet-\int_0^\infty \mathrm{d}k\,\frac{1-\cos k}{k}\frac{1}{e^{\frac{k}{rT}}-1}&=-\int_0^1 \mathrm{d}z\int_0^\infty \mathrm{d}k\,\frac{\sin(kz)}{e^{\frac{k}{rT}}-1}\\
&=-\frac{rT}{2i}\int_0^1 \mathrm{d}z\left[\psi(1+irTz)-\psi(1-irTz)\right]\\
&=\frac{1}{2}\left[\ln\Gamma(1+irT)+\ln\Gamma(1-irT)\right]\,.
\end{aligned}
\tag{E.62}
$$

$$\bullet -\int_0^\infty \mathrm{d}k\,\frac{k-\sin k}{k^2}\frac{1}{e^{\frac{k}{rT}}-1} = -\int_0^1 \mathrm{d}z\int_0^\infty \mathrm{d}k\,\frac{1-\cos(zk)}{k}\frac{1}{e^{\frac{k}{rT}}-1}$$
$$= -\int_0^1 \mathrm{d}z\int_0^\infty \mathrm{d}k\,\frac{1-\cos(k)}{k}\frac{1}{e^{\frac{k}{rTz}}-1}$$
$$= \frac{1}{2}\int_0^1 \mathrm{d}z\,\left[\ln\Gamma(1+irTz)+\ln\Gamma(1-irTz)\right]. \tag{E.63}$$

The logarithm of the gamma function and antiderivatives of that can be expressed through a generalization of the polygamma function $\psi^{(m)}(x)$ to $m\in\mathbb{C}$. However, there are different definitions and conventions in use, so to avoid confusion, we will stick to the expressions above. It is also possible to derive expressions involving derivatives with respect to the first argument of the Hurwitz zeta function, but I do not see how this improves the expression given.

So together we can write:

$$W^{(T)}\left(\gamma_{d)}\right) = \frac{4\alpha_s}{\pi}\left\{\frac{rT}{2i}\int_0^1\frac{\mathrm{d}z}{z}\left[\psi(1+irTz)-\psi(1-irTz)\right]+\frac{1}{2}\left[\ln\Gamma(1+irT)+\ln\Gamma(1-irT)\right]+\right.$$
$$\left.+\frac{1}{2}\int_0^1\mathrm{d}z\,\left[\ln\Gamma(1+irTz)+\ln\Gamma(1-irTz)\right]\right\}. \tag{E.64}$$

We can also derive a series expansion for $rT\ll 1$:

$$W^{(T)}\left(\gamma_{d)}\right) = \frac{g^2}{\pi^2}\int_0^\infty \mathrm{d}k\,\frac{1}{e^{\frac{k}{rT}}-1}\left(\mathrm{Si}(k)-\frac{1-\cos k}{k}-\frac{k-\sin k}{k^2}\right)$$
$$= \frac{g^2}{\pi^2}\int_0^\infty \mathrm{d}k\,\frac{1}{e^{\frac{k}{rT}}-1}\sum_{n=1}^\infty\left(\frac{(-1)^{n-1}}{(2n-1)(2n-1)!}-\frac{(-1)^{n-1}}{(2n)!}-\frac{(-1)^{n-1}}{(2n+1)!}\right)k^{2n-1}$$
$$= \frac{g^2}{\pi^2}\sum_{n=1}^\infty\frac{2(-1)^{n-1}(rT)^{2n}}{(2n-1)(2n+1)!}\int_0^\infty\mathrm{d}k\,\frac{k^{2n-1}}{e^k-1}$$
$$= \frac{g^2}{\pi^2}\sum_{n=1}^\infty\frac{2(-1)^{n-1}(rT)^{2n}}{(2n-1)(2n+1)!}\Gamma(2n)\zeta(2n)$$
$$= \frac{4\alpha_s}{\pi}\sum_{n=1}^\infty\frac{(-1)^{n-1}}{n(4n^2-1)}\zeta(2n)(rT)^{2n}. \tag{E.65}$$

E.7 Divergences of 1T in Feynman gauge

The value of diagram 1T in Feynman gauge is given by:

$$-(ig)^4\left(-\frac{1}{2}C_FC_A\right)\int_0^\beta\mathrm{d}\tau_1\int_0^\beta\mathrm{d}\tau_2\int_0^{\tau_2}\mathrm{d}\tau_3\int_0^{\tau_3}\mathrm{d}\tau_4\sum\!\!\!\!\!\!\int_k\sum\!\!\!\!\!\!\int_q\frac{e^{ik_0(\beta-\tau_1-\tau_3)-i\mathbf{r}\cdot\mathbf{k}}}{k_0^2+\mathbf{k}^2}\frac{e^{iq_0(\tau_2-\tau_4)}}{q_0^2+\mathbf{q}^2}$$
$$= \frac{C_FC_Ag^4}{2}\int_k\frac{e^{-i\mathbf{r}\cdot\mathbf{k}}}{\mathbf{k}^2}\sum\!\!\!\!\!\!\int_q\int_0^\beta\mathrm{d}\tau_2\int_0^{\tau_2}\mathrm{d}\tau_3\,\frac{e^{iq_0\tau_2}}{q_0^2+\mathbf{q}^2}\left[\tau_3\delta_{n_q0}-\frac{e^{-iq_0\tau_3}-1}{iq_0}\left(1-\delta_{n_q0}\right)\right]$$
$$= \frac{C_FC_Ag^4}{2}\int_k\frac{e^{-i\mathbf{r}\cdot\mathbf{k}}}{\mathbf{k}^2}\sum\!\!\!\!\!\!\int_q\frac{1}{q_0^2+\mathbf{q}^2}\int_0^\beta\mathrm{d}\tau_2\left[\frac{\tau_2^2}{2}\delta_{n_q0}+\frac{(1-iq_0\tau_2)e^{iq_0\tau_2}-1}{q_0^2}\left(1-\delta_{n_q0}\right)\right]$$
$$= \frac{C_FC_Ag^4}{2}\int_k\frac{e^{-i\mathbf{r}\cdot\mathbf{k}}}{\mathbf{k}^2}\sum\!\!\!\!\!\!\int_q\frac{1}{q_0^2+\mathbf{q}^2}\left[\frac{\beta^3}{6}\delta_{n_q0}-\frac{2\beta}{q_0^2}\left(1-\delta_{n_q0}\right)\right]$$
$$= \frac{C_FC_Ag^4}{2}\int_k\frac{e^{-i\mathbf{r}\cdot\mathbf{k}}}{\mathbf{k}^2}\int_q\left[\frac{1}{6T^2q^2}-2\beta\sum_{q_0}{}'\frac{1}{q^2}\left(\frac{1}{q_0^2}-\frac{1}{q_0^2+q^2}\right)\right]$$
$$= \frac{C_FC_Ag^4}{2}\int_k\frac{e^{-i\mathbf{r}\cdot\mathbf{k}}}{\mathbf{k}^2}\int_q\left[\frac{1}{6T^2q^2}-\frac{4}{q^2}\frac{\zeta(2)}{(2\pi T)^2}+\frac{2}{Tq^2}\left(\frac{1}{2q}+\frac{1}{q\left(e^{q\beta}-1\right)}-\frac{T}{q^2}\right)\right]$$

$$
\begin{aligned}
&= \frac{C_F C_A g^4}{2} \int_k \frac{e^{-i\mathbf{r}\cdot\mathbf{k}}}{\mathbf{k}^2} \int_q \left[\frac{1}{Tq^3} + \frac{2}{Tq^3} \frac{1}{e^{q\beta} - 1} - \frac{2}{q^4} \right] \\
&= C_F C_A g^4 \int_k \frac{e^{-i\mathbf{r}\cdot\mathbf{k}}}{\mathbf{k}^2} \frac{2T^{d-4}}{(4\pi)^{\frac{d}{2}} \Gamma\left(\frac{d}{2}\right)} \Gamma(d-3)\zeta(d-3) \\
&= C_F g^2 \int_k \frac{e^{-i\mathbf{r}\cdot\mathbf{k}}}{T\mathbf{k}^2} \frac{C_A \alpha_s}{2\pi} \left[\frac{1}{\varepsilon} + 2 + \gamma_E - \ln 4\pi - 2\ln \mu T \right] .
\end{aligned} \tag{E.66}
$$

Taking the Feynman gauge renormalization constants from reference [29], slightly adapted to our notation, we have:

$$
Z_1^{\overline{\text{MS}}} = 1 + \frac{\alpha_s}{4\pi} \left(\frac{2}{3\bar{\varepsilon}} C_A - \frac{4}{3\bar{\varepsilon}} n_f T_F \right) + \mathcal{O}(\alpha_s^2) , \tag{E.67}
$$

$$
Z_3^{\overline{\text{MS}}} = 1 + \frac{\alpha_s}{4\pi} \left(\frac{5}{3\bar{\varepsilon}} C_A - \frac{4}{3\bar{\varepsilon}} n_f T_F \right) + \mathcal{O}(\alpha_s^2) . \tag{E.68}
$$

This gives a line vertex counterterm of

$$
\frac{Z_1^{\overline{\text{MS}}}}{Z_3^{\overline{\text{MS}}}} - 1 = -\frac{C_A \alpha_s}{4\pi\bar{\varepsilon}} + \mathcal{O}(\alpha_s^2) . \tag{E.69}
$$

Combining diagram 1T with the counterterm diagram, we have

$$
C_F g^2 \int_k \frac{e^{-i\mathbf{r}\cdot\mathbf{k}}}{T\mathbf{k}^2} \frac{C_A \alpha_s}{\pi} \left[\frac{1}{4\bar{\varepsilon}} + 1 + \gamma_E - \ln 4\pi - \ln \mu T \right] . \tag{E.70}
$$

So the sum of the divergent contributions of diagrams 1T, 1T' and 3X, respectively, give

$$
\frac{C_F \alpha_s}{rT} \frac{C_A \alpha_s}{4\pi\bar{\varepsilon}} + \frac{C_F \alpha_s}{rT} \frac{C_A \alpha_s}{4\pi\bar{\varepsilon}} + \frac{C_F \alpha_s}{rT} \frac{C_A \alpha_s}{2\pi\bar{\varepsilon}} = \frac{C_F \alpha_s}{rT} \frac{C_A \alpha_s}{\pi\bar{\varepsilon}} , \tag{E.71}
$$

which is exactly the same intersection divergence we got in Coulomb gauge.

References

[1] W. Caswell and G. Lepage, Phys.Lett. **B167**, 437 (1986)

[2] G. T. Bodwin, E. Braaten, and G. Lepage, Phys.Rev. **D51**, 1125 (1995), arXiv:hep-ph/9407339 [hep-ph]

[3] A. Pineda and J. Soto, Nucl.Phys.Proc.Suppl. **64**, 428 (1998), arXiv:hep-ph/9707481 [hep-ph]

[4] N. Brambilla, A. Pineda, J. Soto, and A. Vairo, Nucl.Phys. **B566**, 275 (2000), arXiv:hep-ph/9907240 [hep-ph]

[5] T. Matsui and H. Satz, Phys.Lett. **B178**, 416 (1986)

[6] N. Brambilla, A. Pineda, J. Soto, and A. Vairo, Rev. Mod. Phys. **77**, 1423 (2005), arXiv:hep-ph/0410047

[7] N. Brambilla *et al.*, Eur. Phys. J. **C71**, 1534 (2011), arXiv:1010.5827 [hep-ph]

[8] Y. Burnier, M. Laine, and M. Vepsäläinen, JHEP **01**, 054 (2010), arXiv:0911.3480 [hep-ph]

[9] N. Brambilla, J. Ghiglieri, P. Petreczky, and A. Vairo, Phys.Rev. **D82**, 074019 (2010), arXiv:1007.5172 [hep-ph]

[10] J. Ghiglieri http://nbn-resolving.de/urn/resolver.pl?urn:nbn:de:bvb:91-diss-20110728-1080401-1-3

[11] K. G. Wilson, Phys.Rev. **D10**, 2445 (1974)

[12] L. S. Brown and W. I. Weisberger, Phys.Rev. **D20**, 3239 (1979)

[13] N. Brambilla and A. Vairo(1999), arXiv:hep-ph/9904330

[14] W. Lucha, F. F. Schöberl, and D. Gromes, Phys. Rept. **200**, 127 (1991)

[15] G. Lepage and B. Thacker, Nucl.Phys.Proc.Suppl. **4**, 199 (1988)

[16] V. S. Dotsenko and S. N. Vergeles, Nucl. Phys. **B169**, 527 (1980)

[17] J. G. M. Gatheral, Phys. Lett. **B133**, 90 (1983)

[18] J. Frenkel and J. C. Taylor, Nucl. Phys. **B246**, 231 (1984)

[19] P. Becher, M. Böhm, and H. Joos, *Gauge Theories of Strong and Electroweak Interaction. (in German)* (Stuttgart, F.r. Germany: Teubner Studienbücher: Physik, 1981) pp. 213–216

[20] R. A. Brandt, F. Neri, and M.-a. Sato, Phys. Rev. **D24**, 879 (1981)

[21] G. P. Korchemsky and A. V. Radyushkin, Nucl. Phys. **B283**, 342 (1987)

[22] W. Fischler, Nucl. Phys. **B129**, 157 (1977)

[23] A. Billoire, Phys. Lett. **B92**, 343 (1980)

[24] D. Zwanziger, Nucl. Phys. **B518**, 237 (1998)

[25] A. Andrasi, Eur. Phys. J. **C37**, 307 (2004), arXiv:hep-th/0311118

[26] N. Brambilla, J. Ghiglieri, P. Petreczky, and A. Vairo, Phys.Rev. **D82**, 074019 (2010), arXiv:1007.5172 [hep-ph]

[27] U. W. Heinz, K. Kajantie, and T. Toimela, Ann. Phys. **176**, 218 (1987)

[28] M. Le Bellac, *Thermal Field Theory* (Cambridge University Press, 2000) pp. 239–241

[29] W. Celmaster and R. J. Gonsalves, Phys.Rev. **D20**, 1420 (1979)